High performance polyurethanes

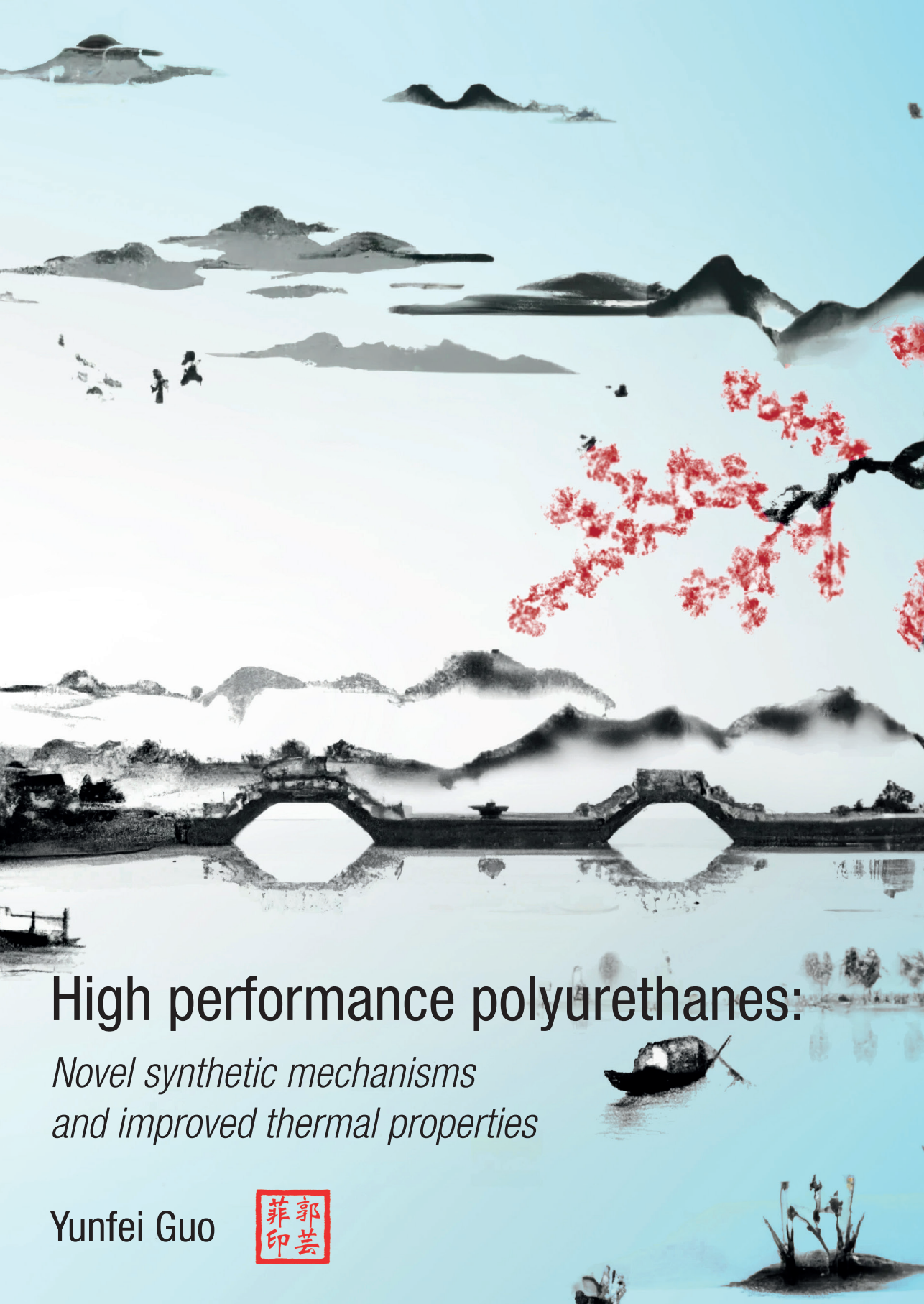

High performance polyurethanes:

Novel synthetic mechanisms and improved thermal properties

Yunfei Guo

郭芸菲印

High performance polyurethanes: Novel synthetic mechanisms and improved thermal properties

PROEFSCHRIFT

ter verkrijging van de graad van doctor aan de Technische Universiteit Eindhoven,
op gezag van de rector magnificus prof. dr. S.K. Lenaerts,
voor een commissie aangewezen door het College voor Promoties,
in het openbaar te verdedigen op dinsdag 23 mei 2023 om 13:30 uur

door

Yunfei Guo

geboren te Shanghai, China

Dit proefschrift is goedgekeurd door de promotoren en de samenstelling van de promotiecommissie is als volgt:

Voorzitter:	Prof. dr. A.P.H.J. Schenning
Promotoren:	Prof. dr. Ž. Tomović
	Prof. dr. R.P. Sijbesma
Promotiecommissieleden:	Prof. dr. ir. A.R.A. Palmans
	Prof. dr. B. Eling (Universität Hamburg)
	Dr. ir. J.P.A. Heuts
Adviseur:	Dr. A.M. Cristadoro (BASF Polyurethanes GmbH)

Het onderzoek dat in dit proefschrift wordt beschreven is uitgevoerd in overeenstemming met de TU/e Gedragscode Wetenschapsbeoefening.

Dedicated to my family

High performance polyurethanes: Novel synthetic mechanisms and improved thermal properties

Yunfei Guo

Eindhoven University of Technology, the Netherlands, 2023

Cover design cogenerated by artificial intelligence programs DALL·E 2 (openai.com), adapted and recreated by Özgün Dağlar and ProefschriftMaken

Printed by ProefschriftMaken

A catalogue record is available from the Eindhoven University of Technology Library

ISBN: 978-90-386-5732-5

The work presented in this thesis was financially supported by BASF Polyurethanes GmbH, Germany

Contents

Chapter 1

Introduction

Images of this figure are obtained from BASF website.

1.1 Motivation

1.1.1 Polyurethane in our daily life

Plastics are inseparable from our daily life. The annual world plastic production keeps increasing. From 2016 to 2020, the plastic production increased by 32 million tons in 5 years (**Figure 1-1a**).[1] Zeroing in to data from 2019, 368 million tons of plastics were produced. Among these plastics, the mostly produced polymers are polyethylene (PE) and polypropylene (PP), followed by polyvinyl chloride (PVC), polyurethane (PU) and polyethylene terephthalate (PET) (**Figure 1-1b**).[2] In 2019, the annual consumption of PUs was around 8% of the global plastics production, corresponding to 29 million tons. As the fourth mostly produced plastic, PUs are made into daily necessities such as artificial leathers, artificial sponges, mattresses, foam sealant and Elastane (Lycra). Moreover, PUs are applied in construction industry such as in rigid foams for thermal insulation, sealants, adhesives and in coatings; in consumer products such as shoe soles, packaging; in automotive applications such as seats, door panels, sound absorption and vibration dampening; in appliances such as insulation of refrigerators and freezers.[3-6]

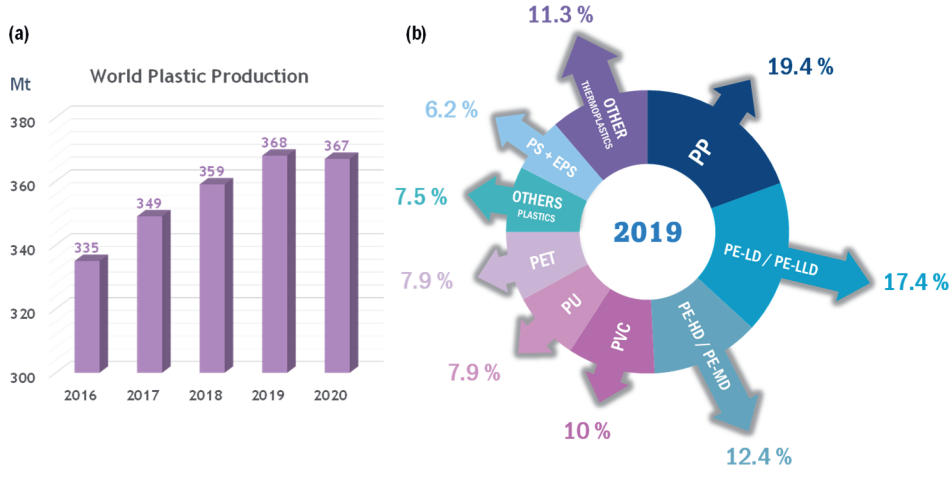

Figure 1-1. (a) Annual world plastic production from 2016-2020 and (b) plastics demand distribution in 2019 by polymer type.[1,2] In 2019, around 29 million tons of PUs were produced in the world.

After the invention of polyurethane by Bayer *et al*. in 1937, polyurethane chemistry has been developing prosperously for 85 years.[7] With the fast development of material science and the material industry, the demands on high-performance PU materials are increasing. These properties include heat resistance and fire safety, mechanical properties, stimuli-responsive functions, biocompatibility, sustainability and

recyclability.[3-6,8-13] Among these properties, flame retardancy is of special interests to the market as for construction and automotive applications.

1.1.2 Flame retardant PU materials

PU plays an important role in many applications, in which fire safety is a crucial topic. Every year, fire causes significant property loss, injuries and even death. However, most of the fire cases can be prevented or controlled. Scientists and engineers have not only been studying fire, but have also been seeking to provide fire protection in our daily life, to which the development of thermally stable and flame retardant plastics can contribute. The term fire retardancy means that when the material is exposed to a flame, it has the property to "either retard the growth and propagation of that flame, or retard (slow) the growth and propagation of any flames that may come from the material once it has been ignited".[14] In other words, if a fire starts by accident, a flame retardant material can be rapidly extinguished by itself, or be used to extinguish the fire before it expands, which can prevent loss of life and property damage. The improvement of flame retardancy of PUs is especially important because they are mostly used in construction, automotive and furniture applications.[4,8]

From the aspect of the flame retardant mechanism, flame retardancy is generally achieved in either the gas phase or/and the condensed polymer phase during combustion (**Figure 1-2a**).[15] In the gas phase, the flame retardation is realized (I) through the capture of reactive free radicals formed during combustion, or (II) through dilution of combustible or combustion-supporting gases. In the condensed phase, the flame retardation is realized *via* several methods such as heat absorption, heat dissipation and barrier protection.

From the aspect of preparation methods, there are typically two ways to achieve flame retardancy and thermal stability in polymers, namely, "additive" and "reactive" types. Many flame retardants (*e.g.*, halogen, phosphorous, boron, nitrogen-based compounds and inorganic compounds) have been reported as additives or fillers to improve the flame retardancy of PU materials (**Figure 1-2b**).[14-19] However, these flame retardant additives may have poor compatibility with PUs, and they may leach out or migrate to the material surface, leading to deterioration in the mechanical properties of the materials. In addition, although halogen-based compounds are one of the most widely used conventional flame retardants in PUs, they have two clear disadvantages.[20] The halogen-based flame retardants are hazardous themselves, and more pressingly, they have the potential to release corrosive and toxic gases (hydrogen halides) during combustion. As a result, the use of halogen-based flame retardants in PUs is gradually being restricted by an increasing number of regulations.

In order to improve the environmental friendliness and compatibility of the flame retardants with the PU materials, many researchers have developed "reactive" type new flame retardants and introduced them into PUs *via* chemical (covalent) bonds (**Figure 1-2c**). Chemical motifs such as reactive phosphorous-containing or phosphorous-nitrogen containing alcohols, melamine-based compounds, isocyanurate and aromatic imide structures enhance the intrinsic thermal stability and flame retardancy of PU materials, which helps to reduce the use of conventional flame retardant additives.[19,21-33]

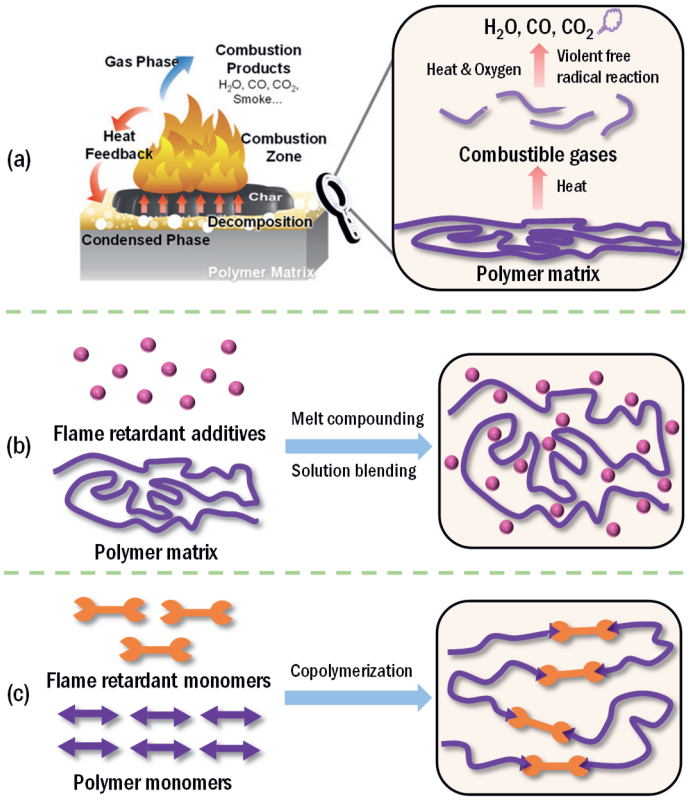

Figure 1-2. (a) Illustration of burning process of the polymer material. Gas phase (free radicals, combustible gases) and condensed phase (polymer matrix) are involved in the burning process; (b) illustration of flame retardants as additives or fillers in the polymer; (c) illustration of flame retardants introduced in polymer *via* covalent bonds. Reproduced from ref. 15 Copyright (2022), with permission from Wiley-VCH GmbH.

Motivated by these developments in "reactive" type flame retardants, this thesis focuses on the introduction of isocyanurate and imide motifs in PU elastomers as a potential approach to large-scale production of these materials. A more detailed explanation of the synthesis and applications of these chemical motifs is presented in the coming sections of this chapter.

1.2 Isocyanurate/polyisocyanurate (PIR) structures in PU

Due to the outstanding thermal and mechanical properties, polyisocyanurate (PIR) is important for polyurethane industry. The synthesis of PIR and the underlying cyclotrimerization mechanism have been widely investigated and the PIR structures have been applied in various PU materials.

1.2.1 Synthesis of isocyanurates

Polyurethane chemistry includes six main isocyanate-based reactions (**Scheme 1-1**), leading to various structures such as urethane (carbamate), allophanate, urea, biuret, uretdione and isocyanurate. Isocyanurates are generally synthesized *via* cyclotrimerization of three isocyanate molecules, which is the main focus of this thesis. Whereas the reaction mechanisms of the other five structures are known, the cyclotrimerization mechanism of isocyanates is still under investigation. Typically, the reaction mechanism of the trimerization reaction is dependent on the catalyst that is used. Thus, in order to elucidate the underlying mechanism, the type of catalyst must be considered.

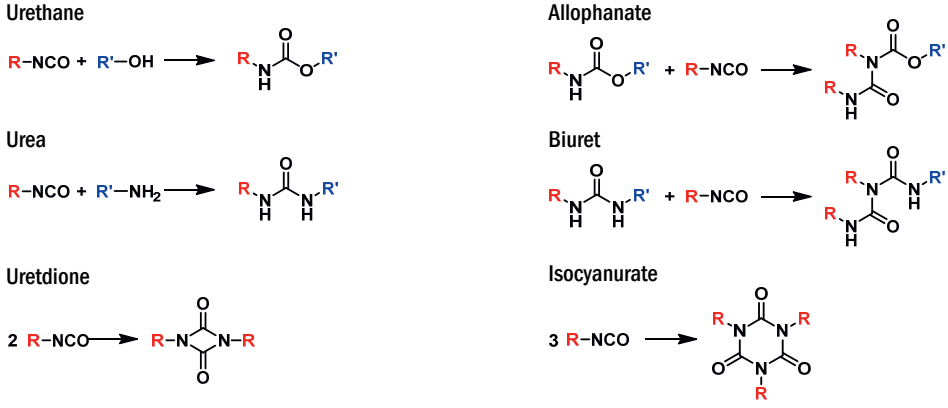

Scheme 1-1. Common structures in PU chemistry. Urethane is formed from the reaction between isocyanate and alcohol; allophanate is formed from the reaction between isocyanate and urethane; urea is formed from the reaction between isocyanate and amine; biuret is formed from the reaction between isocyanate and urea; uretdione is obtained from dimerization of isocyanates; isocyanurate is obtained from trimerization of isocyanates.

The cyclotrimerization catalysts can be divided into two categories: catalysts operating *via* Lewis base cyclotrimerization mechanism and metal-containing catalysts.[34]

Catalysts that operate cyclotrimerization *via* a Lewis base mechanism are generally anions, zwitterions or other functional groups with lone electron pairs. The catalytic

mechanism of these bases has been extensively discussed in the literature (**Scheme 1-2**): the reaction is considered to be initiated by straightforward nucleophilic addition of an anion or lone electron pair of the catalyst to the electrophilic isocyanate carbon forming an anionic intermediate (**2**).[4,35-39] This intermediate reacts further with a second and third molecule of isocyanate in a stepwise manner, and forms isocyanurate (**5**) after ring closure and elimination of the catalyst. Among the Lewis basic catalysts, carboxylates are the most common cyclotrimerization catalysts used in industrial applications. In terms of the cyclotrimerization mechanism using carboxylate as a catalyst, the cyclotrimerization still follows an anionic pathway, while the actual catalytic species changes. A strongly nucleophilic and basic deprotonated amide species is formed irreversibly after the reaction between carboxylate anion and isocyanate, which serves as the actual catalyst.[40-43] The detailed mechanism is explained in **Chapter 2**.

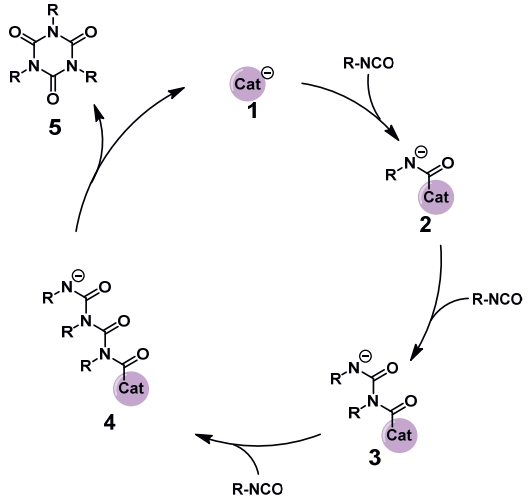

Scheme 1-2. Generally proposed and accepted anionic cyclotrimerization mechanism.

Formulations used for the synthesis of PU materials contain alcohols, which are known to have high reactivity towards isocyanates.[4,6] The proton donors such as alcohols, carbamates or allophanates, after deprotonation by Lewis bases, can also accelerate the cyclotrimerization of isocyanates.[44-47] The nucleophilic catalysts actively catalyze the reaction between alcohol and isocyanate, the formed carbamate not only reacts rapidly with isocyanate but it also deprotonates other protic groups such as urethane, allophanate, urea and biuret groups in the PU system, whose corresponding anions have been shown to be active PIR catalysts.[42,43] Therefore, a mixture of catalytically active species is expected to be present during cyclotrimerization. On the other hand, because tertiary amines are Brønsted bases that

are not nucleophilic enough to directly catalyze the cyclotrimerization of isocyanates, proton donors are required in the reaction. The role of tertiary amine is to deprotonate the proton donors to generate a more nucleophilic catalyst, which in turn catalyze the cyclotrimerization of isocyanates.

In addition to catalysts that operate *via* a Lewis base cyclotrimerization mechanism, many metal-containing catalysts have also been reported to catalyze cyclotrimerization of isocyanates. Most of them are coordination complexes, and others are heavy metal salts with an organic counterion. The cyclotrimerization mechanism of metal-containing catalysts varies. Some of the catalysts promote cyclotrimerization following an anionic catalytic pathway, while other catalysts operate *via* a Lewis acid pathway.[48-51] Some special metal-containing species catalyze cyclotrimerization of isocyanates *via* coordination-insertion mechanism, starting from repeated insertion of isocyanates in the metal coordination bond, followed by elimination of isocyanurate and regeneration of catalyst.[52-56]

As a general reminder, in the majority of the studies about cyclotrimerization catalysts and corresponding reaction mechanisms, model compounds such as phenyl isocyanate, tolyl isocyanate and hexyl isocyanate were used. As mentioned earlier, the presence of polyols and water, the bulk condition, the compatibility of catalysts, and the large-scale reaction can all influence the efficiency of the cyclotrimerization catalysts in real industrial PU systems and applications. Therefore, various factors should be considered when choosing the most suitable catalysts for these applications.

1.2.2 PIR-containing materials

Based on the isocyanate types, the isocyanurates can be divided into aliphatic and aromatic isocyanurates, which exhibit different chemical, physical and mechanical properties that suit various application demands. The literature has established that the isocyanurate exhibits higher thermal decomposition temperature compared to other isocyanate-derived structures such as urethane, urea and allophanate.[4,6,19,57-60] The decomposition temperature of aromatic PIR structures is higher than aliphatic PIR structures.[58] As a result, the introduction of aromatic PIR structures can greatly improve the thermal stability and flame retardancy of PU materials. The aromatic PIR network is typically applied in rigid foams, which are widely manufactured in industry and are used as housing insulation (**Figure 1-3**).[4,61-66] Elastomers with aromatic PIR structures also show good thermal stability as well as harder and stiffer mechanical properties.[60,67,68]

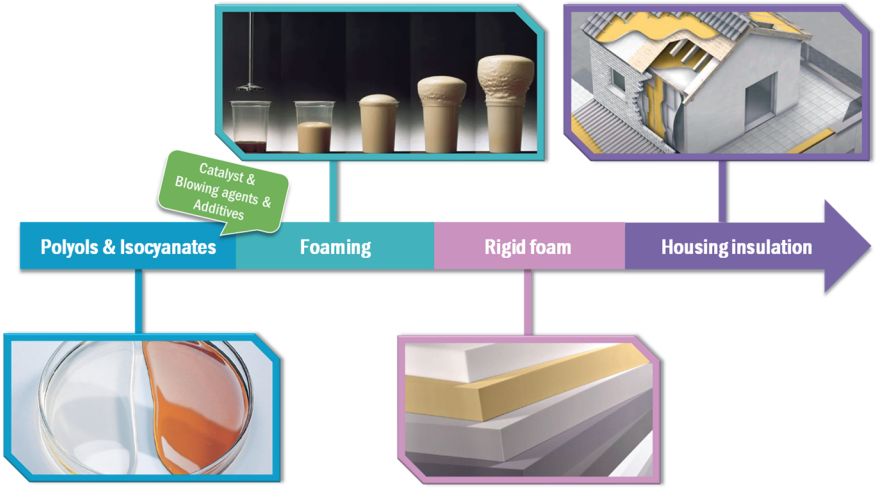

Figure 1-3. From the one-pot synthesis to construction applications of PIR-PU rigid foams. The isocyanates and polyols are reacted in molar ratio from 2:1 to 5:1 (index 200 to 500) with presence of trimerization catalysts, urethane catalysts, surfactants or other additives. After the foaming process, PIR rigid foams are obtained. These foams can be used in houses to provide good thermal insulation. Images obtained from BASF website.

Most of these PIR-containing PU materials are prepared *via* either one of two pathways: by one-pot synthesis with isocyanates, polyols and chain extender reacting simultaneously in the presence of trimerization catalyst, or by trimerization of isocyanate prepolymers obtained from the reaction between excess of isocyanate and long chain polyols.[22,68-72] However, the rigidity of the PIR network leads to fast increase of viscosity and poor catalyst diffusion during trimerization reactions in both cases, resulting in a relatively low PIR content in the PIR-containing PU materials. In order to increase the PIR content, cyclotrimerization of aromatic diisocyanates without alcohols has been studied.[73,74] Whereas the decomposition temperature of the PIR materials increased due to the absence of carbamate bonds, it is difficult to achieve full conversion during trimerization of diisocyanates. The materials obtained are glassy and brittle due to the stiffness of aromatic PIR structures.

To improve the processability and keep the high PIR content, co-trimerization of mono- and di-functional isocyanates has been reported in the literature as an alternative approach to generate a flexible PIR network. For instance, Moritsugu *et al*. co-trimerized 4,4'-methylene diphenyl diisocyanate (4,4'-MDI) with different mono-functional aliphatic or aromatic isocyanates, providing flexible PIR films with decomposition temperature of 5% weight loss higher than 400 ºC (**Figure 1-4**).[75,76] In their work, the utilization of mono-functional isocyanates with different feeding ratio allowed tuning of the flexibility while maintaining similar thermal stability of the PIR network.

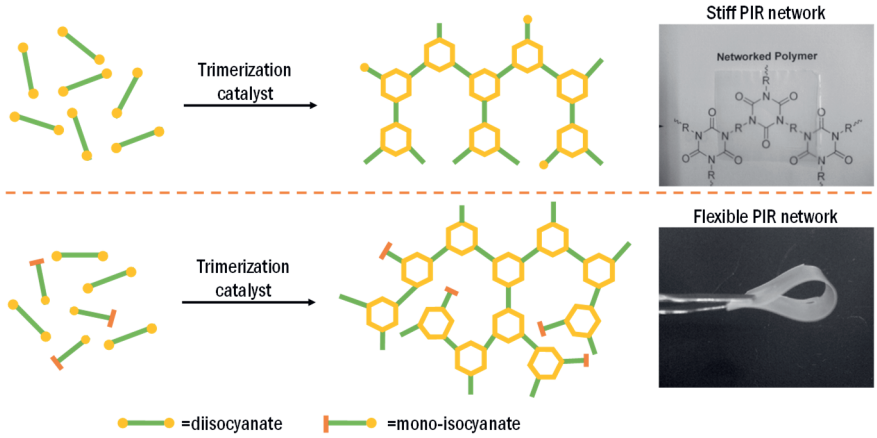

Figure 1-4. Illustration of different PIR networks. The trimerization of neat diisocyanates leads to stiff and highly crosslinked PIR networks as well as incomplete reaction. The co-trimerization of mono- and diisocyanates leads to lower crosslink density as well as flexible PIR networks. The materials shown in this figure was adapted from ref. 76 Copyright (2011), with permission from Wiley Periodicals, Inc.

In addition to aromatic isocyanurates, isocyanurates obtained from trimerization of aliphatic isocyanates have also been studied in great detail. They are typically used as crosslinkers for high-performance PU coatings with outstanding weatherability.[69,77-81] These aliphatic PIR networks are also made into hydrogels that show improved mechanical properties, good optical properties and biocompatibility, and low biofouling propensity.[71,72] PU aerogels that contain aliphatic isocyanurates exhibit shape memory and elastic properties.[82]

In addition, some commercially available isocyanurate moieties are not synthesized from cyclotrimerization of isocyanates (**Figure 1-5**).[83-85] These moieties can not only be introduced in PU materials, but can also be used to improve the thermal stability or mechanical properties of other polymers such as PP, PVC, polylactide (PLA), acrylates, PET and collagen.[86-95] However, these isocyanurate structures are outside of the scope of this thesis and will not be discussed in the later chapters.

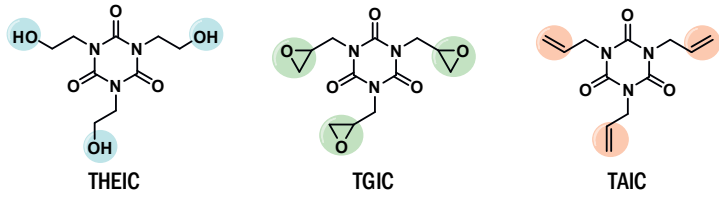

Figure 1-5. Structures of commercially available, well-defined isocyanurate monomers: 1,3,5-tris(2-hydroxyethyl)isocyanurate (THEIC), triallyl isocyanurate (TAIC) and triglycidyl isocyanurate (TGIC).

1.3 Aromatic imide/polyimide (PI) structures in PU

In addition to the wide use of PIR structures in PU, polyimide also has a great prospect of improving the thermal and mechanical properties of PU. A straightforward synthetic way to introduce imide motifs in PU is *via* reaction between anhydrides and isocyanates. Whereas the underlying mechanism of this reaction has not yet been fully understood, some imide containing PU materials have been reported in literature.

1.3.1 Synthesis of aromatic imides

Imides are monoacyl derivatives of amides or lactams that can be divided into aliphatic imides and aromatic imides, among which aromatic polyimides present a class of well-known high-performance polymers with outstanding thermal, mechanical, and electrical properties.[96–103] Due to the excellent combination of these properties, polyimides have been widely studied in both academic and industrial literatures.

There are mainly two ways to synthesize imides. One of the synthetic pathways is *via* the reaction between aromatic anhydride and aromatic amine, which is the mostly adopted way to produce PIs or PI-containing polymers. It is generally accepted that the amine-anhydride reaction follows a two-step mechanism (**Scheme 1-3**). First, the nucleophilic nitrogen atom of the amine attacks one of the carbonyl carbon atoms of the anhydride, followed by ring opening of anhydride and formation of an amic acid. Next, the imidization takes place, where the amic acid undergoes ring closure *via* the elimination of a water molecule, forming an imide structure. The imidization requires either high temperature, or acid anhydrides dehydrating agents (*e.g.*, acetic anhydride and benzoic anhydride). The use of dehydrating agents demands dipolar aprotic solvents or tertiary amine catalysts such as *N*-methylmorpholine and trialkylamines.[99–101,104,105]

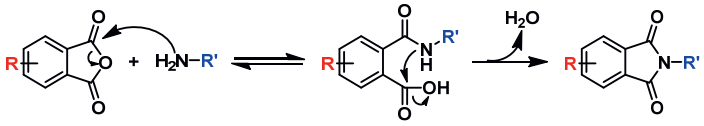

Scheme 1-3. Generally accepted imide formation from a two-step reaction between anhydride and amine.

Whereas the mechanism of anhydride-amine reaction is known, another pathway to obtain imides is *via* the reaction between anhydride and isocyanate, of which the much more complicated mechanism is still under debate (**Scheme 1-4**). Two distinct mechanisms have been proposed for the formation of imides from reaction of aromatic isocyanates with anhydrides. One point of view is that an isocyanate reacts with an anhydride forming a seven-membered-ring, followed by imidization with elimination of

a carbon dioxide molecule.[106–112] The other point of view is that the reaction requires catalyst such as water. The hydrolysis of two isocyanates leads to a urea molecule, which further reacts with anhydride, forming an imide.[113,114] So far, there are no reliable kinetic or mechanistic studies that prove either of the proposals. In addition, there is a common feature of all the studies that the isocyanate-anhydride reactions were carried out in highly polar solvents such as NMP, DMAc, DMF. These solvents may not only ensure the solubility for reactants and products, but also inevitably contain water, which catalyzes the reaction.

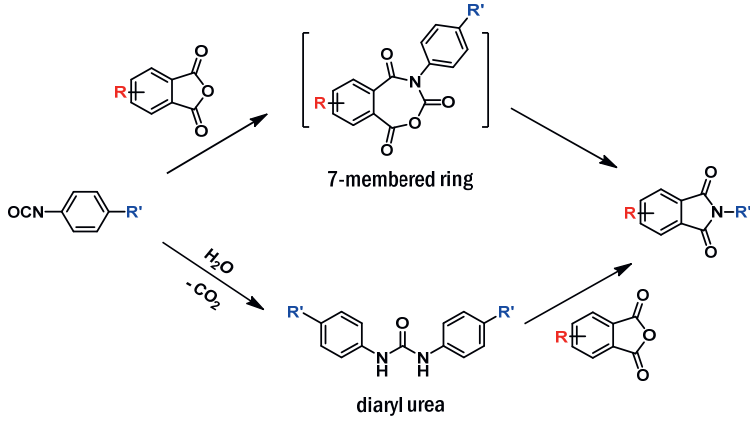

Scheme 1-4. Two proposed mechanisms of imide formation from reaction between anhydride and isocyanate.

To address these gaps in the knowledge of imide formation mechanisms behind the reaction of anhydride and isocyanate, state-of-art experimental and computational methods were used. We proposed that the catalytic cycle is driven by the urea obtained from the hydrolysis of isocyanates. We also showed that with a secondary amine as a pre-catalyst and tertiary amine as a co-catalyst, the reaction proceeds fast without a need for additional solvent. More details of these exclusive findings are described in **Chapter 5**.

1.3.2 Aromatic polyimide-containing materials

Aromatic polyimides (PI) are well-known as high performance polymers that exhibit high thermal stability, chemical resistance to many solvents, high mechanical strength, good electrical and optical properties.[97,99,101,102,115,116] The first commercially available aromatic PI (Kapton®) was manufactured by Dupont, which was obtained from the reaction of pyromellitic dianhydride (PMDA) and 4,4'-oxydianiline. The Kapton® exhibits a high glass transition temperature (T_g = 390 °C), outstanding thermal stability as well as mechanical properties.[117] After that, polyimides are widely used in various applications such as films, coatings, gas separation membranes, filtration membranes,

3D printing materials and energy storage materials.[101,102,104,118-120] However, due to the high rigidity and stability, PI has poor thermal and solvent processability, which leads to high production costs. In order to improve the solubility or thermoplasticity (melt processability) of PIs, a common way is to modify the amines with flexible spacers before imide reactions.[121-125]

Another way to improve the processibility of PI is *via* co-polymerization with other polymers. Most of these co-polymerizations are realized *via* reaction between amines and anhydrides containing other functional groups. Examples of such copolymers are poly(ether imide)s, poly(ester imide)s and poly(amide imide)s (**Figure 1-6a**, **6b** and **6c**).[100,119,126-131] The aromatic polyimides in turn help to enhance the thermal and mechanical properties of such copolymers. On the other hand, PI has also been introduced into moieties such as benzimidazole and benzoxazole to improve their processability, leading to various poly (benzimidazole imide) and poly(benzoxazole imide) copolymers (**Figure 1-6d** and **6e**).[132-135] These copolymers exhibit superior mechanical and thermal properties.

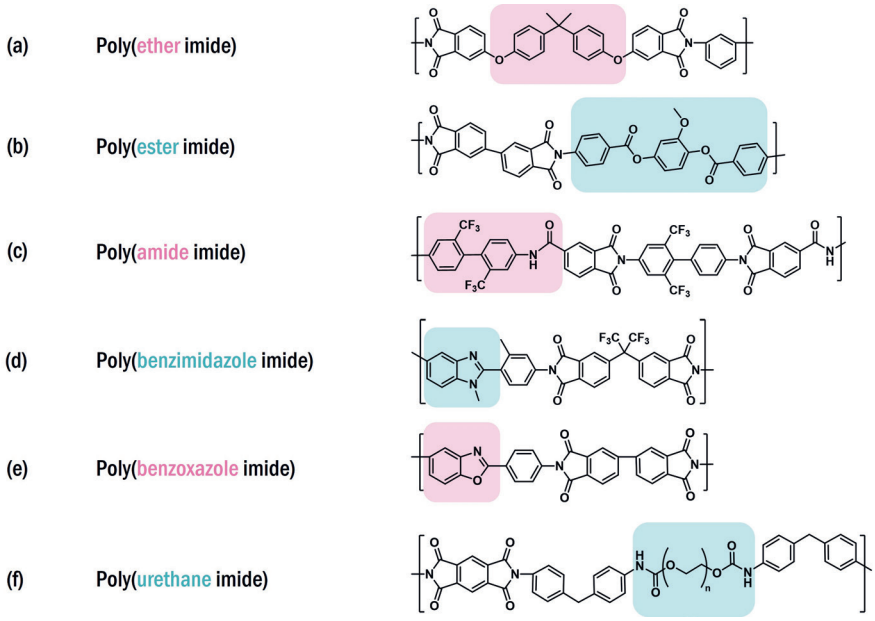

Figure 1-6. Examples of copolymer materials that contain (a) ether-*co*-imide; (b) ester-*co*-imide; (c) amide-*co*-imide; (d) benzimidazole-*co*-imide; (e) benzoxazole-*co*-imide; (f) urethane-*co*-imide repeating units.[127,129,131,133,134,136]

In addition, PIs are introduced in PUs as building blocks, leading to poly(urethane imide) (PUI) materials with improved thermal stability and flame retardancy (Figure 1-

6f). PUI containing thermoplastics,[25,137-143] rigid foams[24,113,144-147] and coatings [136,148-150] have been reported to exhibit better physical properties than conventional PU materials without imide structures. Unlike the other copolymers, the imide structures can be introduced in PUs *via* either reaction of isocyanates and anhydrides, and/or reaction of amines and anhydrides.

The most typical way to obtain PUI materials is *via* reaction of long-chain isocyanate terminated prepolymer with dianhydrides. For example, Meena *et al*. synthesized PUI films *via* two steps.[136] An isocyanate-terminated prepolymer was first prepared by reacting excess diisocyanates and polyethylene glycol in bulk. Then the prepolymer was reacted with equimolar of PMDA in DMF, leading to PUI films (**Figure 1-7**). These films exhibit higher decomposition temperatures (T_{max1} ≈ 420 °C), better flame retardancy, higher hydrophilicity and breathability compared to analogous PU, which can be potentially used as coating on a base fabric. In addition, it is also possible to first functionalize the isocyanate prepolymer before reacting with dianhydrides. Nair *et al*. synthesized PUI polymers by functionalizing the long-chain isocyanate prepolymer with diamines, followed by reacting the prepolymer with dianhydrides in DMAc.[139] Gnanarajan et al. obtained PUI polymers by blocking the long-chain isocyanate prepolymer with *N*-methylaniline before reacting the prepolymer with dianhydrides in DMPU.[141]

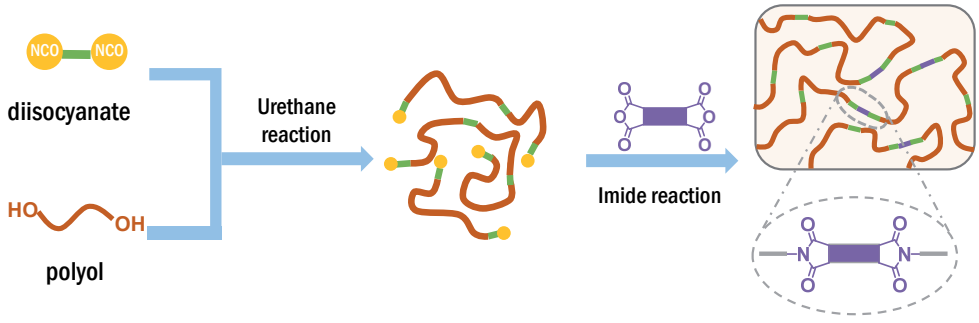

Figure 1-7. Illustration of preparation of PUI polymers by reacting long-chain isocyanate terminated prepolymer with dianhydrides. First the isocyanate prepolymer was synthesized *via* reaction of excess diisocyanates and polyol. Then the dianhydrides were reacted with prepolymer, forming PUI films.

However, the common feature of these preparations of PUI materials is the use of strong polar aprotic solvents such as DMF, DMAc and DMPU that are hazardous and difficult to be removed after synthesis, which is not applicable for industrial production.[151,152] Therefore, it is necessary to develop a new synthetic pathway to prepare PUI materials in solvent-free conditions.

1.4 Scope and outline of the thesis

The aim of this thesis is to investigate new synthetic pathways to incorporate aromatic isocyanurate or aromatic imide motifs in PU elastomers. We expect that the PU elastomers containing either of these chemical motifs intrinsically exhibit enhanced thermal stability, flame retardancy and mechanical property, which will meet the increasing need for high-performance PU materials. In addition, in order to pave a way from lab synthesis to industrial production, solvent-free synthetic pathway is required. To achieve these two targets, the mechanism behind the synthesis of isocyanurates and imides was first studied. Based on the mechanism studies, the isocyanurates or imides were introduced in PU elastomers and the chemical, thermal as well as mechanical properties of the materials were investigated.

This thesis can be divided into two parts based on two chemical motifs. The first part of the thesis focuses on using aromatic isocyanurate/PIR as a chemical motif in PU materials. In **Chapter 2**, we studied the formation of isocyanurate *via* cyclotrimerization of aromatic isocyanates using acetate as an anion. Based on computational and experimental studies, we demonstrated that the acetate anion is only a pre-catalyst in the reaction. The reaction of an acetate anion with an excess of aromatic isocyanates leads to an irreversible formation of a deprotonated amide species with elimination of a carbon dioxide molecule. The deprotonated amide species serves as a new active catalyst and catalyzes the cyclotrimerization of aromatic isocyanates following an anionic mechanism. Moreover, analogue amide species were also found in cyclotrimerizations using other carboxylate anions as catalysts, from which we propose that the cyclotrimerization mechanism discovered is generally adopted for carboxylate catalysts.

Furthermore, we developed PIR-containing PU elastomers in **Chapter 3** and **Chapter 4**. In order to reduce the brittleness of PIR network and increase the PIR content in the material, co-trimerization of mono- and di-functional isocyanate was used to generate a liquid PIR prepolymer containing a flexible PIR network. The mono-functional isocyanate was synthesized *via* reaction between 4,4'-methylene diphenyl diisocyanate (4,4'-MDI) and mono-functional alcohol, 2-ethyl-1-hexanol or diethyl(hydroxymethyl) phosphonate (DEHP). The liquid PIR prepolymer obtained was further used to prepare PIR elastomers in both solvent and solvent-free conditions. We found that the mechanical and thermal properties of the PIR elastomers varied with different mono-functional alcohols. When 2-ethyl-1-hexanol was used, the PIR elastomers exhibited outstanding mechanical properties. On the other hand, the phosphorus atoms from DEHP, together with PIR network, provided a combined flame retardant effect that greatly enhanced the thermal properties of the PU elastomers.

The second part of this thesis focuses on introducing aromatic imide/PI motif in PU materials. A straightforward synthetic pathway to prepare the PUI materials is *via* reaction between isocyanate and anhydride. Before material preparation, a better understanding of the underlying mechanism behind isocyanate-anhydride reaction is crucial. In **Chapter 5**, we investigated this reaction mechanism in the presence of catalytic amounts of water. Our experimental and computational studies demonstrated that the preferred reaction pathway involves formation of urea as a hydrolysis product. When anhydride reacts with excess isocyanates, urea instead of water is the actual catalyst that drives the catalytic cycle. We also found that secondary amines are better pre-catalysts than water and that addition of a nucleophilic co-catalyst considerably reduces the reaction time. With such pre-catalyst and co-catalyst present, the isocyanate-anhydride reaction proceeds fast without a need of solvent.

Using the knowledge from this mechanism study, we prepared imide-containing isocyanate-terminated prepolymers in **Chapter 6** by reacting pyromellitic dianhydride (PMDA) with excess aromatic or aliphatic isocyanates in completely solvent-free condition. The subsequent PUI elastomers prepared from these prepolymers in bulk exhibited enhanced thermal stability and stiffness. Moreover, the PUI elastomer prepared from aromatic isocyanates showed improved flame retardancy in comparison to the PU elastomers without imide structures.

This thesis reveals in depth the mechanisms behind cyclotrimerization of aromatic isocyanates and aromatic isocyanate-anhydride reaction. Our work also demonstrates that the introduction of aromatic isocyanurate or imide motifs improves the intrinsic thermal stability and flame retardancy of the PU elastomers, which could help to reduce the use of conventional flame retardant additives. Our contribution breaks the limitation of current synthesis routes, such as brittleness of the PIR network and the use of the solvents. Based on this modular research, we foresee the potential use of aromatic isocyanurate or imide motifs in real PU applications (*e.g.*, rigid foams, compact elastomers, thermosets and adhesives), where thermal stability, flame retardancy and solvent-free synthesis are required.

1.5 References

(1) Plastics Europe. *Plastics - the Facts 2021*; 2021.
(2) Plastics Europe. *Plastics - the Facts 2020*; 2020.
(3) Engels, H. W.; Pirkl, H. G.; Albers, R.; Albach, R. W.; Krause, J.; Hoffmann, A.; Casselmann, H.; Dormish, J. Polyurethanes: Versatile Materials and Sustainable Problem Solvers for Today's Challenges. *Angew. Chemie - Int. Ed.* **2013**, *52*, 9422–9441.
(4) Randall, D.; Lee, S. *The Polyurethanes Book*; Wiley, 2003.
(5) Eling, B.; Tomović, Ž.; Schädler, V. Current and Future Trends in Polyurethanes: An Industrial Perspective. *Macromol. Chem. Phys.* **2020**, *2000114*, 1–11.
(6) Delebecq, E.; Pascault, J. P.; Boutevin, B.; Ganachaud, F. On the Versatility of Urethane/Urea

Bonds: Reversibility, Blocked Isocyanate, and Non-Isocyanate Polyurethane. *Chem. Rev.* **2013**, *113*, 80–118.
(7) Bayer, O.; Rinke, H.; Siefken, W.; Orthner, L.; Schild, H. IG Farben. DRP 728981, 1937.
(8) Akindoyo, J. O.; Beg, M. D. H.; Ghazali, S.; Islam, M. R.; Jeyaratnam, N.; Yuvaraj, A. R. Polyurethane Types, Synthesis and Applications-a Review. *RSC Adv.* **2016**, *6*, 114453–114482.
(9) Chattopadhyay, D. K.; Raju, K. V. S. N. Structural Engineering of Polyurethane Coatings for High Performance Applications. *Prog. Polym. Sci.* **2007**, *32*, 352–418.
(10) Cherng, J. Y.; Hou, T. Y.; Shih, M. F.; Talsma, H.; Hennink, W. E. Polyurethane-Based Drug Delivery Systems. *Int. J. Pharm.* **2013**, *450*, 145–162.
(11) Gama, N. V.; Ferreira, A.; Barros-Timmons, A. Polyurethane Foams: Past, Present, and Future. *Materials (Basel).* **2018**, *11*, 1841.
(12) Sikdar, P.; Dip, T. M.; Dhar, A. K.; Bhattacharjee, M.; Hoque, M. S.; Ali, S. Bin. Polyurethane (PU) Based Multifunctional Materials: Emerging Paradigm for Functional Textiles, Smart, and Biomedical Applications. *J. Appl. Polym. Sci.* **2022**, *139*, e52832.
(13) Vahabi, H.; Rastin, H.; Movahedifar, E.; Antoun, K.; Brosse, N.; Saeb, M. R. Flame Retardancy of Bio-Based Polyurethanes: Opportunities and Challenges. *Polymers (Basel).* **2020**, *12*.
(14) Wilkie, C. A.; Morgan, A. B. *Fire Retardancy of Polymeric Materials, Second Edition*; CRC Press, 2009.
(15) Liu, B. W.; Zhao, H. B.; Wang, Y. Z. Advanced Flame-Retardant Methods for Polymeric Materials. *Adv. Mater.* **2022**, *2107905*, 1–36.
(16) Dasari, A.; Yu, Z. Z.; Cai, G. P.; Mai, Y. W. Recent Developments in the Fire Retardancy of Polymeric Materials. *Prog. Polym. Sci.* **2013**, *38*, 1357–1387.
(17) Yadav, A.; Souza, F. M. De; Dawsey, T.; Gupta, R. K. Recent Advancements in Flame-Retardant Polyurethane Foams : A Review. *Ind. Eng. Chem. Res.* **2022**.
(18) Toldy, A.; Harakály, G.; Szolnoki, B.; Zimonyi, E.; Marosi, G. Flame Retardancy of Thermoplastics Polyurethanes. *Polym. Degrad. Stab.* **2012**, *97*, 2524–2530.
(19) Chattopadhyay, D. K.; Webster, D. C. Thermal Stability and Flame Retardancy of Polyurethanes. *Prog. Polym. Sci.* **2009**, *34*, 1068–1133.
(20) Lu, S. Y.; Hamerton, I. Recent Developments in the Chemistry of Halogen-Free Flame Retardant Polymers. *Prog. Polym. Sci.* **2002**, *27*, 1661–1712.
(21) Sivriev, C.; Zabski, L. Flame Retarded Rigid Polyurethane Foams by Chemical Modification with Phosphorus- and Nitrogen-Containing Polyols. *Eur. Polym. J.* **1994**, *30*, 509–514.
(22) Reymore, H. E.; Lockwood, R. J.; Ulrich, H. Novel Isocyanurate Foams Containing No Flame Retardant Additives. *J. Cell. Plast.* **1978**, *14*, 332–340.
(23) Duan, L.; Yang, H.; Song, L.; Hou, Y.; Wang, W.; Gui, Z.; Hu, Y. Hyperbranched Phosphorus/Nitrogen-Containing Polymer in Combination with Ammonium Polyphosphate as a Novel Flame Retardant System for Polypropylene. *Polym. Degrad. Stab.* **2016**, *134*, 179–185.
(24) Tian, H.; Yao, Y.; Zhang, S.; Wang, Y.; Xiang, A. Enhanced Thermal Stability and Flame Resistance of Rigid Polyurethane-Imide Foams by Varying Copolymer Composition. *Polym. Test.* **2018**, *67*, 68–74.
(25) Tang, Q.; Song, Y.; He, J.; Yang, R. Synthesis and Characterization of Inherently Flame-Retardant and Anti-Dripping Thermoplastic Poly(Imides-Urethane)s. *J. Appl. Polym. Sci.* **2014**, *131*, 9524–9533.
(26) Sykam, K.; Meka, K. K. R.; Donempudi, S. Intumescent Phosphorus and Triazole-Based Flame-Retardant Polyurethane Foams from Castor Oil. *ACS Omega* **2019**, *4*, 1086–1094.
(27) Yuan, Y.; Yang, H.; Yu, B.; Shi, Y.; Wang, W.; Song, L.; Hu, Y.; Zhang, Y. Phosphorus and Nitrogen-Containing Polyols: Synergistic Effect on the Thermal Property and Flame Retardancy of Rigid Polyurethane Foam Composites. *Ind. Eng. Chem. Res.* **2016**, *55*, 10813–10822.
(28) Rao, W. H.; Xu, H. X.; Xu, Y. J.; Qi, M.; Liao, W.; Xu, S.; Wang, Y. Z. Persistently Flame-Retardant Flexible Polyurethane Foams by a Novel Phosphorus-Containing Polyol. *Chem. Eng. J.* **2018**, *343*, 198–206.
(29) Borreguero, A. M.; Velencoso, M. M.; Rodríguez, J. F.; Serrano, Á.; Carrero, M. J.; Ramos, M. J. Synthesis of Aminophosphonate Polyols and Polyurethane Foams with Improved Fire Retardant Properties. *J. Appl. Polym. Sci.* **2019**, *136*, 1–10.
(30) Zhu, H.; Xu, S. Preparation of Flame-Retardant Rigid Polyurethane Foams by Combining Modified Melamine-Formaldehyde Resin and Phosphorus Flame Retardants. *ACS Omega* **2020**, *5*, 9658–9667.

(31) Liu, Y.; He, J.; Yang, R. The Synthesis of Melamine-Based Polyether Polyol and Its Effects on the Flame Retardancy and Physical-Mechanical Property of Rigid Polyurethane Foam. *J. Mater. Sci.* **2017**, *52*, 4700–4712.

(32) Jia, D.; Yang, J.; He, J.; Li, X.; Yang, R. Melamine-Based Polyol Containing Phosphonate and Alkynyl Groups and Its Application in Rigid Polyurethane Foam. *J. Mater. Sci.* **2021**, *56*, 870–885.

(33) Gao, S.; Zhao, X.; Liu, G. Synthesis of Tris(2-Hydroxyethyl) Isocyanurate Homopolymer and Its Application in Intumescent Flame Retarded Polypropylene. *J. Appl. Polym. Sci.* **2017**, *134*, 1–10.

(34) Guo, Y.; Muuronen, M.; Lucas, F.; Sijbesma, R. P.; Tomović, Ž. Catalysts for Isocyanate Cyclotrimerization. *ChemCatChem* **2023**, e202201362.

(35) Moghaddam, F. M.; Dekamin, M. G.; Khajavi, M. S.; Jalili, S. Efficient and Selective Trimerization of Aryl and Alkyl Isocyanates Catalyzed by Sodium P-Toluenesulfinate in the Presence of TBAI in a Solvent-Free Condition. *Bull. Chem. Soc. Jpn.* **2002**, *75*, 851–852.

(36) Nambu, Y.; Endo, T. Synthesis of Novel Aromatic Isocyanurates by the Fluoride-Catalyzed Selective Trimerization of Isocyanates. *J. Org. Chem.* **1993**, *58*, 1932–1934.

(37) Li, C.; Zhao, W.; He, J.; Zhang, Y. Highly Efficient Cyclotrimerization of Isocyanates Using N-Heterocyclic Olefins under Bulk Conditions. *Chem. Commun.* **2019**, *55*, 12563–12566.

(38) Dekamin, M. G.; Mallakpour, S.; Ghassemi, M. Sulfate Catalysed Multicomponent Cyclisation Reaction of Aryl Isocyanates under Green Conditions. *J. Chem. Res.* **2005**, *3*, 177–179.

(39) Heift, D.; Benko, Z.; Grützmacher, H.; Jupp, A. R.; Goicoechea, J. M. Cyclo-Oligomerization of Isocyanates with $Na(PH_2)$ or Na(OCP) as "P^-" Anion Sources. *Chem. Sci.* **2015**, *6*, 4017–4024.

(40) Hoffman, D. K. Model System for a Urethane-Modified Isocyanurate Foam. *J. Cell. Plast.* **1984**, *20*, 129–137.

(41) Bechara, I. S.; Mascioli, R. L. The Mechanism of the Hydroxyalkyl Quaternary Ammonium Carboxylate Catalyzed Reactions of Phenyl Isocyanate. *J. Cell. Plast.* **1979**, *15*, 321–332.

(42) Guo, Y.; Muuronen, M.; Deglmann, P.; Lucas, F.; Sijbesma, R. P.; Tomović, Ž. Role of Acetate Anions in the Catalytic Formation of Isocyanurates from Aromatic Isocyanates. *J. Org. Chem.* **2021**, *86*, 5651–5659.

(43) Siebert, M.; Sure, R.; Deglmann, P.; Closs, A. C.; Lucas, F.; Trapp, O. Mechanistic Investigation into the Acetate-Initiated Catalytic Trimerization of Aliphatic Isocyanates: A Bicyclic Ride. *J. Org. Chem.* **2020**, *85*, 8553–8562.

(44) Schwetlickt, K.; Noack, R. Kinetics and Catalysis of Consecutive Isocyanate Reactions. Formation of Carbamates, Allophanates and Isocyanurates. *J. Chem. Soc., Perkin Trans. 2* **1995**, 395–402.

(45) Špírková, M.; Kubín, M.; Špaček, P.; Krakovský, I.; Dušek, K. Cyclotrimerization of Isocyanate Groups. II. Catalyzed Reactions of Phenyl Isocyanate in the Presence of 1-Butanol or Butyl-*N*-Phenylurethane. *J. Appl. Polym. Sci.* **1994**, *53*, 1435–1446.

(46) Al Nabulsi, A.; Cozzula, D.; Hagen, T.; Leitner, W.; Müller, T. E. Isocyanurate Formation during Rigid Polyurethane Foam Assembly: A Mechanistic Study Based on: In Situ IR and NMR Spectroscopy. *Polym. Chem.* **2018**, *9*, 4891–4899.

(47) Kogon, I. C. New Reactions of Phenyl Isocyanate and Ethyl Alcohol. *J. Am. Chem. Soc.* **1956**, *78*, 4911–4914.

(48) Foley, S. R.; Zhou, Y.; Yap, G. P. A.; Richeson, D. S. Synthesis of $M(II)[N(SiMe_3)_2][Me_3SiNC(^tBu)NSiMe_3]$ (M = Sn, Ge) from Amidinate Precursors: Active Catalysts for Phenyl Isocyanate Cyclization. *Inorg. Chem.* **2000**, *39*, 924–929.

(49) Sharpe, H. R.; Geer, A. M.; Williams, H. E. L.; Blundell, T. J.; Lewis, W.; Blake, A. J.; Kays, D. L. Cyclotrimerisation of Isocyanates Catalysed by Low-Coordinate Mn(II) and Fe(II) *m*-Terphenyl Complexes. *Chem. Commun.* **2017**, *53*, 937–940.

(50) Wu, X.; Mason, J.; North, M. Isocyanurate Formation During Oxazolidinone Synthesis from Epoxides and Isocyanates Catalysed by a Chromium(Salphen) Complex. *Chem. Eur. J.* **2017**, *23*, 12937–12943.

(51) Villa, J. F.; Powell, H. B. The Reaction of Some Inorganic Lewis Bases and Acids with Organic Isocyanates. *Synth. React. Inorg. Met. Chem.* **1976**, *6*, 59–63.

(52) Srinivas, B.; Chang, C.; Chen, C.; Chiang, M. Y.; Chen, I.; Wang, Y.; Lee, G. Synthesis, Characterization and Crystal Structures of Isothiocyanate and Carbodiimide Complexes Derived from Organomagnesium Reagents: Insertion into Mg-X (X = C or N) Bonds. *J. Chem. Soc., Dalt. Trans.* **1997**, 957–963.

(53) Bahili, M. A.; Stokes, E. C.; Amesbury, R. C.; Ould, D. M. C.; Christo, B.; Horne, R. J.; Kariuki, B. M.; Stewart, J. A.; Taylor, R. L.; Williams, P. A.; Jones, M. D.; Harris, K. D. M.; Ward, B. D. Aluminium-Catalysed Isocyanate Trimerization, Enhanced by Exploiting a Dynamic Coordination Sphere. *Chem. Commun.* **2019**, *55*, 7679–7682.

(54) Zhu, X.; Fan, J.; Wu, Y.; Wang, S.; Zhang, L.; Yang, G.; Wei, Y.; Yin, C.; Zhu, H.; Wu, S.; Zhang, H. Synthesis, Characterization, Selective Catalytic Activity, and Reactivity of Rare Earth Metal Amides with Different Metal-Nitrogen Bonds. *Organometallics* **2009**, *28*, 3882–3888.

(55) Wang, H. M.; Li, H. X.; Yu, X. Y.; Ren, Z. G.; Lang, J. P. Cyclodimerization and Cyclotrimerization of Isocyanates Promoted by One Praseodymium Benzenethiolate Complex $[Pr(SPh)_3(THF)_3]$. *Tetrahedron* **2011**, *67*, 1530–1535.

(56) Yi, W.; Zhang, J.; Hong, L.; Chen, Z.; Zhou, X. Insertion of Isocyanate and Isothiocyanate into the Ln-P σ-Bond of Organolanthanide Phosphides. *Organometallics* **2011**, *30*, 5809–5814.

(57) Kordomenos, P. I.; Kresta, J. E. Thermal Stability of Isocyanate-Based Polymers. 1. Kinetics of the Thermal Dissociation of Urethane, Oxazolidone, and Isocyanurate Groups. *Macromolecules* **1981**, *14*, 1434–1437.

(58) Kordomenos, P. I.; Kresta, J. E.; Frisch, K. C. Thermal Stability of Isocyanate-Based Polymers. 2. Kinetics of the Thermal Dissociation of Model Urethane, Oxazolidone, and Isocyanurate Block Copolymers. *Macromolecules* **1987**, *20*, 2077–2083.

(59) Duff, D. W.; Maciel, G. E. Monitoring the Thermal Degradation of an Isocyanurate-Rich MDI-Based Resin by ^{15}N and ^{13}C CP/MAS NMR. *Macromolecules* **1991**, *24*, 651–658.

(60) Wang, C. L.; Klempner, D.; Frisch, K. C. Morphology of Polyurethane- Isocyanurate Elastomers. *J. Appl. Polym. Sci.* **1985**, *30*, 4337–4344.

(61) Reymore, H. E.; Carleton, P. S.; Kolakowski, R. A.; Sayigh, A. A. R. Isocyanurate Foams: Chemistry, Properties and Processing. *J. Cell. Plast.* **1975**, *11*, 328–344.

(62) Dick, C.; Dominguez-Rosado, E.; Eling, B.; Liggat, J. J.; Lindsay, C. I.; Martin, S. C.; Mohammed, M. H.; Seeley, G.; Snape, C. E. The Flammability of Urethane-Modified Polyisocyanurates and Its Relationship to Thermal Degradation Chemistry. *Polymer (Guildf).* **2001**, *42*, 913–923.

(63) Nicholas, L.; Gmitter, G. T. Heat Resistant Rigid Foams by Trimerization of Isocyanate Terminated Prepolymers. *J. Cell. Plast.* **1965**, *1*, 85–90.

(64) Nawata, T.; Kresta, J. E.; Frisch, K. C. Comparative Studies of Isocyanurate and Isocyanurate-Urethane Foams. *J. Cell. Plast.* **1975**, *11*, 267–278.

(65) Reignier, J.; Méchin, F.; Sarbu, A. Chemical Gradients in PIR Foams as Probed by ATR-FTIR Analysis and Consequences on Fire Resistance. *Polym. Test.* **2021**, *93*, 106972.

(66) Lehmann, P.; Malotki, P. von; Tomasi, G.; Peden, G.; Hensiek, R. Polyisocyanurate Rigid Foam and Method for the Production Thereof. US 20080234402 A1, 2008.

(67) Li, J.; Jiang, S.; Ding, L.; Wang, L. Reaction Kinetics and Properties of MDI Base Poly (Urethane-Isocyanurate) Network Polymers. *Des. Monomers Polym.* **2021**, *24*, 265–273.

(68) Samborska-Skowron, R.; Balas, A. An Overview of Developments in Poly(Urethane-Isocyanurates) Elastomers. *Polym. Adv. Technol.* **2002**, *13*, 653–662.

(69) Driest, P. J.; Dijkstra, D. J.; Stamatialis, D.; Grijpma, D. W. The Trimerization of Isocyanate-Functionalized Prepolymers: An Effective Method for Synthesizing Well-Defined Polymer Networks. *Macromol. Rapid Commun.* **2019**, *40*, 1–6.

(70) Sasaki, N.; Yokoyama, T.; Tanaka, T. Properties of Isocyanurate-Type Crosslinked Polyurethanes. *J. Polym. Sci. Polym. Chem. Ed.* **1973**, *11*, 1765–1779.

(71) Driest, P. J.; Dijkstra, D. J.; Stamatialis, D.; Grijpma, D. W. Tough Combinatorial Poly(Urethane-Isocyanurate) Polymer Networks and Hydrogels Synthesized by the Trimerization of Mixtures of NCO-Prepolymers. *Acta Biomater.* **2020**, *105*, 87–96.

(72) Driest, P. J.; Allijn, I. E.; Dijkstra, D. J.; Stamatialis, D.; Grijpma, D. W. Poly(Ethylene Glycol)-Based Poly(Urethane Isocyanurate) Hydrogels for Contact Lens Applications. *Polym. Int.* **2020**, *69*, 131–139.

(73) Kresta, J. E.; Shen, C. S. Oligomerization of Isocyanates by Cyclic Sulfonium Zwitterions. *Polym. Bull.* **1979**, *1*, 325–328.

(74) Duff, D. W.; Maciel, G. E. ^{13}C and ^{15}N CP/MAS NMR Characterization of MDI-Polyisocyanurate Resin Systems. *Macromolecules* **1990**, *23*, 3069–3079.

(75) Moritsugu, M.; Sudo, A.; Endo, T. Development of High-Performance Networked Polymers Based on Cyclotrimerization of Isocyanates: Control of Properties by Addition of

Monoisocyanates. *J. Polym. Sci. Part A Polym. Chem.* **2012**, *50*, 4365–4367.

(76) Moritsugu, M.; Sudo, A.; Endo, T. Development of High-Performance Networked Polymers Consisting of Isocyanurate Structures Based on Selective Cyclotrimerization of Isocyanates. *J. Polym. Sci. Part A Polym. Chem.* **2011**, *49*, 5186–5191.

(77) Wang, G.; Li, K.; Zou, W.; Hu, A.; Hu, C.; Zhu, Y.; Chen, C.; Guo, G.; Yang, A.; Drumright, R.; Argyropoulos, J. Synthesis of HDI/IPDI Hybrid Isocyanurate and Its Application in Polyurethane Coating. *Progess Org. Coatings* **2015**, *78*, 225–233.

(78) Driest, P. J.; Lenzi, V.; Marques, L. S. A.; Ramos, M. M. D.; Dijkstra, D. J.; Richter, F. U.; Stamatialis, D.; Grijpma, D. W. Aliphatic Isocyanurates and Polyisocyanurate Networks. *Polym. Adv. Technol.* **2017**, *28*, 1299–1304.

(79) Wang, G.; Li, K.; Zou, W.; Hu, A.; Hu, C.; Zhu, Y.; Chen, C.; Guo, G.; Yang, A.; Drumright, R.; Argyropoulos, J. Synthesis of ADI/HDI Hybrid Isocyanurate and Its Application in Polyurethane Coating. *J. Coatings Technol. Res.* **2015**, *12*, 543–553.

(80) Zeng, J.; Yang, Y.; Tang, Y.; Xu, X.; Chen, X.; Li, G.; Chen, K.; Li, H.; Ouyang, P.; Tan, W.; Ma, J.; Liu, Y.; Liang, R. Synthesis, Monomer Removal, Modification, and Coating Performances of Biobased Pentamethylene Diisocyanate Isocyanurate Trimers. *Ind. Eng. Chem. Res.* **2022**, *61*, 2403–2416.

(81) Chattopadhyay, D. K.; Raju, K. V. S. N. Structural Engineering of Polyurethane Coatings for High Performance Applications. *Prog. Polym. Sci.* **2007**, *32*, 352–418.

(82) Donthula, S.; Mandal, C.; Leventis, T.; Schisler, J.; Saeed, A. M.; Sotiriou-Leventis, C.; Leventis, N. Shape Memory Superelastic Poly(Isocyanurate-Urethane) Aerogels (PIR-PUR) for Deployable Panels and Biomimetic Applications. *Chem. Mater.* **2017**, *29*, 4461–4477.

(83) Lavallée, F. A. Preparation of This(2-Hydroxylethyl)Isocyanruate (THEIC). US 6046326 A, 2000.

(84) Werle, P.; Krimmer, H.-P.; Schmidt, M.; Stadtmüller, K.; Trageser, M. Process for Preparing Triallyl Isocyanurate (TAIC). WO 2008006661 A2, 2008.

(85) Patil, P.; Bendre, S.; Jagtap, A.; Roy, M. Process for Preparation of Triglycidyl Isocyanurate (TGIC). US 20150232458 A1, 2015.

(86) Zhang, H.; Zhou, C.; Peng, J.; Chen, B.; Pan, X.; Xiong, W.; Zhang, X.; Xu, Z.; Luo, X.; Liu, Y. A Substrate-Independent Transparent UV-Curable Coating with Excellent Anti-Smudge Performance. *Prog. Org. Coatings* **2022**, *173*, 107185.

(87) Shen, M. Y.; Kuan, C. F.; Kuan, H. C.; Ke, C. Y.; Chiang, C. L. Flame Retardance and Char Analysis of an Eco-Friendly Polyurethane Hyperbranched Hybrid Using the Sol–Gel Method. *Sustain.* **2021**, *13*, 1–14.

(88) Chen, W.; Yuan, S.; Sheng, Y.; Liu, G. Effect of Charring Agent THEIC on Flame Retardant Properties of Polypropylene. *J. Appl. Polym. Sci.* **2015**, *132*.

(89) Jia, P.; Hu, L.; Feng, G.; Bo, C.; Zhou, J.; Zhang, M.; Zhou, Y. Design and Synthesis of a Castor Oil Based Plasticizer Containing THEIC and Diethyl Phosphate Groups for the Preparation of Flame-Retardant PVC Materials. *RSC Adv.* **2017**, *7*, 897–903.

(90) Yuan, S.; Chen, W.; Liu, G. Synergistic Effect of THEIC-Based Charring Agent on Flame Retardant Properties of Polylactide. *J. Appl. Polym. Sci.* **2015**, *132*.

(91) White, T. J.; Natarajan, L. V.; Tondiglia, V. P.; Lloyd, P. F.; Bunning, T. J.; Guymon, C. A. Holographic Polymer Dispersed Liquid Crystals (HPDLCs) Containing Triallyl Isocyanurate Monomer. *Polymer (Guildf).* **2007**, *48*, 5979–5987.

(92) Thite, A. G.; Krishnanand, K.; Panda, P. K. Electron Beam-Induced Crosslinking of Silk Fibers Using Triallyl Isocyanurate for Enhanced Properties. *J. Appl. Polym. Sci.* **2019**, *136*.

(93) Zhong, J.; Hao, M.; Li, R.; Bai, L.; Yang, G. Preparation and Characterization of Poly(Triallyl Isocyanurate *-co-*Trimethylolpropane Triacrylate) Monolith and Its Applications in the Separation of Small Molecules by Liquid Chromatography. *J. Chromatogr. A* **2014**, *1333*, 79–86.

(94) Di, Y.; Heath, R. J. Collagen Stabilization and Modification Using a Polyepoxide, Triglycidyl Isocyanurate. *Polym. Degrad. Stab.* **2009**, *94*, 1684–1692.

(95) Ge, Y.; Yao, S.; Xu, M.; Gao, L.; Fang, Z.; Zhao, L.; Liu, T. Improvement of Poly(Ethylene Terephthalate) Melt-Foamability by Long-Chain Branching with the Combination of Pyromellitic Dianhydride and Triglycidyl Isocyanurate. *Ind. Eng. Chem. Res.* **2019**, *58*, 3666–3678.

(96) Hergenrother, P. M. The Use, Design, Synthesis and Properties of High Performance/High Temperature Polymer: An Overview. *High Perform. Polym.* **2003**, *15*, 3–45.

(97) David, C. Chapter 1 Thermal Degradation of Polymers. In *Degradation of Polymers*; Bamford,

C. H., Tipper, C. F. H., Eds.; Comprehensive Chemical Kinetics; Elsevier, 1975; Vol. 14, pp 1–173.
(98) Dodda, J. M.; Bělský, P. Progress in Designing Poly(Amide Imide)s (PAI) in Terms of Chemical Structure, Preparation Methods and Processability. *Eur. Polym. J.* **2016**, *84*, 514–537.
(99) Sroog, C. E. Polyimides. *J. Polym. sci., Macromol. Rev.* **1976**, *11*, 161–208.
(100) Liou, G. S.; Yen, H. J. *Polyimides*; 2012; Vol. 5.
(101) Ghosh, M. *Polyimides: Fundamentals and Applications*; Plastics Engineering; CRC Press, 2018.
(102) Sezer Hicyilmaz, A.; Celik Bedeloglu, A. Applications of Polyimide Coatings: A Review. *SN Appl. Sci.* **2021**, *3*, 1–22.
(103) Liu, X. J.; Zheng, M. S.; Chen, G.; Dang, Z. M.; Zha, J. W. High-Temperature Polyimide Dielectric Materials for Energy Storage: Theory, Design, Preparation and Properties. *Energy Environ. Sci.* **2022**, *15*, 56–81.
(104) Xu, Z.; Croft, Z. L.; Guo, D.; Cao, K.; Liu, G. Recent Development of Polyimides: Synthesis, Processing, and Application in Gas Separation. *J. Polym. Sci.* **2021**, *59*, 943–962.
(105) Bryant, R. G. Polyimide. In *Encyclopedia of Polymer Science and Technology*; 2002; Vol. 7, pp 529–555.
(106) Meyers, R. A. The Polymerization of Pyromellitic Dianhydride with Diphenylmethane Diisocyanate. *J. Polym. Sci. Part A Polym. Chem.* **1969**, *7*, 2757–2762.
(107) Barikani, M.; Yeganeh, H.; Ataei, S. M. Synthesis and Characterization of New Soluble and Thermostable Polyimides *via* Novel Diisocyanates. *Polym. Int.* **1999**, *48*, 1264–1268.
(108) Barikani, M.; Ataei, S. M. Preparation and Properties of Polyimides and Polyamideimides from Diisocyanates. *J. Polym. Sci. Part A Polym. Chem.* **1999**, *37*, 2245–2250.
(109) Barikani, M.; Mehdipour-ataei, S. Aromatic/Cycloaliphatic Polyimides and Polyamide-Imide from Trans-1 ,4-Cyclohexane Diisocyanate: Synthesis and Properties. *J. Appl. Polym. Sci.* **2000**, *77*, 1102–1107.
(110) Jeon, J. Y.; Tak, T. M. Synthesis and Characterization of Block Copoly(Urethane-Imide). *J. Appl. Polym. Sci.* **1996**, *62*, 763–769.
(111) Chidambareswarapattar, C.; Larimore, Z.; Sotiriou-Leventis, C.; Mang, J. T.; Leventis, N. One-Step Room-Temperature Synthesis of Fibrous Polyimide Aerogels from Anhydrides and Isocyanates and Conversion to Isomorphic Carbons. *J. Mater. Chem.* **2010**, *20*, 9666–9678.
(112) Sun, G.; Zhang, S.; Yang, Z.; Wang, J.; Chen, R.; Sun, L.; Yang, Z.; Han, S. Fabrication and Mechanical, Electrical Properties Study of Isocyanate-Based Polyimide Films Modified by Reduced Graphene Oxide. *Prog. Org. Coatings* **2020**, *143*, 105611.
(113) Farrissey, W. J.; Rose, J. S.; Carleton, P. S. Preparation of a Polyimide Foam. *J. Appl. Polym. Sci.* **1970**, *14*, 1093–1101.
(114) Carleton, P. S.; Farrissey, W. J.; Rose, J. S. The Formation of Polyimides from Anhydrides and Isocyanates. *J. Appl. Polym. Sci.* **1972**, *16*, 2983–2989.
(115) Ding, M. Isomeric Polyimides. *Prog. Polym. Sci.* **2007**, *32*, 623–668.
(116) Hasegawa, M.; Horie, K. Photophysics, Photochemistry, and Optical Properties of Polyimides. *Prog. Polym. Sci.* **2001**, *26*, 259–335.
(117) Edwards, W. M. Aromatic Polyimides and the Process for Preparing Them. US 3179634 A, 1965.
(118) Weyhrich, C. W.; Long, T. E. Additive Manufacturing of High-Performance Engineering Polymers: Present and Future. *Polym. Int.* **2022**, *71*, 532–536.
(119) Vanherck, K.; Koeckelberghs, G.; Vankelecom, I. F. J. Crosslinking Polyimides for Membrane Applications: A Review. *Prog. Polym. Sci.* **2013**, *38*, 874–896.
(120) Song, Z.; Zhan, H.; Zhou, Y. Polyimides: Promising Energy-Storage Materials. *Angew. Chemie - Int. Ed.* **2010**, *49*, 8444–8448.
(121) Kumar, D. New Polypyromellitimide Films Based on Cyclotriphosphazene and Bisaspartimide Derived Diamines. *J. Polym. Sci. A1.* **1984**, *22*, 3439–3446.
(122) Kumar, D.; Gupta, A. D. Novel Processable Aromatic Thermoplastic Polyimides: Films, Adhesives, Moldings, and Graphite Composites. *Polym. Adv. Technol.* **1992**, *3*, 1–7.
(123) Tamai, S.; Yamaguchi, A.; Ohta, M. Melt Processible Polyimides and Their Chemical Structures. *Polymer (Guildf).* **1996**, *37*, 3683–3692.
(124) Bower, G. M.; Frost, L. W. Aromatic Polyimides. *J. Polym. Sci. Part A Polym. Chem.* **1963**, *1*, 3135–3150.
(125) Luo, Y.; Sun, J.; Wang, J.; Jin, K.; He, F.; Fang, Q. A Novel Thermo-Polymerizable Aromatic Diamine: Synthesis and Application in Enhancement of the Properties of Conventional

Polyimides. *Macromol. Chem. Phys.* **2016**, *217*, 856–862.

(126) Cao, K.; Guo, Y.; Zhang, M.; Arrington, C. B.; Long, T. E.; Odle, R. R.; Liu, G. Mechanically Strong, Thermally Stable, and Flame Retardant Poly(Ether Imide) Terminated with Phosphonium Bromide. *Macromolecules* **2019**, *52*, 7361–7368.

(127) Xu, Z.; Gehui, L.; Cao, K.; Guo, D.; Serrano, J.; Esker, A.; Liu, G. Solvent-Resistant Self-Crosslinked Poly(Ether Imide). *Macromolecules* **2021**, *54*, 3405–3412.

(128) Zhou, J.; Li, M.; Wu, J.; Zhang, C.; He, Z.; Xiao, Y.; Tong, G.; Zhu, X. One-Pot Synthesis of Hydroxyl Terminated Hyperbranched Semi-Aromatic Poly(Ester-Imide)s. *Polymer (Guildf).* **2022**, *253*, 124970.

(129) Kim, S. D.; Lee, B.; Byun, T.; Chung, I. S.; Park, J.; Shin, I.; Ahn, N. Y.; Seo, M.; Lee, Y.; Kim, Y.; Kim, W. Y.; Kwon, H.; Moon, H.; Yoo, S.; Kim, S. Y. Poly(Amide-Imide) Materials for Transparent and Flexible Displays. *Sci. Adv.* **2018**, *4*, eaau1956.

(130) Canto-Acosta, R. J.; Loría-Bastarrachea, M. I.; Carrillo-Escalante, H. J.; Hernández-Núñez, E.; Aguilar-Vega, M.; Santiago-García, J. L. Synthesis and Characterization of Poly(Amide-Imide)s Derived from a New: Ortho -Functional Unsymmetrical Dicarboxylic Acid. *RSC Adv.* **2018**, *8*, 284–290.

(131) Hasegawa, M.; Hishiki, T. Poly (Ester Imide)s Possessing Low Coefficients of Themal Expansion and Low Water Absorption (V). Effects of Ester-Linked Diamines with Different Lengths and Sustituents. *Polymers (Basel).* **2020**, *12*, 859.

(132) Lian, M.; Zheng, F.; Lu, X.; Lu, Q. Tuning the Heat Resistance Properties of Polyimides by Intermolecular Interaction Strengthening for Flexible Substrate Application. *Polymer (Guildf).* **2019**, *173*, 205–214.

(133) Yan, X.; Dai, F.; Ke, Z.; Yan, K.; Chen, C.; Qian, G.; Li, H. Synthesis of Colorless Polyimides with High *T*g from Asymmetric Twisted Benzimidazole Diamines. *Eur. Polym. J.* **2022**, *164*, 110975.

(134) Yang, Z.; Chen, Y.; Wang, Q.; Wang, T. High Performance Multiple-Shape Memory Behaviors of Poly(Benzoxazole-Co-Imide)s. *Polymer (Guildf).* **2016**, *88*, 19–28.

(135) Jiao, Y.; Chen, G.; Mushtaq, N.; Zhou, H.; Chen, X.; Li, Y.; Fang, X. Synthesis and Properties of Poly(Benzoxazole Imide)s Derived from Two Isomeric Diamines Containing a Benzoxazole Moiety. *Polym. Chem.* **2020**, *11*, 1937–1946.

(136) Meena, M.; Kerketta, A.; Tripathi, M.; Roy, P.; Jacob, J. Thermally Stable Poly(Urethane-Imide)s with Enhanced Hydrophilicity for Waterproof-Breathable Textile Coatings. *J. Appl. Polym. Sci.* **2022**, *139*, e52508.

(137) Lin, M. F.; Shu, Y. C.; Tsen, W. C.; Chuang, F. S. Synthesis of Polyurethane-Imide (PU-Imide) Copolymers with Different Dianhydrides and Their Properties. *Polym. Int.* **1999**, *48*, 433–445.

(138) Sokolova, M. P.; Bugrov, A. N.; Smirnov, M. A.; Smirnov, A. V.; Lahderanta, E.; Svetlichnyi, V. M.; Toikka, A. M. Effect of Domain Structure of Segmented Poly(Urethane-Imide) Membranes with Polycaprolactone Soft Blocks on Dehydration of *n*-Propanol *via* Pervaporation. *Polymers (Basel).* **2018**, *10*, 1222.

(139) Nair, P. R.; Nair, C. P. R.; Francis, D. J. Imide-Modified Polyurethanes, Syntheses, Thermal, and Mechanical Characteristics. *J. Appl. Polym. Sci.* **1998**, *70*, 1483–1491.

(140) Asai, K.; Inoue, S. I.; Okamoto, H. Preparation and Properties of Imide-Containing Elastic Polymers from Elastic Polyureas and Pyromellitic Dianhydride. *J. Polym. Sci. Part A Polym. Chem.* **2000**, *38*, 715–723.

(141) Philip Gnanarajan, T.; Padmanabha Iyer, N.; Sultan Nasar, A.; Radhakrishnan, G. Preparation and Properties of Poly(Urethane-Imide)s Derived from Amine-Blocked-Polyurethane Prepolymer and Pyromellitic Dianhydride. *Eur. Polym. J.* **2002**, *38*, 487–495.

(142) Liu, J.; Dezhu, M. Study on Synthesis and Thermal Properties of Polyurethane-Imide Copolymers with Multiple Hard Segments. *J. Appl. Polym. Sci.* **2002**, *84*, 2206–2215.

(143) Takeichi, T.; Ujiie, K.; Inoue, K. High Performance Poly(Urethane-Imide) Prepared by Introducing Imide Blocks into the Polyurethane Backbone. *Polymer (Guildf).* **2005**, *46*, 11225–11231.

(144) Müeller-Cristadoro, A.; Prissok, F. Producing Polymer Foams Comprising Imide Groups. WO 2014023796 A1, 2014.

(145) Kashiwame, J.; Ashida, K. Preparation and Properties of Polyimide Foams. *J. Appl. Polym. Sci.* **1994**, *54*, 477–486.

(146) Xi, K.; Shieh, D. J.; Wu, L.; Singh, S. Polyurethane Foam Composition Comprising an Aromatic Polyester Polyol Compound and Products Made Thereform. WO 2021030115 A1, 2021.

(147) Li, C.; Hui, B.; Ye, L. Highly Reinforcing and Thermal Stabilizing Effect of Imide Structure on Polyurethane Foam. *Polym. Int.* **2019**, *68*, 464–472.
(148) Mishra, A. K.; Chattopadhyay, D. K.; Sreedhar, B.; Raju, K. V. S. N. FT-IR and XPS Studies of Polyurethane-Urea-Imide Coatings. *Prog. Org. Coatings* **2006**, *55*, 231–243.
(149) Mishra, A. K.; Chattopadhyay, D. K.; Sreedhar, B.; Raju, K. V. S. N. Thermal and Dynamic Mechanical Characterization of Polyurethane-Urea-Imide Coatings. *J. Appl. Polym. Sci.* **2006**, *102*, 3158–3167.
(150) Chattopadhyay, D. K.; Mishra, A. K.; Sreedhar, B.; Raju, K. V. S. N. Thermal and Viscoelastic Properties of Polyurethane-Imide/Clay Hybrid Coatings. *Polym. Degrad. Stab.* **2006**, *91*, 1837–1849.
(151) Reichardt, C.; Welton, T. *Solvents and Solvent Effects in Organic Chemistry, Fourth Edition*; WILEY-VCH Verlag GmbH & Co., 2011.
(152) Prat, D.; Wells, A.; Hayler, J.; Sneddon, H.; McElroy, C. R.; Abou-Shehada, S.; Dunn, P. J. CHEM21 Selection Guide of Classical- and Less Classical-Solvents. *Green Chem.* **2015**, *18*, 288–296.

Chapter 2

Role of Acetate Anions in the Catalytic Formation of Isocyanurates from Aromatic Isocyanates

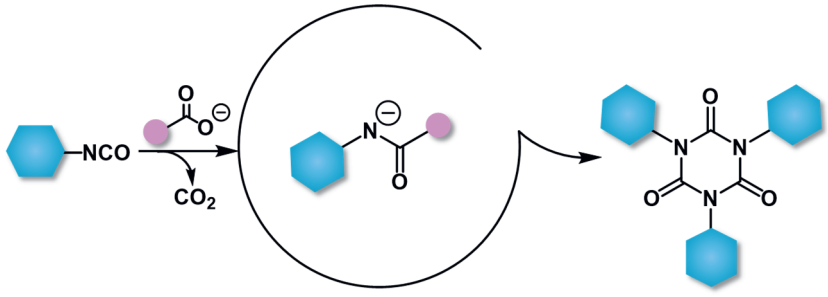

This chapter is based on published work:
Guo, Y.; Muuronen, M.; Deglmann, P.; Lucas, F.; Sijbesma, R. P.; Tomović, Ž., Role of acetate anions in the catalytic formation of isocyanurates from aromatic isocyanates. *J. Org. Chem.* **2021**, *86*, 5651–5659.
Yunfei Guo and Mikko Muuronen contributed equally to the work described in this scientific publication. The experiments and measurements presented in this chapter were performed by Yunfei Guo. The theoretical calculations presented in this chapter were performed by Mikko Muuronen.

Formation of isocyanurates *via* cyclotrimerization of aromatic isocyanates is widely used to enhance the physical properties of a variety of polyurethanes. The industrially most commonly used catalysts are carboxylates for which the exact catalytically active species have remained controversial. We investigated how acetate and other carboxylates react with aromatic isocyanates in a stepwise manner and identified that the carboxylates are only pre-catalysts in the reaction. Reaction of carboxylates with excess of aromatic isocyanates leads to irreversible formation of corresponding deprotonated amide species that are strongly nucleophilic and basic. As a result, they are active catalysts during the nucleophilic anionic trimerization, but can also deprotonate urethane and urea species present, which in turn catalyze the isocyanurate formation. The current study also shows how quantum chemical calculations can be used to direct spectroscopic identification of reactive intermediates formed during the active catalytic cycle with predictive accuracy.

2.1 Introduction

Isocyanurates - heterocyclic structures of 1,3,5-triazine-2,4,6-trione - formed *via* cyclotrimerization of isocyanates are widely used to enhance the physical properties of a variety of polyurethanes.[1-4] Whereas the controlled trimerization of aliphatic isocyanates is used for the preparation of isocyanurate cross-linkers for high-performance polyurethane coatings,[5-8] the cyclotrimerization of aromatic isocyanates into polyisocyanurate (PIR) structures is used to improve the thermal stability and flame retardancy of polyurethane rigid foams.[9-17] The initial molar ratio of functional groups and especially the type of catalysts are the main factors influencing the formation of PIR structures. The most commonly used catalysts in industrial applications are based on carboxylates, such as potassium acetate, potassium 2-ethylhexanoate, trimethyl hydroxypropyl ammonium formate, or phenolate such as 2,4,6-tris(dimethylaminomethyl)phenol.[6,18-25] The various industrial and commercial applications of isocyanurate-based polyurethane materials have attracted much attention in developing more effective catalysts for isocyanate trimerization. A number of catalysts for the trimerization of isocyanates have been extensively studied and reported in academic literature, including among others tetrabutylammonium fluoride (TBAF),[26] 2-phosphaethynolate anion (OCP^-),[27] sodium *p*-toluenesulfinate (*p*-$TolSO_2Na$)/tetrabutylammonium iodide (TBAI),[28,29] tetrakis(dimethylamino)ethylene (TDAE),[30] proazaphosphatrane,[31-33] N-heterocyclic carbenes and olefins,[34,35] *etc*. With more and more catalysts being reported, the exact nature of the cyclotrimerization mechanism has raised many interests.

The generally accepted mechanism for the anionic trimerization of aromatic isocyanates is shown in **Scheme 2-1**. In this mechanism, nucleophilic anionic catalyst (**1**) adds to the isocyanate carbon forming a nucleophilic anionic intermediate **2**, which reacts further in the presence of excess isocyanates to form the trimeric isocyanurates (**6**).[26,28,32,34,36] In the case of industrially used acetate-based catalysts, however, the exact nature of the catalytic species is controversial. Most studies consider the catalytically active species to be the acetate anion itself,[37,38] but on the other hand, Hoffman's early experimental work indicated that acetate anions are quickly converted to acetanilide when reacting with aromatic isocyanates, which in turn could potentially act as the anionic catalysts in the active cycle.[39] Further, as the acetanilide anion can be expected to deprotonate urethane, allophanate, urea and biuret groups in the PU matrix depending on their relative acidities, and their corresponding anions have been shown to be active PIR catalysts, the catalytically active species is expected to change several times during the polymerization.[13,19,40] Recently, Siebert *et al*. also suggested that the catalytically active species originating from acetate anions changes several times during the cyclotrimerization of aliphatic isocyanates.[41] The exact species that

catalyze cyclotrimerization of aromatic isocyanates, however, has not been explicitly characterized so far, which hampers the development of new PIR catalysts suitable for large-scale polyurethane production.

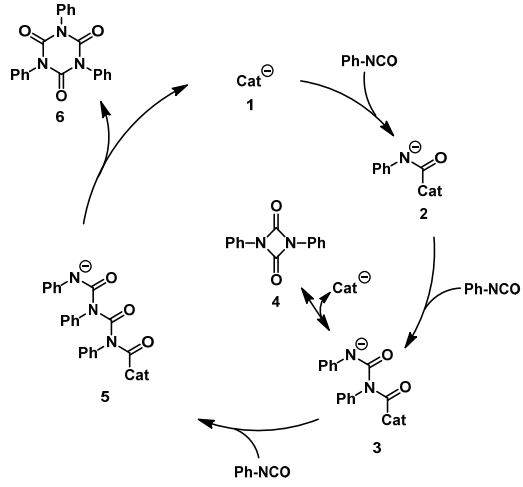

Scheme 2-1. Generally accepted anionic trimerization mechanism of aromatic isocyanates.

Here, we study the role of acetate anions in cyclotrimerization of aromatic isocyanates. Our study is based on first using the state-of-the-art quantum chemical methods to investigate how the acetate anion reacts with aromatic isocyanates in a stepwise manner to identify plausible mechanistic pathways. These are then used to guide spectroscopic identification of the catalytically active species to confirm the predicted mechanistic pathways.

2.2 Results and discussion

We studied the cyclotrimerization of aromatic isocyanates using phenyl and *p*-tolyl isocyanates as model substrates for identifying the species that are formed when acetate anion reacts with an excess of aromatic isocyanates (see **Scheme 2-2**). First, we calculated the relative free energies for several plausible mechanistic pathways for acetate anion-catalyzed cyclotrimerization of phenyl isocyanate in toluene and tetrahydrofuran (THF). Calculations were performed using accurate quantum chemical methods, *i.e.*, all structures were optimized using dispersion-corrected density functional theory, namely the TPSS-D3[42,43] functional with triple-ζ def2-TZVP[44,45] basis sets, and the final relative free energies were calculated using resolution-of-identity random phase approximation (RIRPA)[46] with quadruple-ζ def2-QZVPP basis sets in toluene and THF as described in the methods section. The accuracy of the used methods has been recently discussed elsewhere and is thus not addressed here.[47–49] These data were then used to understand which intermediates are formed during the

active catalytic cycle for guiding their experimental identification directly from the reaction mixture using liquid chromatography-mass spectroscopy (LC-MS) and ^{1}H-^{13}C heteronuclear single quantum coherence (HSQC) nuclear magnetic resonance (NMR) spectroscopy. In the experiments in toluene and THF, catalyst loading of 10 mol% relative to isocyanate was used to ensure that the ionic intermediates are formed in high enough concentrations to be detected with the analytical methods used (see Section 2.4 for full details on computational and experimental methods).

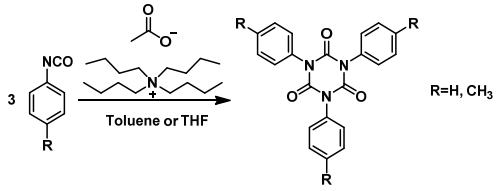

Scheme 2-2. Model reaction for studying the catalyzed trimerization of aromatic isocyanates.

The calculated mechanistic pathways in THF and their corresponding relative free energies are shown in Figure 2-1 (for results in toluene, see **Tables S2-1** and **S2-2**). In the generally accepted reaction mechanism, acetate anions react in a stepwise manner with 3 equiv of isocyanates to form isocyanurates (**6**) (see **Figure 2-1a** and **2b**). The reaction is initiated by straightforward nucleophilic addition of an acetate anion (**1**) to aromatic isocyanate forming an acetate bound isocyanate complex **2**. This nucleophilic intermediate can then react with the second isocyanate to form an allophanate acetate complex **3** that can reversibly cyclize intramolecularly to form 1,3-diphenyl-2,4-uretidinedione (**4**) as the kinetic product or react with the third isocyanate to form intermediate **5**, leading to the formation of isocyanurate **6** *via* its catalyst bound intermediate **6-cat** as the thermodynamic product. Overall, the reaction is strongly exergonic and the calculated low activation free energies agree well with the experimentally observed fast reaction at room temperature, *i.e.*, the rate limiting activation free energies are 65 and 67 kJ/mol in THF and toluene, respectively (**1** → **TS3-5**).

However, while the straightforward mechanism is energetically plausible, we do not consider this mechanism to be the active catalytic cycle, as the allophanate acetate intermediate **3** is predicted to react intramolecularly with lower activation free energy to form intermediate **3b** *via* acetyl migration instead of reacting intermolecularly with isocyanate to form the intermediate **5**. After elimination of CO_2, the intramolecular pathway is calculated to form intermediate **2'** irreversibly, a product of deprotonated amide and isocyanate. The amide could also be formed directly from intermediate **2** *via* a four-membered transition state **TS2-2b**: the free energy difference between transition states **TS2-2b** and **TS2-3** is calculated to be only 12 kJ/mol, indicating that both pathways are plausible or can even coexist.

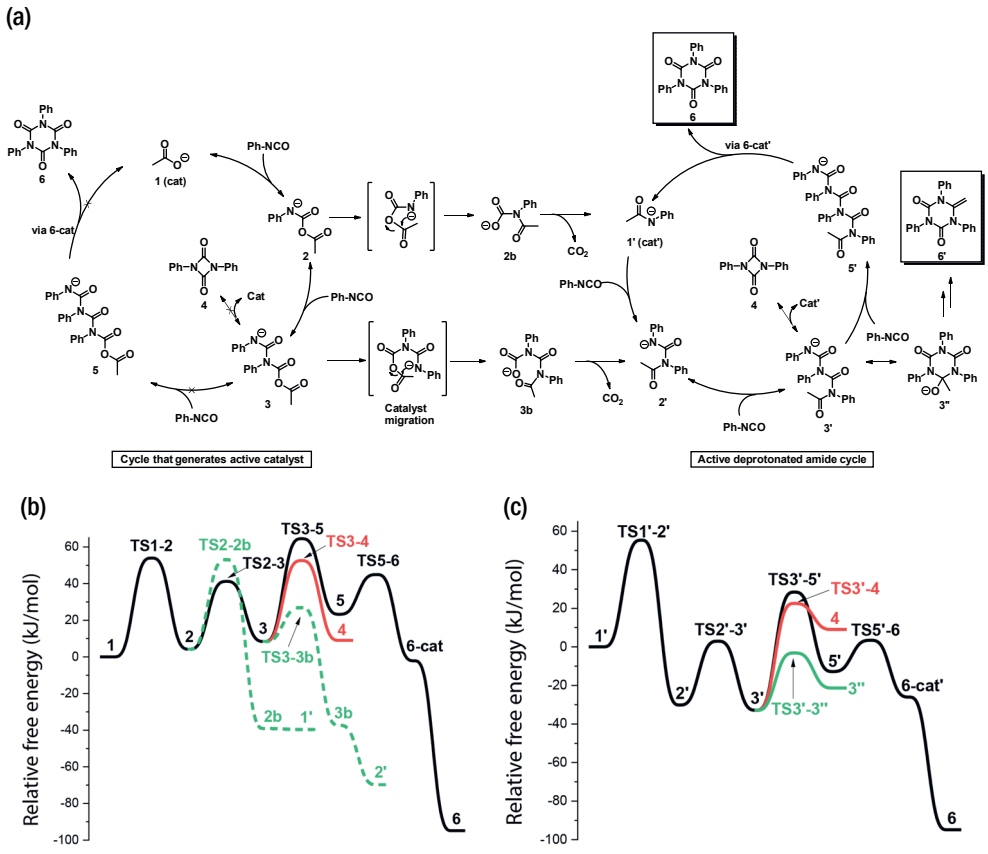

Figure 2-1. Reaction mechanism and the relative free energies (in kJ/mol) for the studied reaction mechanisms. All relative free energies are calculated in THF at 25 °C (see Tables S2-1 and S2-2 for numerical values).

The formed deprotonated aromatic amide **1'** is nucleophilic and reacts with excess isocyanates to form isocyanurate **6** identically to the previously explained catalytic cycle as shown in Figure 2-1. Both catalytic cycles are also energetically very similar with activation free energies of 61 and 60 kJ/mol in THF and toluene, respectively (**3'** → **TS3'-5'**). While in the catalytic cycle on the right, the active species cannot undergo similar catalyst migrations as previously, the allophanate-isocyanate intermediate **3'** is interestingly predicted to reversibly form the cyclized anion **3''**, which we consider to lead to the formation of electron-poor N-heterocyclic olefin **6'** in agreement with recent findings in the cyclotrimerization of aliphatic isocyanates.[41] The total reaction yields one molar equivalent of hydroxyl anions, but we assume the reaction to proceed *via* first protonating **3'** by a trace amount of proton sources and then fragmenting water. Water and hydroxyl anions are well known to lead to formation of urea first by hydrolyzing isocyanate to carbamic acid and forming an aromatic amine after

fragmentation of CO_2.[50] The formed aromatic amine reacts with the second isocyanate equivalent to form urea, which under basic conditions can be deprotonated to form a new anionic catalyst similar to **1'**. Therefore, forming olefin **6'** does not end the catalytic isocyanurate formation, but instead changes the catalytically active species from deprotonated amide to deprotonated urea in agreement with findings for aliphatic isocyanates.[41]

Then, we studied the trimerization reaction experimentally in THF and toluene at room temperature to verify our mechanistic hypothesis. For experiments, we chose phenyl and *p*-tolyl isocyanates as model substrates and tetrabutylammonium acetate (TBAA) as catalyst because of their high solubility in both solvents. The reaction was monitored using Fourier-transform infrared spectroscopy (FT-IR) and once all isocyanates had reacted, the mixture was analyzed using liquid chromatography-mass spectrometry (LC-MS) to detect the reactive intermediates present in the solution (see **Figure 2-2** and **Table 2-1**). The observed signals agree completely with the mechanism depicted in **Figure 2-1a**, being exclusively associated with the deprotonated amide cycle, product **6**, olefinic product **6'**, and urea (see **Table 2-1**). Results were independent of substrate (phenyl or *p*-tolyl isocyanate) or of the solvent (THF or toluene). Therefore, only results from experiments with phenyl isocyanate in THF are discussed below unless otherwise noted. Additional experimental data are found in the supplementary data.

The calculated relative free energies of the reactive intermediates indicate that we should be able to detect intermediates **1'**, **2'** and **3'** but not intermediate **5'** due to its higher relative free energy and fast cyclization to form product **6**. The intermediates **1'** and **2'** are observed in their protonated forms with signals m/z = 136.00, m/z = 255.00, but at the same time intermediate **3'** in its protonated form at m/z = 374.15 is too weak to be conclusively analyzed although it is predicted to be thermodynamically more stable than intermediate **2'** (see **Figure 2-1c**). The rationale for the absence of a peak at m/z = 374.15 is that intermediate **3'** is actually found at m/z = 396.00 as complex with one sodium cation. Intermediate **3'** was also detected as dimer coordinating to one sodium cation (m/z = 768.83).

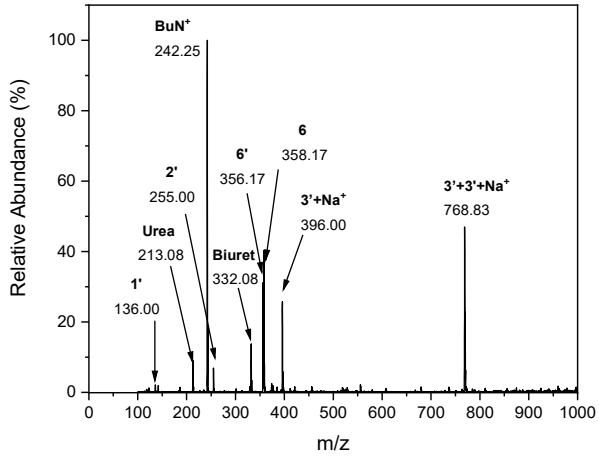

Figure 2-2. LC-MS spectrum after reaction of phenyl isocyanate and 10 mol% TBAA in dry THF and evaporation of the solvent.

Table 2-1. High abundance signals observed from the positive-ion mode of LC-MS analysis of the product after cyclotrimerization of phenyl isocyanate with TBAA in dry THF.

m/z	Abundance (%)	Assignment	*m/z*	Abundance (%)	Assignment
136.00	2	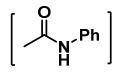	332.08	14	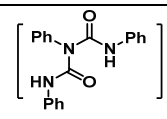
213.08	9	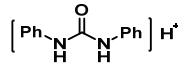	356.17	31	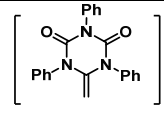
242.25	100	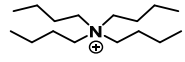	358.17	40	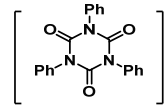
255.00	7	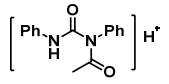	396.00	26	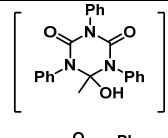 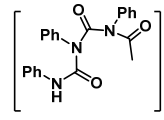

We observed two signals associated with the products: protonated triphenyl isocyanurate (**6**) was detected at *m/z* = 358.17 and the protonated "olefinic isocyanurate" **6'** was found at *m/z* = 356.17. The formation of **6'** was also confirmed by the presence of NMR signals of olefinic CH_2 protons at 3.01 ppm and the associated sp^2 carbon signal at 75.6 ppm in the ^1H-^{13}C-HSQC spectrum (see **Figure 2-3**). Detection of urea at *m/z* = 213.08 and biuret at *m/z* = 332.08 also supports the hypothesis that the eliminated water starts a new catalytic cycle with deprotonated urea as the catalytically active species although trace amounts of water could also have been present as impurities.

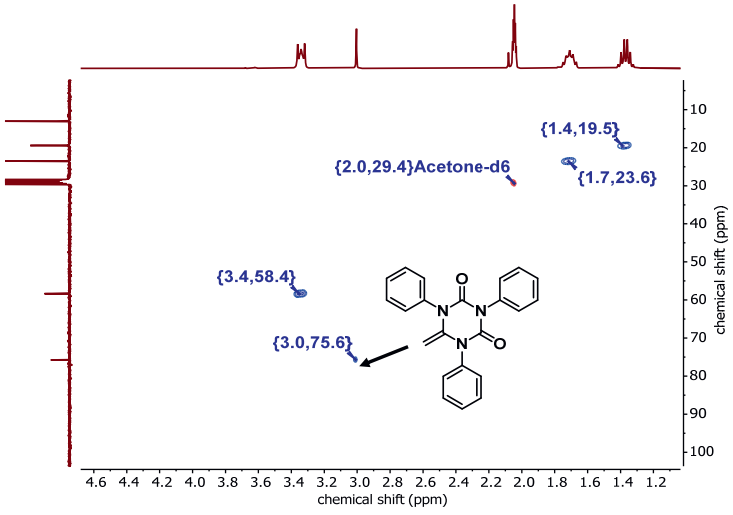

Figure 2-3. ^1H-^{13}C HSQC spectrum in acetone-d_6 after reaction of phenyl isocyanate and 10 mol% TBAA in dry THF and evaporation of the solvent. The peak at ^1H-3.0 ppm, ^{13}C-75.6 ppm is assigned to the terminal CH_2 of the olefin structure.

When *p*-tolyl isocyanate was used as a trimerization starting material, the corresponding isocyanurate **6** was detected as a dimer with one sodium cation at *m/z* = 820.83 (**Figure 2-4**). This assignment was also confirmed by finding the same signal in a purified sample of tris-*p*-tolyl-isocyanurate **6** in LC-MS (**Figure 2-5**), which can be rationalized by the strong tendency of isocyanurate rings to form supramolecular dimers as simulated by Lenzi *et al.*[51]

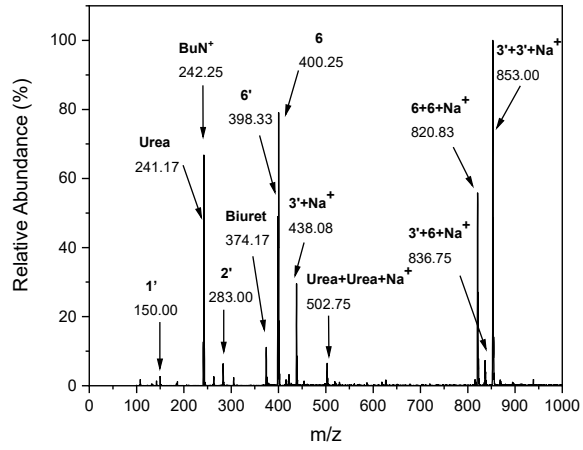

Figure 2-4. LC-MS spectrum after reaction of *p*-tolyl isocyanate and 10 mol% TBAA in THF and evaporation of solvent.

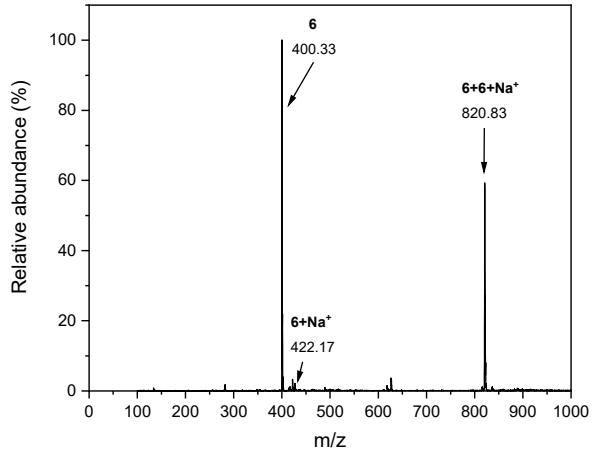

Figure 2-5. LC-MS spectrum of purified tris-*p*-tolyl isocyanurate.

Finally, to verify that deprotonated amides catalyze the reaction, we performed the same reaction using commercially available acetanilide as a catalyst deprotonated *in situ* by excess triethylamine. The reaction was significantly slower due to the unfavorable deprotonation of the amide in toluene and THF, but isocyanurate product **6** was still observed in LC-MS despite the low conversion. Catalysis by deprotonated amides is also supported by early work done by Kogon, who reported the formation of aromatic isocyanate trimers in high yield at elevated temperatures when phenyl

isocyanates were trimerized in the presence of *N*-methylmorpholine and ethyl alcohol or ethyl carbanilate.[13]

To understand how general the observed catalyst migration mechanism is when carboxylates are used as catalysts, we also performed trimerization of *p*-tolyl isocyanate using potassium 2-ethylhexanoate at room temperature and cesium pivalate at 60 °C as the (pre)catalysts in THF (see **Scheme 2-3**). As expected, only intermediates related to the deprotonated amide cycle were found, indicating that the conversion of carboxylates into amides with aromatic isocyanates is general rather than restricted to only sterically small carboxylates such as acetate (**Figure 2-6**). For these two pre-catalysts, 2-ethylhexanoate could, in principle, also form an olefinic isocyanurate structure similar to **6'** *via* deprotonation of the tertiary α-proton, but this was not observed in our experiment.

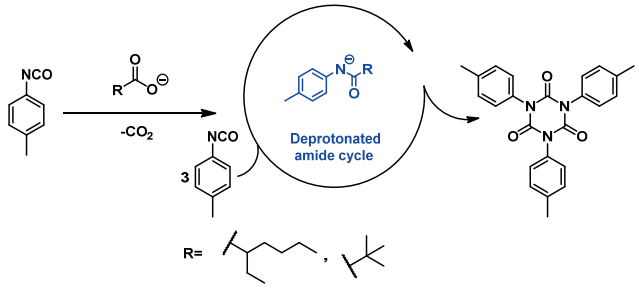

Scheme 2-3. Identified catalytically active species for different carboxylate anions.

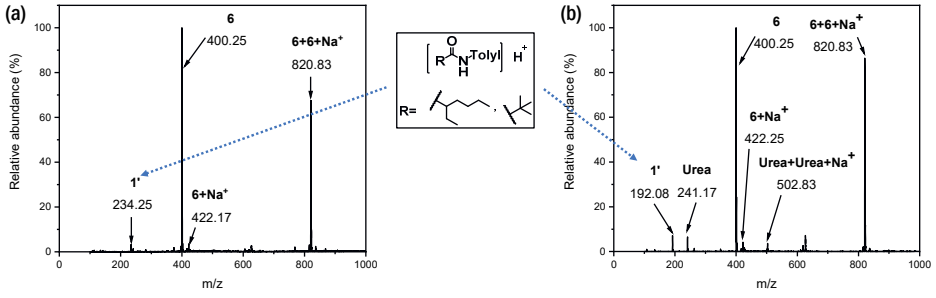

Figure 2-6. LC-MS spectra after reaction of *p*-tolyl isocyanate and 10 mol% (a) potassium 2-ethylhexanoate or (b) cesium pivalate in THF and evaporation of solvent. Nomenclature **1'** refers to 2-ethylhexane or pivalate functionalized amide, respectively.

Finally, we considered the role of the deprotonated amide cycle in catalyzing the trimerization of aromatic isocyanates during the formation of real PU materials. In these cases, several functional groups, *i.e.*, alcohols, water, urethanes, urea, allophanates and biurets, are present that are in deprotonation equilibrium with amide. To establish their roles, we calculated the reaction free energies for proton

transfers between acetate, amide, urethane and urea (see **Scheme 2-4**). The calculations were performed in toluene and THF to understand how the polarity of the reaction media affects the relative stability of the corresponding anions, and in water as a model for a polar protic environment. In all media, the aromatic amide anion is predicted to deprotonate aromatic urethane with exergonic free energies between -7 and -13 kJ/mol, while deprotonation of urea is more dependent on the reaction media that is exergonic in toluene and THF (-23 and -15 kJ/mol, respectively), but endergonic in water (+3 kJ/mol). As expected, acetate itself is calculated to be much less basic than deprotonated amide and direct deprotonation of urethane by acetate is calculated to be endergonic by 20 - 67 kJ/mol depending on the solvent. Therefore, acetate anions form amides and CO_2 with isocyanates, independent of the reaction media, but the amide anion may in turn deprotonate urethanes, urea, allophanates or biurets present, forming new catalytically active anions that are expected to catalyze trimerization in a cycle, which is similar to that of the deprotonated amide. This is supported also by a kinetic study by Schwetlick and Noack,[40] who measured trimerization kinetics of phenyl isocyanate in acetonitrile at 50 °C using tetramethylammonium octanoate as a catalyst in the presence of several X-H active additives such as alcohols, carbamates, phenols and amides. The measured kinetics showed that additives change the rate of isocyanurate formation significantly, confirming our hypothesis that the role of carboxylate pre-catalyst is twofold: first, it generates a strong base out of a weak base by reacting with aromatic isocyanate to generate a deprotonated amide, a reaction that is thermodynamically facilitated by the favorable entropy of the decarboxylation reaction. Second, the amide anion can then catalyze the PIR formation *via* the nucleophilic mechanism of **Scheme 2-1**, but the basic deprotonated amide can also deprotonate functional groups such as urethane and urea groups, which in turn will catalyze the anionic trimerization.

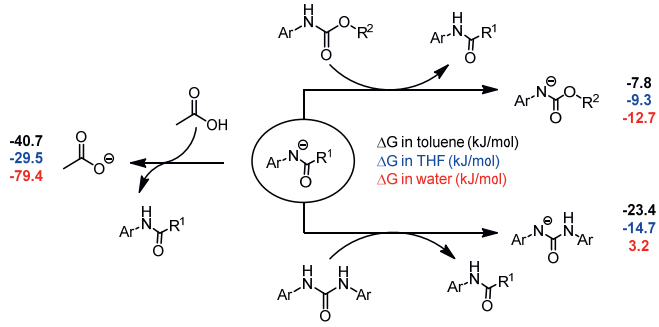

Scheme 2-4. Calculated free energies for proton transfers between deprotonated amide, acetate, urethane and urea species in toluene, THF and water. All free energies are in kJ/mol and calculated for species with Ar = Ph, R^1 = R^2 = Me.

2.3 Conclusion

We investigated the role of acetate anions in the trimerization of aromatic isocyanates by the state-of-the-art experimental and computational methods. Our study reveals that during the anionic cyclotrimerization, the actual catalytically active species changes at least once with the acetate anion only serving as a pre-catalyst. The reaction of acetate anion with an excess of aromatic isocyanates leads eventually to irreversible formation of deprotonated amide species that are formed after intramolecular rearrangement and decarboxylation. The deprotonated amide is the new active catalyst that forms isocyanurate *via* a nucleophilic anionic mechanism. The deprotonated amides are much more basic than the acetate pre-catalyst and, therefore, are capable of deprotonating other protic groups in the system such as urethane and urea groups, which in turn catalyze isocyanurate formation. Carboxylate migration to amide anions is expected to take place regardless of the size of the carboxylate because migration was observed for acetate, 2-ethylhexanoate, and pivalate alike. Acetate, on the other hand, can also lead to the formation of an electron-poor N-heterocyclic olefin and water, which can further lead to a catalytic cycle where deprotonated urea is the active catalytic species. We demonstrated that the qualitative mechanism is independent of the solvent polarity. However, the effect that changes in acid-base equilibrium in protic solvents may have on the mechanism is the subject of further studies. The current study also highlights that mechanistic investigations can greatly be accelerated when using a combination of the state-of-the-art computational and experimental analytic techniques, and importantly discover details that may not be analyzed by either of the methods alone.

2.4 Experimental section

Materials

Phenyl isocyanate (≥98%), *p*-tolyl isocyanate (≥99%) and cesium pivalate (≥98%) were purchased from Sigma-Aldrich, tetrabutylammonium acetate (>90%), triethylamine (>99%) and potassium 2-ethylhexanoate (>95%) were purchased from TCI. All of the reagents above were used directly without treatment. THF (without stabilizer BHT) was directly obtained from dry solvent system; toluene was dried by mol-sieves before use; and pentane was directly used without treatment.

Synthesis

Study of cyclotrimerization mechanism of phenyl and p-tolyl isocyanates using carboxylates (TBAA, potassium 2-ethylhexanoate or cesium pivalate) as catalysts. Phenyl isocyanate (0.53 g, 4.44 mmol) or p-tolyl isocyanate (0.52 g, 3.92 mmol) was dissolved in THF or toluene (5.0 mL) in a dry flask. The catalyst solution was prepared

by dissolving catalyst (10 mol% to NCO groups) in THF or toluene (5.5 mL) in a separate dry flask and then added to the isocyanate solution (concentration of phenyl isocyanate: 0.5 g/10 mL solvent). The reaction was carried out at room temperature for all catalysts except that a temperature of 60 ºC in an oil bath was used for cesium pivalate (due to its poor solubility). All reactions were performed under an Ar atmosphere until the disappearance of NCO stretching vibration at 2270 cm^{-1} as observed by FT-IR spectroscopy. After that, most of the solvent was evaporated in an Ar flow. The so formed sample was diluted in water/acetonitrile (1:1) solution with a concentration of 1 mg/mL for LC-MS measurement and dissolved in acetone-d_6 for NMR spectroscopy measurement.

Study of cyclotrimerization mechanism of phenyl isocyanates using deprotonated acetanilide as a catalyst. Phenyl isocyanate (0.58 g, 4.85 mmol) was dissolved in THF or toluene (5.0 mL) in a dry flask. The catalyst solution was prepared by dissolving acetanilide (10 mol% to NCO groups) and triethylamine (30 mol% to NCO groups) in THF (6.6 mL) in a separate dry flask and then added to the isocyanate solution (concentration of phenyl isocyanate: 0.5 g/10mL solvent). The reaction was carried out at room temperature under an Ar atmosphere overnight. After that, most of the solvent was blown by an Ar flow and wet precipitates were obtained. The sample was diluted in water/acetonitrile (1:1) solution with a concentration of 1mg/mL for LC-MS measurement.

Synthesis and purification of tris-p-tolyl isocyanurate using potassium 2-ethylhexanoate as a catalyst. *p*-Tolyl isocyanate (1.15 g, 8.67 mmol) was dissolved in THF (3.0 mL) in a dry flask. The catalyst solution was prepared by dissolving potassium 2-ethylhexanoate (1 mol% to NCO groups) in THF (2.6 mL) in a separate dry flask and then added to the isocyanate solution. The reaction was carried out in a 40 ºC oil bath under an Ar atmosphere until the disappearance of NCO stretching vibration at 2270 cm^{-1} as observed by FT-IR spectroscopy. After the reaction, 10 mL of THF was added to dissolve all the precipitates at 40 ºC. Then the tris-*p*-tolyl isocyanurate was precipitated by direct pouring the warm solution in cooled pentane. The precipitate was immediately filtered and dried in vacuum oven at 60 ºC overnight, giving tris-*p*-tolyl isocyanurate as a white powder (0.96 g, 2.40 mmol, yield: 83%). ^{1}H NMR (400 MHz, acetone-d_6): δ 7.29 (t, J = 6.1 Hz, 12H), 2.36 (s, 9H) ppm; $^{13}C\{^1H\}$ NMR (100 MHz, acetone-d_6): δ 205.3, 129.4, 128.7, 20.3 ppm.[52]

Characterization

Fourier-transform infrared spectroscopy (FT-IR). FT-IR spectroscopy was carried out in the Attenurated Reflection mode on a Spectrum One (Perkin Elmer) spectrometer at room temperature. Eight scans were performed from 4000 – 450 cm^{-1}.

Liquid chromatography-mass spectrometry (LC-MS). LC-MS measurements were carried out on a LCQ Fleet ESI-MS (Thermo Fisher Scientific) with H_2O (0.1% formic acid) as eluents. As the intermediates are negatively charged, a negative-positive mode LC-MS was adapted, and water and formic acid eluent were used to protonate the intermediates, which provided clear signals in the positive spectrum. The reaction mixtures were further analyzed identically for reactions done with phenyl and *p*-tolyl isocyanates to assist identification of different intermediates in LC-MS spectra by indicating the number of aromatic groups present.

Nuclear magnetic resonance (NMR) spectroscopy. NMR spectroscopy for characterization of the compounds and identification of double bonds were performed using either Bruker UltraShield 400 MHz or Varian Mercury 400 MHz spectrometer at room temperature using acetone-d_6 as solvent.

Computational details

All computations were performed using Turbomole 7.3 program package.[53] Structures were optimized using dispersion corrected TPSS-D3[42,43] density functional with def2-TZVP[44,45] basis sets and by employing multipole-accelerated resolution-of-the-identity approximation for Coulomb term (MARI-J)[54] with the corresponding auxiliary basis sets to speed up the computations.[55] The final energy of each structure was calculated using resolution-of-identity random phase approximation (RIRPA)[46] with def2-QZVPP basis sets and with corresponding auxiliary basis sets.[56,57] RPA calculations were performed using gas-phase TPSS orbitals and the core orbitals were kept frozen for computing the RPA correlation energy. Default settings and convergence criteria of Turbomole were used in all optimizations except a finer integration grid of *m4* was used. In RPA calculations, grid *m5* and a higher threshold for energy convergence (scfconv 7) were used for calculating the TPSS orbitals. Harmonic vibrational frequencies were calculated numerically at the level of optimization for all optimized structures.

Solvation effects were accounted for during structure optimizations using the COSMO solvation model with a dielectric constant of infinity.[58,59] Final solvation free energies were calculated for each structure at 25 °C using the COSMO-RS[60] model in COSMOTherm (version 2018) with the parameter file BP_TZVP_18.ctd based on BP86[61]/def-TZVP level. The Gibbs free energies in solution were then calculated from a thermodynamic cycle $G = E + c.p. + G_{solv}$, where E is the gas-phase energy of the system at the RPA level, *c.p.* is the chemical potential based on standard rigid-rotor harmonic oscillator approximation at 25 °C, and G_{solv} is the free energy of solvation obtained from COSMO-RS. The thermodynamic reference state of the so-obtained free energies refers to a hypothetic mole fraction of 1 for all species, which were converted into a reference state of 1 mol/L using solvent molarities (c) of 9.41 and 12.3 mol/L

for toluene and tetrahydrofuran, respectively, by adding a term RTln(c) to the free energy of all species.

Initial structures that were used for structure optimizations correspond to the lowest energy conformer of each structure obtained from extensive conformational searches performed with respect to all rotatable bonds at the level of optimization without D3 correction. In the case of transition states, the forming and breaking bonds were constrained during the conformer search according to their initial guess structures, which were obtained using the single-ended growing string method.[62–64] Pictures of the computed structures were generated using Cylview.[65]

Supplementary data

Table S2-1. Relative free energies for all minima and transition states in tetrahydrofuran and in toluene for acetate ion catalyzed trimerization of phenyl isocyanate (used to make Figure 2-1b). All free energies are in kJ/mol and relative to intermediate **1** (solvated acetate anion).

	In tetrahydrofuran	In toluene
Acetate ion catalyzed general catalytic cycle		
1	0.0	0.0
2	4.2	6.6
3	8.4	11.0
4	9.0	8.5
5	23.2	25.6
6-cat	-2.1	-1.1
6	-94.9	-92.4
TS1-2	53.9	55.0
TS2-3	41.2	43.5
TS3-4	52.5	55.2
TS3-5	64.5	66.6
TS5-6	44.9	46.4
Catalyst migration		
2b	-39.1	-38.2
3b	-37.4	-36.2
1'	-39.6	-37.4
2'	-69.8	-67.5
TS2-2b	53.1	55.2
TS3-3b	26.8	29.2

Table S2-2. Relative free energies for all minima and transition states in tetrahydrofuran and in toluene for amide anion catalyzed trimerization of phenyl isocyanate (used to make Figure 2-1c). All free energies are in kJ/mol and relative to intermediate **1'** (solvated acetanilide anion).

	In tetrahydrofuran	In toluene
1'	0.0	0.0
2'	-30.2	-30.1
3'	-32.8	-33.0
3''	-21.3	-22.6
4	9.0	8.5
5'	-12.8	-13.0
6-cat'	-26.0	-27.5
6	-94.9	-92.4
TS1'-2'	55.3	55.2
TS2'-3'	2.9	2.6
TS3'-3''	-3.2	-3.8
TS3'-4	22.5	21.9
TS3'-5'	28.4	27.3
TS5'-6'	3.4	2.1

2.5 References

(1) Engels, H. W.; Pirkl, H. G.; Albers, R.; Albach, R. W.; Krause, J.; Hoffmann, A.; Casselmann, H.; Dormish, J. Polyurethanes: Versatile Materials and Sustainable Problem Solvers for Today's Challenges. *Angew. Chemie - Int. Ed.* **2013**, *52*, 9422–9441.

(2) Randall, D.; Lee, S. *The Polyurethanes Book*; Wiley, 2003.

(3) Eling, B.; Tomović, Ž.; Schädler, V. Current and Future Trends in Polyurethanes: An Industrial Perspective. *Macromol. Chem. Phys.* **2020**, *2000114*, 1–11.

(4) Delebecq, E.; Pascault, J. P.; Boutevin, B.; Ganachaud, F. On the Versatility of Urethane/Urea Bonds: Reversibility, Blocked Isocyanate, and Non-Isocyanate Polyurethane. *Chem. Rev.* **2013**, *113*, 80–118.

(5) Wang, G.; Li, K.; Zou, W.; Hu, A.; Hu, C.; Zhu, Y.; Chen, C.; Guo, G.; Yang, A.; Drumright, R.; Argyropoulos, J. Synthesis of HDI/IPDI Hybrid Isocyanurate and Its Application in Polyurethane Coating. *Progess Org. Coatings* **2015**, *78*, 225–233.

(6) Driest, P. J.; Lenzi, V.; Marques, L. S. A.; Ramos, M. M. D.; Dijkstra, D. J.; Richter, F. U.; Stamatialis, D.; Grijpma, D. W. Aliphatic Isocyanurates and Polyisocyanurate Networks. *Polym. Adv. Technol.* **2017**, *28*, 1299–1304.

(7) Laas, H. J.; Halpaap, R.; Pedain, J. Zur Synthese Aliphatischer Polyisocyanate – Lackpolyisocyanate Mit Biuret-, Isocyanurat- Oder Uretdionstruktur. *Journal für Praktische Chemie/Chemiker-Zeitung*. John Wiley & Sons, Ltd January 1, 1994, pp 185–200.

(8) Meier-Westhues, H.-U. *Polyurethanes: Coatings, Adhesives and Sealants*; European Coatings, 2019.

(9) Kordomenos, P. I.; Kresta, J. E. Thermal Stability of Isocyanate-Based Polymers. 1. Kinetics of the Thermal Dissociation of Urethane, Oxazolidone, and Isocyanurate Groups. *Macromolecules* **1981**, *14*, 1434–1437.

(10) Kordomenos, P. I.; Kresta, J. E.; Frisch, K. C. Thermal Stability of Isocyanate-Based Polymers. 2. Kinetics of the Thermal Dissociation of Model Urethane, Oxazolidone, and Isocyanurate Block Copolymers. *Macromolecules* **1987**, *20*, 2077–2083.

(11) Reymore, H. E.; Carleton, P. S.; Kolakowski, R. A.; Sayigh, A. A. R. Isocyanurate Foams: Chemistry, Properties and Processing. *J. Cell. Plast.* **1975**, *11*, 328–344.

(12) Wang, C. L.; Klempner, D.; Frisch, K. C. Morphology of Polyurethane- Isocyanurate Elastomers. *J. Appl. Polym. Sci.* **1985**, *30*, 4337–4344.

(13) Kogon, I. C. New Reactions of Phenyl Isocyanate and Ethyl Alcohol. *J. Am. Chem. Soc.* **1956**, *78*, 4911–4914.

(14) Duff, D. W.; Maciel, G. E. Monitoring the Thermal Degradation of an Isocyanurate-Rich MDI-

Based Resin by ^{15}N and ^{13}C CP/MAS NMR. *Macromolecules* **1991**, *24*, 651–658.
(15) Chattopadhyay, D. K.; Webster, D. C. Thermal Stability and Flame Retardancy of Polyurethanes. *Prog. Polym. Sci.* **2009**, *34*, 1068–1133.
(16) Xu, Q.; Hong, T.; Zhou, Z.; Gao, J.; Xue, L. The Effect of the Trimerization Catalyst on the Thermal Stability and the Fire Performance of the Polyisocyanurate-Polyurethane Foam. *Fire Mater.* **2018**, *42*, 119–127.
(17) Dick, C.; Dominguez-Rosado, E.; Eling, B.; Liggat, J. J.; Lindsay, C. I.; Martin, S. C.; Mohammed, M. H.; Seeley, G.; Snape, C. E. The Flammability of Urethane-Modified Polyisocyanurates and Its Relationship to Thermal Degradation Chemistry. *Polymer (Guildf).* **2001**, *42*, 913–923.
(18) Jozef, B. G.; Eric, H.; Stijn, R.; Marc, V.; Guido, V. H. G. Process for Preparing a Polyisocyanurate Polyurethane Material. US 20080227929 A1, 2008.
(19) Al Nabulsi, A.; Cozzula, D.; Hagen, T.; Leitner, W.; Müller, T. E. Isocyanurate Formation during Rigid Polyurethane Foam Assembly: A Mechanistic Study Based on: In Situ IR and NMR Spectroscopy. *Polym. Chem.* **2018**, *9*, 4891–4899.
(20) Hagquist, J. A. E.; Reid, K. J.; Giorgini, A.; Hill, N. Isocyanurate Embedment Compound. US 5556934 A, 1996.
(21) Burdeniuc, J. J.; Panitzsch, T.; Dewhurst, J. E. Trimerization Catalysts from Sterically Hindered Salts. US 8530534 B2, 2013.
(22) Bechara, I. Some Aspects of Innovative Catalysis of the Isocyanate Trimerization Reaction - Polyisocyanurate Foam Formation and Properties. *J. Cell. Plast.* **1979**, *15*, 102–113.
(23) Driest, P. J.; Dijkstra, D. J.; Stamatialis, D.; Grijpma, D. W. The Trimerization of Isocyanate-Functionalized Prepolymers: An Effective Method for Synthesizing Well-Defined Polymer Networks. *Macromol. Rapid Commun.* **2019**, *40*, 1–6.
(24) Driest, P. J.; Dijkstra, D. J.; Stamatialis, D.; Grijpma, D. W. Tough Combinatorial Poly(Urethane-Isocyanurate) Polymer Networks and Hydrogels Synthesized by the Trimerization of Mixtures of NCO-Prepolymers. *Acta Biomater.* **2020**, *105*, 87–96.
(25) Achten, D.; Matner, M.; Casselmann, H.; Ehlers, M. Polyisocyanurate Plastics Having High Thermal Stability. US 2018/0086875 A1, 2018.
(26) Nambu, Y.; Endo, T. Synthesis of Novel Aromatic Isocyanurates by the Fluoride-Catalyzed Selective Trimerization of Isocyanates. *J. Org. Chem.* **1993**, *58*, 1932–1934.
(27) Heift, D.; Benko, Z.; Grützmacher, H.; Jupp, A. R.; Goicoechea, J. M. Cyclo-Oligomerization of Isocyanates with Na(PH2) or Na(OCP) as "P^-" Anion Sources. *Chem. Sci.* **2015**, *6*, 4017–4024.
(28) Moghaddam, F. M.; Dekamin, M. G.; Khajavi, M. S.; Jalili, S. Efficient and Selective Trimerization of Aryl and Alkyl Isocyanates Catalyzed by Sodium P-Toluenesulfinate in the Presence of TBAI in a Solvent-Free Condition. *Bull. Chem. Soc. Jpn.* **2002**, *75*, 851–852.
(29) Moritsugu, M.; Sudo, A.; Endo, T. Development of High-Performance Networked Polymers Consisting of Isocyanurate Structures Based on Selective Cyclotrimerization of Isocyanates. *J. Polym. Sci. Part A Polym. Chem.* **2011**, *49*, 5186–5191.
(30) Giuglio-Tonolo, A. G.; Spitz, C.; Terme, T.; Vanelle, P. An Expeditious Method for the Selective Cyclotrimerization of Isocyanates Initiated by TDAE. *Tetrahedron Lett.* **2014**, *55*, 2700–2702.
(31) Tang, J.; Mohan, T.; Verkade, J. G. Selective and Efficient Syntheses of Perhydro-1,3,5-Triazine-2,4,6-Triones and Carbodiimides from Isocyanates Using $ZP(MeNCH_2CH_2)_3N$ Catalysts. *J. Org. Chem.* **1994**, *59*, 4931–4938.
(32) Gibb, J. N.; Goodman, J. M. The Formation of High-Purity Isocyanurate through Proazaphosphatrane- Catalysed Isocyanate Cyclo-Trimerisation: Computational Insights. *Org. Biomol. Chem.* **2013**, *11*, 90–97.
(33) Raders, S. M.; Verkade, J. G. An Electron-Rich Proazaphosphatrane for Isocyanate Trimerization to Isocyanurates. *J. Org. Chem.* **2010**, *75*, 5308–5311.
(34) Li, C.; Zhao, W.; He, J.; Zhang, Y. Highly Efficient Cyclotrimerization of Isocyanates Using N-Heterocyclic Olefins under Bulk Conditions. *Chem. Commun.* **2019**, *55*, 12563–12566.
(35) Duong, H. A.; Cross, M. J.; Louie, J. N-Heterocyclic Carbenes as Highly Efficient Catalysts for the Cyclotrimerization of Isocyanates. *Org. Lett.* **2004**, *6*, 4679–4681.
(36) Duff, D. W.; Maciel, G. E. ^{13}C and ^{15}N CP/MAS NMR Characterization of MDI-Polyisocyanurate Resin Systems. *Macromolecules* **1990**, *23*, 3069–3079.
(37) Silva, A. L.; Bordado, J. C. Recent Developments in Polyurethane Catalysis: Catalytic Mechanisms Review. *Catal. Rev. - Sci. Eng.* **2004**, *46*, 31–51.
(38) Krestra, J. E. Reaction Injection Molding and Fast Polymerization Reactions. In *Polymer Science and Technology*; 1982; Vol. 18, pp 147–168.
(39) Hoffman, D. K. Model System for a Urethane-Modified Isocyanurate Foam. *J. Cell. Plast.* **1984**,

20, 129–137.
(40) Schwetlickt, K.; Noacks, R. Kinetics and Catalysis of Consecutive Isocyanate Reactions. Formation of Carbamates, Allophanates and Lsocyanurates. *J. Chem. Soc. Perkin Trans. 2* **1995**, No. 2, 395–402.
(41) Siebert, M.; Sure, R.; Deglmann, P.; Closs, A. C.; Lucas, F.; Trapp, O. Mechanistic Investigation into the Acetate-Initiated Catalytic Trimerization of Aliphatic Isocyanates: A Bicyclic Ride. *J. Org. Chem.* **2020**, *85*, 8553–8562.
(42) Tao, J.; Perdew, J.; Staroverov, V.; Scuseria, G. Climbing the Density Functional Ladder: Nonempirical Meta-Generalized Gradient Approximation Designed for Molecules and Solids. *Phys. Rev. Lett.* **2003**, *91*, 146401.
(43) Grimme, S.; Antony, J.; Ehrlich, S.; Krieg, H. A Consistent and Accurate Ab Initio Parametrization of Density Functional Dispersion Correction (DFT-D) for the 94 Elements H-Pu. *J. Chem. Phys.* **2010**, *132*, 154104.
(44) Weigend, F.; Furche, F.; Ahlrichs, R. Gaussian Basis Sets of Quadruple Zeta Valence Quality for Atoms H-Kr. *J. Chem. Phys.* **2003**, *119*, 12753.
(45) Weigend, F.; Ahlrichs, R. Balanced Basis Sets of Split Valence, Triple Zeta Valence and Quadruple Zeta Valence Quality for H to Rn: Design and Assessment of Accuracy. *Phys. Chem. Chem. Phys.* **2005**, *7*, 3297.
(46) Eshuis, H.; Yarkony, J.; Furche, F. Fast Computation of Molecular Random Phase Approximation Correlation Energies Using Resolution of the Identity and Imaginary Frequency Integration. *J. Chem. Phys.* **2010**, *132*, 234114.
(47) Muuronen, M.; Deglmann, P.; Tomović, Ž. Design Principles for Rational Polyurethane Catalyst Development. *J. Org. Chem.* **2019**, *84*, 8202–8209.
(48) Nguyen, B. D.; Chen, G. P.; Agee, M. M.; Burow, A. M.; Tang, M. P.; Furche, F. Divergence of Many-Body Perturbation Theory for Noncovalent Interactions of Large Molecules. *J. Chem. Theory Comput.* **2020**, *16*, 2258–2273.
(49) Grimme, S. Supramolecular Binding Thermodynamics by Dispersion-Corrected Density Functional Theory. *Chem. - A Eur. J.* **2012**, *18*, 9955–9964.
(50) Mader, P. M. Hydrolysis Kinetics for P-Dimethylaminophenyl Isocyanate in Aqueous Solutions. *J. Org. Chem.* **1968**, *33*, 2253–2260.
(51) Lenzi, V.; Driest, P. J.; Dijkstra, D. J.; Ramos, M. M. D.; Marques, L. S. A. Investigation on the Intermolecular Interactions in Aliphatic Isocyanurate Liquids: Revealing the Importance of Dispersion. *J. Mol. Liq.* **2019**, *280*, 25–33.
(52) Bahili, M. A.; Stokes, E. C.; Amesbury, R. C.; Ould, D. M. C.; Christo, B.; Horne, R. J.; Kariuki, B. M.; Stewart, J. A.; Taylor, R. L.; Williams, P. A.; Jones, M. D.; Harris, K. D. M.; Ward, B. D. Aluminium-Catalysed Isocyanate Trimerization, Enhanced by Exploiting a Dynamic Coordination Sphere. *Chem. Commun.* **2019**, *55*, 7679–7682.
(53) Balasubramani, S. G.; Chen, G. P.; Coriani, S.; Diedenhofen, M.; Frank, M. S.; Franzke, Y. J.; Furche, F.; Grotjahn, R.; Harding, M. E.; Hättig, C.; Hellweg, A.; Helmich-Paris, B.; Holzer, C.; Huniar, U.; Kaupp, M.; Khah, A. M.; Khani, S. K.; Müller, T.; Mack, F.; Nguyen, B. D.; Parker, S. M.; Perlt, E.; Rappoport, D.; Reiter, K.; Roy, S.; Rückert, M.; Schmitz, G.; Sierka, M.; Tapavicza, E.; Tew, D. P.; Wüllen, C. van; Voora, V. K.; Weigend, F.; Wodyński, A.; Yu, J. M. TURBOMOLE: Modular Program Suite for Ab Initio Quantum-Chemical and Condensed-Matter Simulations. *J. Chem. Phys.* **2020**, *152*, 184107.
(54) Sierka, M.; Hogekamp, A.; Ahlrichs, R. Fast Evaluation of the Coulomb Potential for Electron Densities Using Multipole Accelerated Resolution of Identity Approximation. *J. Chem. Phys.* **2003**, *118*, 9136–9148.
(55) Weigend, F. Accurate Coulomb-Fitting Basis Sets for H to Rn. *Phys. Chem. Chem. Phys.* **2006**, *8*, 1057–1065.
(56) Weigend, F.; Häser, M.; Patzelt, H.; Ahlrichs, R. RI-Mp2: Optimized Auxiliary Basis Sets and Demonstration of Efficiency. *Chem. Phys. Lett.* **1998**, *294*, 143.
(57) Hättig, C. Optimization of Auxiliary Basis Sets for RI-MP2 and RI-CC2 Calculations: Core–Valence and Quintuple-ζ Basis Sets for H to Ar and QZVPP Basis Sets for Li to Kr. *Phys. Chem. Chem. Phys.* **2005**, *7*, 59.
(58) Schäfer, A.; Klamt, A.; Sattel, D.; Lohrenz, J. C. W.; Eckert, F. COSMO Implementation in TURBOMOLE: Extension of an Efficient Quantum Chemical Code towards Liquid Systems. *Phys. Chem. Chem. Phys.* **2000**, *2*, 2187–2193.
(59) Klamt, A.; Schueuermann, G. COSMO: A New Approach to Dielectric Screening in Solvents with Explicit Expressions for the Screening Energy and Its Gradient. *J. Chem. Soc., Perkin Trans. 2* **1993**, No. 5, 799–805.

(60) Klamt, A.; Eckert, F. COSMO-RS: A Novel and Efficient Method for the a Priori Prediction of Thermophysical Data of Liquids. *Fluid Phase Equilib.* **2000**, *172*, 43–72.
(61) Becke, A. D. Density-Functional Exchange-Energy Approximation with Correct Asymptotic Behavior. *Phys. Rev. A Gen. Phys.* **1988**, *38*, 3098–3100.
(62) Zimmerman, P. Reliable Transition State Searches Integrated with the Growing String Method. *J. Chem. Theory Comput.* **2013**, *9*, 3043–3050.
(63) Zimmerman, P. M. Growing String Method with Interpolation and Optimization in Internal Coordinates: Method and Examples. *J. Chem. Phys.* **2013**, *138*, 184102.
(64) Zimmerman, P. M. Single-Ended Transition State Finding with the Growing String Method. *J. Comput. Chem.* **2015**, *36*, 601–611.
(65) CYLview C.Y., Legault. Université de Sherbrooke, 2009 (http://www.cylview.org).

Chapter 3

Synthesis of Polyisocyanurate Prepolymer and the Resulting Flexible Elastomers with Tunable Mechanical Properties

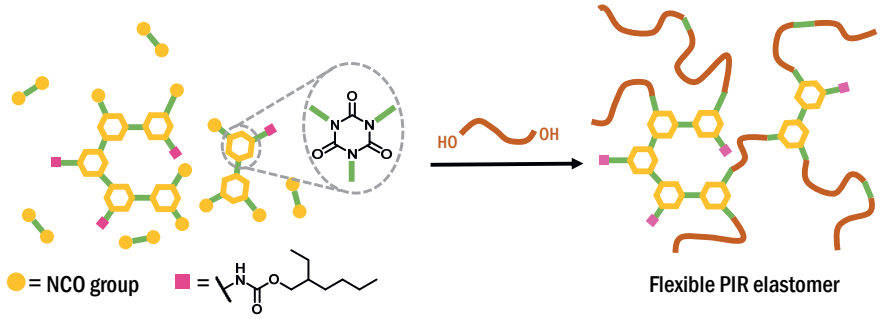

This chapter is based on published work:
Guo, Y.; Kleemann, J.; Bokern, S.; Kamm, A.; Sijbesma, R. P.; Tomović, Ž., Synthesis of polyisocyanurate prepolymer and the resulting flexible elastomers with tunable mechanical properties. *Polym. Chem.* **2023**, *14*, 1923–1932.

Polyurethane (PU) is used in a wide range of applications due to its diverse chemical and physical properties. To meet the increasing demands on thermal and mechanical properties of PU materials, polyisocyanurates (PIRs) have been introduced in PU materials as crosslinkers and due to their high decomposition temperature. We prepared a liquid PIR prepolymer with high PIR content by co-trimerization of 4,4'-methylene diphenyl diisocyanate (4,4'-MDI) and mono-isocyanates. The mono-isocyanate was synthesized *via* reaction between a 4,4'-MDI and a 2-ethyl-1-hexanol. The PIR prepolymer obtained was further reacted with long chain polyols and chain extenders in both solvent and solvent-free conditions, leading to PIR elastomers that exhibited good thermal stability with high char formation, and improved mechanical properties with much higher Young's modulus. This work demonstrates that the liquid PIR prepolymer can potentially be used in various large-scale industrial applications.

3.1 Introduction

Polyurethane (PU) is one of the most common polymers used to provide a wide range of materials, such as soft cushioning foams, rigid thermal insulation foams, elastomers, coatings and adhesives.[1-5] In terms of chemical structures, polyurethanes include various isocyanate-based bonds such as urethane, urea, uretdione, biuret, allophanate and isocyanurate, among which the isocyanurate structure exhibits a higher thermal decomposition temperature.[6-14] Therefore, the thermal stability of PU materials can be greatly enhanced by introducing isocyanurate or polyisocyanurate (PIR) structures, which is especially important for rigid thermal insulation foams.

In addition to PU rigid foams, researchers have been developing PIR elastomers *via* trimerization of isocyanate prepolymers obtained from the reaction between excess of isocyanate and long chain polyols, or *via in situ* synthesis with isocyanates, polyols and chain extender reacting in the presence of a trimerization catalyst.[15-20] However, the resulting PU materials in both cases have a relatively low PIR content due to the fast increase of viscosity and poor catalyst diffusion during trimerization reaction.

An alternative approach to obtain a PIR network with high concentration of isocyanurate structures is *via* direct trimerization of di- or polyisocyanate monomers, leading to a multi-functional PIR-containing isocyanate prepolymer.[21-26] However, high crosslink density as well as rigid isocyanurate structures lead to brittle solid PIR networks. To improve the processability and reduce the brittleness of the materials, co-trimerization of mono- and di-functional isocyanates has been reported to generate a flexible PIR network. For instance, di-functional isocyanate hexamethylene diisocyanate (HDI) was co-trimerized with mono-functional isocyanates such as butyl isocyanate or phenyl isocyanate.[22,27] By changing the ratio between HDI and mono-functional isocyanate, the mechanical properties of the polymer as well as the reaction kinetics can be adjusted. 4,4'-Methylene diphenyl diisocyanate (4,4'-MDI) was also co-trimerized with different mono-functional aliphatic or aromatic isocyanates, providing flexible PIR films with good thermal stability (T_{d5} > 400 ºC).[28,29] These studies provide a good way to prepare liquid PIR-containing isocyanate prepolymers containing controllable isocyanurate content and such prepolymer can be used to prepare PIR-PU elastomers in both solvent and solvent-free conditions. However, commercially available mono-functional isocyanates, such as phenyl and butyl isocyanates, are not suitable for industrial applications due to high toxicity caused by high vapor pressure.

In this chapter, an alternative strategy for synthesis of non-volatile mono-functional isocyanate is explored. The reaction between diisocyanate and mono-functional alcohol is used for the preparation of a mixture containing di- and mono-isocyanates that can be used to prepare flexible PIR prepolymers (**Scheme 3-1**). In this work, a mixture of mono- and di-functional isocyanates was synthesized by reacting excess of

4,4'-MDI with 2-ethyl-1-hexanol in a 1:0.25 molar ratio. The mixture was then co-trimerized and quenched by diethylene glycol bis-chloroformate (DGBCF) before solidification in order to get a liquid PIR prepolymer (**Scheme 3-2**). The PIR prepolymer was further used to prepare PIR elastomers by reacting the prepolymer with long chain polyol and chain extender in both solvent and bulk conditions. The elastomers obtained exhibit superior mechanical properties in addition to good thermal stability. The preparation of a liquid PIR prepolymer with high PIR content is a promising approach for the large-scale, solvent free production of thermally stable and mechanically strong PU materials, which is important for various real industrial applications.

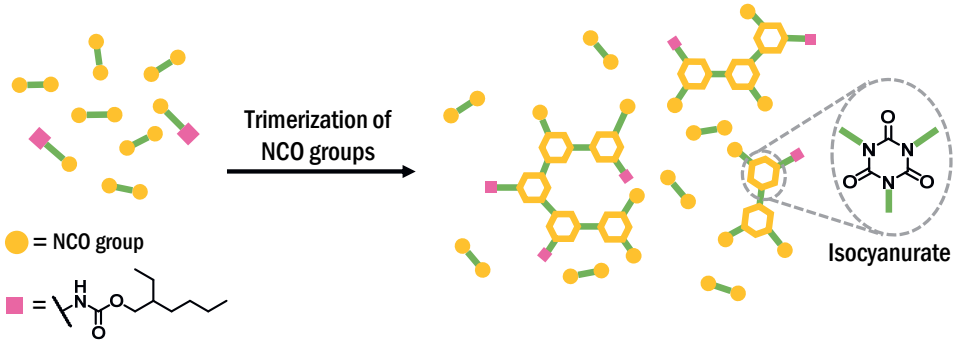

Scheme 3-1. PIR prepolymer obtained *via* co-cyclotrimerization of di- and mono-functional isocyanates.

3.2 Results and discussion

3.2.1 Synthesis of PIR prepolymer

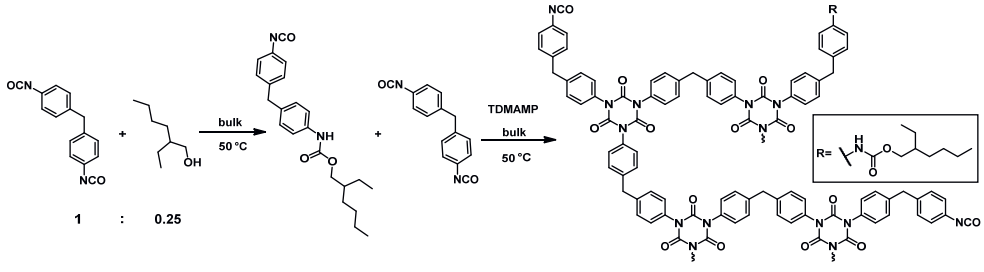

Scheme 3-2. Synthesis of PIR prepolymer.

Statistically, the reaction between 4,4'-MDI with 2-ethyl-1-hexanol leads to the formation of di-urethanes besides mono-urethanes. To minimize formation of di-urethanes, the selectivity of the reaction was studied. 4,4'-MDI was reacted with 2-ethyl-1-hexanol in various molar ratios and the reaction was performed by slowly dropping the alcohol into the isocyanate at the relatively low temperature of 50 °C.

The chemical composition of the obtained mixture was determined by gel permeation chromatography (GPC) (**Figure 3-1**).

With more mono-functional alcohol, the number of di-urethane structures increased. In order to minimize the formation of di-urethanes which do not contribute to the network, and maximize the mono-functional isocyanate content which helps to maintain a flexible PIR network in a final product, the optimized isocyanate-to-alcohol molar ratio of 1:0.25 was chosen, resulting in a mixture containing around 75 mol% di-functional isocyanate and 25 mol% mono-functional isocyanate.

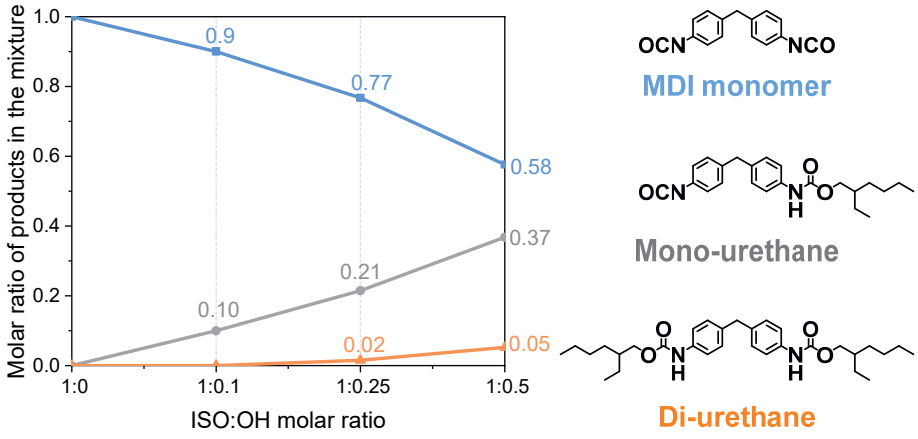

Figure 3-1. Product compositions of reaction mixtures obtained at various 4,4'-MDI to 2-ethyl-1-hexanol molar ratio. The reaction was carried out at 50 °C with 2-ethyl-1-hexanol being added dropwise to 4,4'-MDI. The ratio of different products was determined by GPC measurement.

The mixture obtained was further trimerized using a selection of common trimerization catalysts, mainly based on tertiary amines and Lewis basic salts with nucleophilic anions (**Scheme 3-3**). Various reaction conditions, such as reaction temperature and catalyst concentration, were investigated. 2,4,6-Tris(dimethylaminomethyl)phenol (TDMAMP)[6,31] was found to be the most suitable trimerization catalyst for PIR prepolymer preparation in terms of mildness of reaction conditions, and product processability and solubility. While some catalysts, for example, tetrabutylammonium acetate (TBAA),[32,33] potassium 2-ethylhexanoate[34-37] and 2-{[2-(dimethylamino)ethyl]methylamino}ethanol (DMAEMAE)[38] were too active to be controlled, others, such as sodium *p*-toluenesulfinate (*p*-TolSO$_2$Na)[39] and potassium acetate[40,41] had poor solubility in either solvents or isocyanate. *N,N',N"*-tris(3-dimethylaminopropyl)hexahydro-1,3,5-triazine (TDMAPHT)[7,42,43] provided more allophanate and less isocyanurate than TDMAMP (**Figure S3-1** and **S3-2**), and [HTBD][OAc][30] (a conjugate between 1, 5, 7-triazabicyclo [4.4.0] dec-5-ene and acetic acid), which catalyzes cyclotrimerization of isocyanates *via* synergistic hydrogen

bonding functional catalytic mechanism, was deactivated most probably due to the presence of urethane groups in the mixture.

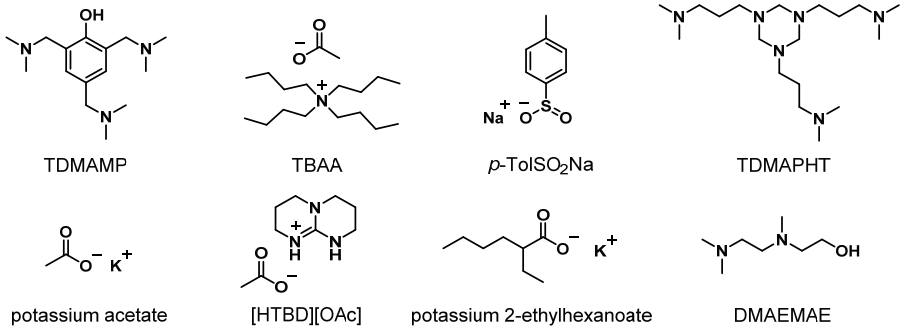

Scheme 3-3. Structures of various cyclotrimerization catalysts.

The isocyanate trimerization mechanism using TDMAMP as a catalyst was further studied by cyclotrimerization of *p*-tolyl isocyanate in the presence of one equivalent 2-ethylhexyl *p*-tolylcarbamate in deuterated acetone at 50 ºC. In agreement with the mechanism proposed by Nabulsi and Schwetlick, the NMR spectroscopy studies show that in the presence of carbamate, the cyclotrimerization follows an allophanate pathway (**Scheme 3-4** and **Figure 3-2**).[41,42] In this mechanism, the isocyanate first reacts with carbamate to form allophanate as a key intermediate. Next, the allophanate decomposes to anionic species **B** or **C** by elimination of carbamate or alcohol, finally followed by ring closure to form isocyanurate. However, in the model reaction, around 10 mol% of allophanate was still present after 34 h reaction due to the limited catalytic activity of the TDMAMP in highly diluted solution.

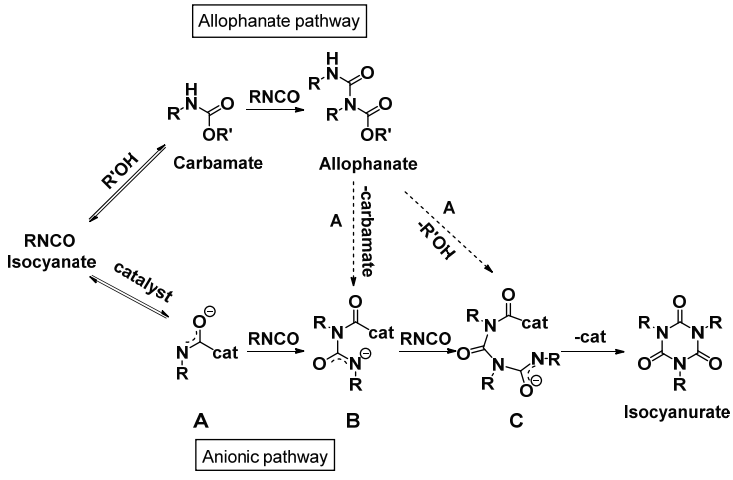

Scheme 3-4. Proposed cyclotrimerization mechanism of isocyanates *via* allophanate and anionic pathways.

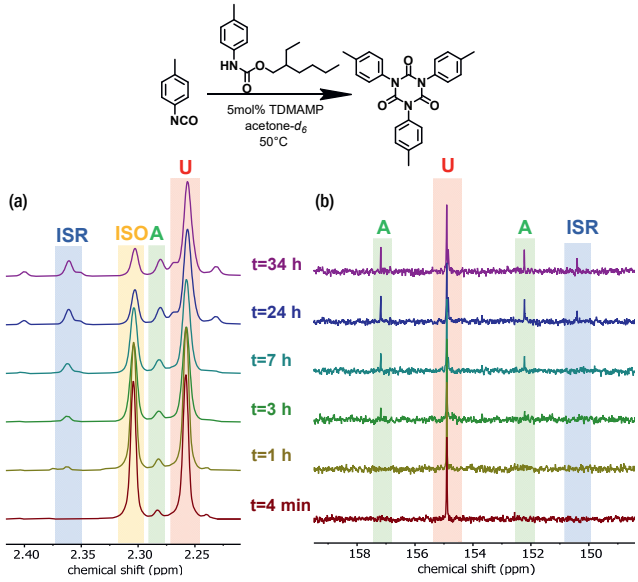

Figure 3-2. (a) ^{1}H NMR spectra (400 MHz, acetone-d_6) and (b) ^{13}C NMR spectra (100 MHz, acetone-d_6) of reaction between *p*-tolyl isocyanate and 2-ethylhexyl *p*-tolylcarbamate in 1:1 molar ratio at 50 °C using 5 mol% TDMAMP as catalyst. The reaction was carried out in an NMR tube in deuterated acetone and monitored by (a) peaks between 2.2 and 2.4 ppm (methyl group protons), and (b) peaks between 148 and 158 ppm (carbonyl carbons). ISO (*p*-tolyl isocyanate); U (carbamate); A (allophanate); ISR (isocyanurate).

Based on the catalyst screening, the trimerization of mono- and di-functional isocyanate mixture was carried out at 50 °C in bulk with TDMAMP as the catalyst; the PIR reaction was quenched with DGBCF before solidification could take place (**Figure 3-3a** and **3b**). The resulting PIR prepolymer was further characterized by quantitative ^{13}C NMR spectroscopy to quantify the molar ratio of urethane (U), allophanate (A) and isocyanurate (ISR) with the help of chromium (III) acetylacetonate ($Cr(acac)_3$) as relaxation agent.[44-46] Carbonyl carbon peaks were assigned to the urethane, allophanate and isocyanurate carbonyl atoms and integrated to give a ratio of U:A:ISR of 1:0.5:1.0 (**Figure 3-3c**).[26,47] In addition, NCO content was determined as 16.0 wt% by back-titration, and the average molar mass of the PIR prepolymer, 660 g/mol, was determined by GPC measurement (**Figure 3-3d**), from which the functionality f_n of the PIR prepolymer was calculated to be 2.5 *via* the following equation:

$$f_n = \frac{NCO\ content \times n_{prepolymer} \times M_{prepolymer}}{n_{prepolymer} \times M_{NCO} \times 100\ wt\%}$$

$$= \frac{16\ wt\% \times 660\ g/mol}{42\ g/mol \times 100\ wt\%} = 2.5$$

where $n_{prepolymer}$ is the mole amount of prepolymer, M_{NCO} is the molecular weight of NCO group, $M_{prepolymer}$ is the number average molecular weight of prepolymer.

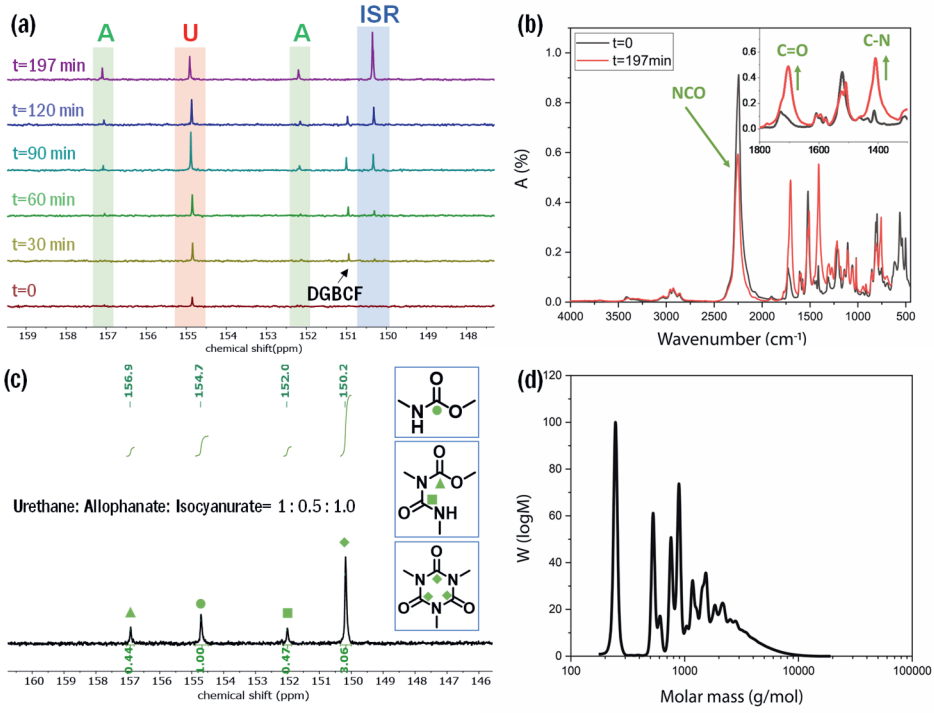

Figure 3-3. (a) ^{13}C NMR spectra (100 MHz, acetone-d_6) of the co-trimerization of mono- and di-functional isocyanates. U (carbamate); A (allophanate); ISR (isocyanurate). (b) FT-IR spectra of PIR prepolymer. (c) Quantitative ^{13}C NMR spectrum (125 MHz, acetone-d_6) of the PIR prepolymer. The ratio of U:A:ISR was determined by integrals of the carbonyl carbon peaks. (d) GPC trace of the PIR-DEHP prepolymer, obtained M_n = 710 g/mol.

3.2.2 Preparation of PIR elastomers in solution

PIR elastomers were prepared by the reaction of a PIR prepolymer with two commercially available polyether polyol or polyester polyol with molecular weight of 2000 g/mol, PolyTHF® 2000 (PTHF) and Lupraphen® 6601/2 (Lupraphen), using different amounts of 1,4-butanediol (BDO) as chain extender (0, 5 wt%, 10 wt%, 15 wt% of the polyol component). The molar ratio of NCO:OH was kept constant at 1.05 (index 105), which was typically used in industrial applications,[48,49] and the elastomers were cast from THF solution (**Table 3-1**). All elastomers were transparent.

In addition, a commercially available polymeric MDI with functionality of 2.7, Lupranate® M20 (M20), was used to compare with PIR prepolymer due to the similar average functionality. Using the same procedure and conditions, M20 elastomers were prepared by reacting M20 and PTHF or Lupraphen with either 0 or 15 wt% BDO. Classical linear 4,4'-MDI-based elastomers are synthesized from reaction of 4,4'-MDI, polyol and BDO without trimerization.

Table 3-1. Recipes (by weight percentage) of solution-cast elastomers (Index 105).

	PIR elastomers				M20 elastomers		4,4'-MDI based elastomer
BDO in polyol component (wt%)	0	5	10	15	0	15	15
PIR prepolymer	21.7	36.3	46.3	53.6	--	--	--
4,4'-MDI	--	--	--	--	--	--	35.4
M20	--	--	--	--	12.3	36.9	--
PTHF/Lupraphen	78.3	60.5	48.3	39.4	87.7	53.6	54.9
BDO	--	3.2	5.4	7.0	--	9.5	9.7

The thermal stability of the PIR elastomers was measured with thermogravimetric analysis (TGA), the results of which are shown in **Table 3-2** and **Figure 3-4**. With a higher BDO content, the decomposition temperatures of PIR elastomers at 5% weight loss (T_{d5}) and 10% weight loss (T_{d10}) slightly decreased due to the presence of more urethane bonds in the material. However, as the amount of PIR structures and the aromatic content also increased, higher char formation was obtained at 596 ºC. The decomposition temperatures and char formation of M20-based elastomers were slightly higher than PIR elastomers, which may be due to a higher crosslink density. On the other hand, all PIR elastomers showed better thermal stability than classical 4,4'-MDI-based elastomers (**Figure 3-4e** and **4f**).

Table 3-2. TGA results of PIR and M20 elastomers with PTHF or Lupraphen polyol, and different amount of BDO.

BDO content (wt%)	Aromatic content[a] (wt%)	PTHF			Lupraphen		
		T_{d5} (ºC)	T_{d10} (ºC)	Char formation (%)	T_{d5} (ºC)	T_{d10} (ºC)	Char formation (%)
PIR elastomers							
0	19	297.8	329.0	7.2	290.8	311.4	7.3
5	32	277.7	306.6	10.4	284.1	302.2	10.6
10	41	270.0	296.2	14.0	275.1	291.5	7.2
15	47	270.1	294.2	15.2	268.5	286.2	14.9
M20 elastomers							
0	12	321.8	345.1	7.8	312.4	336.2	7.5
15	37	294.3	311.0	16.9	289.1	306.5	16.6
4,4'-MDI-based elastomers							
15	35	272.7	285.2	9.3	278.5	294.5	13.0

[a] The aromatic content is calculated based on the weight percentage of aromatic isocyanate in the elastomers (see experimental section).

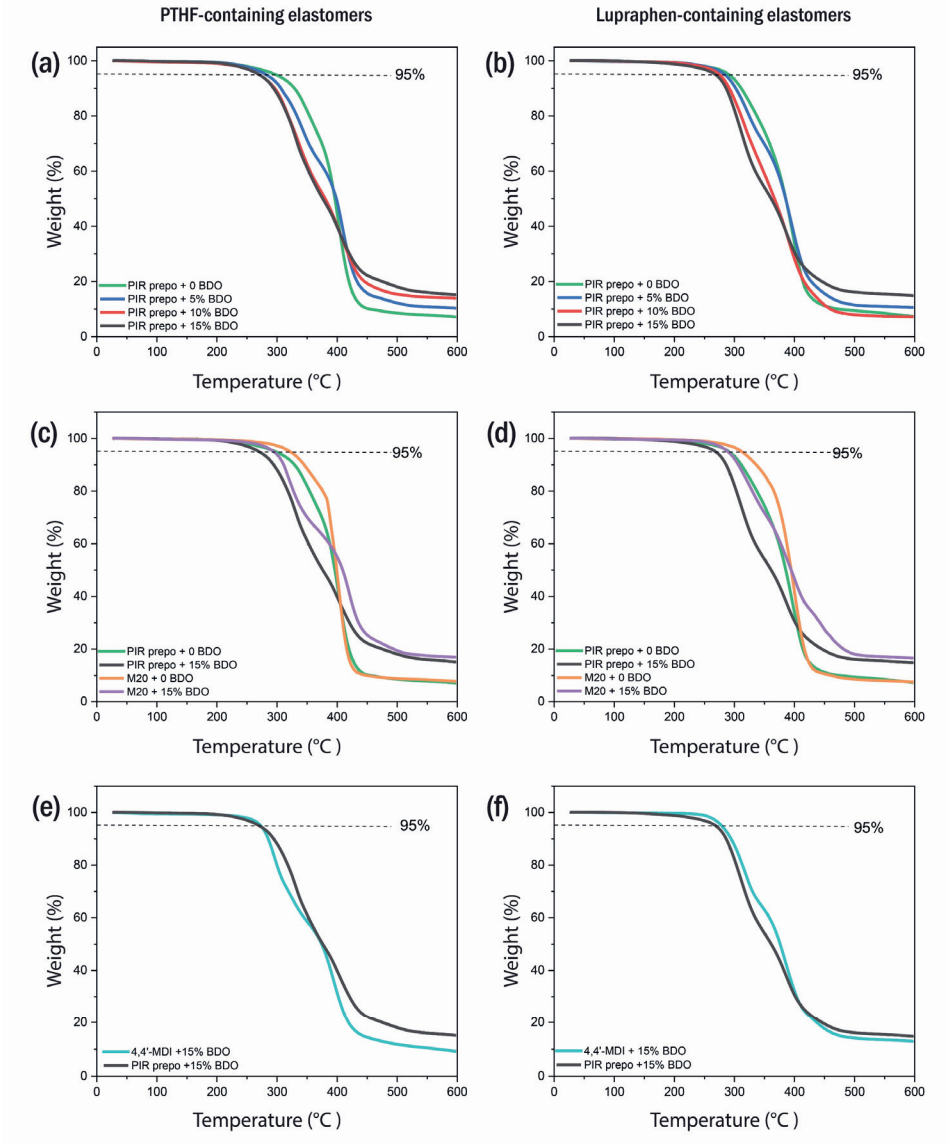

Figure 3-4. TGA curves of (a) PTHF-containing and (b) Lupraphen-containing PIR elastomers with different amount of BDO; (c) PTHF-containing and (d) Lupraphen-containing PIR and M20 elastomers with 0 and 15 wt% BDO; (e) PTHF-containing and (f) Lupraphen-containing PIR and 4,4'-MDI-based elastomers with 15 wt% BDO.

A significant difference in mechanical properties was found between PIR elastomers and M20 elastomers (**Figure 3-5** and **Table 3-3**). Compared to M20 elastomers with the same amount of BDO in polyol component (purple curve), the tensile strength and Young's modulus of PIR elastomer (black curve) was much higher due to a higher aromatic content and the presence of PIR structures. In addition, with alkyl chains that

improved flexibility of the PIR network, the elongation at break of the PIR elastomers was also higher than in the corresponding M20 elastomers. The only exception is that the PIR elastomer containing PTHF and 15 wt% BDO has a slightly lower elongation at break than M20 elastomer with PTHF and with the same amount of BDO in polyol component. The higher Young's modulus leads to lower elongation at break as shown in **Table 3-3**. Although the elastomer based on PIR prepolymer has around 12 times higher Young's modulus relative to M20 based elastomer, the elongation at break is still very high due to the presence of flexible alkyl chains. The same trend is also visible for the Lupraphen-containing elastomers. The obtained absolute values are the result of a complex interplay of different parameters, such as polarity or compatibility of PTHF with hard phase, glass transition temperature (T_g) of elastomers and hard phase content in the PIR prepolymer.

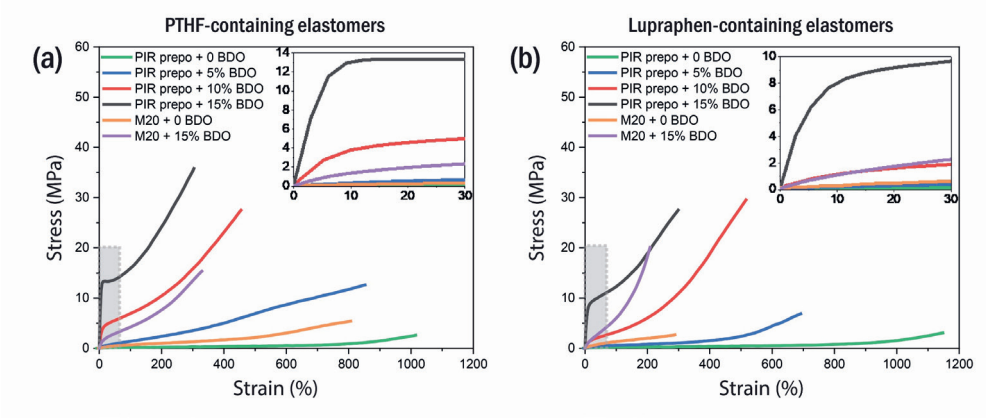

Figure 3-5. Tensile test of PIR and M20 elastomers based on (a) PTHF and (b) Lupraphen, and different amounts of BDO. The inserts show the slopes of the curves which are correlated to Young's modulus of the elastomers.

Table 3-3. Tensile test results of PIR and M20 elastomers with PTHF or Lupraphen polyol, and different amounts of BDO.

BDO content (wt%)	PTHF			Lupraphen		
	Tensile strength (MPa)	Elongation at break (%)	Young's modulus (MPa)[a]	Tensile strength (MPa)	Elongation at break (%)	Young's modulus (MPa)[a]
PIR elastomers						
0	2.5	1000	0.3	2.6	1190	0.3
5	13.5	845	2.9	6.6	703	1.1
10	26.8	453	47.9	28.2	500	8.3
15	36.3	310	173.9	28.7	314	81.1
M20 elastomers						
0	5.4	807	0.9	2.7	288	1.9
15	15.4	329	14.7	20.1	208	12.2

[a] The Young's modulus is calculated by the initial linear slope of the tensile curve.

Dynamic mechanical analysis (DMA) measurements were performed on the polymers and the maximum in the loss tangent tan(δ) was used to determine T_g. The results are shown in **Figure 3-6** and **Table 3-4**. The PIR structures and aromatic content increased with BDO content, and the resulting T_g as well as the storage modulus at rubbery plateau of the PIR elastomers increased. The PIR elastomer based on PTHF without BDO had a narrow tan(δ) peak (green curve in **Figure 3-6a**) with a maximum at -49 °C, which is strongly influenced by the T_g of PTHF polyol. When there was no BDO in the elastomer, cold crystallization with subsequent melting of PTHF was found between -30 to 30 °C.[50] The presence of BDO limited the crystallization tendency of PTHF, thus no cold crystallization peaks were found in the curves of elastomers containing BDO. The broad tan(δ) peaks of PIR elastomers containing PTHF and BDO indicate that there might be phase separation between PTHF and hard segments in the elastomers. On the other hand, due to the good compatibility of the PIR prepolymer and the polyester polyol Lupraphen, only one narrow tan(δ) peak was observed in each Lupraphen-containing elastomer which increased with higher PIR and aromatic content. In comparison to PIR elastomers, M20 elastomers have lower T_g, which was caused by the absence of PIR structures and lower aromatic content.

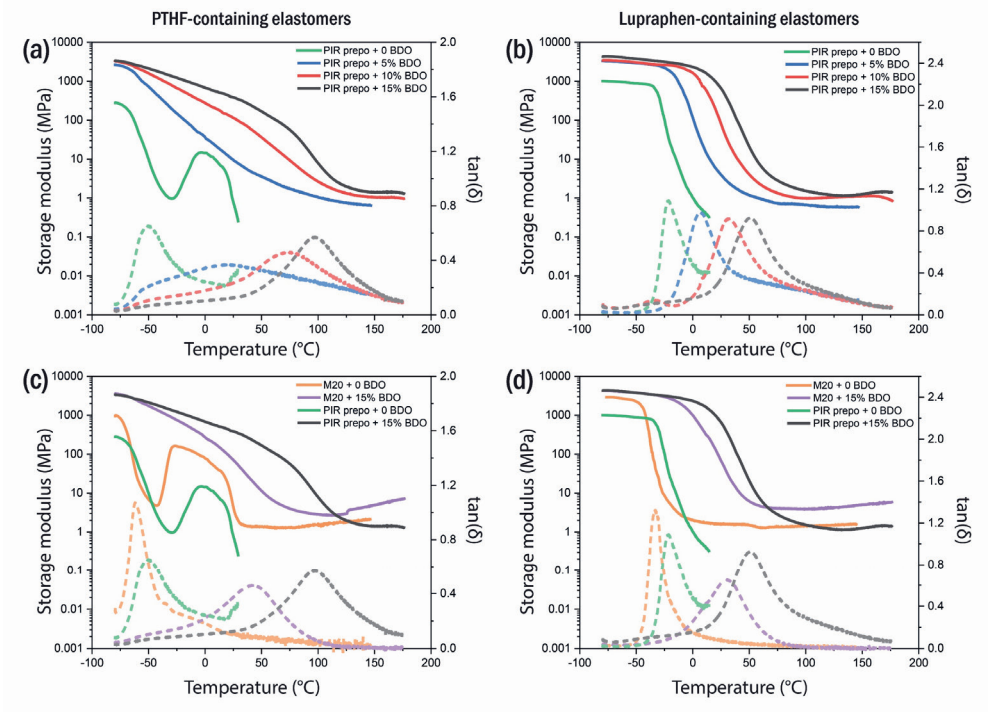

Figure 3-6. DMA results of (a) PTHF-containing and (b) Lupraphen-containing PIR elastomers with different amount of BDO; (c) PTHF-containing and (d) Lupraphen-containing PIR and M20 elastomers with 0 and 15 wt% BDO. Solid line: storage modulus, dash line: tan(δ).

Table 3-4. DMA data of PIR and M20 elastomers with PTHF or Lupraphen polyol, and different amounts of BDO.

PTHF		Lupraphen	
PIR elastomers			
BDO content (wt%)	T_g (°C)	BDO content (wt%)	T_g (°C)
0	-49	0	-22
5	-55, -20	5	7
10	-54, 74	10	32
15	-52, 95	15	51
M20 elastomers			
0	-61	0	-35
15	43	15	30

3.2.3 Preparation of PIR elastomers in bulk

PIR elastomers were also prepared by reacting a PIR prepolymer with Lupraphen without solvent (**Table 3-5**). A PIR prepolymer with NCO content of 16.5 wt% for bulk casting of elastomers was synthesized *via* the same procedure as that for solution casting of elastomers. The PIR prepolymer and the polyol component (Lupraphen, BDO and urethane catalyst) were mixed and the elastomers were prepared at 80 °C in bulk. The trend of increasing char formation and T_g with increasing PIR and aromatic content observed in solvent-cast elastomers was also observed in bulk-cast elastomer (**Figure 3-7**). Similar trends were observed in mechanical properties of elastomers using either of the two preparation methods. When BDO content was increased from 10 wt% to 15 wt%, the Young's modulus of PIR elastomers increased from 2.6 MPa to 116.7 MPa respectively, while the bulk-cast M20 elastomers with Lupraphen and 15 wt% BDO had Young's modulus of only 20.6 MPa. Despite the same trend of mechanical properties, the bulk-cast PIR elastomers with 15 wt% BDO prepared from bulk has higher Young's modulus compared to that prepared from solution (116.7 MPa *vs*. 81.1 MPa).[51]

Table 3-5. Recipes (by weight percentage) of bulk-cast elastomers (Index 105).

	PIR elastomers			M20
BDO in polyol component (wt%)	5	10	15	15
PIR prepolymer	35.5	45.5	52.8	--
M20	--	--	--	36.9
Lupraphen	61.3	49.1	40.1	53.6
BDO	3.2	5.4	7.1	9.5

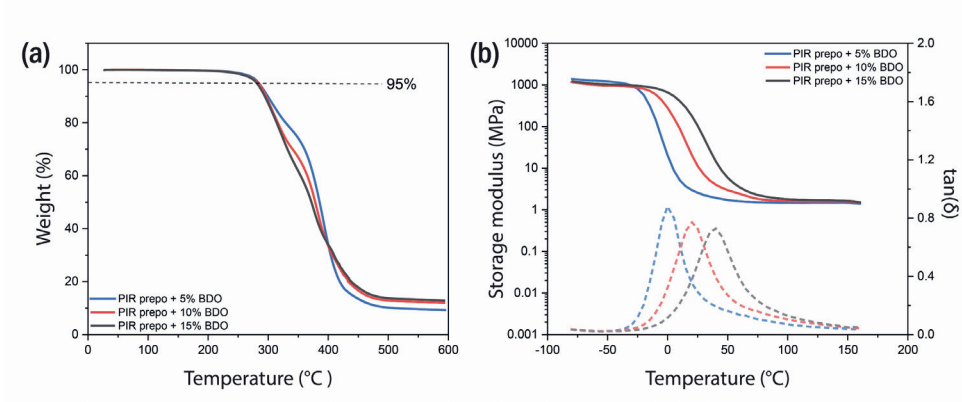

Figure 3-7. (a) TGA and (b) DMA results of the PIR elastomers cast in bulk with Lupraphen as a polyol and different amount of BDO. Solid line: storage modulus, dash line: tan(δ).

3.3 Conclusion

In this work, PIR prepolymers were synthesized from co-trimerization of mono- and di-isocyanates, and isocyanurate containing elastomers were prepared from PIR prepolymers. TDMAMP turned out to be the most suitable catalyst for the preparation of prepolymers due to high isocyanurate content after isocyanate trimerization, mild reaction conditions and the possibility to be quenched after a certain reaction time. In the final products, the PIR elastomers, char formation at 596 °C, T_g as well as Young's modulus increased with increasing PIR and aromatic content. In addition, the mechanical properties of PIR elastomers (stress at break, elongation and Young's moduli) are much better than the elastomers cast from commercially available polymeric MDI.

This study provides an elegant synthetic pathway to obtain liquid, flexible elastomer networks with high PIR content and good thermal stability as well as superior mechanical properties. It is expected that by substituting 2-ethyl-1-hexanol with other mono-functional alcohols, or by adjusting the molar ratio of mono- and di-functional isocyanates, the chemical, physical and mechanical properties, such as polarity, rigidity and thermal stability of the PIR prepolymer can be tuned. The PIR prepolymer with versatile properties will be suitable for diverse large-scale industrial applications.

3.4 Experimental section

Materials

2-Ethyl-1-hexanol (≥99.6%), *p*-tolyl isocyanate (99%), 2,4,6-tris(dimethylaminomethyl)phenol (TDMAMP) (>95%), tetrabutylammonium acetate (97%), sodium *p*-toluenesulfinate (*p*-TolSO_2Na) (95%), potassium acetate (≥99%), 2-{[2-

(dimethylamino)ethyl]methylamino}ethanol (DMAEMAE) (98%), chromium (III) acetylacetonate ($Cr(acac)_3$) (99.99% trace metals basis), 1,4-butanediol (BDO) (99%) and dibutyltin dilaurate (DBTL) (95%) were purchased from Sigma-Aldrich. Potassium 2-ethylhexanoate (>95%) was purchased from TCI. [HTBD][OAc] was synthesized following a literature procedure.[30] 1,4-Butanediol was dried over mol-sieves, all other reagents were used directly without treatment. 4,4'-Methylene diphenyl diisocyanate (4,4'-MDI), polymeric MDI Lupranate® M20 (M20), *N,N',N"*-tris(3-dimethylaminopropyl)hexahydro-1,3,5-triazine (TDMAPHT), diethylene glycol bis-chloroformate (DGBCF), 1,4-diazabicyclo[2.2.2]octane (DABCO)-based urethane gel catalyst Lupragen® N202, PolyTHF® 2000 with molecular weight of 2000 g/mol (OH_v = 56 mg KOH/g), and Lupraphen® 6601/2 with molecular weight of 2000 g/mol (polyester polyol synthesized from adipic acid, 1,4-butanediol and mono ethylene glycol, OH_v = 56 mg KOH/g) were kindly provided by BASF Polyurethanes GmbH. Polyols were dried at 80 ºC under vacuum for 2 h before use. THF (containing BHT as stabilizer) and toluene were purchased from Biosolve, and THF was dried over mol-sieves overnight before use.

Synthesis

Synthesis of PIR prepolymer. 4,4'-MDI (184.0 g, 0.74 mol) in a dry 3-neck flask equipped with a dropping funnel was stirred under an Ar flow at 50 ºC in an oil bath. 2-Ethyl-1-hexanol (24.0 g, 0.18 mol) was added in the dropping funnel and dropped into the flask at a speed of 1 drop every 10 s with the internal temperature kept under 55 ºC. The reaction was immediately completed after addition of the alcohol and the mixture was calculated to have average molecular weight of 282.6 g/mol with f_n of 1.75.

The isocyanate mixture (169.9 g, 0.60 mol) was added to a dry beaker under an Ar flow. Trimerization catalyst TDMAMP (0.1 g, 0.53 mmol) was dissolved in 6 mL THF and was quickly injected into the isocyanate mixture. The mixture was stirred at 50 ºC in an oil bath with an anchor-shape stirrer and the internal temperature as well as the torque were monitored by the mechanical stirrer. After 200 min, the co-trimerization was quenched with DGBCF (0.1 g, 0.53 mmol) in 2 mL THF. The reaction was monitored with ^{13}C NMR spectroscopy and the product was characterized with FT-IR spectroscopy. After that, the NCO content of the PIR prepolymer was titrated and the prepolymer was used for casting elastomers in solution. For bulk-cast elastomers, the same procedure was used except that the catalyst amount was 0.1 mol%.

Synthesis of 2-ethylhexyl-p-tolylcarbamate. *p*-Tolyl isocyanate (1.6 g, 12.18 mmol), 2-ethyl-1-hexanol (1.8 g, 13.39 mmol) and toluene (5 mL) were added in a 3-neck flask equipped with a condenser under an Ar atmosphere. The mixture was stirred and heated to 50 ºC until the NCO stretching band at 2270 cm^{-1} disappeared according to

FT-IR spectroscopy. After that, solvent was evaporated, the mixture was purified by column chromatography and transparent liquid was obtained. ^{1}H NMR (400 MHz, acetone-d_6): δ 8.49 (s, 1H), 7.44 (d, J = 8.2 Hz, 2H), 7.09 (d, 2H), 4.21 – 3.89 (m, 2H), 2.26 (s, 3H), 1.59 (hept, 1H), 1.51 – 1.17 (m, 8H), 1.00 – 0.81 (m, 6H) ppm; ^{13}C NMR (400 MHz, acetone-d_6): δ 153.8, 136.9, 131.6, 129.1, 118.2, 66.4, 39.1, 30.2, 23.5, 22.8, 19.9, 13.5, 10.5 ppm.

Preparation of PIR elastomers in solution. The preparation of PIR elastomer with PolyTHF® 2000 and 15 wt% BDO is used as an example to illustrate the synthetic route: The PIR prepolymer (2.9 g, NCO content = 16.0 wt%) was dissolved in 15 mL dry THF in a dry 1-neck flask at room temperature. The polyol component solution was prepared by dissolving PolyTHF® 2000 (2.1 g, 1.07 mmol), BDO (0.4 g, 4.18 mmol) and DBTL (7.0 mg, 0.01 mmol, 0.1 mol% to the NCO groups) in 5 mL dry THF in another dry 1-neck flask at room temperature. Then the polyol solution was added into the prepolymer solution and the mixture obtained was stirred for 1 min under an Ar atmosphere. The solution was poured on a metal lid which was preheated at 50 ºC in a N_2 oven and the elastomer was cured overnight. After that, the elastomer was dried at 80 ºC vacuum oven for one day to remove solvent. The same procedures and the same conditions were used for the preparation of PIR elastomers, 4,4'-MDI based classical elastomers, and M20 based elastomers in solution.

Calculation of aromatic content. As the PIR prepolymer is trimerized from a mixture containing 184 g 4,4'-MDI and 24 g 2-ethyl-1-hexanol, which means that there is 88.5 wt% isocyanate contained in PIR prepolymer. The aromatic content of PIR elastomers with 15% BDO, for example, can be calculated as: 53.6% × 88.5% = 47%. The aromatic content of 4,4'-MDI based elastomer and M20 elastomers is the amount of isocyanate that was used.

Preparation of elastomers in bulk. The preparation of PIR elastomer with Lupraphen® 6601/2 and 15 wt% BDO is used as an example to illustrate the synthetic route: The PIR prepolymer was kept in a vacuum oven overnight at 50 ºC. The polyol component that consisted of Lupraphen® 6601/2 (64.2 g, 0.03 mol), BDO (11.4 g, 0.13 mol) and Lupragen® N202 (0.1 g) was added in a sealed polypropylene cup and stirred at 1000 rpm under vacuum in a speedmixer for 10 min at 50 ºC. PIR prepolymer (84.5 g, NCO content = 16.5 wt%) was added and the mixture was mixed in a speedmixer for 30 s under vacuum. After that, the mixture was poured on a preheated metal mold at 80 ºC. The elastomers were further cured in an 80 ºC oven overnight. The same procedure and conditions were used for the preparation of PIR and M20 elastomers in bulk.

Characterization

Fourier-transform infrared spectroscopy (FT-IR). FT-IR spectroscopy was carried out in attenuated total reflection mode on a Spectrum Two (Perkin Elmer) spectrometer at room temperature. 8 scans were performed from 4000 - 450 cm^{-1}.

Nuclear magnetic resonance (NMR) spectroscopy. ^{1}H NMR spectroscopy was performed using a Bruker UltraShield 400 MHz or Varian Mercury 400 MHz spectrometer at room temperature using acetone-d_6 as solvent with TMS as internal standard with a delay time of 1s and 32 scans per spectrum. ^{13}C NMR spectroscopy for monitoring the PIR reaction were performed using either Bruker UltraShield 400 MHz or Varian Mercury 400 MHz spectrometer at room temperature using acetone-d_6 as solvent with TMS as internal standard with a delay time of 2 s and 256 scans per spectrum. Quantitative ^{13}C NMR spectroscopy for determining the urethane, allophanate and isocyanurate ratio were performed on a Varian Unit Inova 500 MHz spectrometer using acetone-d_6 as solvent with TMS as internal standard at room temperature with a delay time of 12 s, 2048 scans per spectrum and $Cr(acac)_3$ (20 mg/mL) as a relaxation agent.

Determination of isocyanate content. The titration of NCO groups was performed on a 916 Ti-Touch titration machine (Metrohm) equipped with an electrode using tetraethylammonium bromide (0.4 mol/L in ethylene glycol) as electrolyte. The isocyanate was quenched with excess of dibutylamine and unreacted dibutylamine was titrated with 1M HCl as the titrant. After getting the volume (V_1) at the end of titration of sample as well as the volume (V_0) of the blank titration at the same condition, the NCO content was calculated by the titration machine using the following equation:

$$NCO\ content = \frac{(V_1 - V_0) \times c_{HCl} \times M_{NCO}}{m_{sample}}.$$

Gel permeation chromatography (GPC). The average molecular weight of the PIR prepolymer was measured on a GPC system comprising a series of columns (one PSS-SDV 500 Å (5µm) and three Agilent PL-Gel 500 Å (5µm) columns) and a UV detector. THF was used as the eluent with a flow rate of 1 mL/min and toluene was used as internal standard. Calibration was done with monodisperse PMMA and Lupranate® M20 samples. GPC for studying selectivity of 4,4'-MDI and 2-ethyl-1-hexanol reaction was performed on a series of columns including four Agilent PL-Gel-Columns (1 × 50 Å - 3 × 100 Å) equipped with a UV detector and a differential refractometer. THF was used as the eluent with a flow rate of 0.5 mL/min. The system was calibrated by Basonat® HI 100 NH with molecular weight range 2200 – 168 g/mol.

Thermogravimetric analysis (TGA). TGA measurement was performed on a TA Q500 or TA Q550 (TA Instruments) under N_2 atmosphere. Samples (around 10 mg) were heated from 28 to 600 °C at a rate of 10 °C/min.

Tensile testing. Tensile testing was performed on a EZ20 (Lloyd instrument) with a 500 N load cell. The tensile bars used had an effective length of 12 mm, width of 2 mm and thickness of 0.6 mm. The elongation rate used was 50 mm/min.

Dynamic mechanical analysis (DMA). DMA measurement was measured on a DMA Q850 (TA Instruments) with a film tension setup. The test bars had a width of 5.3 mm, thickness of 0.6 mm and effective length of around 20 mm. For each measurement, a temperature ramp from -80 to 180 °C was programmed with a heating rate of 3 °C/min at a frequency of 1.0 Hz. A preload force of 0.01 N, an amplitude of 100 µm and a force track of 115% were used. The storage and loss modulus were recorded as a function of temperature. The glass transition temperature (T_g) was determined from the peak maximum of the tan(δ).

Supplementary data

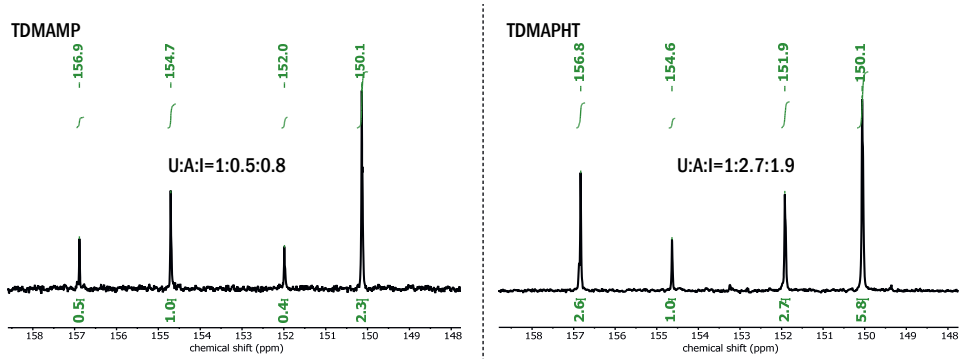

Figure S3-1. ^{13}C NMR spectra (100MHz, acetone-d_6) of synthesized PIR prepolymer using TDMAMP or TDMAPHT as trimerization catalyst. The molar ratio of allophanate to isocyanurate was 0.6:1 and 1.4:1 respectively.

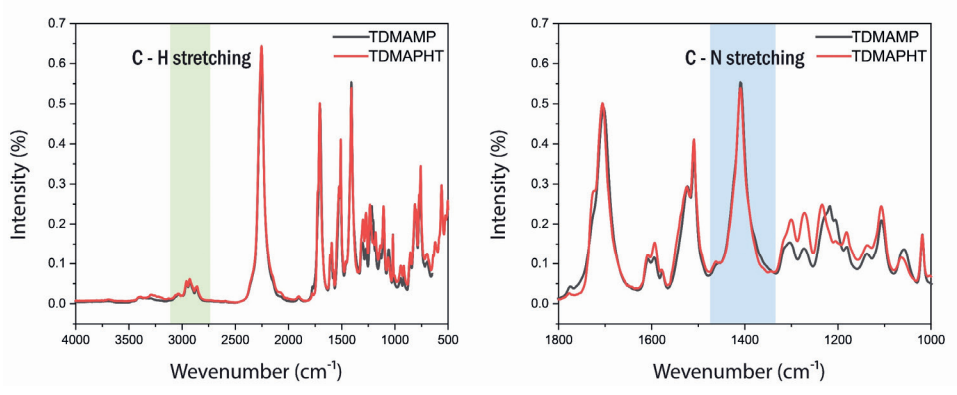

Figure S3-2. FT-IR spectra of PIR prepolymer using TDMAMP or TDMAPHT as trimerization catalyst. After normalization based on the area of C-H stretching (3110-2770 cm^{-1}) of TDMAMP curve, the area of isocyanurate C-N stretching (1474-1338cm^{-1}) was 16.8 and 14.8 respectively, which means that more isocyanurate was formed when TDMAMP was used as trimerization catalyst.

3.5 References

(1) Engels, H. W.; Pirkl, H. G.; Albers, R.; Albach, R. W.; Krause, J.; Hoffmann, A.; Casselmann, H.; Dormish, J. Polyurethanes: Versatile Materials and Sustainable Problem Solvers for Today's Challenges. *Angew. Chemie - Int. Ed.* **2013**, *52*, 9422–9441.

(2) Randall, D.; Lee, S. *The Polyurethanes Book*; Wiley, 2003.

(3) Eling, B.; Tomović, Ž.; Schädler, V. Current and Future Trends in Polyurethanes: An Industrial Perspective. *Macromol. Chem. Phys.* **2020**, *2000114*, 1–11.

(4) Delebecq, E.; Pascault, J. P.; Boutevin, B.; Ganachaud, F. On the Versatility of Urethane/Urea Bonds: Reversibility, Blocked Isocyanate, and Non-Isocyanate Polyurethane. *Chem. Rev.* **2013**, *113*, 80–118.

(5) Akindoyo, J. O.; Beg, M. D. H.; Ghazali, S.; Islam, M. R.; Jeyaratnam, N.; Yuvaraj, A. R. Polyurethane Types, Synthesis and Applications-a Review. *RSC Adv.* **2016**, *6*, 114453–114482.

(6) Kordomenos, P. I.; Kresta, J. E. Thermal Stability of Isocyanate-Based Polymers. 1. Kinetics of the Thermal Dissociation of Urethane, Oxazolidone, and Isocyanurate Groups. *Macromolecules* **1981**, *14*, 1434–1437.

(7) Kordomenos, P. I.; Kresta, J. E.; Frisch, K. C. Thermal Stability of Isocyanate-Based Polymers. 2. Kinetics of the Thermal Dissociation of Model Urethane, Oxazolidone, and Isocyanurate Block Copolymers. *Macromolecules* **1987**, *20*, 2077–2083.

(8) Reymore, H. E.; Carleton, P. S.; Kolakowski, R. A.; Sayigh, A. A. R. Isocyanurate Foams: Chemistry, Properties and Processing. *J. Cell. Plast.* **1975**, *11*, 328–344.

(9) Wang, C. L.; Klempner, D.; Frisch, K. C. Morphology of Polyurethane- Isocyanurate Elastomers. *J. Appl. Polym. Sci.* **1985**, *30*, 4337–4344.

(10) Kogon, I. C. New Reactions of Phenyl Isocyanate and Ethyl Alcohol. *J. Am. Chem. Soc.* **1956**, *78*, 4911–4914.

(11) Duff, D. W.; Maciel, G. E. Monitoring the Thermal Degradation of an Isocyanurate-Rich MDI-Based Resin by ^{15}N and ^{13}C CP/MAS NMR. *Macromolecules* **1991**, *24*, 651–658.

(12) Chattopadhyay, D. K.; Webster, D. C. Thermal Stability and Flame Retardancy of Polyurethanes. *Prog. Polym. Sci.* **2009**, *34*, 1068–1133.

(13) Xu, Q.; Hong, T.; Zhou, Z.; Gao, J.; Xue, L. The Effect of the Trimerization Catalyst on the Thermal Stability and the Fire Performance of the Polyisocyanurate-Polyurethane Foam. *Fire Mater.* **2018**, *42*, 119–127.

(14) Dick, C.; Dominguez-Rosado, E.; Eling, B.; Liggat, J. J.; Lindsay, C. I.; Martin, S. C.; Mohammed, M. H.; Seeley, G.; Snape, C. E. The Flammability of Urethane-Modified Polyisocyanurates and Its Relationship to Thermal Degradation Chemistry. *Polymer (Guildf).* **2001**, *42*, 913–923.

(15) Samborska-Skowron, R.; Balas, A. An Overview of Developments in Poly(Urethane-Isocyanurates) Elastomers. *Polym. Adv. Technol.* **2002**, *13*, 653–662.

(16) Driest, P. J.; Dijkstra, D. J.; Stamatialis, D.; Grijpma, D. W. The Trimerization of Isocyanate-Functionalized Prepolymers: An Effective Method for Synthesizing Well-Defined Polymer Networks. *Macromol. Rapid Commun.* **2019**, *40*, 1–6.

(17) Reymore, H. E.; Lockwood, R. J.; Ulrich, H. Novel Isocyanurate Foams Containing No Flame Retardant Additives. *J. Cell. Plast.* **1978**, *14*, 332–340.

(18) Sasaki, N.; Yokoyama, T.; Tanaka, T. Properties of Isocyanurate-Type Crosslinked Polyurethanes. *J. Polym. Sci. Polym. Chem. Ed.* **1973**, *11*, 1765–1779.

(19) Driest, P. J.; Dijkstra, D. J.; Stamatialis, D.; Grijpma, D. W. Tough Combinatorial Poly(Urethane-Isocyanurate) Polymer Networks and Hydrogels Synthesized by the Trimerization of Mixtures of NCO-Prepolymers. *Acta Biomater.* **2020**, *105*, 87–96.

(20) Driest, P. J.; Allijn, I. E.; Dijkstra, D. J.; Stamatialis, D.; Grijpma, D. W. Poly(Ethylene Glycol)-Based Poly(Urethane Isocyanurate) Hydrogels for Contact Lens Applications. *Polym. Int.* **2020**, *69*, 131–139.

(21) Dabi, S.; Zilkha, A. Foam Polymerization of Hexamethylene Diisocyanate by Cobalt Naphthenate. *Eur. Polym. J.* **1982**, *18*, 549–553.

(22) Dabi, S.; Zilkha, A. Oligotrimerization of Hexamethylene Diisocyanate by Organometallic Catalysts. *Eur. Polym. J.* **1980**, *16*, 831–833.

(23) Wejchan-Judek, M.; Polus, I.; Doczekalska, B.; Pertek, H. Trimerization of 3-Isocyanatomethyl-3,5,5-Trimethylcyclohexyl Isocyanate. *Polymery* **2001**, *46*, 131–132.

(24) Zeng, J.; Yang, Y.; Tang, Y.; Xu, X.; Chen, X.; Li, G.; Chen, K.; Li, H.; Ouyang, P.; Tan, W.; Ma, J.; Liu, Y.; Liang, R. Synthesis, Monomer Removal, Modification, and Coating Performances

of Biobased Pentamethylene Diisocyanate Isocyanurate Trimers. *Ind. Eng. Chem. Res.* **2022**, *61*, 2403–2416.

(25) Kresta, J. E.; Shen, C. S. Oligomerization of Isocyanates by Cyclic Sulfonium Zwitterions. *Polym. Bull.* **1979**, *1*, 325–328.

(26) Duff, D. W.; Maciel, G. E. ^{13}C and ^{15}N CP/MAS NMR Characterization of MDI-Polyisocyanurate Resin Systems. *Macromolecules* **1990**, *23*, 3069–3079.

(27) Hsieh, K. H.; Kresta, J. E. Polycocyclotrimerization of Isocyanates. In *Cyclopolymerization and Polymers with Chain-Ring Structures*; 1982; pp 311–324.

(28) Moritsugu, M.; Sudo, A.; Endo, T. Development of High-Performance Networked Polymers Based on Cyclotrimerization of Isocyanates: Control of Properties by Addition of Monoisocyanates. *J. Polym. Sci. Part A Polym. Chem.* **2012**, *50*, 4365–4367.

(29) Moritsugu, M.; Sudo, A.; Endo, T. Development of High-Performance Networked Polymers Consisting of Isocyanurate Structures Based on Selective Cyclotrimerization of Isocyanates. *J. Polym. Sci. Part A Polym. Chem.* **2011**, *49*, 5186–5191.

(30) Hagquist, J. A. E.; Reid, K. J.; Giorgini, A.; Hill, N. Isocyanurate Embedment Compound. US 5556934 A, 1996.

(31) Guo, Y.; Muuronen, M.; Deglmann, P.; Lucas, F.; Sijbesma, R. P.; Tomović, Ž. Role of Acetate Anions in the Catalytic Formation of Isocyanurates from Aromatic Isocyanates. *J. Org. Chem.* **2021**, *86*, 5651–5659.

(32) Siebert, M.; Sure, R.; Deglmann, P.; Closs, A. C.; Lucas, F.; Trapp, O. Mechanistic Investigation into the Acetate-Initiated Catalytic Trimerization of Aliphatic Isocyanates: A Bicyclic Ride. *J. Org. Chem.* **2020**, *85*, 8553–8562.

(33) Jozef, B. G.; Eric, H.; Stijn, R.; Marc, V.; Guido, V. H. G. Process for Preparing a Polyisocyanurate Polyurethane Material. US 20080227929 A1, 2008.

(34) Burdeniuc, J. J.; Panitzsch, T.; Dewhurst, J. E. Trimerization Catalysts from Sterically Hindered Salts. US 8530534 B2, 2013.

(35) Krakovský, I.; Špírková, M. A Discussion of the Cyclotrimerization Mechanism of Isocyanate. *Collect. Czech. Chem. Commun* **1993**, *58*, 2663–2672.

(36) Špírková, M.; Kubín, M.; Špaček, P.; Krakovský, I.; Dušek, K. Cyclotrimerization of Isocyanate Groups. II. Catalyzed Reactions of Phenyl Isocyanate in the Presence of 1-Butanol or Butyl-N-Phenylurethane. *J. Appl. Polym. Sci.* **1994**, *53*, 1435–1446.

(37) Bechara, I. S.; Carroll, F. P. Unusual Catalysts For Flexible Urethane Foams. *J. Cell. Plast.* **1980**, *16*, 89–101.

(38) Moghaddam, F. M.; Dekamin, M. G.; Khajavi, M. S.; Jalili, S. Efficient and Selective Trimerization of Aryl and Alkyl Isocyanates Catalyzed by Sodium P-Toluenesulfinate in the Presence of TBAI in a Solvent-Free Condition. *Bull. Chem. Soc. Jpn.* **2002**, *75*, 851–852.

(39) Driest, P. J.; Lenzi, V.; Marques, L. S. A.; Ramos, M. M. D.; Dijkstra, D. J.; Richter, F. U.; Stamatialis, D.; Grijpma, D. W. Aliphatic Isocyanurates and Polyisocyanurate Networks. *Polym. Adv. Technol.* **2017**, *28*, 1299–1304.

(40) Al Nabulsi, A.; Cozzula, D.; Hagen, T.; Leitner, W.; Müller, T. E. Isocyanurate Formation during Rigid Polyurethane Foam Assembly: A Mechanistic Study Based on: In Situ IR and NMR Spectroscopy. *Polym. Chem.* **2018**, *9*, 4891–4899.

(41) Schwetlickt, K.; Noack, R. Kinetics and Catalysis of Consecutive Isocyanate Reactions. Formation of Carbamates, Allophanates and Isocyanurates. *J. Chem. Soc., Perkin Trans. 2* **1995**, 395–402.

(42) Wong, S. -W; Frisch, K. C. Catalysis in Competing Isocyanate Reactions. I. Effect of Organotin-Tertiary Amine Catalysts on Phenyl Isocyanate and N-butanol Reaction. *J. Polym. Sci. Part A Polym. Chem.* **1986**, *24*, 2867–2875.

(43) Wu, L.; Liu, W.; Ye, J.; Cheng, R. Fast Cyclotrimerization of a Wide Range of Isocyanates to Isocyanurates over Acid/Base Conjugates under Bulk Conditions. *Catal. Commun.* **2020**, *145*, 106097.

(44) Zhou, Z.; He, Y.; Qiu, X.; Redwine, D.; Potter, J.; Cong, R.; Miller, M. Optimum $Cr(Acac)_3$ Concentration for NMR Quantitative Analysis of Polyolefins. *Macromol. Symp.* **2013**, *330*, 115–122.

(45) Braun, S.; Kalinowski, H. O.; Berger, S. *100 and More Basic NMR Experiments: A Practical Course*; Wiley, 1996.

(46) Harris, L. A.; Goff, J. D.; Carmichael, A. Y.; Riffle, J. S.; Harburn, J. J.; St. Pierre, T. G.; Saunders, M. Magnetite Nanoparticle Dispersions Stabilized with Triblock Copolymers. *Chem. Mater.* **2003**, *15*, 1367–1377.

(47) Lapprand, A.; Boisson, F.; Delolme, F.; Méchin, F.; Pascault, J. P. Reactivity of Isocyanates

with Urethanes: Conditions for Allophanate Formation. *Polym. Degrad. Stab.* **2005**, *90*, 363–373.
(48) Frisch, K. C.; Klempner, D. *Advances in Urethane: Science & Technology, Volume XIV*; CRC Press, 2020.
(49) Dick, J. S.; Annicelli, R. A. *Rubber Technology: Compounding and Testing for Performance*; Hanser eLibrary: Backlist 2014; Hanser Publishers, 2009.
(50) Ziegler, W.; Guttmann, P.; Kopeinig, S.; Dietrich, M.; Amirosanloo, S.; Riess, G.; Kern, W. Influence of Different Polyol Segments on the Crystallisation Behavior of Polyurethane Elastomers Measured with DSC and DMA Experiments. *Polym. Test.* **2018**, *71*, 18–26.
(51) Gunatillake, P. A.; Meijs, G. F.; Rizzardo, E.; Chatelier, R. C.; McCarthy, S. J.; Brandwood, A.; Schindhelm, K. Polyurethane Elastomers Based on Novel Polyether Macrodiols and MDI: Synthesis, Mechanical Properties, and Resistance to Hydrolysis and Oxidation. *J. Appl. Polym. Sci.* **1992**, *46*, 319–328.

Chapter 4

Phosphorus-Containing Polyisocyanurate Elastomers for Flame Retardant Application

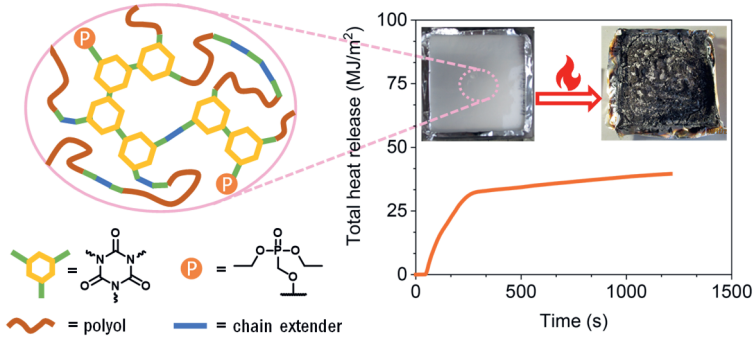

This chapter is based on submitted work:
Guo, Y.; Kleemann, J.; Sijbesma, R. P.; Tomović, Ž., Phosphorus-containing polyisocyanurate (PIR) elastomers for flame retardant application, *under peer review.*

Polyurethanes (PUs) are one of the most common and versatile polymers in many applications, especially in construction and automotive industry, where the improvement of thermal stability and flame retardancy is crucial. As polyisocyanaurate (PIR) is well known to have high decomposition temperature and phosphorus motifs are usually used as flame retardants in polymers, the introduction of PIR and phosphorus motifs in polyurethanes can lead to PUs with high thermal stability and flame retardancy. We investigated a synthesis pathway to introduce polyisocyanurate (PIR) and phosphorus motifs in polyurethanes *via* co-trimerization of 4,4'-methylene diphenyl diisocyanate (4,4'-MDI) and mono-isocyanate which was synthesized from the reaction between diethyl(hydroxymethyl)phosphonate (DEHP) and 4,4'-MDI. The resulting PIR-DEHP prepolymer was used to prepare PIR-DEHP elastomers in both solvent and solvent-free conditions. The elastomer with polyester polyol and 15 wt% 1,4-butanediol in polyol component showed high char formation (25.5 wt%) and 55% reductions in the total heat release (THR) relative to the reference elastomer without PIR and phosphorus content. It is expected that the use of PIR-DEHP prepolymer can be extended to other applications, such as rigid PU foams and compact thermosets where the flame retardancy and bulk reaction conditions are required.

4.1 Introduction

Polyurethane (PU) is one of the most versatile polymers and it is used to provide materials with a wide range of chemical, thermal and mechanical properties.[1-5] Although many different PU materials are available, further improvement of the physical properties, especially thermal stability and flame retardancy, will make them suitable for an increased number of applications and meet the new market demands. The introduction of PIR and phosphorus motifs in polyurethanes can lead to PUs with better thermal properties, as polyisocyanaurate (PIR) is well known to have a high decomposition temperature and phosphorus motifs are usually used as flame retardants in polymers.[6-10] However, the brittleness of PIR networks, and the limited compatibility of phosphorus motifs with the PUs are challenges that need to be improved.

PIRs are widely applied in PU elastomers in order to improve their thermal stability and flame retardant properties.[6,7] These elastomers are generally obtained *via* one of the two most common synthesis routes.[11-16] They can be prepared by trimerization of an isocyanate prepolymer that is obtained from the reaction of excess isocyanates and polyols (**Scheme 4-1a**), or *via* the *in-situ* reaction of isocyanates, polyols, and chain extenders in the presence of a trimerization catalyst (**Scheme 4-1b**). However, both of the synthesis routes lead to PU materials with relatively low PIR content, due to rapid increase of network density and viscosity, and restricted catalyst diffusion in the reaction mixture.

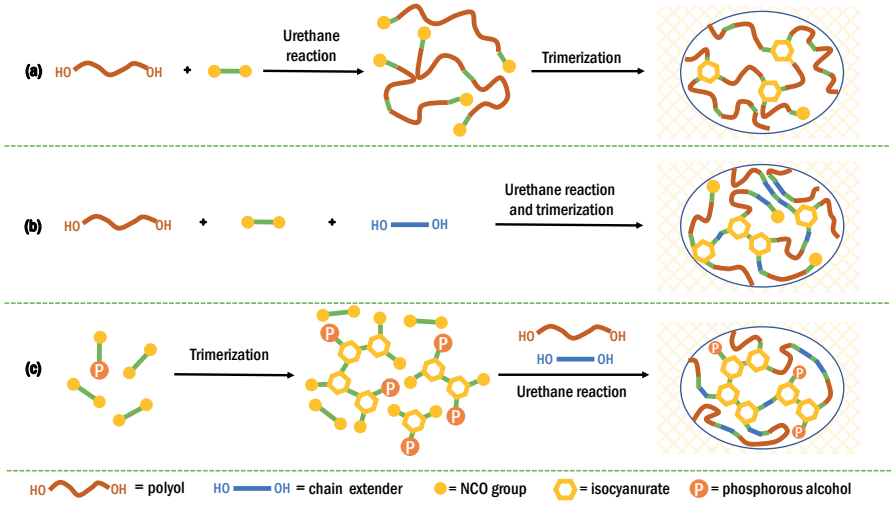

Scheme 4-1. The two most common synthesis pathways to prepare PIR elastomers and the preparation of PIR elastomer in this work: (a) trimerization of isocyanate prepolymer obtained from the reaction between excess of isocyanates and long chain polyols; (b) *in-situ* reaction of isocyanate, polyols and chain extenders in presence of trimerization catalyst; (c) urethane reaction of PIR prepolymer with polyols and chain extenders.

A more elegant way to develop a flexible network with high concentration of PIR structures is to synthesize a PIR-containing isocyanate prepolymer (**Scheme 4-1c**), which has been already discussed in **Chapter 3**. In order to control the crosslink density of the PIR prepolymer and to reduce the brittleness of the network, co-trimerization of mono- and di-functional isocyanates is used to create a flexible PIR network.[17-20] However, the commercially available mono-functional isocyanates, such as butyl and phenyl isocyanates, are too volatile and toxic to be used in large scale industrial applications. As an alternative approach, mono-functional isocyanates can be synthesized *in situ* by reacting mono-functional alcohols with diisocyanates and used in subsequent co-trimerization with diisocyanates to form PIR networks, as shown in **Chapter 3**.

Although phosphorus containing compounds are well known as flame retardants which are typically added in polyurethanes as fillers or additives,[21-28] they may leach out or migrate to the sample surface, leading to deterioration of the mechanical properties of the materials. In order to improve the compatibility of phosphorus compounds, phosphorus-containing polyols have been synthesized and introduced into PU materials *via* covalent bonds.[22,29-34] The flame retardancy can be realized *via* condensed- and gas-phase mechanisms, and many phosphorus containing compounds utilize both.[22,24,35,36] In the condensed-phase, many phosphorus flame retardants mediate the formation of char, which reduces the release of volatiles. Some phosphorus flame retardants also give intumescence, which produces a protective layer and slows down heat transfer to the underlying material. In parallel with condensed-phase mechanisms, phosphorus compounds also act as flame retardants in the gas-phase, which significantly improves the flame retardancy of the materials. It is generally accepted that PO· radicals formed from phosphorus-containing compounds play an important role to provide flame retardancy. During combustion, OH· radicals are replaced by PO· radicals which are formed from the decomposition of phosphorus flame retardants. The PO· radicals are less reactive, thus slow down or interrupt the oxidation of hydrocarbons. Therefore, the addition of phosphorus-containing motifs can be used to inhibit flames and reduce the heat production upon combustion, which enhances the flame retardancy of the material.

This work aims to combine both PIR and phosphorus motifs in PU elastomers in order to greatly enhance the intrinsic thermal stability and flame retardancy of these materials. Firstly, a mono-functional phosphonate alcohol, diethyl(hydroxymethyl) phosphonate (DEHP), was synthesized and introduced into a PIR matrix by reacting with 4,4'-methylene diphenyl diisocyanate (4,4'-MDI) in 0.25:1 molar ratio to produce a mixture containing both mono- and di-isocyanates. Then, the mixture was trimerized and quenched by acid before solidification in order to get liquid PIR-DEHP prepolymer (**Scheme 4-2**). Finally, PIR-DEHP elastomers were prepared by reacting the PIR-DEHP

prepolymer and long chain polyols with different amount of 1,4-butanediol as a chain extender in both solution and bulk conditions. Initial cone calorimetry tests were performed and the PIR-DEHP elastomer exhibited enhanced flame retardancy, which promises the potential use of PIR-DEHP network in various polyurethane applications such as rigid foams, compact elastomers, thermosets and adhesives, where flame retardancy is required. Our approach helps to improve the intrinsic flame retardancy of PU materials and to reduce the use of classical flame retardant additives.

4.2 Results and discussion

4.2.1 Preparation of PIR-DEHP prepolymer

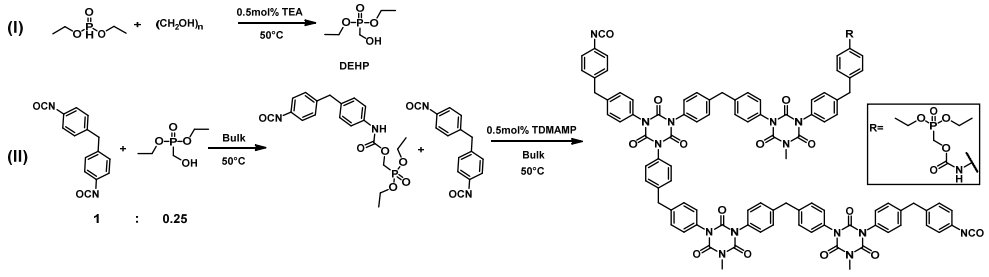

Scheme 4-2. Synthesis of DEHP (I) and PIR-DEHP prepolymer (II).

Mono-functional phosphonate alcohol, diethyl(hydroxymethyl)phosphonate (DEHP) was synthesized from diethyl phosphite and paraformaldehyde with triethylamine as a catalyst.[37] After the reaction, pure DEHP was obtained by evaporation of the triethylamine under reduced pressure.

To maximize the phosphorus content and to keep the viscosity low enough to perform trimerization in bulk afterwards, 4,4'-MDI and DEHP were reacted in a molar ratio of 1:0.25 resulting in an isocyanate mixture with 75 mol% di-functional isocyanate and 25 mol% mono-functional isocyanate, as shown in **Chapter 3**.

The trimerization of di- and mono-functional isocyanate mixture was carried out in bulk at 50 ºC using 2,4,6-tris(dimethylaminomethyl)phenol (TDMAMP) as the trimerization catalyst. As soon as the viscosity increased strongly, the reaction was quenched by diethylene glycol bis-chloroformate (DGBCF). The formation of isocyanurate was monitored with both ^{13}C NMR spectroscopy at 150.2 ppm (carbonyl carbon),[38,39] and with FT-IR spectroscopy at 1704 cm^{-1} (C=O stretching) and 1410 cm^{-1} (C-N stretching) (**Figure 4-1a** and **1b**).[40] After reaction, the urethane (U), allophanate (A) and isocyanurate (ISR) ratio in the PIR-DEHP prepolymer was further determined by ^{13}C NMR spectroscopy. In order to allow quantitative integration of the carbonyl peaks, 25 s of relaxation delay was required and chromium (III) acetylacetonate ($Cr(acac)_3$)

was used as relaxation agent.[41-43] In the quantitative ^{13}C NMR spectrum shown in **Figure 4-1c**, the peaks at 153.6, 151.6, 156.0 and 150.2 ppm were assigned to carbonyl carbon atoms of urethane, allophanate (2 peaks) and isocyanurate respectively.[38,39] The molar ratio of urethane: allophanate: isocyanurate (U:A:ISR) was calculated as 1:0.9:1.5 based on the integrals of carbonyl carbon peaks. In addition, an NCO content of 14.5 wt% was determined by back-titration and the average molar mass of the PIR-DEHP prepolymer, 710 g/mol, was determined with GPC (**Figure 4-1d**), from which the average functionality of the PIR-DEHP prepolymer was calculated to be 2.5 *via* the following equation:

$$f_n = \frac{NCO\ content \times M_{prepolymer}}{M_{NCO} \times 100\ wt\%} = \frac{14.5\ wt\% \times 710\ g/mol}{42\ g/mol \times 100\ wt\%} = 2.5,$$

where $n_{prepolymer}$ is the mole amount of prepolymer, M_{NCO} is the molecular weight of NCO group, $M_{prepolymer}$ is the number average molecular weight of prepolymer.

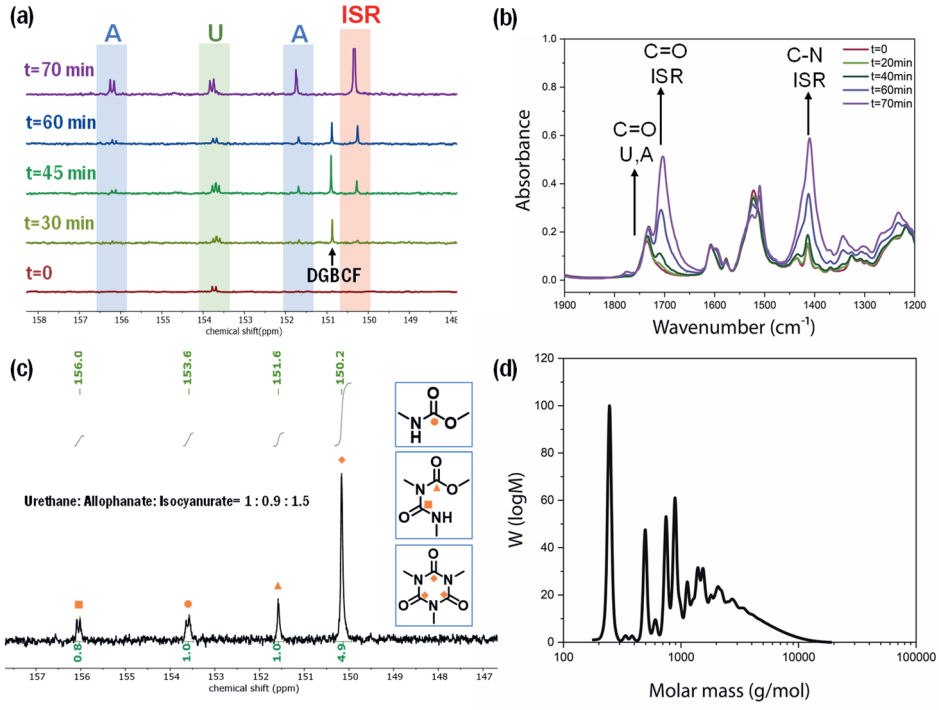

Figure 4-1. (a) ^{13}C NMR spectra (100 MHz, acetone-d_6) and (b) FT-IR spectra of co-trimerization of mono- and di-functional isocyanates. (c) Quantitative ^{13}C NMR spectrum (125 MHz, acetone-d_6) of the PIR-DEHP prepolymer. The ratio of U:A:ISR was determined by integrals of the carbonyl carbon peaks. U (carbamate); A (allophanate); ISR (isocyanurate). (d) GPC trace of the PIR-DEHP prepolymer, obtained M_n = 710 g/mol.

4.2.2 Preparation and characterization of solution cast PIR-DEHP elastomers

The PIR-DEHP elastomers were prepared by the reaction of PIR-DEHP prepolymer with commercially available polyether polyol or polyester polyol with average molecular weight of 2000 g/mol such as PolyTHF® 2000 (PTHF) and Lupraphen® 6601/2 (Lupraphen), and various amounts of 1,4-butanediol (BDO) as a chain extender (0, 5 wt%, 10 wt%, or 15 wt% of the polyol component). The molar ratio of NCO:OH was kept constant at 1.05 (index 105),[44,45] and the elastomers were solution-cast from THF (**Table 4-1**). The PIR-DEHP elastomers prepared with PTHF were white turbid and those with Lupraphen were transparent. Commercially available polymeric MDI, Lupranate® M20 (M20), which has a slightly higher functionality of 2.7, was also used to prepare M20-based elastomers as reference materials. M20 was reacted with either PTHF or Lupraphen polyol and 15 wt% BDO under the same casting condition used for PIR elastomers.

Table 4-1. Recipes (by weight) of solution cast elastomers (Index 105).

	PIR-DEHP elastomers				M20 elastomer	4,4'-MDI based elastomer
BDO in polyol component (wt%)	0	5	10	15	15	15
PIR-DEHP prepolymer	23.6	38.8	48.9	56.4	--	--
4,4'-MDI	--	--	--	--	--	35.4
M20	--	--	--	--	36.9	--
PTHF/Lupraphen	76.4	58.2	46.0	37.1	53.6	54.9
BDO	--	3.1	5.1	6.5	9.5	9.7

Dynamic mechanical analysis (DMA) of the elastomers was shown in **Figure 4-2** and **Table 4-2**. Together with the turbidity of the PTHF containing PIR-DEHP elastomers, phase separation is confirmed by the presence of two glass transition temperatures (T_g's) in the elastomers. The lower T_g at around -60 ºC is strongly influenced by the T_g of PTHF polyol and the higher T_g at around 120 ºC is influenced by the T_g of PIR structures. When there was no BDO in the elastomer, cold crystallization with subsequent melting of PTHF was found between -29 to 35 ºC (green curve).[46] The addition of BDO limited the crystallization tendency of PTHF, thus no cold crystallization peaks were found in the curves of elastomers containing BDO. For the Lupraphen-containing PIR-DEHP elastomers, only one narrow tan(δ) peak was observed, which indicates that the PIR structures have good compatibility with polyester polyol. The T_g of the elastomers increased with increasing amount of PIR structure as well as aromatic content. Compared to the M20 elastomers, PIR-DEHP elastomers had higher T_g as they contained PIR structures and have a higher aromatic content.

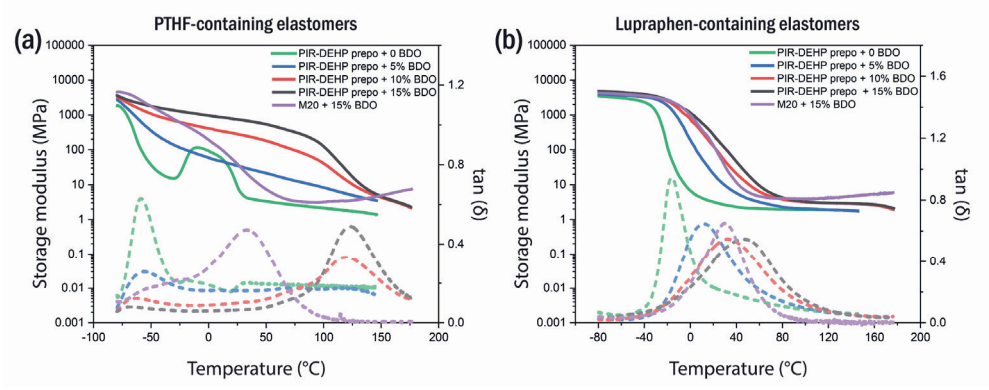

Figure 4-2. DMA curves of (a) PTHF-containing and (b) Lupraphen-containing PIR-DEHP and M20 elastomers with different amount of BDO. Solid line: storage modulus; dash line: tan(δ).

Table 4-2. DMA measurement data of PIR-DEHP and M20 elastomers with different polyols and different amount of BDO.

PTHF			Lupraphen		
PIR elastomers					
BDO content (wt%)	Aromatic content[a] (%)	T_g (°C)	BDO content (wt%)	Aromatic content[a] (%)	T_g (°C)
0	20	-59	0	20	-16
5	33	-56, 120	5	33	12
10	42	-61, 119	10	42	33
15	48	-69, 123	15	48	46
M20 elastomers					
15	37	34	15	37	18

[a] The aromatic content is calculated based on the weight percentage of aromatic isocyanate in the elastomers (see experimental section).

The mechanical properties of the PIR-DEHP elastomers with different amounts of BDO as well as M20 elastomer containing 15 wt% BDO were measured by tensile test (**Figure 4-3** and **Table 4-3**). The PIR-DEHP elastomers became stiffer with higher isocyanurate content. As a result, the stress at break and the Young's modulus increased while the elongation at break decreased. The M20 elastomers, which contain no isocyanurate, had lower stress at break and lower Young's modulus. This could also be explained by the lower T_g of M20 elastomers with either PTHF or Lupraphen polyol and 15 wt% BDO, which was around room temperature (34 and 18 °C respectively), thus the material was more rubbery and easier to break than the isocyanurate containing materials.

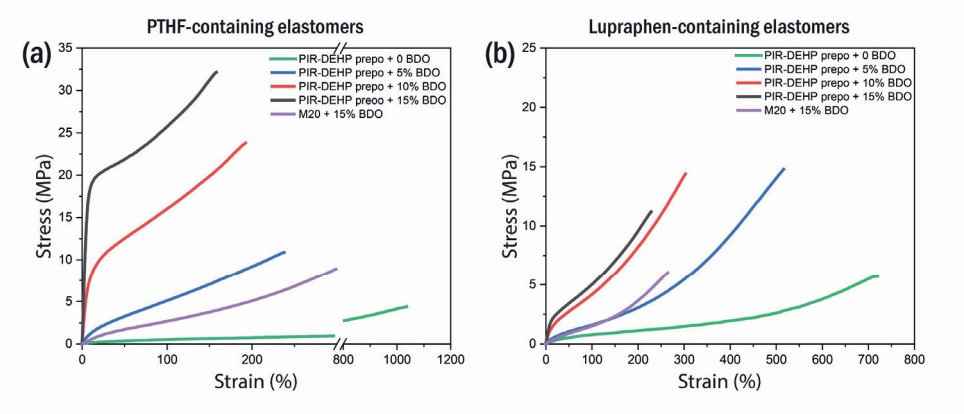

Figure 4-3. Tensile test of (a) PTHF-containing and (b) Lupraphen-containing PIR-DEHP and M20 elastomers with different amount of BDO.

Table 4-3. Tensile test results of PIR-DEHP and M20 elastomers with PTHF or Lupraphen polyol, and different amount of BDO.

BDO content (wt%)	PTHF		Lupraphen	
	Tensile strength (MPa)	Elongation at break (%)	Tensile strength (MPa)	Elongation at break (%)
PIR elastomers				
0	4.0	976	5.9	766
5	10.5	234	15.4	517
10	23.5	190	14.9	296
15	33.0	167	11.5	226
M20 elastomers				
15	11.2	358	6.0	264

Finally, thermogravimetric analysis (TGA) of these elastomers was measured (**Figure 4-4**). The decomposition temperature at 5% weight loss (T_{d5}), 10% weight loss (T_{d10}) and char formation at 596 ºC are shown in Table 4-4. The T_{d5} and T_{d10} are mainly dependent on the decomposition of urethane bonds and decrease with higher BDO content. For PTHF-containing PIR-DEHP elastomers, with more BDO, the amount of isocyanurate structures as well as aromatic content increased, leading to higher char formation. The char formation of Lupraphen-containing elastomers was higher than PTHF-containing elastomers, but it did not significantly change with the amount of BDO. Nevertheless, all PIR-DEHP elastomers showed higher char formation than classical 4,4'-MDI-based elastomers which were synthesized from 4,4'-MDI, polyol and BDO without trimerization (**Figure 4-4c** and **4d**). With PTHF and 15 wt% of BDO, M20 elastomers had slightly higher char formation than PIR-DEHP elastomers. However, with Lupraphen and the same amount of BDO (15 wt%) in polyol component, the char formation of PIR-DEHP elastomers was much higher than M20 elastomers.

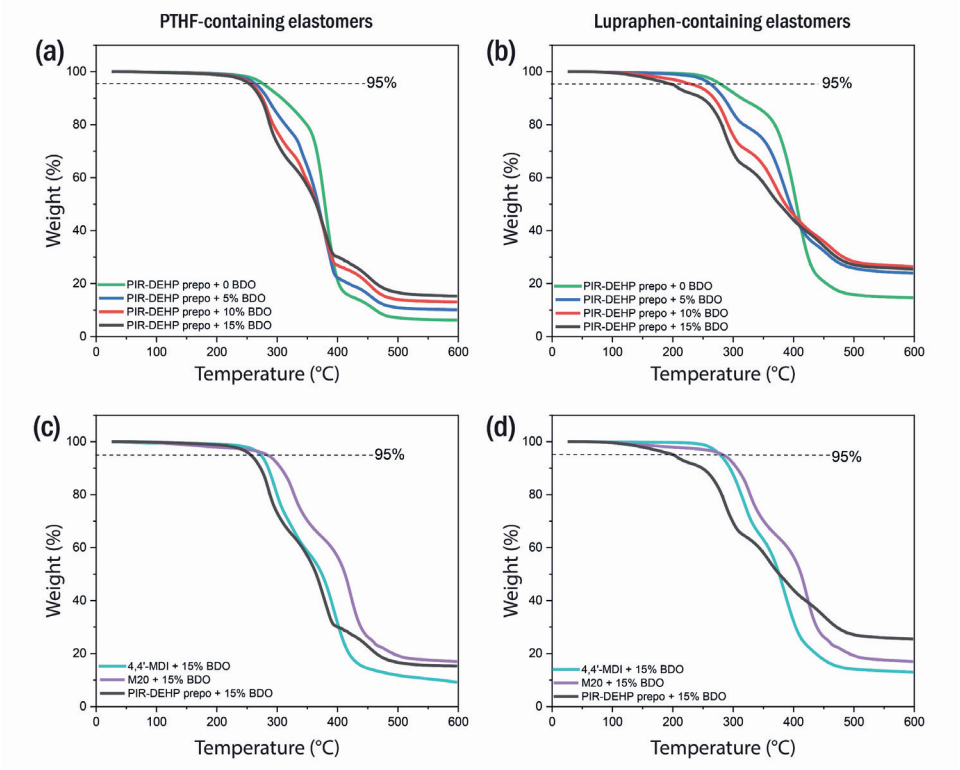

Figure 4-4. TGA curves of (a) PTHF-containing and (b) Lupraphen-containing PIR-DEHP and M20 elastomers with different amount of BDO; (c) PTHF-containing and (d) Lupraphen-containing PIR-DEHP and 4,4'-MDI-based elastomers with 15 wt% BDO.

Table 4-4. TGA measurement data of PTHF-containing and Lupraphen-containing PIR-DEHP and M20 elastomers with different amount of BDO.

BDO content (wt%)	Aromatic content[a] (wt%)	PTHF			Lupraphen		
		T_{d5} (°C)	T_{d10} (°C)	Char formation (%)	T_{d5} (°C)	T_{d10} (°C)	Char formation (%)
PIR elastomers							
0	20	279.5	307.5	6.2	281.2	313.7	14.7
5	33	266.3	283.8	10.1	264.5	284.5	24.0
10	42	259.3	275.3	13.1	234.9	268.1	26.4
15	48	256.1	272.5	15.3	201.8	248.6	25.5
M20 elastomer							
15	37	283.7	306.2	17.0	218.2	284.3	16.3
4,4'-MDI-based elastomer							
15	35	272.7	285.2	9.3	278.5	294.5	13.0

[a] The aromatic content is calculated based on the weight percentage of aromatic isocyanate in the elastomers.

4.2.3 Flame retardancy of PIR-DEHP elastomers

As PIR-DEHP prepolymer is still a liquid, it is also possible to use this prepolymer to cast elastomers without solvent, which is advantageous for industrial applications. To study the flame retardancy of the elastomers, three samples were prepared using Lupraphen as the polyol due to the high char formation as shown in **Figure 4-4**. First, PIR-DEHP elastomer was prepared by reacting PIR-DEHP prepolymer with Lupraphen and 15 wt% BDO in solvent-free condition. The used PIR-DEHP prepolymer had NCO content = 18.1 wt%, M_n = 590 g/mol, calculated f_n = 2.5 and molar ratio of U:A:ISR was 1:0.5:0.8 (**Figure 4-5**).

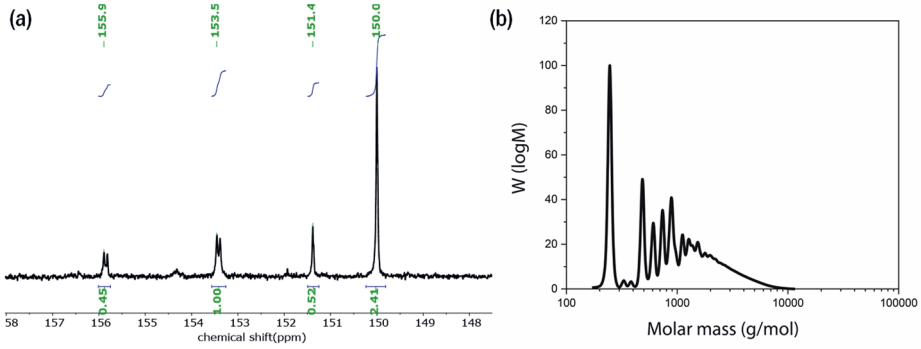

Figure 4-5. (a) Quantitative ^{13}C NMR spectrum (125 MHz, acetone-d_6) of PIR-DEHP prepolymer used for casting cone calorimetry specimens. The ratio of urethane, allophanate and isocyanurate is determined by integrals as 1:0.5:0.8. (b) GPC trace of the PIR-DEHP prepolymer used for casting cone calorimetry specimens, obtained M_n = 590 g/mol.

In order to compare the thermal stability of PIR structures with polymeric MDI regardless of the effects of phosphorus content, M20-DEHP prepolymer was prepared by reacting M20 with the same amount of DEHP as in the PIR-DEHP prepolymer. After that, the M20-DEHP elastomer was prepared by reacting M20-DEHP prepolymer with Lupraphen and 15 wt% BDO in polyol component. Another M20 elastomer was prepared by reacting M20 with Lupraphen and 15 wt% BDO in polyol component. Both of the elastomers were cast using the same procedure as PIR-DEHP elastomer in bulk condition (**Table 4-5**).

Table 4-5. Recipes (by weight) of PIR-DEHP, M20-DEHP and M20 elastomers for cone calorimetry measurement.

PIR-DEHP elastomer		M20-DEHP elastomer		M20 elastomer	
PIR-DEHP prepolymer	50.4	M20	38.0	M20	36.9
[DEHP content][a]	7.2	DEHP	7.2	--	--
Lupraphen	42.2	Lupraphen	46.5	Lupraphen	53.6
BDO	7.4	BDO	8.2	BDO	9.5

[a] The amount of DEHP contained in PIR-DEHP prepolymer.

The TGA and DMA results of three elastomers are shown in **Figure 4-6**. With the same amount of DEHP as well as similar amount of aromatic content, polyol and BDO, the PIR-DEHP and M20-DEHP elastomers had similar T_{d5} ≈ 265 °C, char formation ≈ 23% and T_g ≈ 40 °C. However, without DEHP and PIR, M20 elastomer showed a lower char formation of only 16%.

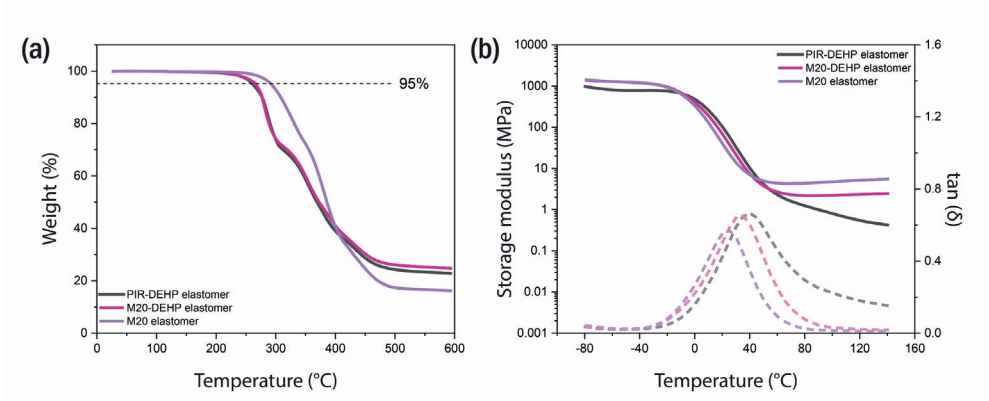

Figure 4-6. (a) TGA and (b) DMA curves of PIR-DEHP, M20-DEHP and M20 elastomers. Solid line: storage modulus; dash line: tan(δ).

The combustion behavior of the PIR-DEHP, M20-DEHP and M20 elastomers was initially evaluated by cone calorimetry and the time to ignition (TTI, s), peak of heat release rate (PHRR, kW/m^2), time to PHRR (t_p, s), total heat release (THR, MJ/m^2), average effective heat of combustion (AEHC, MJ/kg), maximum average rate of heat emission (MARHE, kW/m^2), total smoke production (TSP, m^2), time to extinguishment (t_e) and mass residue (wt%) are shown in **Table 4-6** and **Figure 4-7**.

Table 4-6. Cone calorimetry results of PIR-DEHP, M20-DEHP and M20 elastomers measured under a heat flux of 35 kW/m^2.

Sample	TTI (s)	PHRR[a] (kW/m^2)	t_p (s)	THR (MJ/m^2)	AEHC (MJ/kg)	MARHE (kW/m^2)	TSP (m^2)	t_e (s)	Residue (wt%)
PIR-DEHP	48	320.6	56	39.2	19.0	137	7.8	1185	17
M20-DEHP	62	234.4	182	72.8	19.0	153	14.1	782	26
M20	72	361.1	98	86.9	19.8	191	15.0	930	13

[a] The highest PHRR is shown.

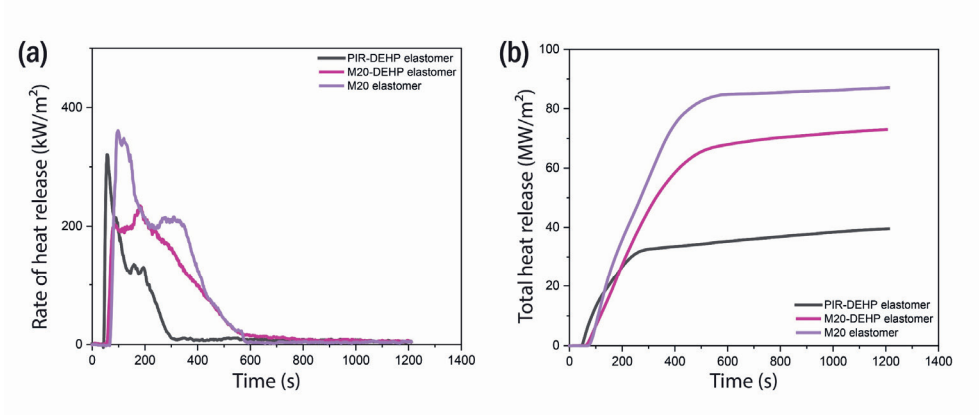

Figure 4-7. (a) HRR and (b) THR curves of PIR-DEHP, M20-DEHP and M20 elastomers measured by cone colorimeter under a heat flux of 35 kW/m^2.

From **Figure 4-7a**, it is noted that the HRR curves of all the elastomers show two peaks associated with two-step decomposition, which is also evident from the TGA curves in **Figure 4-6**. Typically, the first decomposition step corresponds to the decomposition of urethane bonds in PU and the second step is caused by the decomposition of the soft segment.[26,28,47] The higher first PHRR peak of PIR-DEHP elastomer compared to that of M20-DEHP elastomer may be due to the additional rupture of allophanate bonds. The endothermic decomposition of the PIR structures and the effect of phosphorus content are attributed to a fast decrease of HRR after reaching the PHRR, leading to a reduction of 55% in THR compared to M20 elastomer.[48-50] The decomposition of PIR structures also leads to lower char residue compared to M20-DEHP elastomer.[51,52] On the other hand, the M20-DEHP elastomer has the lowest PHRR and a shortest combustion time, leading to a high char residue, whereas the broad HRR curve results in higher THR in comparison to PIR-DEHP elastomer. In addition, an important factor to show the activity of flame retardants in the gas phase is EHC, which means the combustion extent of volatile in gas phase.[28,34,53] Despite the differences in HRR and char residue, the PIR-DEHP and M20-DEHP elastomers have similar average EHC, slightly reduced relative to M20 elastomer, indicating that the phosphorus content has minor effect in the gas phase. Finally, PIR-DEHP elastomer

showed the lowest TSP compared to the other two elastomers. As the smoke production is one of the major hazards of fire, lowering the TSP helps to improve the fire safety of the material. The PIR structures, in combination with phosphorus content, help to reduce the TSP during the combustion.

The scanning electron microscopy (SEM) images of the char residues after cone calorimetry measurements are shown in **Figure 4-8**. The porous char of both PIR-DEHP and M20-DEHP elastomers might be the result of decomposition of the elastomers and the release of volatiles. It is also notable that the surface and inside char images of PIR-DEHP elastomer are similar, but that they differ a lot for M20-DEHP elastomer. According to the char residue images (**Figure 4-9**), the PIR-DEHP elastomer had no expansion, resulting in a more even morphology of the char residue. However, the expansion of the M20-DEHP elastomer led to a different morphology with higher concentration of pores on the surface. Although the interior of the elastomer sample cracked to smaller pieces due to expansion, less pores were observed. M20 elastomer was combusted to a great extent with a lot of ashes and dense char observed.

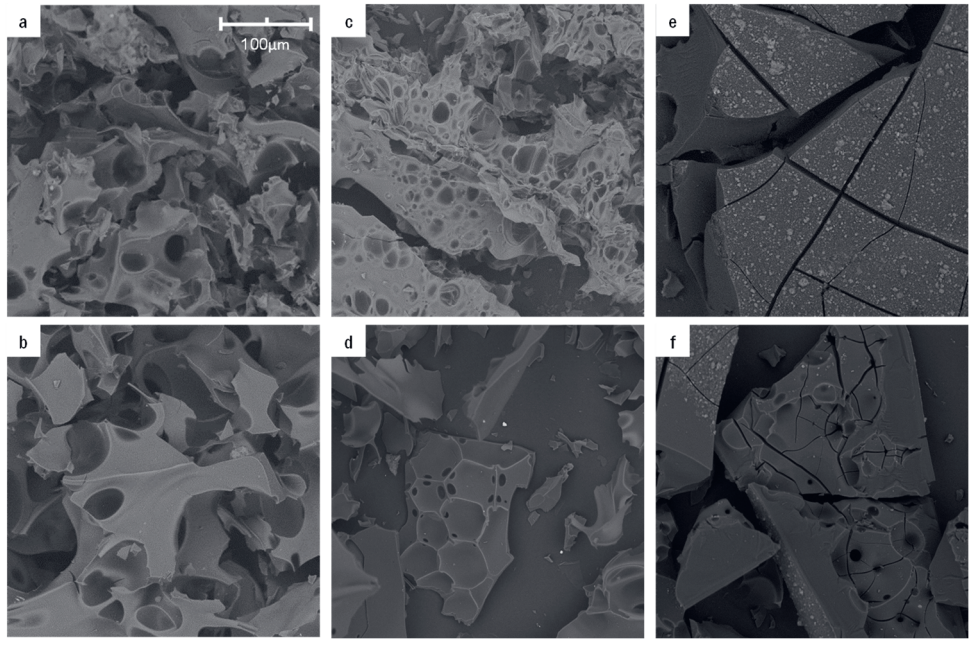

Figure 4-8. SEM images (100µm, 780×, 10kV) of elastomer char residues obtained from (a) PIR-DEHP elastomer surface, (b) PIR-DEHP elastomer interior, (c) M20-DEHP elastomer surface, (d) M20-DEHP elastomer interior, (e) M20 elastomer surface and (f) M20 elastomer interior.

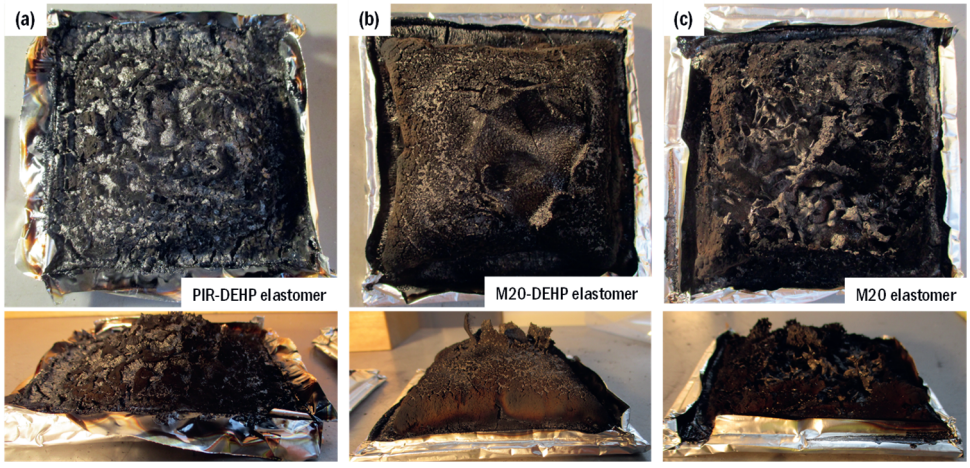

Figure 4-9. Photos of char residues after cone calorimetry measurement (a) PIR-DEHP elastomer, (b) M20-DEHP elastomer, (c) M20 elastomer.

The char residues of the elastomers were further studied with Raman spectrometry as shown in **Figure 4-10**. Two strong, overlapping peaks were observed at 1348 and 1586 cm^{-1}, which are attributed to D band (amorphous structure) and G band (graphitic structure) of C=C bonds, respectively. The integral ratio of D band to G band is often used as characteristic parameter for the graphitization degree of the char residues.[31,54] A lower value of I_D/I_G, indicates a higher degree of graphitization that reduces the release of polymer volatiles from the char. After peak deconvolution, the integrals of D band and G band were obtained and the ratio of I_D/I_G was calculated. The I_D/I_G ratio of PIR-DEHP, M20-DEHP and M20 elastomers are 1.90, 2.31 and 1.95, respectively. This indicates that the combination of phosphorus and PIR content in the PIR-DEHP elastomer helps to promote amorphous char into a graphitic structure, leading to low I_D/I_G ratios.

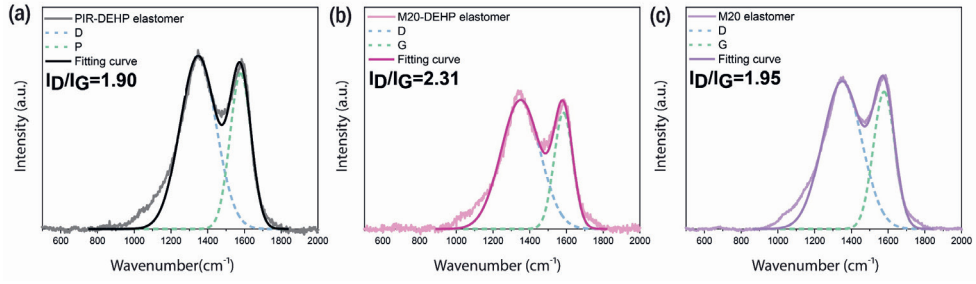

Figure 4-10. Raman spectra of PIR-DEHP, M20-DEHP, M20 elastomer char residues. The overlapping two peaks were deconvoluted by fitting to Gaussian peak shapes.

4.3 Conclusion

We investigated a synthetic pathway to incorporate PIR and phosphorus motifs (DEHP) in PU elastomers *via* covalent bonds in order to improve their thermal stability as well as flame retardancy. The PIR-DEHP elastomers are stiff and exhibit a high T_g. Moreover, they show high char formation according to TGA measurement, and low THR and TSP according to initial cone calorimetry measurements.

Our current study highlights the preparation of liquid PIR-DEHP prepolymer with a high concentration of isocyanurate structures *via* cyclotrimerization of mono- and di-functional isocyanates. The use of a phosphorus-containing alcohol also creates a way to introduce covalently bound phosphorus atoms in PU materials instead of using phosphorus-containing additives. The combination effect of PIR and phosphorus motifs improves the char formation and flame retardancy of the PU materials. This effect could be further studied by additional fire behavior tests such as UL94, limiting oxygen index (LOI) and gas chromatography–mass spectrometry (GC-MS) measurement.

The liquid PIR-DEHP prepolymer also offers prospects for the use of the PIR-DEHP prepolymer in other industrial applications such as rigid PU foams, compact thermosets and coatings where a solvent-free synthesis and flame retardancy are required. By improving the intrinsic flame retardancy of PU materials, the use of conventional flame retardant additives can be reduced. Moreover, it is expected that the physical properties, thermal stability and flame retardancy of the PU materials based on PIR prepolymers can be tuned by varying phosphorus compounds.

4.4 Experimental section

Materials

Diethyl phosphite (>98%), paraformaldehyde (>95%), triethylamine (≥99.5%), 2,4,6-tris(dimethylaminomethyl)phenol (TDMAMP) (>95%), chromium (III) acetylacetonate ($Cr(acac)_3$) (99.99% trace metals basis), 1,4-butanediol (BDO) (99%) and dibutyltin dilaurate (DBTL) (95%), 2-ethyl-1-hexanol (≥99.6%) were purchased from Sigma-Aldrich. 1,4-Butanediol was dried over mol-sieves, all other reagents were used directly without treatment. 4,4'-Methylene diphenyl diisocyanate (4,4'-MDI), polymeric MDI Lupranate® M20 (NCO content = 31.5 wt%, f_n = 2.7), diethylene glycol bis-chloroformate (DGBCF), 1,4-diazabicyclo[2.2.2]octane (DABCO)-based urethane gel catalyst Lupragen® N202, PolyTHF® 2000 with molecular weight 2000 g/mol (OH_v = 56 mg KOH/g), and Lupraphen® 6601/2 with molecular weight 2000 g/mol (OH_v = 56 mg KOH/g, polyester polyol synthesized from adipic acid, 1,4-butanediol and mono ethylene glycol) were kindly provided by BASF Polyurethanes GmbH. Polyols were dried

at 80 °C under vacuum for 2 h before use. Tetrahydrofuran (THF) (containing stabilizer BHT) was purchased from Biosolve and dried over mol-sieves before use.

Synthesis

Synthesis of diethyl(hydroxymethyl)phosphonate (DEHP). Diethyl phosphite (250.5g, 1.81 mol) and paraformaldehyde (54.5 g, 1.81mol) were added in a dry 3-neck flask equipped with a condenser. Then triethylamine (9.2 g, 0.09 mol) was added in the flask. The reaction was carried out at 50 °C in an oil bath under Ar flow. After stirring for 20 min, the temperature increased dramatically to 156 °C for a few seconds and the suspension mixture became transparent when temperature reached around 100 °C. After the heat release, the solution was stirred for another 1 h at 50 °C. DEHP was obtained as a transparent liquid after evaporation of triethylamine under reduced pressure at 50 °C. ^{1}H NMR (400 MHz, chloroform-*d*): δ 4.88 (s, 1H), 4.26 - 4.09 (m, 4H), 3.91 (d, *J* = 6.0 Hz, 2H), 1.35 (t, *J* = 7.1 Hz, 6H) ppm; ^{31}P NMR (162 MHz, chloroform-*d*): δ 24.5 ppm.

Synthesis of PIR-DEHP prepolymer. 4,4'-MDI (188.3 g, 0.75 mol) in a dry 3-neck flask equipped with a dropping funnel was stirred under Ar flow at 50 °C in an oil bath. DEHP (31.6 g, 0.19 mol) was added in the dropping funnel and dropped into the flask at a speed of 1 drop every 10 s with the internal temperature kept under 55 °C. The reaction was immediately completed after addition of the alcohol and the mixture was calculated to have average molecular weight of 292.2 g/mol with f_n of 1.75.

The isocyanate mixture (186.4 g, 0.64 mol) was added to a dry beaker under Ar flow. Trimerization catalyst TDMAMP (1.5 g, 5.58 mmol) was dissolved in 6 mL THF and was quickly injected into the isocyanate mixture. The mixture was stirred at 50 °C in an oil bath with an anchor-shape stirrer and the internal temperature as well as the torque were monitored by the mechanical stirrer. After 70 min, the co-trimerization was quenched with DGBCF (1.3 g, 5.58 mmol) in 2 mL THF. The reaction was monitored with ^{13}C NMR spectroscopy and FT-IR spectroscopy. After that, the NCO content of the PIR prepolymer was titrated and the prepolymer was used for casting elastomers in solution. For PIR prepolymer that was used for bulk-cast elastomers, the same procedure was used except that the co-trimerization was quenched earlier to obtain prepolymer with lower viscosity.

Preparation of elastomers in solution. The preparation of PIR-DEHP elastomer with Lupraphen® 6601/2 and 15 wt% BDO is used as an example to illustrate the general synthetic route: the PIR-DEHP prepolymer (6.0 g, NCO content = 14.5 wt%) was dissolved in 25 mL dry THF in a dry 1-neck flask at room temperature. The polyol component solution was prepared by dissolving Lupraphen® 6601/2 (4.0 g, 2.00 mmol), BDO (0.7 g, 7.83 mmol) and DBTL (13.2 mg, 0.02 mmol, 0.1 mol% to the NCO groups) in 5 mL dry THF in another dry 1-neck flask at room temperature. Then the polyol

solution was added into the prepolymer solution and the mixture obtained was stirred for 1 min under Ar atmosphere. The solution was poured on a metal lid which was preheated at 50 ºC in N_2 oven and the elastomer was cured overnight. After that, the obtained elastomer was dried at 80 ºC vacuum oven for one day to remove solvent. The same procedures and the same conditions were used for the preparation of solution-cast 4,4'-MDI-based classical elastomers, and M20-based elastomers.

Aromatic content calculation. The PIR prepolymer is trimerized from a mixture containing 188.3 g 4,4'-MDI and 31.6 g DEHP, which means that there is 85.6 wt% isocyanate contained in PIR prepolymer. The aromatic content of PIR elastomers with 15 wt% BDO, for example, can be calculated as: 56.4% × 85.6% = 48%. The aromatic content of 4,4'-MDI based elastomer and M20 elastomer is the amount of isocyanate that was used.

Preparation of elastomers in bulk. The preparation of PIR-DEHP elastomer for cone calorimetry measurement is used as an example to illustrate the general synthetic route: the PIR-DEHP prepolymer was kept in a vacuum oven overnight at 50 ºC. The polyol component consisted of Lupraphen® 6601/2 (67.5 g, 0.03 mol), BDO (11.8 g, 0.13 mol) and Lupragen® N202 (0.1 g) was added in a sealed polypropylene cup and stirred at 1000 rpm under vacuum in a speedmixer for 10 min at 50 ºC. PIR-DEHP prepolymer (80.6 g, NCO content = 18.1 wt%) was added and the mixture was mixed in a speedmixer for 30 s under vacuum. After that, the mixture was poured on a preheated metal mold at 80 ºC. The elastomers were further cured in an 80 ºC oven overnight. The same procedure and conditions were used for the preparation of M20-DEHP and M20 elastomers cast in bulk. For M20-DEHP elastomer, the M20-DEHP prepolymer was pre-synthesized by slowly dropping DEHP into Lupranate® M20 at 50 ºC.

Characterization

Fourier-transform infrared spectroscopy (FT-IR). FT-IR spectroscopy was carried out in attenuated total reflection mode on a Spectrum Two (Perkin Elmer) spectrometer at room temperature. 8 scans were performed from 4000 - 450 cm^{-1}.

Nuclear magnetic resonance (NMR) spectroscopy. ^{1}H NMR and ^{31}P NMR spectroscopy for measuring DEHP was performed using a Bruker UltraShield 400 MHz spectrometer at room temperature using chloroform-*d* as solvent with TMS as internal standard with a delay time of 1s and 32 scans per spectrum. ^{13}C NMR spectroscopy for monitoring the PIR reaction were performed using a Bruker UltraShield 400 MHz or Varian Mercury 400 MHz spectrometer at room temperature using acetone-d_6 as solvent with TMS as internal standard with a delay time of 2 s and 256 scans per spectrum. Quantitative ^{13}C NMR spectroscopy for determining the urethane, allophanate and isocyanurate ratio were performed in a Varian Unit Inova 500 MHz spectrometer using acetone-d_6 as

solvent with TMS as internal standard at room temperature with a delay time of 25 s, 2048 scans per spectrum and $Cr(acac)_3$ (20 mg/mL) as a relaxation agent.

Determination of isocyanate content. NCO titration was performed on a 916 Ti-Touch titration machine (Metrohm) equipped with an electrode using tetraethylammonium bromide (0.4 mol/L in ethylene glycol) as electrolyte. The isocyanate was quenched with excess of dibutylamine and the unreacted dibutylamine was titrated with 1M HCl as the titrant. After getting the volume (V_1) at the end of titration of sample as well as the volume (V_0) of the blank titration at the same condition, the NCO content was calculated by the titration machine using the following equation:

$$NCO\ content = \frac{(V_1 - V_0) \times c_{HCl} \times M_{NCO}}{m_{sample}}.$$

Gel permeation chromatography (GPC). The average molecular weight of the PIR prepolymer was measured by a GPC system comprising a series of columns (one PSS-SDV 500 Å (5µm) and three Agilent PL-Gel 500 Å (5µm) packed columns) and a UV detector. THF was used as the eluent with a flow rate of 1 mL/min and toluene as internal standard. Calibration was done with monodisperse PMMA and Lupranate® M20 samples.

Thermogravimetric analysis (TGA). TGA measurement was performed on a TA Q500 or TA Q550 (TA Instruments) under N_2 atmosphere. Samples (around 10 mg) were heated from 28 to 600 ºC at a rate of 10 ºC/min.

Tensile testing. Tensile testing was performed on a EZ20 (Lloyd instrument) with a 500 N load cell. The tensile bars used had an effective length of 12 mm, width of 2 mm and thickness of 1.2 mm. The elongation rate used was 50 mm/min.

Dynamic mechanical analysis (DMA). DMA measurement was performed on a DMA Q850 (TA Instruments) with a film tension setup. The test bars had a width of 5.3 mm, thickness of 1.2 mm and effective length of around 20 mm. For each measurement, a temperature ramp from -80 to 150 ºC for soft samples, or from -80 to 180 ºC for hard samples was programmed with a heating rate of 3 ºC/min at a frequency of 1.0 Hz. A preload force of 0.01 N, an amplitude of 100 µm and a force track of 115 % were used. The storage and loss modulus were recorded as a function of temperature. The glass transition temperature (T_g) was determined from the peak maximum of the tan(δ).

Cone calorimetry. Cone calorimetry measurement was performed on an iCone calorimeter (Fire Testing Technology Limited) under a heat flux of 35 kW/m^2 according to ISO 5660-1:2015-03/Amd 1:2019-08 standard. The samples were cut into 100×100×3 mm^3 size and wrapped with aluminum foil for measurement. The obtained results are based on single measurements.

Scanning electron microscopy (SEM). SEM images were obtained using a Phenom ProX instrument with an acceleration of 10kV. Both surface and interior char residue were investigated with 100 µm scale.

Raman spectroscopy. Raman spectroscopy measurement was performed on a Confocal Raman microscope WITec WMT 50 (WITEC) with a laser of 532.3 nm.

4.5 References

(1) Engels, H. W.; Pirkl, H. G.; Albers, R.; Albach, R. W.; Krause, J.; Hoffmann, A.; Casselmann, H.; Dormish, J. Polyurethanes: Versatile Materials and Sustainable Problem Solvers for Today's Challenges. *Angew. Chemie - Int. Ed.* **2013**, *52*, 9422–9441.

(2) Randall, D.; Lee, S. *The Polyurethanes Book*; Wiley, 2003.

(3) Eling, B.; Tomović, Ž.; Schädler, V. Current and Future Trends in Polyurethanes: An Industrial Perspective. *Macromol. Chem. Phys.* **2020**, *2000114*, 1–11.

(4) Delebecq, E.; Pascault, J. P.; Boutevin, B.; Ganachaud, F. On the Versatility of Urethane/Urea Bonds: Reversibility, Blocked Isocyanate, and Non-Isocyanate Polyurethane. *Chem. Rev.* **2013**, *113*, 80–118.

(5) Akindoyo, J. O.; Beg, M. D. H.; Ghazali, S.; Islam, M. R.; Jeyaratnam, N.; Yuvaraj, A. R. Polyurethane Types, Synthesis and Applications-a Review. *RSC Adv.* **2016**, *6*, 114453–114482.

(6) Chattopadhyay, D. K.; Webster, D. C. Thermal Stability and Flame Retardancy of Polyurethanes. *Prog. Polym. Sci.* **2009**, *34*, 1068–1133.

(7) Levchik, S. V.; Weil, E. D. Thermal Decomposition, Combustion and Fire-Retardancy of Polyurethanes - A Review of the Recent Literature. *Polym. Int.* **2004**, *53*, 1585–1610.

(8) Schartel, B.; Perret, B.; Dittrich, B.; Ciesielski, M.; Krämer, J.; Müller, P.; Altstädt, V.; Zang, L.; Döring, M. Flame Retardancy of Polymers: The Role of Specific Reactions in the Condensed Phase. *Macromol. Mater. Eng.* **2016**, *301*, 9–35.

(9) Lenz, J.; Pospiech, D.; Paven, M.; Albach, R. W.; Günther, M.; Schartel, B.; Voit, B. Improving the Flame Retardance of Polyisocyanurate Foams by Dibenzo[d,f][1,3,2]Dioxaphosphepine 6-Oxide-Containing Additives. *Polymers (Basel).* **2019**, *11*, 1242.

(10) Günther, M.; Lorenzetti, A.; Schartel, B. Fire Phenomena of Rigid Polyurethane Foams. *Polymers (Basel).* **2018**, *10*.

(11) Samborska-Skowron, R.; Balas, A. An Overview of Developments in Poly(Urethane-Isocyanurates) Elastomers. *Polym. Adv. Technol.* **2002**, *13*, 653–662.

(12) Driest, P. J.; Dijkstra, D. J.; Stamatialis, D.; Grijpma, D. W. The Trimerization of Isocyanate-Functionalized Prepolymers: An Effective Method for Synthesizing Well-Defined Polymer Networks. *Macromol. Rapid Commun.* **2019**, *40*, 1–6.

(13) Reymore, H. E.; Lockwood, R. J.; Ulrich, H. Novel Isocyanurate Foams Containing No Flame Retardant Additives. *J. Cell. Plast.* **1978**, *14*, 332–340.

(14) Sasaki, N.; Yokoyama, T.; Tanaka, T. Properties of Isocyanurate-Type Crosslinked Polyurethanes. *J. Polym. Sci. Polym. Chem. Ed.* **1973**, *11*, 1765–1779.

(15) Driest, P. J.; Dijkstra, D. J.; Stamatialis, D.; Grijpma, D. W. Tough Combinatorial Poly(Urethane-Isocyanurate) Polymer Networks and Hydrogels Synthesized by the Trimerization of Mixtures of NCO-Prepolymers. *Acta Biomater.* **2020**, *105*, 87–96.

(16) Driest, P. J.; Allijn, I. E.; Dijkstra, D. J.; Stamatialis, D.; Grijpma, D. W. Poly(Ethylene Glycol)-Based Poly(Urethane Isocyanurate) Hydrogels for Contact Lens Applications. *Polym. Int.* **2020**, *69*, 131–139.

(17) Hsieh, K. H.; Kresta, J. E. Polycocyclotrimerization of Isocyanates. In *Cyclopolymerization and Polymers with Chain-Ring Structures*; 1982; pp 311–324.

(18) Dabi, S.; Zilkha, A. Oligotrimerization of Hexamethylene Diisocyanate by Organometallic Catalysts. *Eur. Polym. J.* **1980**, *16*, 831–833.

(19) Moritsugu, M.; Sudo, A.; Endo, T. Development of High-Performance Networked Polymers Based on Cyclotrimerization of Isocyanates: Control of Properties by Addition of Monoisocyanates. *J. Polym. Sci. Part A Polym. Chem.* **2012**, *50*, 4365–4367.

(20) Moritsugu, M.; Sudo, A.; Endo, T. Development of High-Performance Networked Polymers Consisting of Isocyanurate Structures Based on Selective Cyclotrimerization of Isocyanates. *J. Polym. Sci. Part A Polym. Chem.* **2011**, *49*, 5186–5191.

(21) Levchik, S. V.; Weil, E. D. A Review of Recent Progress in Phosphorus-Based Flame Retardants. *J. Fire Sci.* **2006**, *24*, 345–364.
(22) Velencoso, M. M.; Battig, A.; Markwart, J. C.; Schartel, B.; Wurm, F. R. Molecular Firefighting—How Modern Phosphorus Chemistry Can Help Solve the Challenge of Flame Retardancy. *Angew. Chemie - Int. Ed.* **2018**, *57*, 10450–10467.
(23) Liang, S.; Neisius, M.; Mispreuve, H.; Naescher, R.; Gaan, S. Flame Retardancy and Thermal Decomposition of Flexible Polyurethane Foams: Structural Influence of Organophosphorus Compounds. *Polym. Degrad. Stab.* **2012**, *97*, 2428–2440.
(24) Schartel, B. Phosphorus-Based Flame Retardancy Mechanisms-Old Hat or a Starting Point for Future Development? *Materials (Basel).* **2010**, *3*, 4710–4745.
(25) Toldy, A.; Harakály, G.; Szolnoki, B.; Zimonyi, E.; Marosi, G. Flame Retardancy of Thermoplastics Polyurethanes. *Polym. Degrad. Stab.* **2012**, *97*, 2524–2530.
(26) Sut, A.; Metzsch-Zilligen, E.; Großhauser, M.; Pfaendner, R.; Schartel, B. Rapid Mass Calorimeter as a High-Throughput Screening Method for the Development of Flame-Retarded TPU. *Polym. Degrad. Stab.* **2018**, *156*, 43–58.
(27) Zhou, F.; Ma, C.; Zhang, K.; Chan, Y. Y.; Xiao, Y.; Schartel, B.; Doring, M.; Wang, B.; Hu, W.; Hu, Y. Synthesis of Ethyl (Diethoxymethyl)Phosphinate Derivatives and Their Flame Retardancy in Flexible Polyurethane Foam: Structure-Flame Retardancy Relationships. *Polym. Degrad. Stab.* **2021**, *188*, 109557.
(28) Chan, Y. Y.; Ma, C.; Zhou, F.; Hu, Y.; Schartel, B. A Liquid Phosphorous Flame Retardant Combined with Expandable Graphite or Melamine in Flexible Polyurethane Foam. *Polym. Adv. Technol.* **2022**, *33*, 326–339.
(29) Weil, E. D.; Levchik, S. V. Commercial Flame Retardancy of Polyurethanes. *J. Fire Sci.* **2004**, *22*, 183–210.
(30) Rao, W. H.; Xu, H. X.; Xu, Y. J.; Qi, M.; Liao, W.; Xu, S.; Wang, Y. Z. Persistently Flame-Retardant Flexible Polyurethane Foams by a Novel Phosphorus-Containing Polyol. *Chem. Eng. J.* **2018**, *343*, 198–206.
(31) Yuan, Y.; Yang, H.; Yu, B.; Shi, Y.; Wang, W.; Song, L.; Hu, Y.; Zhang, Y. Phosphorus and Nitrogen-Containing Polyols: Synergistic Effect on the Thermal Property and Flame Retardancy of Rigid Polyurethane Foam Composites. *Ind. Eng. Chem. Res.* **2016**, *55*, 10813–10822.
(32) Sykam, K.; Meka, K. K. R.; Donempudi, S. Intumescent Phosphorus and Triazole-Based Flame-Retardant Polyurethane Foams from Castor Oil. *ACS Omega* **2019**, *4*, 1086–1094.
(33) Zhou, F.; Zhang, T.; Zou, B.; Hu, W.; Wang, B.; Zhan, J.; Ma, C.; Hu, Y. Synthesis of a Novel Liquid Phosphorus-Containing Flame Retardant for Flexible Polyurethane Foam: Combustion Behaviors and Thermal Properties. *Polym. Degrad. Stab.* **2020**, *171*, 109029.
(34) Rao, W. H.; Zhu, Z. M.; Wang, S. X.; Wang, T.; Tan, Y.; Liao, W.; Zhao, H. B.; Wang, Y. Z. A Reactive Phosphorus-Containing Polyol Incorporated into Flexible Polyurethane Foam: Self-Extinguishing Behavior and Mechanism. *Polym. Degrad. Stab.* **2018**, *153*, 192–200.
(35) Liu, B. W.; Zhao, H. B.; Wang, Y. Z. Advanced Flame-Retardant Methods for Polymeric Materials. *Adv. Mater.* **2022**, *2107905*, 1–36.
(36) Duquesne, S.; Bras, M. Le; Bourbigot, S.; Delobel, R.; Camino, G.; Eling, B.; Lindsay, C.; Roels, T.; Vezin, H. Mechanism of Fire Retardancy of Polyurethanes Using Ammonium Polyphosphate. *J. Appl. Polym. Sci.* **2001**, *82*, 3262–3274.
(37) Stowell, J. K.; Francisco, G.; Weil, E. Method of Making Hydroxymethylphosphonate, Polyurethane Foam-Forming Compositions, Polyurethane Foam and Articles Made Therefrom. WO 2014062313 A1, 2014.
(38) Lapprand, A.; Boisson, F.; Delolme, F.; Méchin, F.; Pascault, J. P. Reactivity of Isocyanates with Urethanes: Conditions for Allophanate Formation. *Polym. Degrad. Stab.* **2005**, *90*, 363–373.
(39) Duff, D. W.; Maciel, G. E. ^{13}C and ^{15}N CP/MAS NMR Characterization of MDI-Polyisocyanurate Resin Systems. *Macromolecules* **1990**, *23*, 3069–3079.
(40) Reignier, J.; Méchin, F.; Sarbu, A. Chemical Gradients in PIR Foams as Probed by ATR-FTIR Analysis and Consequences on Fire Resistance. *Polym. Test.* **2021**, *93*, 106972.
(41) Zhou, Z.; He, Y.; Qiu, X.; Redwine, D.; Potter, J.; Cong, R.; Miller, M. Optimum $Cr(Acac)_3$ Concentration for NMR Quantitative Analysis of Polyolefins. *Macromol. Symp.* **2013**, *330*, 115–122.
(42) Braun, S.; Kalinowski, H. O.; Berger, S. *100 and More Basic NMR Experiments: A Practical Course*; Wiley, 1996.
(43) Harris, L. A.; Goff, J. D.; Carmichael, A. Y.; Riffle, J. S.; Harburn, J. J.; St. Pierre, T. G.; Saunders, M. Magnetite Nanoparticle Dispersions Stabilized with Triblock Copolymers. *Chem.*

Mater. **2003**, *15*, 1367–1377.
(44) Frisch, K. C.; Klempner, D. *Advances in Urethane: Science & Technology, Volume XIV*; CRC Press, 2020.
(45) Dick, J. S.; Annicelli, R. A. *Rubber Technology: Compounding and Testing for Performance*; Hanser, 2009.
(46) Ziegler, W.; Guttmann, P.; Kopeinig, S.; Dietrich, M.; Amirosanloo, S.; Riess, G.; Kern, W. Influence of Different Polyol Segments on the Crystallisation Behavior of Polyurethane Elastomers Measured with DSC and DMA Experiments. *Polym. Test*. **2018**, *71*, 18–26.
(47) Chan, Y. Y.; Korwitz, A.; Pospiech, D.; Schartel, B. Flame Retardant Combinations with Expandable Graphite/Phosphorus/CuO/Castor Oil in Flexible Polyurethane Foams. *ACS Appl. Polym. Mater*. **2023**, *5*, 1891–1901.
(48) Perret, B.; Schartel, B.; Stöß, K.; Ciesielski, M.; Diederichs, J.; Döring, M.; Krämer, J.; Altstädt, V. Novel DOPO-Based Flame Retardants in High-Performance Carbon Fibre Epoxy Composites for Aviation. *Eur. Polym. J*. **2011**, *47*, 1081–1089.
(49) Xu, Q.; Hong, T.; Zhou, Z.; Gao, J.; Xue, L. The Effect of the Trimerization Catalyst on the Thermal Stability and the Fire Performance of the Polyisocyanurate-Polyurethane Foam. *Fire Mater*. **2018**, *42*, 119–127.
(50) Gao, L.; Zheng, G.; Zhou, Y.; Hu, L.; Feng, G.; Zhang, M. Synergistic Effect of Expandable Graphite, Diethyl Ethylphosphonate and Organically-Modified Layered Double Hydroxide on Flame Retardancy and Fire Behavior of Polyisocyanurate-Polyurethane Foam Nanocomposite. *Polym. Degrad. Stab*. **2014**, *101*, 92–101.
(51) Duff, D. W.; Maciel, G. E. Monitoring the Thermal Degradation of an Isocyanurate-Rich MDI-Based Resin by ^{15}N and ^{13}C CP/MAS NMR. *Macromolecules* **1991**, *24*, 651–658.
(52) Chambers, J.; Jiricny, J.; Reese, C. B. The Thermal Decomposition of Polyurethanes and Polyisocyanurates. *Fire Mater*. **1981**, *5*, 133–141.
(53) Zhang, Z.; Li, D.; Xu, M.; Li, B. Synthesis of a Novel Phosphorus and Nitrogen-Containing Flame Retardant and Its Application in Rigid Polyurethane Foam with Expandable Graphite. *Polym. Degrad. Stab*. **2020**, *173*, 109077.
(54) Ferrari, A. C.; Robertson, J. Interpretation of Raman Spectra of Disordered and Amorphous Carbon. *Phys. Rev. B* **2000**, *61*, 14095–14107.

Chapter 5

A Mechanism of Amine Catalyzed Aromatic Imide Formation from the Reaction of Isocyanates with Anhydrides

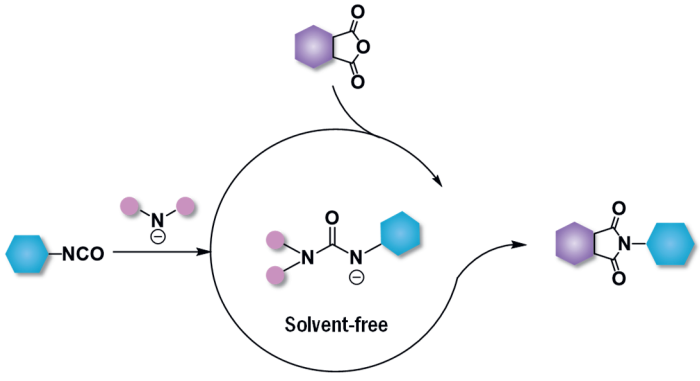

This chapter is based on published work:
Guo, Y.; Spicher, S.; Cristadoro, A.; Deglmann, P.; Sijbesma, R. P.; Tomović, Ž., Towards high-performance polyurethanes: A mechanism of amine catalyzed aromatic imide formation from the reaction of isocyanates with anhydrides, *Polym. Chem.* **2023**, *14*, 1773-1780.
The experiments and measurements presented in this chapter were performed by Yunfei Guo. The theoretical calculations presented in this chapter were performed by Sebastian Spicher.

Poly(urethane imide)s (PUIs) with improved thermal properties and flame retardancy can be made in a direct way by the reaction of isocyanates with anhydrides to give aromatic imides. We investigated the mechanism of this reaction in the presence of water with experimental studies and quantum chemical calculations. The catalytic cycle is driven by the urea obtained from the hydrolysis of isocyanates. We show that with a secondary amine as a pre-catalyst and tertiary amine as a co-catalyst, the reaction proceeds fast without a need for additional solvent. The insights in the underlying mechanism provided by the computational study have guided the development of a solvent-free synthetic method that provides a pathway to produce PUIs on an industrial scale.

5.1 Introduction

Polyurethanes (PUs) are among the most widely produced plastics worldwide.[1] Showing versatile properties, PUs are used for construction, consumer products, furniture and in the automotive industry.[2-5] Although many different PU materials are available, further improvement of the physical properties of the materials will make them suitable for an increased number of applications, providing new market opportunities. Aromatic polyimides present a class of well-known high-performance polymers with outstanding thermal, mechanical, and electrical properties.[6-13] They have been used to improve the properties of a variety of polymer matrixes (*e.g.*, poly(ether imide)s, poly(ester imide)s, poly(amide imide)s).[10,14-18] Especially the co-polymerization of prepolymers containing aromatic polyimide structures with conventional PU raw materials results in significant improvements in thermal stability and flame retardancy and hence, poly(urethane imide)s are promising building blocks for the development of new thermoplastics,[19-25] rigid foams[26-30] and coatings.[31-34]

Aromatic imides are usually introduced in poly(urethane-imide)s by the reaction of amines or isocyanates with anhydrides.[9-11] It is generally accepted that the amine-anhydride reaction follows a two-step mechanism. First, the nucleophilic amine attacks one of the carbonyl carbon atoms of the anhydride, forming an amic acid. Second, imidization of the amic acid leads to the release of a molecule of water.[9,11,35] Whereas the mechanism of the reaction of anhydrides with amines is known, the much more complicated mechanism of imide formation from reaction of anhydrides with aromatic isocyanates is still under debate.[11]

Two distinct mechanisms have been proposed for the formation of imides from reaction of aromatic isocyanates with anhydrides. Based on Fourier-transform infrared spectroscopy (FT-IR) studies, several groups proposed that the reaction between aromatic isocyanate and anhydride forms a seven-membered-ring, followed by imidization with elimination of a CO_2 molecule (**Scheme 5-1a**).[36-40] Later, these findings were challenged by Carleton *et al*. who postulated that the spectroscopic evidence points to a hydrolysis product rather than an intermediate with a seven-membered ring, because they discovered that the polymerization rate increased with water concentration.[28,41] Accordingly, they proposed that the aromatic imide is obtained from the reaction of anhydride with a urea (**Scheme 5-1b**), accelerated by water and other nucleophiles. However, no reliable kinetic or mechanistic studies are currently available to give conclusive evidence for either proposed mechanism.

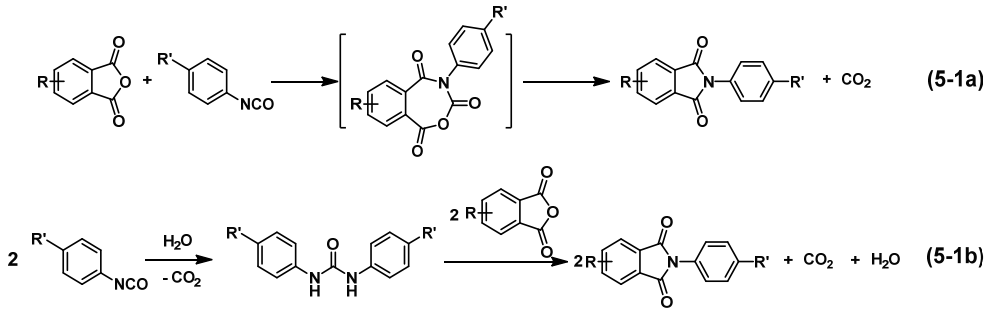

Scheme 5-1. Proposed mechanisms of aromatic isocyanate-anhydride reaction from literature: (a) 7-membered ring mechanism;[36] (b) urea-dianhydride mechanism, where urea is formed from the intermediary amine hydrolysis product of isocyanate.[41]

A better understanding of the mechanism of aromatic isocyanate-dianhydride reactions will allow further development of poly(urethane-imide) chemistry, by guiding optimization of the reaction conditions. Here, the reaction mechanism of imide formation from aromatic isocyanates and dianhydrides in the presence of catalytic amounts of water was investigated with nuclear magnetic resonance spectroscopy (NMR), liquid chromatography-mass spectrometry (LC-MS), and quantum mechanical (QM) computations. The results reveal (I) that the preferred pathway involves formation of urea as a hydrolysis product, and (II) in the reaction of excess isocyanate with anhydrides, urea instead of water is the actual catalyst in the reaction. Furthermore, we demonstrate that secondary amines are better pre-catalysts than water and that addition of a nucleophilic co-catalyst considerably reduces reaction time. These novel insights of the underlying mechanism will help to pave the way towards a completely solvent-free synthetic route to imides, which is important for developing poly(urethane-imide)s in industrial applications.

5.2 Results and discussion

5.2.1 Hydrolysis products in aromatic isocyanate-anhydride reactions

The reaction between phthalic anhydride and phenyl isocyanate (this combination giving rise to a soluble imide) in the presence of water was used to determine the hydrolysis products (**Scheme 5-2**). First, model reaction 5-2 was carried out in an NMR tube in DMSO-d_6. The reaction was monitored with NMR spectroscopy at room temperature and the formation of *N*-phenylphthalimide was observed. However, neither the proton nor the carbon NMR spectra showed evidence of an intermediate with a seven-membered-ring (see supplementary data). To shed some light on this mechanism, we also performed QM calculations for the seven-membered-ring pathway. The results given in the supplementary data (**Scheme S5-1**) show no indication of the

formation of such an intermediate, due to a high kinetic barrier resulting from a very high activation energy for its formation.

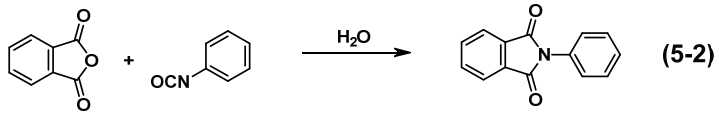

Scheme 5-2. Formation of *N*-phenylphthalimide from reaction between phthalic anhydride and phenyl isocyanate.

When water is present in the reaction mixture, isocyanate or anhydride can be hydrolyzed to urea or the diacid, respectively. To verify the formation of these hydrolysis products, model reaction 5-2 was further dissected by studying reactions 5-3a and 3b, in which each one of the phthalic anhydride or phenyl isocyanate hydrolysis products was allowed to react with the other component in a 1:1 molar ratio (**Scheme 5-3**).

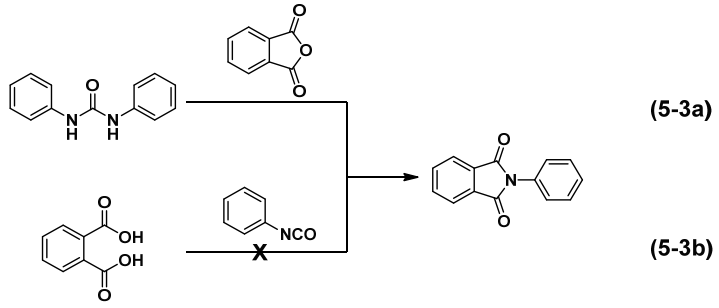

Scheme 5-3. Formation of *N*-phenylphthalimide from reaction between (a) 1,3-diphenylurea and phthalic anhydride; (b) phthalic acid and phenyl isocyanate.

According to ^{13}C NMR spectra (**Figure 5-1a**), full conversion to *N*-phenylphthalimide was achieved after reacting 1,3-diphenyl urea and phthalic anhydride (reaction 5-3a) in DMF at 140 ºC for 22 h, while no *N*-phenylphthalimide was obtained by carrying out the reaction at lower temperature (*e.g.*, at 66 ºC in refluxing THF). Reaction of phthalic acid with phenyl isocyanate (reaction 5-3b) in refluxing THF only gave mono- and di-amides. Interestingly, the formation of phthalic anhydride (carbonyl carbon at 164.0 ppm) and 1,3-diphenylurea (carbonyl carbon at 153.5 ppm) were observed (**Figure 5-1b**).[42,43] In DMF at 140 ºC, phthalic anhydride and diphenylurea were formed within 15 min, and a small amount of imide was produced. Comparison of reactions 5-3a and 5-3b suggests that urea is more readily formed than diacid, and that the reaction between urea and anhydride requires high temperatures.

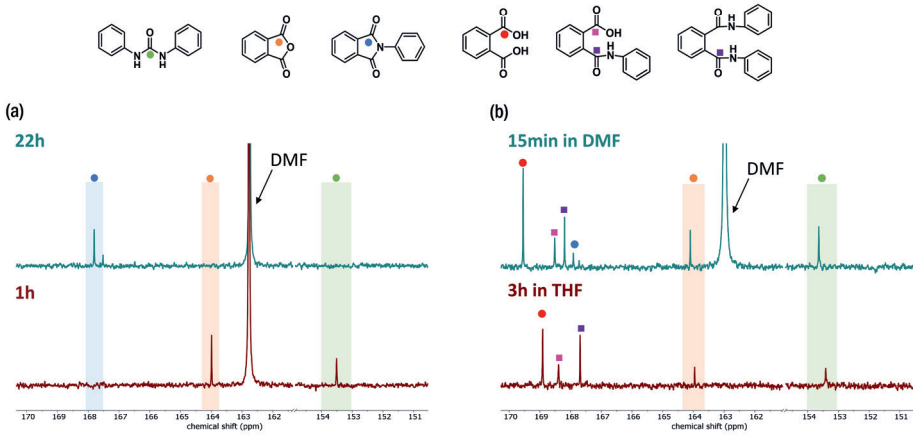

Figure 5-1. ^{13}C NMR spectra (100 MHz, acetone-d_6) of the product obtained from reaction between (a) 1,3-diphenylurea and phthalic anhydride in DMF at 140 °C; (b) phthalic acid and phenyl isocyanate in THF reflux or DMF at 140 °C.

Nevertheless, the mechanism of the reaction between urea and anhydride needs further investigation because it is not clear how urea reacts with two molecules of anhydride under the release of one molecule of each CO_2 and H_2O. Therefore, LC-MS was used to identify the intermediates in the isocyanate-anhydride reaction in the presence of water. To speed up the reaction, a highly reactive anhydride, pyromellitic dianhydride (PMDA) was used, while the solubility of the imide product for LC-MS measurement was improved by using hexyl isocyanate. Model reaction 5-4 between PMDA and hexyl isocyanate was carried out in refluxing THF containing 1 mol% water (**Scheme 5-4**). After 21 h, new peaks in the ^1H NMR spectrum between 3.65-3.80 ppm (**Figure 5-2a**) indicated formation of dihexylurea and imide. In LC-MS of the mixture obtained (**Figure 5-2b** and **Table 5-1**), a peak with a signal at m/z = 548.25 was observed, which was assigned to the ring-opened product of the reaction of PMDA with 1,3-dihexylurea (**VI** and **VII**). This is a strong indication that a urea is involved as intermediate in the formation of imide from reaction of isocyanate with anhydride.

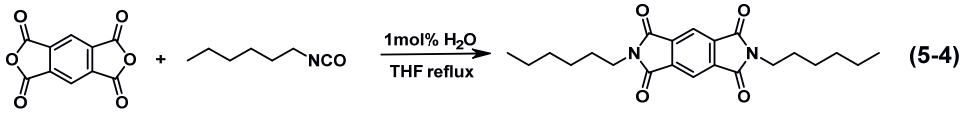

(5-4)

Scheme 5-4. Model reaction of pyromellitic anhydride and hexyl isocyanate in the presence of catalytic amount of water. The reaction was used to identify the intermediate during the isocyanate-anhydride reaction.

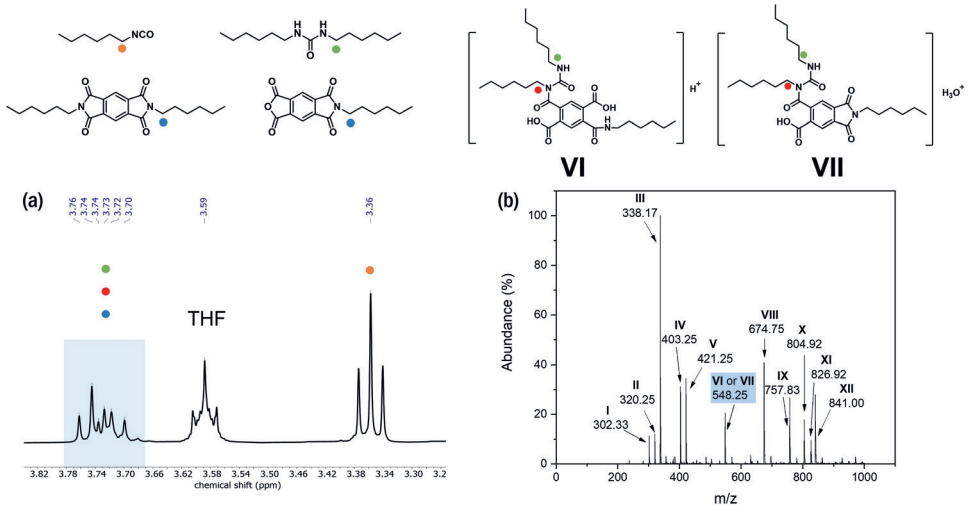

Figure 5-2 (a) ^{1}H NMR spectrum (400 MHz, acetone-d_6) and (b) LC-MS spectrum of the intermediates obtained in model reaction 5-4.

Table 5-1. LC-MS analysis of the intermediates obtained in the model reaction 5-4.

	m/z	Abundance (%)	Assignment
I	302.33	11	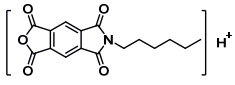
II	320.25	12	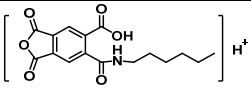
III	338.17	100	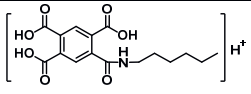
IV	403.25	31	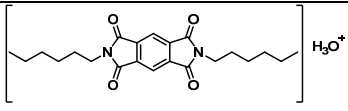
V	421.25	35	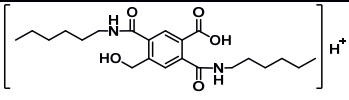
VI	548.25	21	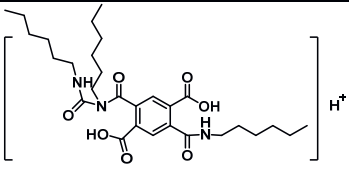

VII	548.25	21	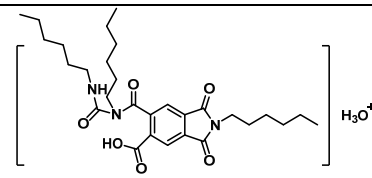
VIII	674.75	41	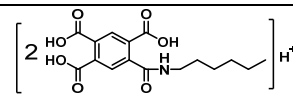
IX	757.83	27	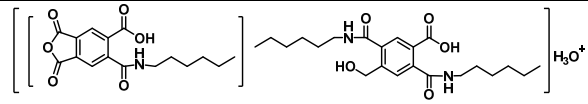
X	804.92	18	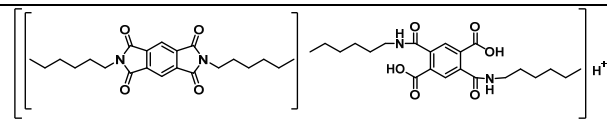
XI	826.92	10	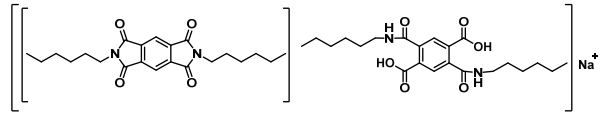
XII	841.00	28	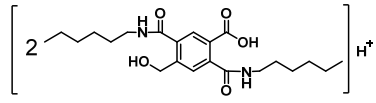

5.2.2 Optimization of the aromatic isocyanate-anhydride reaction

Based on the observation of a signal with m/z = 548.25 in LC-MS, we proposed that during the aromatic isocyanate-anhydride reaction, the urea is deprotonated and attacks the positively charged carbonyl carbon of PMDA, forming an amic acid. After the ring closure of the amic acid and formation of an imide, the urea is released. To accelerate this reaction, we systematically investigated different pre-catalysts, other than water in combination with additional co-catalysts.

Reaction conditions were optimized with PMDA as a substrate. PMDA is one of the most reactive dianhydrides due to its high electron affinity,[9,44] and thus, it is commonly used to react with excess of isocyanates to prepare isocyanate prepolymers that contain imides. The imide-containing prepolymer is used to prepare different polyurethane materials such as compact materials and rigid foams with enhanced thermal properties. In our optimization experiments, PMDA was reacted with polymeric methylene diphenyl diisocyanate (pMDI), Lupranate® M20 (NCO = 31.5 wt%, f_n = 2.7) in a 1:19 weight ratio to investigate and optimize the pre-catalyst as well as co-catalyst (**Scheme 5-5**). The dosing amount of the pre-catalyst and co-catalyst was based on the

mole amount of pMDI. Model reaction 5-5 was carried out at 140 ºC in bulk with 10 vol% triethyl phosphate (TEP) as an additive to avoid sublimation of PMDA. The reaction was followed with ^{13}C NMR spectroscopy, monitoring the carbonyl carbon peaks of anhydride and imide products. When an excess of isocyanate reacted with PMDA in the presence of water, we have demonstrated that urea was the only hydrolysis product (**Figure S5-2**). This also supports the proposal that urea is the real catalyst of the reaction, with water only acting as a pre-catalyst.

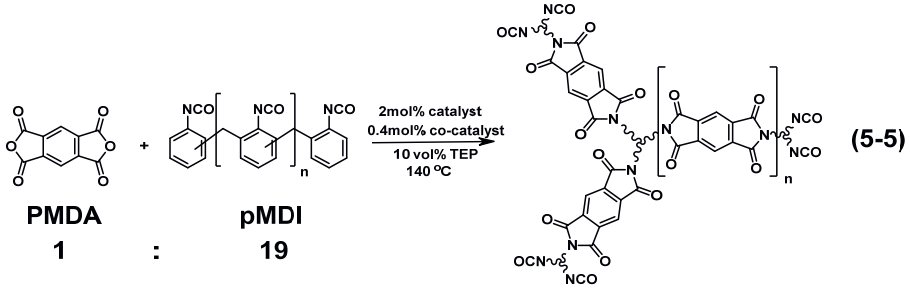

Scheme 5-5. Model reaction between PMDA and pMDI in a 1:19 weight ratio.

To generate different urea's, various primary and secondary amines were used as pre-catalysts (**Figure 5-3**). The reaction time to achieve full conversion is listed in **Table 5-2**. It was found that dibutylamine, a secondary amine, was able to accelerate the reaction.

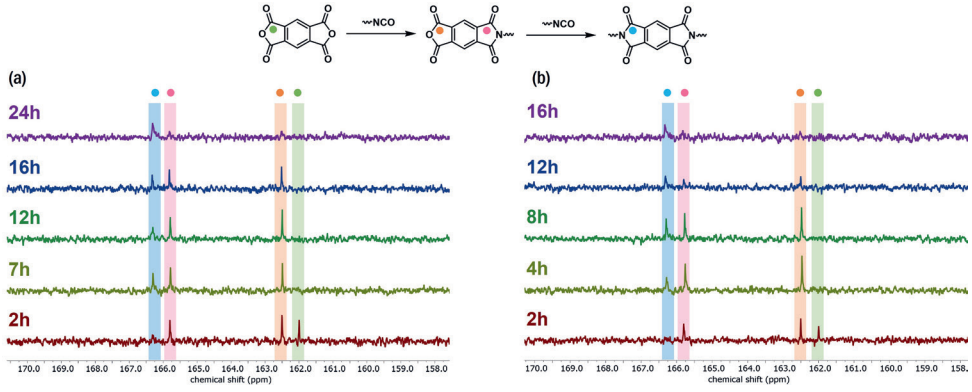

Figure 5-3. ^{13}C NMR spectra (100 MHz, acetone-d_6) of model reaction 5-5 using (a) water or (b) dibutylamine as a catalyst. The reaction was monitored at the carbonyl carbon region. During the reaction, the PMDA carbonyl carbon peak at 162.0 ppm disappeared and the two carbonyl peaks of one-sided imide structure were found at 162.5 and 165.8 ppm, respectively. Further, when PMDA was fully converted to di-imide structure, only one carbonyl carbon peak at 166.3 ppm was observed.

Table 5-2. Reaction time of model reaction 5-5 using different amines as pre-catalysts (dosing amount 2 mol%) without co-catalyst.

Entry	Pre-catalyst	Reaction time[a]
5-5-1	Water	24 h
5-5-2	*N*-Butylamine	>21 h
5-5-3	Dibutylamine	16 h

[a] The time when there was only di-imide carbonyl peak in ^{13}C NMR spectra was defined as reaction time.

Next, using dibutylamine as a pre-catalyst, basic or nucleophilic tertiary amines were used as co-catalysts to deprotonate urea (**Table 5-3**). With the help of co-catalysts, the reaction time was significantly reduced, particularly when co-catalysts with little steric hindrance were used. However, the more nucleophilic the co-catalyst was, the more likely it was to catalyze the cyclotrimerization of isocyanates after the isocyanate-dianhydride reaction (entries 5-5-8 to 5-5-10).[45]

Table 5-3. Reaction time of model reaction 5-5 using 2 mol% dibutylamine as a pre-catalyst and different tertiary amine as co-catalysts (dosing amount 0.4 mol%).

Entry	Co-catalyst	Reaction time[a]
5-5-4	*N*,*N*-Diisopropylethylamine	8 h
5-5-5	Tributylamine	8 h
5-5-6	*N*,*N*-Dimethylcyclohexylamine	6 h
5-5-7	4-Methylmorpholine	>18 h
5-5-8	4-(Dimethylamino)pyridine	Isocyanurate formation
5-5-9	1,4-Diazabicyclo[2.2.2]octane	Isocyanurate formation
5-5-10	1,5,7-Triazabicyclo[4.4.0]dec-5-en	Isocyanurate formation

[a] The time when there was only di-imide carbonyl peak in ^{13}C NMR spectra was defined as reaction time.

Based on results shown in **Table 5-3**, *N*,*N*-dimethylcyclohexylamine (DMCHA) was chosen as the optimal co-catalyst and various secondary amines were evaluated as a pre-catalyst (**Table 5-4**). *N*-methylaniline turned out to be a better secondary amine pre-catalyst than dibutylamine. When *N*-methylaniline was used as a pre-catalyst and DMCHA was used as a co-catalyst, the reaction time was greatly shortened from 24 h (entry 5-5-1) to 4 h (entry 5-5-11).

Table 5-4. Reaction time of model reaction 5-5 using 0.4 mol% DMCHA as a co-catalyst and different secondary amine as pre-catalysts (dosing amount 2 mol%).

Entry	Pre-catalyst	Reaction time[a]
5-5-11	*N*-methylaniline	4 h
5-5-12	4-Methoxy-*N*-methylaniline	6 h
5-5-13	*N*-Methyl-*o*-toluldine	7 h
5-5-14	Imidazole	7 h
5-5-15	Diphenylamine	6 h
5-5-16	ε-Caprolactam	5 h
5-5-17	Phthalimide	8 h

[a] The time when there was only di-imide carbonyl peak in ^{13}C NMR spectra was defined as reaction time.

Based on these experimental findings, we conclude that water or amines function as pre-catalysts in the aromatic isocyanate-anhydride reaction, while the urea obtained out of it is the real catalyst. Additional experiments were performed by replacing secondary amines with urea as catalysts in model reaction 5-5; also here, imide structures were obtained in the end (see supplementary data).

5.2.3 Computational studies of aromatic isocyanate-anhydride reaction with secondary amines as pre-catalysts

To obtain further insights into the thermodynamics and kinetics of the isocyanate-anhydride reaction, computer simulations were additionally applied. Quantum chemical calculations serve nowadays as an indispensable tool to reveal reaction mechanism at an atomic level. Therefore, in state-of-the-art computational workflows, efficient screening techniques are combined with highly accurate density functional theory (DFT) methods for postprocessing.[46] In this work, we employ the widely used CREST algorithm combined with extended tight-binding QM methods (GFN2-xTB) to explore the low-energy conformational space.[46] Conformational screening was followed by DFT re-optimization (TPSS-D3/def2-TZVP)[47–50] and final single-point energies were computed with the M06-2x[51] density functional approximation in a large def2-QZVP basis set. Bulk phenyl isocyanate was taken as the solvent and accounted for implicitly by COSMO-RS[52,53] theory. For further computational details see Section 5.4.

The free energy diagram of the imide-forming reaction is given in **Figure 5-5** (black line). As an upstream process, *N*-methylaniline is added to phenyl isocyanate to form 1-methyl-1,3-diphenyl-urea, or simply urea from now on. In the transition state TS_0 (see **Figure 5-4a**), water acts as a hydrogen shuttle and forms a six-membered ring. With secondary amines, the urea formation is 30 kJ/mol higher in energy, underlining the assumption that water is the pre-catalyst for fast urea generation. Urea is then deprotonated by DMCHA, yielding the effective catalyst of the imide-forming reaction

mechanism. Please note, from this point on, the reaction path occurs *via* charged species. In a nucleophilic addition, the urea anion ring-opens the anhydride **A** to form intermediate **B.** The reaction is facilitated by hydrogen-bonding between $DMCHA^+$ and PMDA within the transition state TS_1 (**Figure 5-4b**), showing an activation barrier ($\Delta G^‡$) of 9 kJ/mol. As none of the two nitrogen atoms within this intermediate are good nucleophiles, ring-closure at this stage of the reaction cycle is not possible. Instead, the carboxylate group of **B** adds one more equivalent of phenyl isocyanate to form the second intermediate **C** *via* TS_2 (**Figure 5-4c**) with a $\Delta G^‡$ of 63 kJ/mol. In the rate determining step of the reaction, CO_2 is released *via* TS_3 that occurs *via* a four-membered ring (**Figure 5-4d**). The activation barrier for the CO_2 release amounts to 52 kJ/mol. It is now the nucleophilic nitrogen atom in **D** that initializes the ring closure by formation of the tetrahedral intermediate **E**. Elimination of the catalytically acting urea anion finally yields the desired imide **F**.

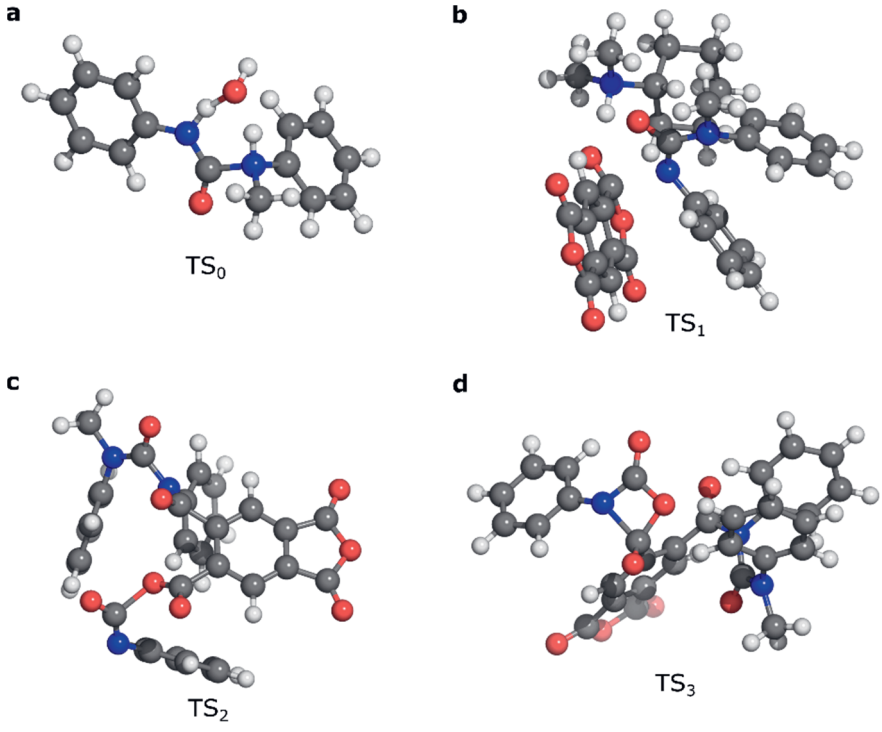

Figure 5-4. Refined transition state structures at the TPSS-D3/def2-TZVP level of theory within the reaction of PMDA and phenyl isocyanate to form the imide.

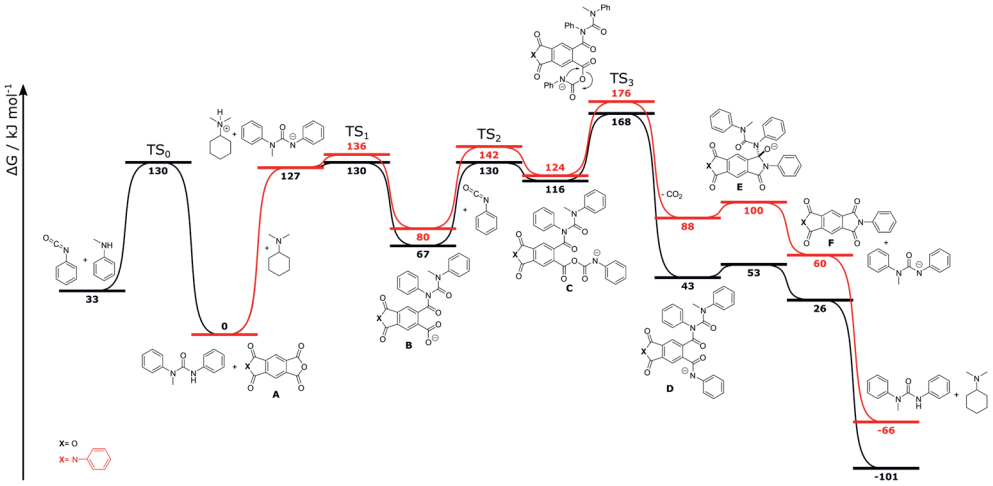

Figure 5-5. Free energy diagram of the conversion of PMDA and phenyl isocyanate to form an (di)imide at the M06-2x/def2-QZVP+COSMO-RS(phenyl isocyanate)//TPSS-D3(COSMO(∞))/def2-TZVP level of theory. All free energies are given in kJ/mol.

Our quantum chemical computer simulations prove that water only acts as a pre-catalyst, while urea, or to be more precise its deprotonated form, acts as the actual catalyst. All findings can be summarized in a single catalytic cycle shown in **Scheme 5-6** (black lines).

Further theoretical insights were needed to explain a fast initial release of CO_2 (minutes) that was observed experimentally, followed by a slower release of CO_2 over the next few hours. NMR spectroscopy studies suggested that the symmetric anhydride PMDA reacts in a two-step process *via* a one-sided imide to a di-imide (**Figure 5-6**). Therefore, the QM simulation of the reaction cycle of imide formation was repeated, starting from the half-imide-half-anhydride structure (**Figure 5-5** and **Scheme 5-6** red line). The change in the electronic structure caused by the half-imide formation leads to an upshift in energy of the reaction path compared to PMDA. Especially at the highest energy point (TS_3), according to transition state theory,[54] a relative increase of 8 kJ/mol causes the reaction to last more than ten times longer (hours instead of minutes). This good agreement between computer simulations and experimental findings further establishes the correctness of the identified reaction mechanism.

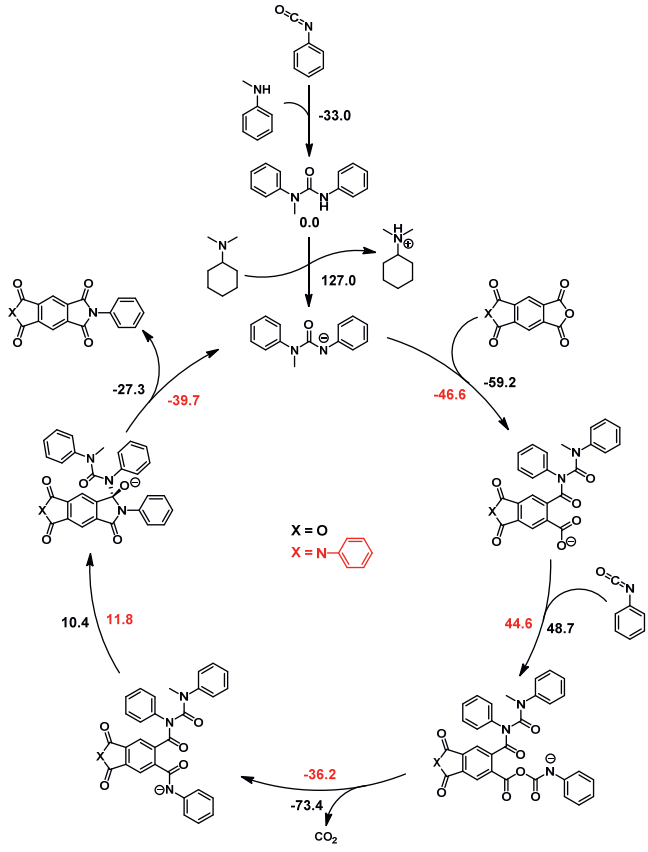

Scheme 5-6. Catalytic cycle of the aromatic isocyanate-dianhydride reaction using *N*-methylaniline as a pre-catalyst and DMCHA as a co-catalyst. The computed activation free energies ($\Delta G^{\ddagger}$) for all transition states and reaction free energies (ΔG) are given in kJ/mol.

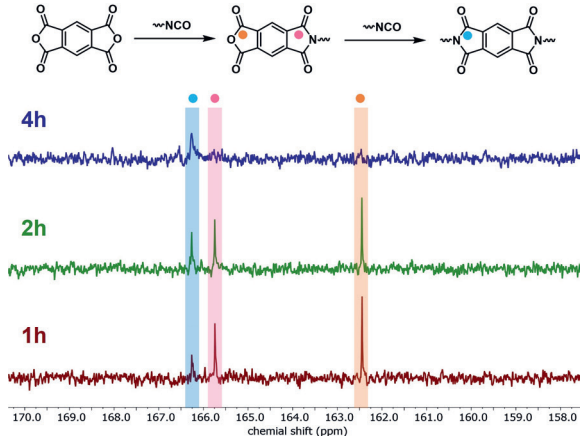

Figure 5-6. ^{13}C NMR spectra (100 MHz, acetone-d_6) of model reaction 5-5 using *N*-methylaniline as a pre-catalyst and DMCHA as a co-catalyst.

There is a discrepancy between experimental observations and absolute theoretically computed activation barriers. With optimal catalysts (*N*-methylaniline, DMCHA) and additives (TEP) the reaction finishes within four hours, whereas it would take days to overcome the highest activation barrier (TS_3) of 168 kJ/mol with respect to the catalytic resting state. It can be expected that the applied implicit COSMO(-RS) solvation model does not accurately describe the charge separation leading to free anions. Especially because of the high temperatures (140 ºC), the validity of the applied solvation model is questionable. Since the importance of additive TEP is experimentally known, yet the implicit incorporation of 10 vol% within COSMO-RS shows no significant energy lowering of the ionic species, we added an explicit TEP molecule for stabilization. Exemplary, the deprotonation of urea by DMCHA was explicitly solvated with TEP, lowering the free energy of the resulting complex by -10 kJ/mol. Since the explicit incorporation of TEP within the entire catalytic cycle is computationally too demanding, we assume that this energy lowering can be transferred to all ionic species along the reaction path. This simple example of explicit solvent addition already significantly reduces the divergence between experiment and theory. It highlights the importance of an accurate description of solvation effects and shows that in current solvent models there is still room for improvement if ionic species are concerned.

5.3 Conclusion

We investigated the reaction mechanism of aromatic isocyanates and dianhydrides in the presence of water to form imides. Our study revealed that during the reaction urea, formed as the hydrolysis product from isocyanate, acted as the actual catalyst in the reaction. Secondary amines, with the help of tertiary amine bases, were further discovered as better pre-catalysts (or, rather, co-catalysts) than water. The reaction time strongly decreased from 24 h with water as a pre-catalyst to 4 h with *N*-methylaniline and *N,N*-dimethylcyclohexylamine as pre-catalyst and co-catalyst respectively. Further, the combination of experimental and computational results revealed exclusive insights in the reaction of aromatic isocyanates and dianhydrides, starting from the deprotonated urea, which ring-opens the anhydrides to form an amic acid intermediate. After this step, the carboxylate of the acid intermediate reacts with one more isocyanate molecule, followed by release of a CO_2 molecule and ring closure, forming the imide structure.

Our current study highlights how the combination of state-of-art experimental and computational techniques allows for unique mechanistic insights and is able to answer questions that have been open for debate for quite a while. These exclusive insights into the underlying mechanism demonstrate the possibility of producing poly(urethane-imide)s under completely solvent-free conditions with a short reaction time. This is

especially important for industrial applications in terms of green chemistry and low costs. Our results provide convincing evidence that the revealed mechanism of aromatic imide formation can also be applied in the reaction between various aliphatic isocyanates and dianhydrides to form aliphatic imides. These aliphatic imides can potentially help to improve the thermal stability of materials that are synthesized from aliphatic isocyanates such as PU coatings, sealants, and adhesives.

5.4 Experimental section

Materials

Phthalic anhydride (≥99%), phthalic acid (≥99.5%), phenyl isocyanate (≥98%), 1,3-diphenylurea (98%), triethylamine (99.5%), pyromellitic dianhydride (97%), hexyl isocyanate (97%), triethyl phosphate (≥99.8%), *N*-butylamine (≥99.5%), dibutylamine (≥99.5%), *N*,*N*-diisopropylethylamine (≥99%), tributylamine (≥99.5%), *N*,*N*-dimethylcyclohexylamine (99%), 4-methylmorpholine (≥99.5%), 4-(dimethylamino)pyridine (≥99%), 1,4-diazabicyclo[2.2.2]octane (DABCO) (≥99%), 1,5,7-triazabicyclo[4.4.0]dec-5-en (TBD) (98%), *N*-methylaniline (98%), 4-methoxy-*N*-methylaniline (98%), *N*-methyl-*o*-toluldine (≥95%), imidazole (99%), diphenylamine (99%), *ε*-caprolactam (for synthesis), phthalimide (≥99%), *p*-tolyl isocyanate (99%) were purchased from Sigma-Aldrich and all the reagents were used directly without treatment. Polymeric MDI, Lupranate® M20 (NCO content = 31.5%, f_n = 2.7) was kindly provided by BASF Polyurethanes GmbH. Dimethylformamide (DMF) and tetrahydrofuran (THF, without stabilizer BHT) were directly obtained from the dry solvent system. Triethyl phosphate (≥99.8%) was purchased from Sigma-Aldrich and dried with mol-sieves before use.

Synthesis

Study of reaction between phthalic anhydride and phenyl isocyanate (5-2). Phthalic anhydride (28.0 mg, 0.19 mmol) and phenyl isocyanate (22.6 mg, 0.19 mmol) were dissolved by DMSO-d_6 (ampule) in an NMR tube. The reaction was monitored with ^{1}H and ^{13}C NMR spectroscopy.

Study of reaction between phthalic anhydride and 1,3-diphenyl urea (5-3a). Phthalic anhydride (0.6 g, 4.07 mmol) and 1,3-diphenyl urea (0.43 g, 2.03 mmol) were dissolved in 5.3 mL DMF in a dry 2-neck flask equipped with a condenser. The reaction was carried out at 140 °C in an oil bath under an Ar atmosphere overnight and monitored with ^{13}C NMR spectroscopy.

Study of reaction between phthalic acid and phenyl isocyanate (5-3b). Phthalic acid (0.9 g, 5.23 mmol) and phenyl isocyanate (0.6 g, 5.23 mmol) were dissolved in 7.5 mL THF in a dry 2-neck flask equipped with a condenser. The reaction was carried out at

80 ºC in an oil bath in THF reflux under an Ar atmosphere for 5 h and then triethylamine (5 mg, 0.05 mmol) was added in the solution. The solution was stirred overnight and the reaction was monitored with ^{13}C NMR spectroscopy.

Study of reaction between pyromellitic dianhydride and hexyl isocyanate (5-4). Pyromellitic dianhydride (1.6 g, 7.45 mmol) and hexyl isocyanate (1.9 g, 14.90 mmol) were dissolved in 18 mL THF in a dry 2-neck flask equipped with a condenser. Then water (2.7 mg, 0.15 mmol) was added in the solution and the reaction was carried out at 80 ºC in an oil bath in THF reflux under an Ar atmosphere overnight. After that, most of the solvent was blown by an Ar flow. The reaction was monitored with ^{1}H NMR spectroscopy and obtained product was analyzed using LC-MS measurement.

Study of reaction between pyromellitic dianhydride and polymeric MDI (5-5). The reaction between pyromellitic dianhydride and polymeric MDI using *N*-methylaniline as a pre-catalyst and *N,N*-dimethylcyclohexylamine as a co-catalyst is used as an example to illustrate the general synthetic route: A mixture of pyromellitic dianhydride (1.1 g, 4.83 mmol) and Lupranate® M20 (20.0 g) in a dry 2-neck flask and was heated to 100 ºC under an Ar atmosphere. A pre-catalyst solution was prepared by dissolving *N*-methylaniline (0.1 g, 1.11 mmol) and *N,N*-dimethylcyclohexylamine (28.5 mg, 0.22 mmol) in 2 mL triethyl phosphate. Then the pre-catalyst solution was added into the flask and the reaction was carried out at 140 ºC in an oil bath. The reaction was monitored with ^{13}C NMR spectroscopy and the time when carbonyl peaks of anhydride and mono-imides could no longer be observed was defined as reaction time. Dark brown liquid was obtained at 140 ºC, which solidified over the time at room temperature.

Synthesis of 1-methyl-1-phenyl-3-(p-tolyl) urea. *N*-Methylaniline (1.8 g, 17.12 mmol) and p-tolyl isocyanate (2.3 g, 17.12 mmol) were dissolved in 10 mL $CHCl_3$ and the reaction was carried out at room temperature for 2 h. After that, $CHCl_3$ was removed by vacuum and the obtained solid was dried at 80 ºC oven overnight. Slightly yellow solid was obtained (4.0 g, 16.66 mmol, yield 97%). ^{1}H NMR (400 MHz, acetone-d_6): δ 7.51 - 7.41 (m, 2H), 7.41 - 7.34 (m, 2H), 7.34 - 7.27 (m, 3H), 7.16 (s, 1H), 7.00 (d, J = 8.2 Hz, 2H), 3.28 (s, 3H), 2.22 (s, 3H) ppm; ^{13}C NMR (100 MHz, acetone-d_6): δ 154.35, 143.91, 137.69, 131.15, 129.81, 128.76, 127.08, 126.75, 119.34, 36.79, 19.80 ppm.

Synthesis of 1,1-dibutyl-3-(p-tolyl) urea. Dibutylamine (1.9 g, 14.70 mmol) and *p*-tolyl isocyanate (2.0 g, 14.70 mmol) were dissolved in 10 mL $CHCl_3$ and the reaction was carried out at room temperature for 1 h. After that, $CHCl_3$ was removed by vacuum and the obtained solid was dried at 80 ºC oven overnight. White solid was obtained (3.7 g, 14.11 mmol, 95% yield). ^{1}H NMR (400 MHz, acetone-d_6): δ 7.44 (s, 1H), 7.41 - 7.33 (m, 2H), 7.01 (d, J = 8.0 Hz, 2H), 3.35 (t, J= 7.5 Hz, 4H), 2.23 (s, 3H), 1.66 – 1.49 (m,

4H), 1.36 (h, *J* = 7.5 Hz, 4H), 0.92 (t, *J* = 7.4 Hz, 6H) ppm; ^{13}C NMR (100 MHz, acetone-d_6): δ 154.85, 138.38, 130.68, 128.63, 119.76, 46.55, 30.72, 19.84, 19.80, 13.35 ppm.

Characterization

Liquid chromatography-mass spectrometry (LC-MS). LC-MS measurement for identification of intermediates was carried out on a LCQ Fleet ESI-MS (Thermo Fisher Scientific) with H_2O containing 0.1% formic acid as eluents. Sample was diluted in water/acetonitrile (1:1) solution with a concentration of 1 mg/mL for LC-MS measurement.

Nuclear magnetic resonance (NMR) spectroscopy. ^{1}H NMR spectroscopy was performed using either Bruker UltraShield 400 MHz or Varian Mercury 400 MHz spectrometer at room temperature using acetone-d_6 or DMSO-d_6 as solvent with 32 scans per spectrum. ^{13}C NMR spectroscopy for monitoring the reactions was performed using either Bruker UltraShield 400 MHz or Varian Mercury 400 MHz spectrometer at room temperature using acetone-d_6 or DMSO-d_6 as solvent with 256 scans per spectrum. For characterization of compounds, a number of 1024 scans were used.

Computational details

DFT calculations were employed to compute the reaction free energies of the investigated species to decipher the underlying reaction mechanism and to rationalize the experimental observations. For the protocol, the input structures of all molecules were generated by applying the conformer-rotamer ensemble sampling tool (CREST)[54] at the GFN2-xTB[55] and GFN-FF[56] level of theory with the implicit GBSA(THF) solvation model.[57] The energetically lowest-lying conformers were then determined out of both runs. These conformers (up to 200 structures) were further optimized using the DFT method TPSS with a def2-TZVP basis set.[58] The D3 dispersion correction and the implicit COSMO solvation model ($\varepsilon = \infty$) were applied throughout.[49,50] Free energies were calculated based on the optimized geometries by utilizing a multilevel approach. High level single-point energies were calculated with the hybrid density functional M06-2x[51] with a large def2-QZVP basis set. Solvation contributions to the free energy were calculated with COSMO-RS,[52,53] also including the volume work to convert an ideal gas at 1 bar to a solution of 1 mol/L. All quantum mechanical calculations were performed with the TURBOMOLE 7.5.1 (DFT) and xtb 6.4.1 (GFN2-xTB, and GFN-FF) program packages.[59,60]

For the COSMO-RS free energy, two single-point calculations with BP86/TZ, one in the gas phase and one in an ideal conductor, were performed. The output of these calculations was then processed by the COSMOtherm program. For the COSMO-RS free energy, the BP_TZVP_C30_1601 parameterization was used. Bulk phenyl isocyanate with 10 vol% of TEP was chosen as solvent. Thermostatistical contributions to the free

energy were calculated at the same level of theory as the geometry optimization (TPSS-D3/def2-TZVP) applying the rigid-rotor-harmonic-oscillator scheme (RRHO). The temperature was set to 413.15 K.

In the computational approach, total free energies were calculated as sum of the electronic gas phase binding energy ΔE (single-point energy), including the London dispersion contribution, thermostatistical (ΔG_{RHHO}) and solvation ($\Delta\delta G_{solv}$) contribution according to Equation below. The prefix Δ refers to the differences regarding the reaction from reactants to products.

$$\Delta G = \Delta E + \Delta G_{RRHO} + \Delta\delta G_{solv}$$

Supplementary data

Investigation of the 7-member ring mechanism. The model reaction between phthalic anhydride and phenyl isocyanate was monitored by ^{1}H and ^{13}C NMR spectroscopy in DMSO-d_6 (ampule) at room temperature in order to capture the intermediate (**Figure S5-1**). No evidence of 7-member ring was found. The formation of *N*-phenylphthalimide may be due to the presence of catalytic amount of water in DMSO-d_6.

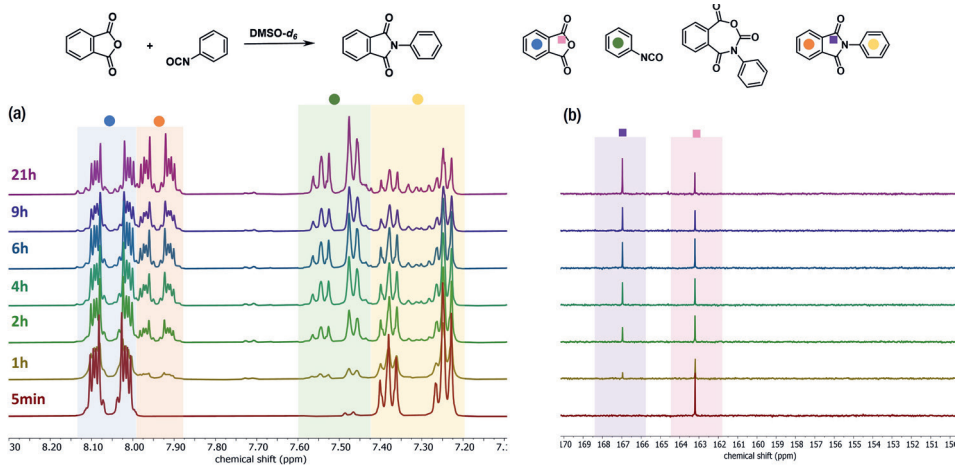

Figure S5-1. (a) ^{1}H NMR spectra (400 MHz, DMSO-d_6) and (b) ^{13}C NMR spectra (100 MHz, DMSO-d_6) of reaction between phthalic anhydride and phenyl isocyanate.

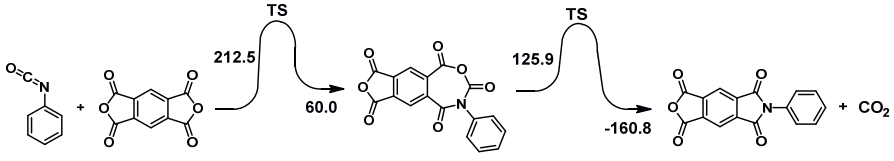

Scheme S5-1. QM studies on the proposed seven-member ring reaction mechanism of aromatic isocyanate-anhydride reaction. All values are given in kJ/mol.

Hydrolysis product in model reaction 5-5. In order to confirm that urea is the only hydrolysis product in model reaction 5-5, pyromellitic acid instead of PMDA was used to react with pMDI in a 1:19 weight ratio. With excess of isocyanates, pyromellitic acid loses one H_2O molecule and forms PMDA. The carbonyl peak of PMDA was not shown in the ^{13}C NMR spectra due to its bad solubility in isocyanate, but the urea formed from the reaction between isocyanate and H_2O was found (**Figure S5-2a**). Similar result was also observed by reacting phthalic acid with pMDI in a 1:19 weight ratio. With excess of isocyanates, phthalic acid loses one H_2O molecule and forms phthalic anhydride (**Figure S5-2b**).

Thus, if an excess of isocyanates reacts with pyromellitic dianhydride in the presence of water, the hydrolysis product can only be urea. This also supports our proposal that water only acts as a pre-catalyst for the formation of urea, which is the real catalyst of the reaction.

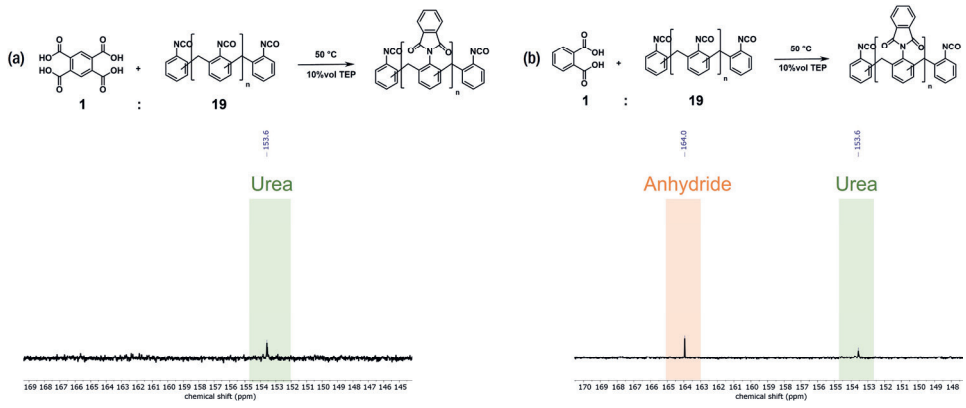

Figure S5-2. (a)^{13}C NMR spectrum (100 MHz, acetone-d_6) of the reaction between pyromellitic acid and pMDI in 1:19 weight ratio at 50 ºC with 10 vol% TEP. (b)^{13}C NMR spectrum (100 MHz, acetone-d_6) of the reaction between phthalic acid and pMDI in a 1:19 weight ratio at 50 ºC with 10 vol% TEP. In both cases, strong bubbling was observed after 15 min and only carbonyl peak for urea was found.

Experimental verification of urea obtained from reaction between secondary amine and isocyanate as the real catalyst. *N*-methylaniline was reacted with *p*-tolyl isocyanate in 1:1 molar ratio to obtain 1-methyl-1-phenyl-3-(*p*-tolyl) urea (**Figure S5-3a**). After that, the urea obtained was used as a catalyst instead of *N*-methylaniline in model reaction 5-5, entry 5-5-11. The reaction was completed in 8 h, which was slower than that using *N*-methylaniline as a catalyst. The slower reaction time may be due to different solubility of urea's that are obtained from *N*-methylaniline reacted with different isocyanates (**Figure S5-3b**). Similarly, 1,1-dibutyl-3-(*p*-tolyl) urea obtained

from the reaction between dibutylamine and p-tolyl isocyanate in 1:1 molar ratio was also able to catalyze reaction 5-5; imide structures were obtained in the end (see **Figure S5-3c** and **3d**).

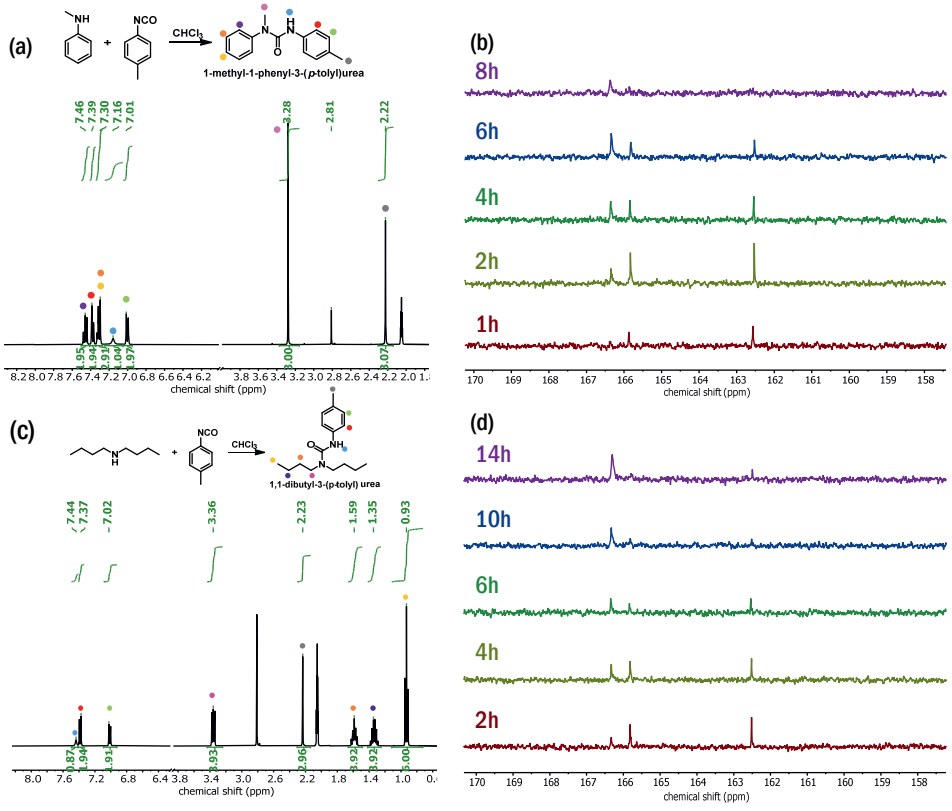

Figure S5-3. (a) ^{1}H NMR spectrum (400MHz, acetone-d_6) of 1-methyl-1-phenyl-3-(*p*-tolyl) urea obtained from the reaction between *N*-methylaniline and *p*-tolyl isocyanate. (b) ^{13}C NMR spectra (100 MHz, acetone-d_6) of model reaction 5-5 using 1-methyl-1-phenyl-3-(*p*-tolyl) urea as a catalyst. (c) ^{1}H NMR spectrum (400MHz, acetone-d_6) of 1,1-dibutyl-3-(*p*-tolyl) urea obtained from the reaction between dibutylamine and *p*-tolyl isocyanate. (d) ^{13}C NMR spectra (100 MHz, acetone-d_6) of model reaction 5-5 using 1,1-dibutyl-3-(*p*-tolyl) urea as a catalyst.

5.5 References

(1) Engels, H. W.; Pirkl, H. G.; Albers, R.; Albach, R. W.; Krause, J.; Hoffmann, A.; Casselmann, H.; Dormish, J. Polyurethanes: Versatile Materials and Sustainable Problem Solvers for Today's Challenges. *Angew. Chemie - Int. Ed.* **2013**, *52*, 9422–9441.

(2) Gama, N. V.; Ferreira, A.; Barros-Timmons, A. Polyurethane Foams: Past, Present, and Future. *Materials (Basel).* **2018**, *11*, 1841.

(3) Randall, D.; Lee, S. *The Polyurethanes Book*; Wiley, 2003.

(4) Eling, B.; Tomović, Ž.; Schädler, V. Current and Future Trends in Polyurethanes: An Industrial Perspective. *Macromol. Chem. Phys.* **2020**, *2000114*, 1–11.

(5) Delebecq, E.; Pascault, J. P.; Boutevin, B.; Ganachaud, F. On the Versatility of Urethane/Urea

Bonds: Reversibility, Blocked Isocyanate, and Non-Isocyanate Polyurethane. *Chem. Rev.* **2013**, *113*, 80–118.
(6) Hergenrother, P. M. The Use, Design, Synthesis and Properties of High Performance/ High Temperature Polymer: An Overview. *High Perform. Polym.* **2003**, *15*, 3–45.
(7) David, C. Chapter 1 Thermal Degradation of Polymers. In *Degradation of Polymers*; Bamford, C. H., Tipper, C. F. H., Eds.; Comprehensive Chemical Kinetics; Elsevier, 1975; Vol. 14, pp 1–173.
(8) Dodda, J. M.; Bělský, P. Progress in Designing Poly(Amide Imide)s (PAI) in Terms of Chemical Structure, Preparation Methods and Processability. *Eur. Polym. J.* **2016**, *84*, 514–537.
(9) Sroog, C. E. Polyimides. *J. Polym. sci., Macromol. Rev.* **1976**, *11*, 161–208.
(10) Liou, G. S.; Yen, H. J. *Polyimides*; 2012; Vol. 5.
(11) Ghosh, M. *Polyimides: Fundamentals and Applications*; Plastics Engineering; CRC Press, 2018.
(12) Sezer Hicyilmaz, A.; Celik Bedeloglu, A. Applications of Polyimide Coatings: A Review. *SN Appl. Sci.* **2021**, *3*, 1–22.
(13) Liu, X. J.; Zheng, M. S.; Chen, G.; Dang, Z. M.; Zha, J. W. High-Temperature Polyimide Dielectric Materials for Energy Storage: Theory, Design, Preparation and Properties. *Energy Environ. Sci.* **2022**, *15*, 56–81.
(14) Li, L.; Xu, Y.; Che, J.; Ye, Z. Synthesis and Optical Properties of Novel Soluble and Optically Transparent Semifluorinated Poly(Ether Imide)s. *Polym. Adv. Technol.* **2019**, *30*, 120–127.
(15) Cao, K.; Guo, Y.; Zhang, M.; Arrington, C. B.; Long, T. E.; Odle, R. R.; Liu, G. Mechanically Strong, Thermally Stable, and Flame Retardant Poly(Ether Imide) Terminated with Phosphonium Bromide. *Macromolecules* **2019**, *52*, 7361–7368.
(16) Banu, P.; Radhakrishnan, G. Thermoplastic Poly(Ester-Imide)s Derived from Anhydride-Terminated Polyester Prepolymer and Diisocyanate. *J. Polym. Sci. Part A Polym. Chem.* **2003**, *42*, 341–350.
(17) Zhu, G.; Lao, H.; Feng, F.; Wang, M.; Fang, X.; Chen, G. Synthesis and Characterization of Poly(Amide-Imide)s with High T_g and Low CTE Derived from Isomeric Amide-Containing Diamines. *Eur. Polym. J.* **2022**, *179*, 111558.
(18) Kim, S. D.; Lee, B.; Byun, T.; Chung, I. S.; Park, J.; Shin, I.; Ahn, N. Y.; Seo, M.; Lee, Y.; Kim, Y.; Kim, W. Y.; Kwon, H.; Moon, H.; Yoo, S.; Kim, S. Y. Poly(Amide-Imide) Materials for Transparent and Flexible Displays. *Sci. Adv.* **2018**, *4*, eaau1956.
(19) Tang, Q.; Song, Y.; He, J.; Yang, R. Synthesis and Characterization of Inherently Flame-Retardant and Anti-Dripping Thermoplastic Poly(Imides-Urethane)s. *J. Appl. Polym. Sci.* **2014**, *131*, 9524–9533.
(20) Lin, M. F.; Shu, Y. C.; Tsen, W. C.; Chuang, F. S. Synthesis of Polyurethane-Imide (PU-Imide) Copolymers with Different Dianhydrides and Their Properties. *Polym. Int.* **1999**, *48*, 433–445.
(21) Sokolova, M. P.; Bugrov, A. N.; Smirnov, M. A.; Smirnov, A. V.; Lahderanta, E.; Svetlichnyi, V. M.; Toikka, A. M. Effect of Domain Structure of Segmented Poly(Urethane-Imide) Membranes with Polycaprolactone Soft Blocks on Dehydration of *n*-Propanol *via* Pervaporation. *Polymers (Basel).* **2018**, *10*, 1222.
(22) Nair, P. R.; Nair, C. P. R.; Francis, D. J. Imide-Modified Polyurethanes, Syntheses, Thermal, and Mechanical Characteristics. *J. Appl. Polym. Sci.* **1998**, *70*, 1483–1491.
(23) Asai, K.; Inoue, S. I.; Okamoto, H. Preparation and Properties of Imide-Containing Elastic Polymers from Elastic Polyureas and Pyromellitic Dianhydride. *J. Polym. Sci. Part A Polym. Chem.* **2000**, *38*, 715–723.
(24) Philip Gnanarajan, T.; Padmanabha Iyer, N.; Sultan Nasar, A.; Radhakrishnan, G. Preparation and Properties of Poly(Urethane-Imide)s Derived from Amine-Blocked-Polyurethane Prepolymer and Pyromellitic Dianhydride. *Eur. Polym. J.* **2002**, *38*, 487–495.
(25) Liu, J.; Dezhu, M. Study on Synthesis and Thermal Properties of Polyurethane-Imide Copolymers with Multiple Hard Segments. *J. Appl. Polym. Sci.* **2002**, *84*, 2206–2215.
(26) Müeller-Cristadoro, A.; Prissok, F. Producing Polymer Foams Comprising Imide Groups. WO 2014023796 A1, 2014.
(27) Tian, H.; Yao, Y.; Zhang, S.; Wang, Y.; Xiang, A. Enhanced Thermal Stability and Flame Resistance of Rigid Polyurethane-Imide Foams by Varying Copolymer Composition. *Polym. Test.* **2018**, *67*, 68–74.
(28) Farrissey, W. J.; Rose, J. S.; Carleton, P. S. Preparation of a Polyimide Foam. *J. Appl. Polym. Sci.* **1970**, *14*, 1093–1101.
(29) Kashiwame, J.; Ashida, K. Preparation and Properties of Polyimide Foams. *J. Appl. Polym. Sci.* **1994**, *54*, 477–486.
(30) Xi, K.; Shieh, D. J.; Wu, L.; Singh, S. Polyurethane Foam Composition Comprising an Aromatic

Polyester Polyol Compound and Products Made Thereform. WO 2021030115 A1, 2021.
(31) Mishra, A. K.; Chattopadhyay, D. K.; Sreedhar, B.; Raju, K. V. S. N. FT-IR and XPS Studies of Polyurethane-Urea-Imide Coatings. *Prog. Org. Coatings* **2006**, *55*, 231–243.
(32) Mishra, A. K.; Chattopadhyay, D. K.; Sreedhar, B.; Raju, K. V. S. N. Thermal and Dynamic Mechanical Characterization of Polyurethane-Urea-Imide Coatings. *J. Appl. Polym. Sci.* **2006**, *102*, 3158–3167.
(33) Chattopadhyay, D. K.; Mishra, A. K.; Sreedhar, B.; Raju, K. V. S. N. Thermal and Viscoelastic Properties of Polyurethane-Imide/Clay Hybrid Coatings. *Polym. Degrad. Stab.* **2006**, *91*, 1837–1849.
(34) Meena, M.; Kerketta, A.; Tripathi, M.; Roy, P.; Jacob, J. Thermally Stable Poly(Urethane-Imide)s with Enhanced Hydrophilicity for Waterproof-Breathable Textile Coatings. *J. Appl. Polym. Sci.* **2022**, *139*, e52508.
(35) Xu, Z.; Croft, Z. L.; Guo, D.; Cao, K.; Liu, G. Recent Development of Polyimides: Synthesis, Processing, and Application in Gas Separation. *J. Polym. Sci.* **2021**, *59*, 943–962.
(36) Meyers, R. A. The Polymerization of Pyromellitic Dianhydride with Diphenylmethane Diisocyanate. *J. Polym. Sci. Part A Polym. Chem.* **1969**, *7*, 2757–2762.
(37) Barikani, M.; Ataei, S. M. Preparation and Properties of Polyimides and Polyamideimides from Diisocyanates. *J. Polym. Sci. Part A Polym. Chem.* **1999**, *37*, 2245–2250.
(38) Barikani, M.; Mehdipour-ataei, S. Aromatic/Cycloaliphatic Polyimides and Polyamide-Imide from Trans-1 ,4-Cyclohexane Diisocyanate: Synthesis and Properties. *J. Appl. Polym. Sci.* **2000**, *77*, 1102–1107.
(39) Jeon, J. Y.; Tak, T. M. Synthesis and Characterization of Block Copoly(Urethane-Imide). *J. Appl. Polym. Sci.* **1996**, *62*, 763–769.
(40) Chidambareswarapattar, C.; Larimore, Z.; Sotiriou-Leventis, C.; Mang, J. T.; Leventis, N. One-Step Room-Temperature Synthesis of Fibrous Polyimide Aerogels from Anhydrides and Isocyanates and Conversion to Isomorphic Carbons. *J. Mater. Chem.* **2010**, *20*, 9666–9678.
(41) Carleton, P. S.; Farrissey, W. J.; Rose, J. S. The Formation of Polyimides from Anhydrides and Isocyanates. *J. Appl. Polym. Sci.* **1972**, *16*, 2983–2989.
(42) Sorenson, W. R. Reaction of an Isocyanate and a Carboxylic Acid in Dimenthyl Sulfoxide. *J. Org. Chem.* **1959**, *24*, 978–980.
(43) Fry, A. A Tracer Study of the Reaction of Isocyanates with Carboxylic Acids. *J. Am. Chem. Soc* **1953**, *75*, 2686–2688.
(44) Mundhenke, R. F.; Willis, T. S. Chemistry and Properties of 4,4'-Oxydiphthalic Anhydride Based Polyimides. *High Perform. Polym.* **1990**, *2*, 57–66.
(45) Guo, Y.; Muuronen, M.; Deglmann, P.; Lucas, F.; Sijbesma, R. P.; Tomović, Ž. Role of Acetate Anions in the Catalytic Formation of Isocyanurates from Aromatic Isocyanates. *J. Org. Chem.* **2021**, *86*, 5651–5659.
(46) Grimme, S.; Bohle, F.; Hansen, A.; Pracht, P.; Spicher, S.; Stahn, M. Efficient Quantum Chemical Calculation of Structure Ensembles and Free Energies for Nonrigid Molecules. *J. Phys. Chem. A* **2021**, *125*, 4039–4054.
(47) Tao, J.; Perdew, J.; Staroverov, V.; Scuseria, G. Climbing the Density Functional Ladder: Nonempirical Meta-Generalized Gradient Approximation Designed for Molecules and Solids. *Phys. Rev. Lett.* **2003**, *91*, 146401.
(48) Perdew, J. P.; Ruzsinszky, A.; Csonka, G. I.; Constantin, L. A.; Sun, J. Workhorse Semilocal Density Functional for Condensed Matter Physics and Quantum Chemistry. *Phys. Rev. Lett.* **2009**, *103*, 10–13.
(49) Grimme, S.; Antony, J.; Ehrlich, S.; Krieg, H. A Consistent and Accurate Ab Initio Parametrization of Density Functional Dispersion Correction (DFT-D) for the 94 Elements H-Pu. *J. Chem. Phys.* **2010**, *132*, 154104.
(50) Klamt, A.; Schüürmann, G. COSMO: A New Approach to Dielectric Screening in Solvents with Explicit Expressions for the Screening Energy and Its Gradient. *J. Chem. Soc. Perkin Trans. 2* **1993**, 799–805.
(51) Zhao, Y.; Truhlar, D. G. The M06 Suite of Density Functionals for Main Group Thermochemistry, Thermochemical Kinetics, Noncovalent Interactions, Excited States, and Transition Elements: Two New Functionals and Systematic Testing of Four M06-Class Functionals and 12 Other Function. *Theor. Chem. Acc.* **2008**, *120*, 215–241.
(52) Klamt, A. Conductor-like Screening Model for Real Solvents: A New Approach to the Quantitative Calculation of Solvation Phenomena. *J. Phys. Chem.* **1995**, *99*, 2224–2235.
(53) Klamt, A.; Jonas, V.; Bürger, T.; Lohrenz, J. C. W. Refinement and Parametrization of COSMO-RS. *J. Phys. Chem. A* **1998**, *102*, 5074–5085.

(54) Truhlar, D. G.; Garrett, B. C.; Klippenstein, S. J. Current Status of Transition-State Theory. *J.Phys. Chem.* **1996**, *100*, 12771–12800.
(55) Bannwarth, C.; Ehlert, S.; Grimme, S. GFN2-XTB - An Accurate and Broadly Parametrized Self-Consistent Tight-Binding Quantum Chemical Method with Multipole Electrostatics and Density-Dependent Dispersion Contributions. *J. Chem. Theory Comput.* **2019**, *15*, 1652–1671.
(56) Spicher, S.; Grimme, S. Robust Atomistic Modeling of Materials, Organometallic, and Biochemical Systems. *Angew. Chemie - Int. Ed.* **2020**, *59*, 15665–15673.
(57) Ehlert, S.; Stahn, M.; Spicher, S.; Grimme, S. Robust and Efficient Implicit Solvation Model for Fast Semiempirical Methods. *J. Chem. Theory Comput.* **2021**, *17*, 4250–4261.
(58) Perdew, J. P.; Ernzerhof, M.; Burke, K. Rationale for Mixing Exact Exchange with Density Functional Approximations. *J. Chem. Phys.* **1996**, *105*, 9982–9985.
(59) Furche, F.; Ahlrichs, R.; Hättig, C.; Klopper, W.; Sierka, M.; Weigend, F. Turbomole. *Wiley Interdiscip. Rev. Comput. Mol. Sci.* **2014**, *4*, 91–100.
(60) Ahlrichs, R.; Bär, M.; Häser, M.; Horn, H.; Kölmel, C. Electronic Structure Calculations on Workstation Computers: The Program System Turbomole. *Chem. Phys. Lett.* **1989**, *162*, 165–169.

Chapter 6

Solvent-Free Preparation of Thermally Stable Poly(Urethane-Imide) Elastomers

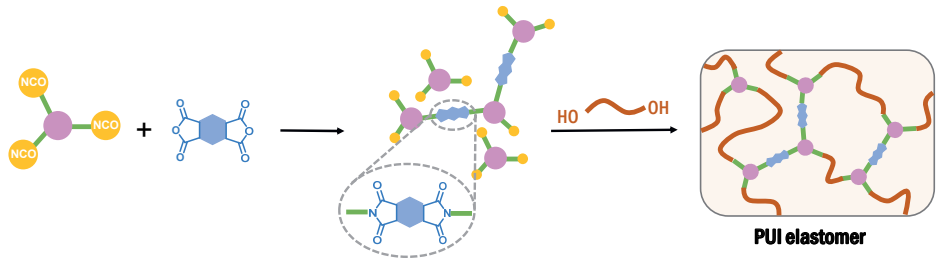

This chapter is based on submitted work:
Guo, Y.; Cristadoro, A.; Kleemann J.; Bokern, S.; Sijbesma, R. P.; Tomović, Ž., Solvent-free preparation of thermally stable poly(urethane-imide) (PUI) elastomers, *under peer review.*

Polyurethanes (PUs) are widely used in many applications due to their versatile chemical and physical properties. To meet the increasing demands on PU with respect to intrinsic mechanical and thermal properties, they can be modified with thermally stable aromatic imide structures to form poly(urethane imide)s (PUIs). However, the preparation of PUI materials is limited by the need for strong polar solvents, which hinder their industrial scale development. In this chapter, we prepare imide containing isocyanate terminated prepolymers *via* reaction of polymeric aromatic or aliphatic isocyanates and pyromellitic dianhydride in completely solvent-free conditions. The subsequent PUI elastomers made from these prepolymers exhibit enhanced thermal stability and stiffness, among which the aromatic PUI elastomer shows improved flame retardancy. This work demonstrates the potential use of imide prepolymers in other PU applications where high thermal stability and flame retardancy is required. The solvent-free synthesis also paves a way for large-scale production of PUI materials.

6.1 Introduction

Polyurethanes (PUs) are among the most versatile polymers and exhibit a wide range of chemical, thermal and mechanical properties.[1-5] They are used in a variety of applications such as soft cushioning foams, rigid thermal insulation foams, thermoplastic elastomers, coatings and adhesives. With the fast development of the PU market, further improvement of the chemical and physical properties of PU materials will make them meet the increasing demands on high-performance materials and suit a rising number of applications. This can be achieved by the chemical modification of PU with thermally stable chemical motifs such as aromatic polyimides, which are one of the most remarkable structures in respect to their outstanding thermal, mechanical and electrical properties.[6-12] As aromatic polyimides have been used to enhance the thermal properties of various polymer matrices such as poly(ether imide)s, poly(ester imide)s, poly(amide imide)s,[9,13-19] the incorporation of aromatic polyimides in PU promises the development of new thermoplastics,[20-26] rigid foams[27-32] and coatings[33-36] with significantly enhanced thermal stability and flame retardancy, which is especially important for construction and automotive industry.

Most imides are introduced in polymer matrices *via* the reaction between amine and anhydride.[9,10] As isocyanates are used during PU synthesis, another more direct synthetic way to introduce imides is *via* the reaction between isocyanate and anhydride. Thus, the poly(urethane imide) (PUI) materials are typically prepared by reaction of long-chain isocyanate terminated prepolymers with dianhydrides.[20,25,32,33,36-40] PUI preparations are also reported to be prepared from reaction of hydroxy functionalized imide oligomers and diisocyanates,[41,42] or the reaction of amine functionalized isocyanate prepolymers with dianhydrides.[23] However, a common feature of these preparations is the use of strong polar aprotic solvents such as DMF, NMP, DMAc that are hazardous and difficult to be removed, which limit the development of PUI materials in industrial scale production.[43,44]

As discussed in **Chapter 5**, we have discovered that it is possible to perform the reaction of aromatic isocyanates and anhydrides in solvent-free condition with high conversion. The use of secondary amine as a pre-catalyst and tertiary amine as a co-catalyst compensates the lack of catalytic effect from strong polar solvents and accelerates the reaction speed.[45] We also discovered that during the imide formation from aromatic isocyanate and anhydride with secondary amine as a pre-catalyst, the urea that forms from the reaction of aromatic isocyanate and secondary amine is the actual active catalyst. With the help of a tertiary amine as a co-catalyst, the deprotonated urea opens the ring of an anhydride to form an amic acid intermediate. The carboxyl group of the intermediate reacts with one more isocyanate group, followed by imidization with release of CO_2 and the urea catalyst.

Using the knowledge from this mechanism study, we prepared PUI elastomers with high thermal stability in completely solvent-free conditions in this work. As pyromellitic dianhydride (PMDA) is one of the most reactive dianhydrides due to the high electron deficiency of its anhydride groups, it was chosen to prepare imide-containing isocyanate-terminated prepolymers.[8,46] The imide prepolymer was first synthesized *via* the reaction of PMDA with aromatic or aliphatic polyisocyanates in a 1:19 weight ratio using *N*-methylaniline (for aromatic isocyanates) or dibutylamine (for aliphatic isocyanates) as a pre-catalyst, and *N,N*-dimethylcyclohexylamine (DMCHA) as a co-catalyst. Then the PUI elastomers were prepared by reacting the imide-containing isocyanate prepolymer and polyester polyol with 1,4-butanediol as a chain extender in bulk conditions. Both PUI elastomers obtained from aromatic and aliphatic isocyanates exhibited enhanced thermal and mechanical properties. Moreover, initial cone calorimetry tests were performed and PUI elastomer synthesized from aromatic isocyanate also showed improved flame retardancy. Due to the concern of industrial production, this work paves a way for a completely solvent-free production of high-performance PUI materials with inherent thermal stability and flame retardancy. In addition, the current work also helps to reduce the use of conventional flame retardance additives.

6.2 Results and discussion

6.2.1 PUI elastomers prepared from aromatic isocyanates

The imide prepolymer based on an aromatic isocyanate (PI-1) was synthesized *via* reaction of PMDA and polymeric methylene diphenyl diisocyanate (pMDI) in a 1:19 weight ratio at 140 ºC with 2 mol% *N*-methylaniline as a pre-catalyst, 1 mol% DMCHA as a co-catalyst and 1.5 vol% triethyl phosphate (TEP) as an additive to prevent the sublimation of PMDA at high temperature (**Scheme 6-1**). During the reaction, it was found that the PMDA reacted in a two-step process. One-side imides were formed in the first hour and di-imides were formed within the next 6 hours (**Figure 6-1**). The PI-1 prepolymer obtained had an NCO content of 28.1 wt%, which was determined by back-titration method (see Section 6.4).

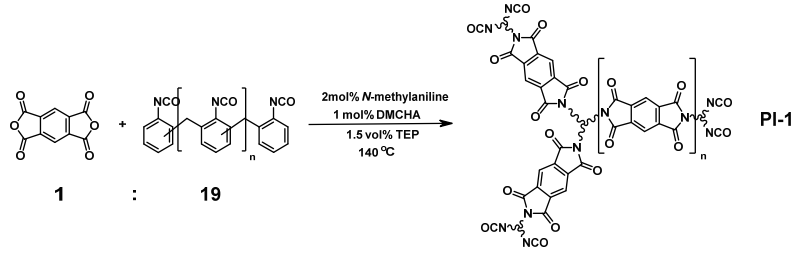

Scheme 6-1. Synthesis of imide prepolymer PI-1 from aromatic isocyanate.

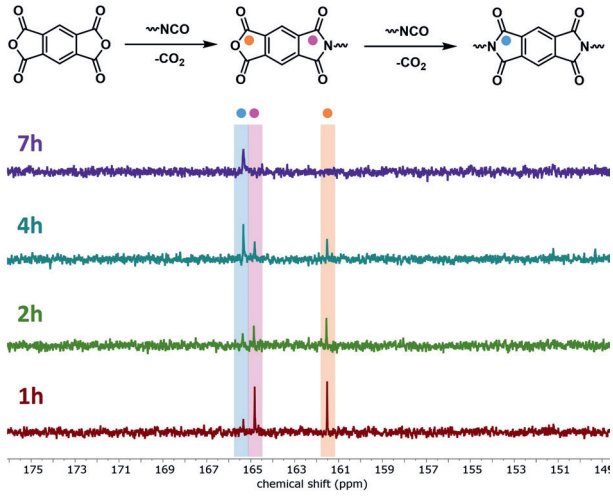

Figure 6-1. ^{13}C NMR spectra (100 MHz, acetone-d_6) of reaction between PMDA and pMDI in a 1:19 weight ratio with *N*-methylaniline as a pre-catalyst, DMCHA as a co-catalyst and TEP as an additive. Full conversion was achieved after 7 h.

PUI-1 elastomer was prepared by the reaction of PI-1 prepolymer and commercially available polyester polyol Lupraphen® 6601/2 (Lupraphen) with molecular weight of 2000 g/mol, using 1,4-butanediol (BDO) as a chain extender (15 wt% of the polyol component) in bulk condition. The molar ratio of NCO:OH was 1.02 (index 102). As DMCHA remained in the prepolymer, it also served as a urethane catalyst. 0.03 wt% Diethylene glycol bis-chloroformate (DGBCF) was added to the imide-modified prepolymer to partially neutralize DMCHA, which slowed down the urethane formation reaction during the elastomer synthesis for easier handling. The synthesis recipe can be found in **Table 6-1**.

Table 6-1. Recipes in weight percentage of PUI-1 and Reference 1 and 2 elastomers.

	PUI-1	Reference 1	Reference 2
PI-1	38.9	--	--
pMDI	--	37.0	36.0
Lupraphen	51.9	51.7	53.9
BDO	9.2	9.0	9.4
BDM	--	1.7	--
DGBCF	0.03	--	--
Lupragen N202	--	0.1	0.1
TEP	--	0.5	0.5

As a reference, elastomer (Reference 1) was prepared in bulk by reacting pMDI with same amount of Lupraphen and BDO, and benzenedimethanol (BDM) as a replacement of PMDA (index 102). As BDM has similar molecular weight (138.2 g/mol) as the effective molecular weight of PMDA ($M_{eff} = M_{PMDA} - 2M_{CO2}$ = 218.1 g/mol - 44.0 g/mol × 2 = 130.1 g/mol) in the PI-1 prepolymer, the aromatic content as well as the amount of polyol and BDO in the reference elastomer were almost the same as those in PUI-1 elastomer, with the key difference that BDM does not form imide bonds. A second reference elastomer (Reference 2) was prepared by reacting pMDI with Lupraphen and 15 wt% BDO using the same index in bulk.

The elastomers were characterized by thermogravimetric analysis (TGA), tensile test and dynamic mechanical analysis (DMA) (**Table 6-2** and **Figure 6-2**). With the similar aromatic content, the decomposition temperatures of PUI-1 elastomer at 5% weight loss (T_{d5}) and 10% weight loss (T_{d10}) were similar to reference elastomers. However, the PUI-1 elastomer showed significantly higher char formation at 800 ºC, which indicates the improvement of thermal stability due to the presence of imide structures. In addition, the rigid imide structures led to a stiffer PUI-1 elastomer with higher Young's modulus and lower elongation at break. Due to the low aromatic content and absence of imide structures, the Young's modulus of the Reference 2 elastomer was the lowest. The increase of the stiffness of PUI-1 elastomer can also be explained by phase separation, as shown in DMA result. Compared to the reference elastomers that had only one narrow tan(δ) peak around 32 ºC, the two tan(δ) peaks of PUI-1 elastomer indicate the occurrence of phase separation. The lower glass transition temperature (T_g) is dominated by soft segments, and the higher T_g is dominated by hard segments which are mainly based on imide structures.

Table 6-2. TGA, tensile test and DMA results of PUI-1 elastomer and reference elastomers without imide structures.

	PUI-1	Reference 1	Reference 2
Aromatic content[a] (%)	39	39	36
T_{d5} (ºC)	300	293	294
T_{d10} (ºC)	316	309	311
Char at 800 ºC (%)	16.9	10.9	12.4
Young's modulus (MPa)	55 ± 2	15 ± 2	10 ± 2
Stress at break (MPa)	15 ± 1	25 ± 1	19 ± 1
Elongation (%)	60	110	110
T_g (ºC)	-10, 48	34	31

[a] The aromatic content is determined by the total weight percentage of aromatic compounds (isocyanates, imides and BDM) in the elastomers.

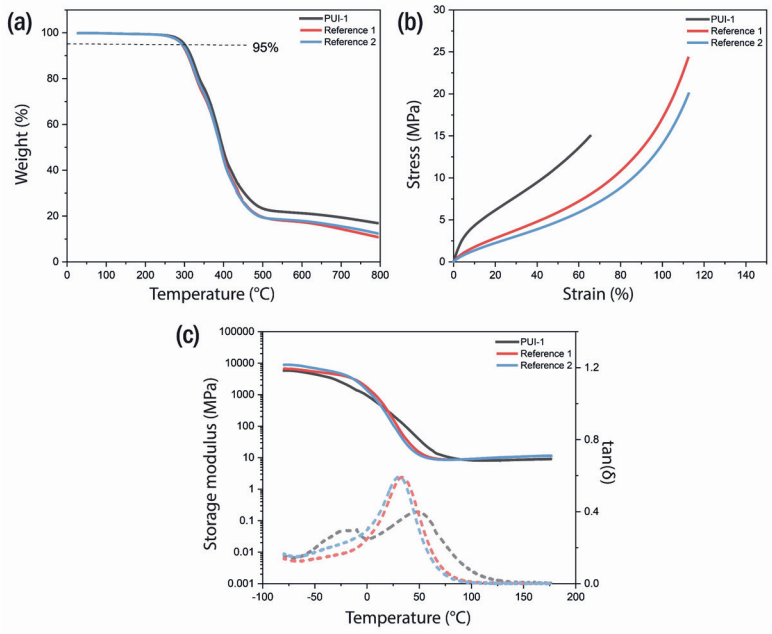

Figure 6-2. (a) TGA curves, (b) tensile test and (c) DMA curves (solid line: storage modulus; dash line: tan(δ)) of PUI-1 elastomer and reference elastomers without imide structures.

6.2.2 PUI elastomers prepared from aliphatic isocyanates

In addition to aromatic imide prepolymer, we found that imide prepolymers could also be prepared from the reaction between aliphatic isocyanates and dianhydride. Instead of *N*-methylaniline used in the synthesis of aromatic imide prepolymer, dibutylamine was used as a pre-catalyst for the synthesis of imide prepolymers from aliphatic isocyanates in terms of shorter reaction time. The aliphatic isocyanate-based imide prepolymer (PI-2) was synthesized *via* reaction of PMDA and hexamethylene diisocyanate (HDI) trimer in a 1:19 weight ratio at 140 ºC with 2 mol% dibutylamine as a pre-catalyst, 1 mol% DMCHA as a co-catalyst and 1.5 vol% TEP as an additive (**Scheme 6-2**). The full conversion to the imide-containing prepolymer was achieved after 12 h (**Figure 6-3**). According to back-titration method, the PI-2 prepolymer had an NCO content of 18.0 wt%.

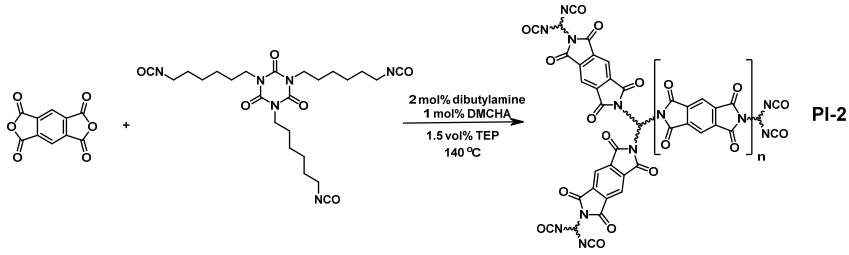

Scheme 6-2. Synthesis of imide prepolymer PI-2 from aliphatic isocyanate.

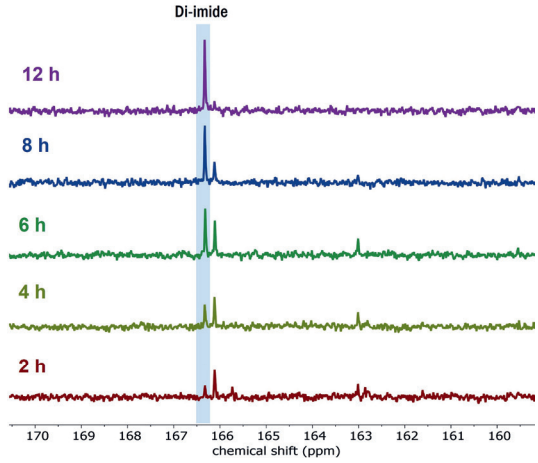

Figure 6-3. ^{13}C NMR spectra (100 MHz, acetone-d_6) of reaction between PMDA and HDI trimer in a 1:19 weight ratio with dibutylamine as a pre-catalyst, DMCHA as a co-catalyst and TEP as an additive.

The PUI elastomer based on aliphatic isocyanate (PUI-2) was prepared by reacting PI-2 prepolymer with Lupraphen polyol and BDO as a chain extender (15 wt% of the polyol component) in bulk condition (index 102). DGBCF (0.02 wt%) was also used to slow down the urethane reaction. As a reference, elastomer (Reference 3) was prepared by reacting HDI trimer with Lupraphen and 15 wt% BDO using the same index in bulk. The synthesis recipes can be found in **Table 6-3**.

Table 6-3. Recipes in weight percentage of PUI-2 and Reference 3 elastomers.

	PUI-2	Reference 3
PI-2	50.0	--
HDI trimer	--	44.6
Lupraphen	42.5	46.6
BDO	7.5	8.2
DGBCF	0.02	--
TEP	--	0.6

The TGA, tensile test and DMA results of the elastomers prepared from aliphatic isocyanates are shown in **Figure 6-4** and **Table 6-4**. Compared to Reference 3, the elastomer with no imide structure but the same amount of BDO in polyol component, PUI-2 had similar decomposition temperature while the char formation was slightly higher. The rigid imide structures also led to higher Young's modulus, stress at break as well as a higher T_g of PUI-2 elastomer than Reference 3 elastomer. Although only small improvement in the physical properties was observed due to the low imide amount (2.5 wt%), this still indicates that the imide structures can be potentially used to improve the mechanical properties of the aliphatic isocyanate-based elastomers.

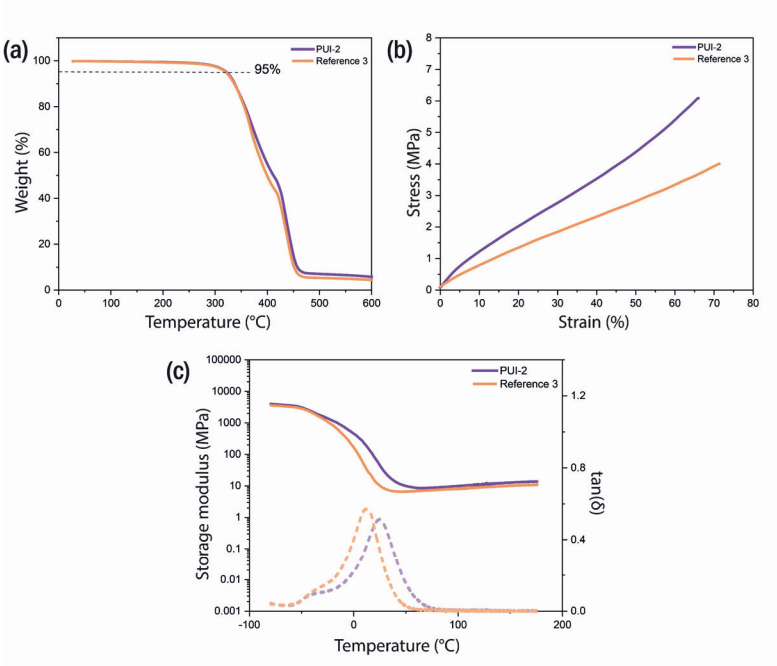

Figure 6-4. (a) TGA curves, (b) tensile test and (c) DMA curves (solid line: storage modulus; dash line: tan(δ)) of PUI-2 and Reference 3 elastomers.

Table 6-4. TGA, tensile test and DMA results of the PUI-2 and Reference 3 elastomers.

	PUI-2	Reference 3
T_{d5} (°C)	322	320
T_{d10} (°C)	337	337
Char at 600 °C (%)	5.7	4.4
Young's modulus (MPa)	10 ± 0.6	8 ± 0.4
Stress at break (MPa)	5 ± 0.6	4 ± 0.3
Elongation (%)	61	70
T_g (°C)	25	12

6.2.3 Flame retardancy of PUI elastomers prepared from aromatic isocyanates

Based on the TGA results of PUI-1 and PUI-2 elastomers, the PUI elastomer prepared from aromatic isocyanates exhibits better thermal stability and higher char formation at high temperature, which implies good combustion behavior. Therefore, the flame retardancy of PUI-1 elastomer as well as Reference 1 and 2 elastomers were preliminary evaluated by cone calorimetry measurement. The time to ignition (TTI, s), peak of heat release rate (PHRR, kW/m^2), time to PHRR (t_p, s), total heat release (THR, MJ/m^2), total smoke production (TSP, m^2), time to extinguishment (t_e) and mass residue (wt%) are shown in **Figure 6-5** and **Table 6-5**.

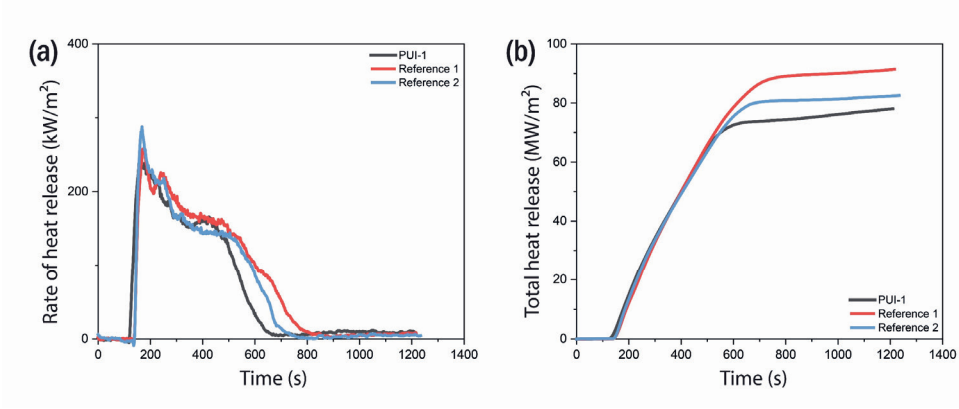

Figure 6-5. HRR (a) and THR (b) curves of PUI-1, Reference 1 and 2 elastomers measured by cone colorimeter under a heat flux of 25 kW/m^2.

Table 6-5. Cone calorimetry results of PUI-1, Reference 1 and 2 elastomers measured under a heat flux of 25 kW/m^2.

Sample	TTI (s)	PHRR (kW/m^2)	t_p (s)	THR (MJ/m^2)	TSP (m^2)	t_e (s)	Mass residue (wt%)
PUI-1	121	244.3	166	78.0	12.5	741	28.9
Reference 1	140	257.6	170	91.2	15.7	852	28.9
Reference 2	140	288.0	168	82.3	18.3	789	26.9

In terms of the flame retardancy, the flame retardants generally contributes to either or both gas phase and condensed polymer phase during the combustion.[47] The heterocyclic imides incorporated into the polymer main chains realize the flame retardation in the condensed phase. The lower PHRR of PUI-1 elastomer compared to reference elastomers was attributed to the imides that accelerated the formation a thick char layer on the material surface after ignition. The char layer insulated the

remaining material, retarding the pyrolysis and shielding the material surface from heat and oxidation.[20] As a result, the effective combustion time of PUI-1 elastomer was 575 s, while it took 682 s and 621 s for the Reference 1 and 2 elastomers to extinguish. The subsequent THR of PUI-1 elastomer was 78 MJ/m^2, which was lower than the values of both reference elastomers, indicating the better flame retardancy of PUI-1 elastomer even with only 2 wt% imide structures. In addition to lowering the THR, reducing the smoke production is another important target for the flame retardant materials, as the gas released during combustion is one of the fire hazards. The TSP of PUI-1 elastomer was much lower than the reference elastomers, which is due to the thick char layer that reduced the smoke production.

The char residues of PUI-1, Reference 1 and Reference 2 elastomers obtained after cone calorimetry measurement (**Figure 6-6**) were further studied by scanning electron microscopy (SEM), as shown in **Figure 6-7**. Due to the accelerating effect of imides on char formation, a clear dense char layer was formed on the surface of PUI-1 elastomer (**Figure 6-6a** and **Figure 6-7a**), which provided an effective barrier protection from the flame. Without the imides, a less pronounced char layer was formed on the surface of reference elastomers. Thus, both surface and interior char residues of reference elastomers were more fragmented.

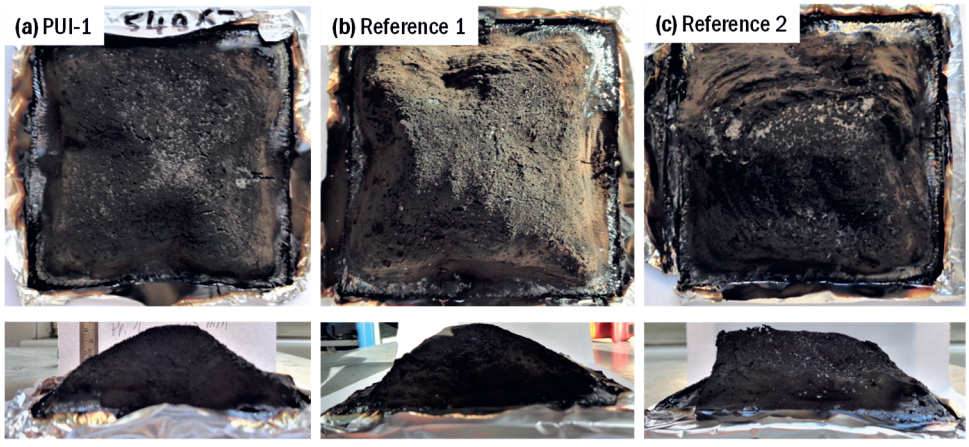

Figure 6-6. Photos of char residues after cone calorimetry measurement. (a) PUI-1 elastomer, (b) Reference 1 elastomer, (c) Reference 2 elastomer.

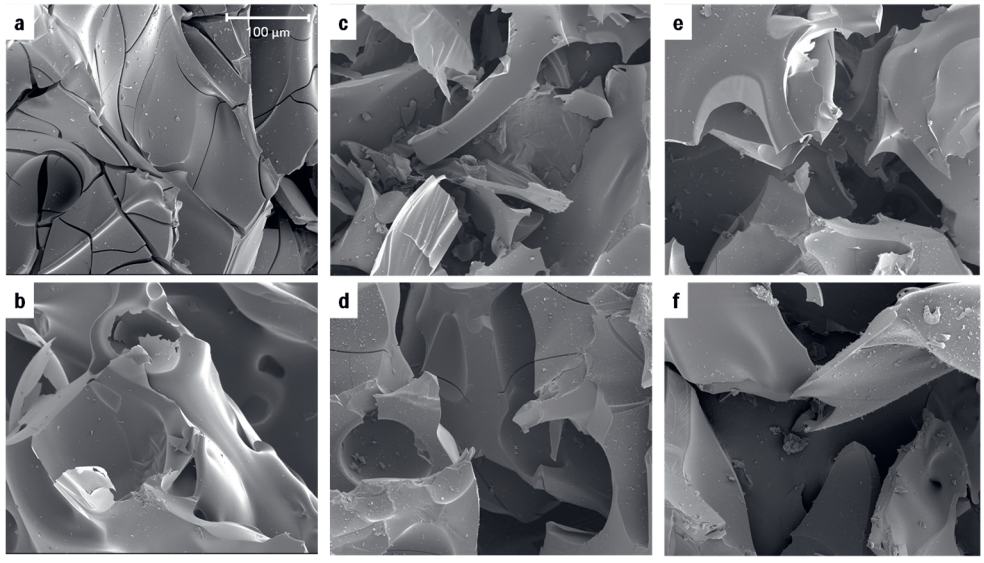

Figure 6-7. SEM images (100 µm, 5kV) of elastomer char residues obtained from (a) PUI-1 elastomer surface, (b) PUI-1 elastomer interior, (c) Reference 1 elastomer surface, (d) Reference 1 elastomer interior, (e) Reference 2 elastomer surface and (f) Reference 2 elastomer interior.

The char residue was also studied by Raman spectroscopy as shown in **Figure 6-8.** The two strong, overlapping peaks at 1348 and 1586 cm^{-1} are assigned to D band (amorphous structure) and G band (graphitic structure) of C=C bonds, respectively. After deconvoluted of the overlapping peaks by fitting to Gaussian peak shape, the integral ratio of D band to G band is used as a characteristic parameter to determine the graphitization degree of the char residues.[48] The lower the value of I_D/I_G, the higher the degree of graphitization is, which indicates the better capability of the char to prevent polymer volatiles from external release. The I_D/I_G ratio of PUI-1, Reference 1 and Reference 2 elastomers are 1.88, 1.94 and 2.06, respectively. The imides in the elastomers helped to promote char into a graphitic structure, leading to low I_D/I_G ratios.

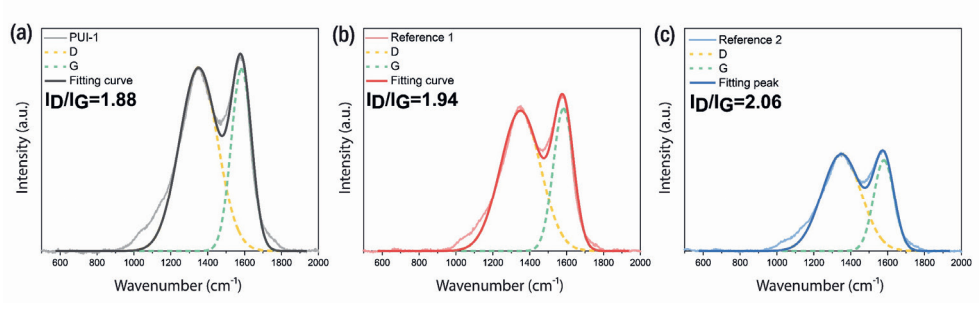

Figure 6-8. Raman spectra of char residues obtained from the surface of (a) PUI-1, (b) Reference 1 and (c) Reference 2 elastomers.

6.3 Conclusion

The combination of imides and polyurethanes leads to PUI materials with improved inherent thermal and mechanical properties. In the current work, we investigated a two-step, completely solvent-free synthetic way to introduce imides in PUs. Isocyanate terminated imide prepolymers were first prepared. The subsequent aromatic and aliphatic isocyanate-based PUI elastomers (PUI-1 and PUI-2) exhibited better thermal stability as well as higher stiffness compared to elastomers without imide structures. Moreover, the PUI-1 elastomer showed enhanced flame retardancy with lower PHRR, THR and TSP.

The new solvent-free synthetic route of imide prepolymer removes current limitations caused by the use of organic solvents, and allows greener and more processable large-scale industrial production. The improved thermal stability, especially flame retardancy of the PU materials, demonstrates the potential use of aromatic imide prepolymers in other PU applications, such as rigid foams and compact thermosets, where thermal stability and flame retardancy are required. The thermal properties of PUI materials could be further improved by increasing the content of imide motifs in imide prepolymers. In addition, the use of imide motifs helps to improve the intrinsic thermal properties of PU materials and reduces the need of conventional flame retardant additives. Synergy with other flame retardant strategies like PIR formation or flame retardant additives may also be expected, and this is a relevant topic for future investigations.

Despite the focus of this work on thermal stability, the PUI materials may also have other improved physical properties. As imide structures exhibit high surface energy, a low dielectric constant, low refractive index and low coefficient of thermal expansion, it is expected that the combination of imides and polyurethane will lead to PUI materials that can be used in, for instance, adhesive applications, electrical devices and as photoconductors.[9,49,50]

6.4 Experimental section

Materials

Pyromellitic dianhydride (97%), triethyl phosphate (≥99.8%), *N*-methylaniline (98%), dibutylamine (≥99.5%), *N,N*-dimethylcyclohexylamine (99%) and 1,4-butanediol (BDO) (99%) were purchased from Sigma-Aldrich. 1,4-Benzenedimethanol (>99%) was purchased from TCI. 1,4-Butanediol was dried on mol-sieves, all other reagents were used directly without treatment. Polymeric methylene diphenyl diisocyanate Lupranate® M20 (pMDI, NCO content = 31.5 wt%), hexamethylene diisocyanate trimer

Basonat® HI 100 NG (HDI trimer, NCO content=22 wt%), diethylene glycol bis-chloroformate (DGBCF), and Lupraphen® 6601/2 with molecular weight 2000 g/mol (OH_v = 56, polyester polyol synthesized from adipic acid, 1,4-butanediol and mono ethylene glycol) were kindly provided by BASF Polyurethanes GmbH. The polyol was dried at 80 ºC under vacuum for 2 h before use.

Synthesis

Preparation of PI-1 prepolymer. Pyromellitic dianhydride (10.5 g, 48.26 mmol) and pMDI (200.0 g) were added in a dry 3-neck flask and the mixture was heated to 100 ºC under an Ar atmosphere. A catalyst solution was prepared by dissolving *N*-methylaniline (1.2 g, 11.11 mmol) and *N,N*-dimethylcyclohexylamine (0.7 g, 5.56 mmol) in 2.5 mL triethyl phosphate. Then the catalyst solution was added into the flask and the internal reaction temperature was kept at 140 ºC. The reaction was monitored by ^{13}C NMR spectroscopy and the time when all dianhydride converted to di-imide structures was defined as reaction time. Dark brown liquid was obtained at 140 ºC, which solidified over the time at room temperature. After the reaction, the NCO content of prepolymer was titrated as 28.1 wt%.

Preparation of PI-2 prepolymer. Pyromellitic dianhydride (10.5 g, 48.26 mmol) and HDI trimer (200.0 g) were added in a dry 3-neck flask and the mixture was heated to 100 ºC under an Ar atmosphere. A catalyst solution was prepared by dissolving dibutylamine (1.4 g, 11.11 mmol) and *N,N*-dimethylcyclohexylamine (0.7 g, 5.56 mmol) in 2.5 mL triethyl phosphate. Then the catalyst solution was added into the flask and the internal reaction temperature was kept at 140 ºC. The reaction was monitored by ^{13}C NMR spectroscopy and the time when all dianhydride converted to di-imide structures was defined as reaction time. Dark brown liquid was obtained. After the reaction, the NCO content of prepolymer was titrated as 18.0 wt%.

Preparation of elastomers. The preparation of PUI-1 elastomer is used as an example to illustrate the general synthetic route: The PI-1 prepolymer was added in sealed polypropylene cup and stirred at 800 rpm under vacuum in a speedmixer for 30 min at 140 ºC before use. The polyol component that consisted of Lupraphen (106.8 g, 0.05 mol), BDO (18.9 g, 0.21 mol) and DGBCF (0.06 g, 0.26 mmol) was added in a sealed polypropylene cup and stirred at 800 rpm under vacuum in a speedmixer for 20 min at 80 ºC. PI-1 prepolymer (80.0 g, NCO content = 28.1 wt%) was added to the polyol component and the mixture was mixed in a speedmixer for 30 s under vacuum. After that, the mixture was poured on a metal mold which was pre-heated at 80 ºC. After the polymerization of the mixture, the material was further cured in 90 ºC oven overnight. The same procedure and conditions were used for the preparation of PUI-2 and reference elastomers in bulk.

Characterization

Nuclear magnetic resonance (NMR) spectroscopy. ^{13}C NMR spectroscopy for monitoring the imide formation were performed using either a Bruker UltraShield 400 MHz or Varian Mercury 400 MHz spectrometer at room temperature with a delay time of 2 s and 256 scans per spectrum, using acetone-d_6 as solvent with TMS as internal standard.

Determination of isocyanate content. The NCO titration was performed on a 916 Ti-Touch titration machine (Metrohm) equipped with an electrode using tetraethylammonium bromide (0.4 mol/L in ethylene glycol) as electrolyte. The isocyanate was quenched with excess of dibutylamine and the unreacted dibutylamine was titrated with 1 M HCl as the titrant. After getting the volume (V_1) at the end of titration of sample as well as the volume (V_0) of the blank titration at the same condition, the NCO content was calculated by the titration machine using the following equation:

$$NCO\ content = \frac{(V_1 - V_0) \times c_{HCl} \times M_{NCO}}{m_{sample}}.$$

Thermogravimetric analysis (TGA). TGA measurement was performed on a TA Q550 (TA Instruments) under N_2 atmosphere. Samples (around 5 mg) were heated from 28 to 800 °C (or 600 °C for aliphatic isocyanate-based elastomers) at a rate of 10 °C/min.

Tensile testing. Tensile testing was performed on a Z010 (Zwick/Roell) with a 500 N load cell using dumbbell-shaped specimens. The specimens had an effective length of 33 mm, width of 6 mm and thickness of 2 mm. The elongation rate used was 20 mm/min.

Dynamic mechanical analysis (DMA). DMA measurement was performed on a DMA Q850 (TA Instruments) with a film tension setup. The test bars had a width of 5.3 mm, thickness of 1.2 mm and effective length of around 15 mm. For each measurement, a temperature ramp from -80 to 180 °C was programmed with a heating rate of 3 °C/min at a frequency of 1.0 Hz. A preload force of 0.01 N, an amplitude of 100 µm and a force track of 115 % were used. The storage and loss modulus were recorded as a function of temperature. The glass transition temperature (T_g) was determined from the peak maximum of the tan(δ).

Cone calorimetry. Cone calorimetry measurement was carried out in iCone calorimeter (Fire Testing Technology Limited) under a heat flux of 25 kW/m^2 according to ISO 5660-1:2015-03/Amd 1:2019-08 standard. The samples were cut into 100×100×4 mm^3 size and wrapped with aluminum foil for measurement. The obtained results are based on single measurements.

Scanning electron microscopy (SEM). SEM images were obtained in a FEI Quanta 200 3D instrument using an acceleration of 5 kV. Both surface and inside parts of char residue were investigated with 100 μm scale. Before SEM observation, the samples were sputter-coated with gold.

Raman spectroscopy. Raman spectroscopy was performed on a Confocal Raman microscope WITec WMT 50 (WITEC) with laser of 532.3 nm.

6.5 References

(1) Randall, D.; Lee, S. *The Polyurethanes Book*; Wiley, 2003.
(2) Engels, H. W.; Pirkl, H. G.; Albers, R.; Albach, R. W.; Krause, J.; Hoffmann, A.; Casselmann, H.; Dormish, J. Polyurethanes: Versatile Materials and Sustainable Problem Solvers for Today's Challenges. *Angew. Chemie - Int. Ed.* **2013**, *52*, 9422–9441.
(3) Eling, B.; Tomović, Ž.; Schädler, V. Current and Future Trends in Polyurethanes: An Industrial Perspective. *Macromol. Chem. Phys.* **2020**, *2000114*, 1–11.
(4) Delebecq, E.; Pascault, J. P.; Boutevin, B.; Ganachaud, F. On the Versatility of Urethane/Urea Bonds: Reversibility, Blocked Isocyanate, and Non-Isocyanate Polyurethane. *Chem. Rev.* **2013**, *113*, 80–118.
(5) Gama, N. V.; Ferreira, A.; Barros-Timmons, A. Polyurethane Foams: Past, Present, and Future. *Materials (Basel).* **2018**, *11*, 1841.
(6) Hergenrother, P. M. The Use, Design, Synthesis and Properties of High Performance/High Temperature Polymer: An Overview. *High Perform. Polym.* **2003**, *15*, 3–45.
(7) David, C. Chapter 1 Thermal Degradation of Polymers. In *Degradation of Polymers*; Bamford, C. H., Tipper, C. F. H., Eds.; Comprehensive Chemical Kinetics; Elsevier, 1975; Vol. 14, pp 1–173.
(8) Sroog, C. E. Polyimides. *J. Polym. sci., Macromol. Rev.* **1976**, *11*, 161–208.
(9) Liou, G. S.; Yen, H. J. *Polyimides*; 2012; Vol. 5.
(10) Ghosh, M. *Polyimides: Fundamentals and Applications*; Plastics Engineering; CRC Press, 2018.
(11) Sezer Hicyilmaz, A.; Celik Bedeloglu, A. Applications of Polyimide Coatings: A Review. *SN Appl. Sci.* **2021**, *3*, 1–22.
(12) Liu, X. J.; Zheng, M. S.; Chen, G.; Dang, Z. M.; Zha, J. W. High-Temperature Polyimide Dielectric Materials for Energy Storage: Theory, Design, Preparation and Properties. *Energy Environ. Sci.* **2022**, *15*, 56–81.
(13) Cao, K.; Guo, Y.; Zhang, M.; Arrington, C. B.; Long, T. E.; Odle, R. R.; Liu, G. Mechanically Strong, Thermally Stable, and Flame Retardant Poly(Ether Imide) Terminated with Phosphonium Bromide. *Macromolecules* **2019**, *52*, 7361–7368.
(14) Li, L.; Xu, Y.; Che, J.; Ye, Z. Synthesis and Optical Properties of Novel Soluble and Optically Transparent Semifluorinated Poly (Ether Imide)S. *Polym. Adv. Technol.* **2019**, *30*, 120–127.
(15) Zhou, J.; Li, M.; Wu, J.; Zhang, C.; He, Z.; Xiao, Y.; Tong, G.; Zhu, X. One-Pot Synthesis of Hydroxyl Terminated Hyperbranched Semi-Aromatic Poly(Ester-Imide)s. *Polymer (Guildf).* **2022**, *253*, 124970.
(16) Serbezeanu, D.; Homocianu, M.; Macsim, A. M.; Enache, A. A.; Vlad-Bubulac, T. Flexible Thin Films Based on Poly(Ester Imide) Materials for Optoelectronic Applications. *Polym. Int.* **2022**, *71*, 98–106.
(17) Dodda, J. M.; Bělský, P. Progress in Designing Poly(Amide Imide)s (PAI) in Terms of Chemical Structure, Preparation Methods and Processability. *Eur. Polym. J.* **2016**, *84*, 514–537.
(18) Zhu, G.; Lao, H.; Feng, F.; Wang, M.; Fang, X.; Chen, G. Synthesis and Characterization of Poly(Amide-Imide)s with High *T*g and Low CTE Derived from Isomeric Amide-Containing Diamines. *Eur. Polym. J.* **2022**, *179*, 111558.
(19) Canto-Acosta, R. J.; Loría-Bastarrachea, M. I.; Carrillo-Escalante, H. J.; Hernández-Núñez, E.; Aguilar-Vega, M.; Santiago-García, J. L. Synthesis and Characterization of Poly(Amide-Imide)s Derived from a New: Ortho -Functional Unsymmetrical Dicarboxylic Acid. *RSC Adv.* **2018**, *8*, 284–290.
(20) Tang, Q.; Song, Y.; He, J.; Yang, R. Synthesis and Characterization of Inherently Flame-Retardant and Anti-Dripping Thermoplastic Poly(Imides-Urethane)s. *J. Appl. Polym. Sci.* **2014**,

131, 9524–9533.
(21) Lin, M. F.; Shu, Y. C.; Tsen, W. C.; Chuang, F. S. Synthesis of Polyurethane-Imide (PU-Imide) Copolymers with Different Dianhydrides and Their Properties. *Polym. Int.* **1999**, *48*, 433–445.
(22) Sokolova, M. P.; Bugrov, A. N.; Smirnov, M. A.; Smirnov, A. V.; Lahderanta, E.; Svetlichnyi, V. M.; Toikka, A. M. Effect of Domain Structure of Segmented Poly(Urethane-Imide) Membranes with Polycaprolactone Soft Blocks on Dehydration of *n*-Propanol *via* Pervaporation. *Polymers (Basel)*. **2018**, *10*, 1222.
(23) Nair, P. R.; Nair, C. P. R.; Francis, D. J. Imide-Modified Polyurethanes, Syntheses, Thermal, and Mechanical Characteristics. *J. Appl. Polym. Sci.* **1998**, *70*, 1483–1491.
(24) Asai, K.; Inoue, S. I.; Okamoto, H. Preparation and Properties of Imide-Containing Elastic Polymers from Elastic Polyureas and Pyromellitic Dianhydride. *J. Polym. Sci. Part A Polym. Chem.* **2000**, *38*, 715–723.
(25) Philip Gnanarajan, T.; Padmanabha Iyer, N.; Sultan Nasar, A.; Radhakrishnan, G. Preparation and Properties of Poly(Urethane-Imide)s Derived from Amine-Blocked-Polyurethane Prepolymer and Pyromellitic Dianhydride. *Eur. Polym. J.* **2002**, *38*, 487–495.
(26) Liu, J.; Dezhu, M. Study on Synthesis and Thermal Properties of Polyurethane-Imide Copolymers with Multiple Hard Segments. *J. Appl. Polym. Sci.* **2002**, *84*, 2206–2215.
(27) Mueller-Cristadoro, A.; Prissok, F. Producing Polymer Foams Comprising Imide Groups. WO 2014023796 A1, 2014.
(28) Tian, H.; Yao, Y.; Zhang, S.; Wang, Y.; Xiang, A. Enhanced Thermal Stability and Flame Resistance of Rigid Polyurethane-Imide Foams by Varying Copolymer Composition. *Polym. Test.* **2018**, *67*, 68–74.
(29) Farrissey, W. J.; Rose, J. S.; Carleton, P. S. Preparation of a Polyimide Foam. *J. Appl. Polym. Sci.* **1970**, *14*, 1093–1101.
(30) Kashiwame, J.; Ashida, K. Preparation and Properties of Polyimide Foams. *J. Appl. Polym. Sci.* **1994**, *54*, 477–486.
(31) Xi, K.; Shieh, D. J.; Wu, L.; Singh, S. Polyurethane Foam Composition Comprising an Aromatic Polyester Polyol Compound and Products Made Thereform. WO 202130115 A1, 2021.
(32) Li, C.; Hui, B.; Ye, L. Highly Reinforcing and Thermal Stabilizing Effect of Imide Structure on Polyurethane Foam. *Polym. Int.* **2019**, *68*, 464–472.
(33) Mishra, A. K.; Chattopadhyay, D. K.; Sreedhar, B.; Raju, K. V. S. N. FT-IR and XPS Studies of Polyurethane-Urea-Imide Coatings. *Prog. Org. Coatings* **2006**, *55*, 231–243.
(34) Mishra, A. K.; Chattopadhyay, D. K.; Sreedhar, B.; Raju, K. V. S. N. Thermal and Dynamic Mechanical Characterization of Polyurethane-Urea-Imide Coatings. *J. Appl. Polym. Sci.* **2006**, *102*, 3158–3167.
(35) Chattopadhyay, D. K.; Mishra, A. K.; Sreedhar, B.; Raju, K. V. S. N. Thermal and Viscoelastic Properties of Polyurethane-Imide/Clay Hybrid Coatings. *Polym. Degrad. Stab.* **2006**, *91*, 1837–1849.
(36) Meena, M.; Kerketta, A.; Tripathi, M.; Roy, P.; Jacob, J. Thermally Stable Poly(Urethane-Imide)s with Enhanced Hydrophilicity for Waterproof-Breathable Textile Coatings. *J. Appl. Polym. Sci.* **2022**, *139*, e52508.
(37) Jeon, J. Y.; Tak, T. M. Synthesis and Characterization of Block Copoly(Urethane-Imide). *J. Appl. Polym. Sci.* **1996**, *62*, 763–769.
(38) Sokolova, M. P.; Bugrov, A. N.; Smirnov, M. A.; Smirnov, A. V.; Lahderanta, E.; Svetlichnyi, V. M.; Toikka, A. M. Effect of Domain Structure of Segmented Poly(Urethane-Imide) Membranes with Polycaprolactone Soft Blocks on Dehydration of *n*-Propanol *via* Pervaporation. *Polymers (Basel)*. **2018**, *10*, 1222.
(39) Gnanarajan, T. P.; Nasar, A. S.; Iyer, N. P.; Radhakrishnan, G. Synthesis of Poly(Urethane-Imide) Using Aromatic Secondary Amine-Blocked Polyurethane Prepolymer. *J. Polym. Sci. Part A Polym. Chem.* **2000**, *38*, 4032–4037.
(40) Liu, X.; Zhou, P.; Zhang, R. Organic-Inorganic Hybrid Isocyanate-Based Polyimide Foams with Excellent Fire Resistance and Thermal Insulation Performance. *ACS Appl. Polym. Mater. Polym. Mater.* **2022**, *4*, 9015–9024.
(41) Avc, A.; Şirin, K. Thermal, Fluorescence, and Electrochemical Characteristics of Novel Poly(Urethane-Imide)s. *Des. Monomers Polym.* **2014**, *17*, 380–389.
(42) Yeganeh, H.; Barikani, M.; Noei Khodabadi, F. Synthesis and Properties of Novel Thermoplastic Poly(Urethane-Imide)s. *Eur. Polym. J.* **2000**, *36*, 2207–2211.
(43) Reichardt, C.; Welton, T. *Solvents and Solvent Effects in Organic Chemistry, Fourth Edition*; WILEY-VCH Verlag GmbH & Co., 2011.
(44) Prat, D.; Wells, A.; Hayler, J.; Sneddon, H.; McElroy, C. R.; Abou-Shehada, S.; Dunn, P. J.

CHEM21 Selection Guide of Classical- and Less Classical-Solvents. *Green Chem.* **2015**, *18*, 288–296.
(45) Guo, Y.; Spicher, S.; Cristadoro, A.; Deglmann, P.; Sijbesma, R. P.; Tomović, Ž. Towards High-Performance Polyurethanes : A Mechanism of Amine Catalyzed Aromatic Imide Formation from the Reaction of Isocyanates with Anhydrides. *Polym. Chem.* **2023**, *14*, 1773-1780.
(46) Mundhenke, R. F.; Willis, T. S. Chemistry and Properties of 4,4'-Oxydiphthalic Anhydride Based Polyimides. *High Perform. Polym.* **1990**, *2*, 57–66.
(47) Liu, B. W.; Zhao, H. B.; Wang, Y. Z. Advanced Flame-Retardant Methods for Polymeric Materials. *Adv. Mater.* **2022**, *2107905*, 1–36.
(48) Ferrari, A. C.; Robertson, J. Interpretation of Raman Spectra of Disordered and Amorphous Carbon. *Phys. Rev. B* **2000**, *61*, 14095–14107.
(49) Lu, Q. H.; Zheng, F. *Polyimides for Electronic Applications*; Elsevier Inc., 2018.
(50) Hasegawa, M.; Horie, K. Photophysics, Photochemistry, and Optical Properties of Polyimides. *Prog. Polym. Sci.* **2001**, *26*, 259–335.

Chapter 7

Epilogue

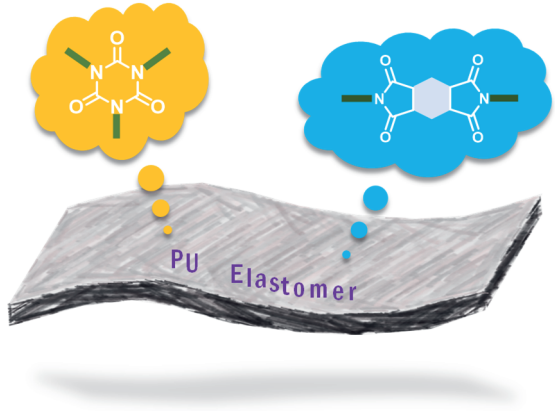
PU Elastomer

The work presented in this thesis describes the use of two chemical motifs, aromatic isocyanurate and aromatic imides, in polyurethane (PU) elastomers. Our modular study revealed the mechanism behind the cyclotrimerization of aromatic isocyanates using acetate anion as a catalyst, and a mechanism of imide formation from reaction between aromatic isocyanate and anhydride in the presence of water or amines. We also showed that the PU elastomers containing either of these two motifs exhibit enhanced thermal stability and flame retardancy. Our new synthetic pathways highlight the solvent-free reaction conditions, which paves the way from lab synthesis towards industrial applications.

In addition to the novel PU elastomers that we have prepared, there are some limitations and unanswered questions arising from the previous chapters. To solve these problems, further investigations are required. Herein, we provide suggestions to gain deeper insights into the underlying reaction mechanisms, and propose future research directions to develop high-performance PU materials that harness the isocyanurate or imide motifs to a greater extent.

7.1 General discussion

7.1.1 Mechanism studies

During the mechanism studies of cyclotrimerization and imide formation, our proposed mechanisms were consistent with the experimental results and were further supported by quantum chemical calculations. Despite these exclusive insights to the mechanisms, some questions still remain to be explored.

In **Chapter 2**, we used phenyl and *p*-tolyl isocyanates as model substrates and tetrabutylammonium acetate as a catalyst to investigate the cyclotrimerization mechanism. However, in the industrial production of PU, the efficiency of the cyclotrimerization catalysts can be influenced by various factors (*e.g.*, the presence of polyols and water, and the compatibility of catalysts). The presence of polyols and water leads to the formation of proton doners such as carbamate, allophanate, urea and biuret. As we discussed in **Chapter 2**, the deprotonated amide formed from the reaction between acetate anion and isocyanate may in turn deprotonate these proton donors, forming new catalytically active anions that are expected to catalyze the cyclotrimerization. Although the deprotonation is calculated to be possible (**Scheme 2-4**), and is supported by a kinetic study from Schwetlick and Noack,[1] more experimental verifications need to be done. Moreover, different carboxylate anions may vary the cyclotrimerization mechanisms. For instance, a benchmark cyclotrimerization catalyst, potassium acetate, needs to be dissolved in alcohols or water before use, which leads to the carbamate and urea formation. When 2-

ethylhexanoate or pivalate anion was used as a catalyst, no olefinic isocyanurate structure was observed as shown in **Figure 2-6**. Therefore, detailed cyclotrimerization mechanisms need to be specified based on different catalysts, even though they all follow anionic cyclotrimerization pathway.

In **Chapter 5**, we studied aromatic imide formation from reaction between isocyanates and anhydrides. As we discussed in **Scheme 5-1**, there are mainly two distinct mechanisms proposed for this reaction. Based on our investigations, we proposed that the urea, hydrolysis product of isocyanates, is the actual catalyst, which supports the opinion from Carleton *et al.*[2,3] However, we did not manage to observe the seven-membered ring intermediate since we could not perform the reaction of isocyanates and anhydrides in completely dry conditions.

In addition, we found that by using *N*-methylaniline as a pre-catalyst and *N,N*-dimethylcyclohyxylamine (DMCHA) as a co-catalyst, the reaction time of model reaction 5-5 (**Scheme 7-1**) is shortened to 4 h. However, this initial investigation is based on pyromellitic dianhydride (PMDA), which has high reactivity towards nucleophiles, *i.e.*, strong tendency to accept electrons.[4,5] When 3,3',4,4'-benzophenonetetracarboxylic dianhydride (BPTDA) was used to replace PMDA in model reaction 5-5, di-imide was formed within 10 h with disappearance of the carbonyl carbon of the ketone (**Figure 7-1**). When 4,4-oxydiphthalic anhydride (OPDA) was used to replace PMDA in model reaction 5-5, no imide formation was observed. Both BPTDA and OPDA have lower electron affinity (E_a = 1.55 and 1.30 eV, respectively) in comparison to PMDA with E_a = 1.90 eV.[5,6] Phthalic anhydride also cannot react readily with aromatic isocyanates. It is reported that temperature as high as 180 ºC, and long reaction time are required for the reaction between phthalic anhydride and phenyl isocyanate.[7] Even with our optimized pre-catalyst and co-catalyst, only a small number of imides was formed after reaction at 160 ºC for 2 h, while the high temperature also promoted the cyclotrimerization of isocyanates. Therefore, in order to perform the reactions between aromatic isocyanates and anhydrides such as BPTDA, OPDA and phthalic anhydrides in bulk, more mechanism investigations are necessary and optimization of catalysts is required.

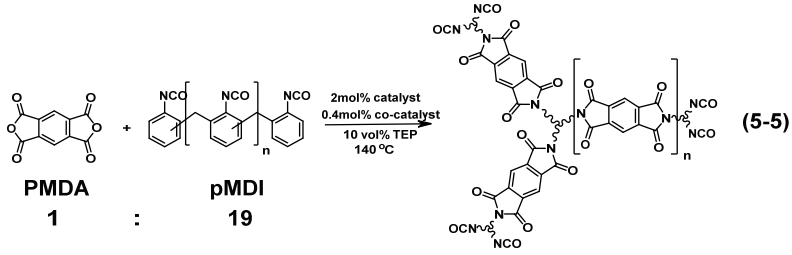

Scheme 7-1. Model reaction 5-5 between PMDA and pMDI in a 1:19 weight ratio.

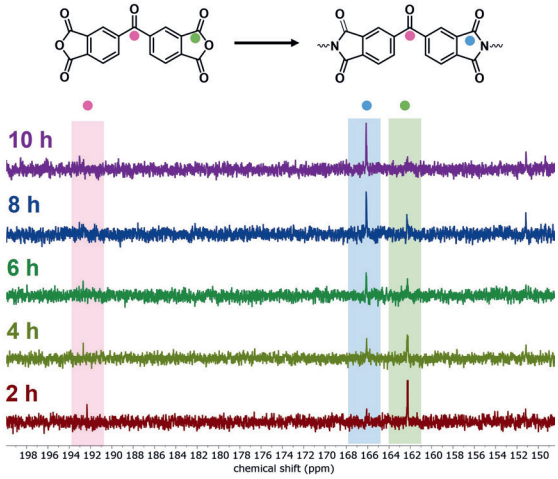

Figure 7-1. In situ ^{13}C NMR spectra (100 MHz, acetone-d_6) of the reaction between BPTDA and polymeric methylene diphenyl diisocyanate in a 1:19 weight ratio. The reaction was carried out at 140 °C using 2 mol% dibuylamine as a pre-catalyst, 0.4 mol% DMCHA as a co-catalyst and 10 vol% of TEP as an additive.

7.1.2 Polyisocyanurate (PIR)-containing and polyimide (PI)-containing PU elastomers

In **Chapter 3** and **Chapter 4**, we have prepared PIR-containing isocyanate prepolymers, which lead to PU elastomers with enhanced thermal stability and flame retardancy. While increasing the PIR content in the prepolymer will further improve the inherent thermal properties of PU materials, the increase of rigid isocyanurate structures also leads to high viscosity of subsequent isocyanate prepolymer, which remains challenging for the next-step synthesis.

In addition, we prepared flexible PIR prepolymers by co-cyclotrimerization of mono- and di-functional isocyanates. In order to avoid the use of commercially available volatile mono isocyanates, the mono-functional isocyanates were synthesized by reacting di-isocyanates with mono-functional alcohols, resulting in mono-functional isocyanates containing carbamate structures. However, this leads to allophanate formation during co-cyclotrimerization, which has a relatively low dissociation temperature (106 °C).[8,9] Although optimization have been done in **Chapter 3**, allophanate was still present as shown in **Figure 3-5** and **Figure 4-1**. The presence of allophanate inevitably decreases the thermal stability of the PIR prepolymer and the resulting PU elastomers. Compared to the work reported by Endo *et al*. who prepared flexible PIR film with decomposition temperature at 5% weigh loss (T_{d5}) higher than 400 °C *via* co-trimerization of 4,4'-methylene diphenyl diisocyanate (4,4'-MDI) and mono-functional isocyanates such as butyl or phenyl isocyanates, our synthetic pathway still

needs to be optimized in order to reduce allophanate formation during preparation of PIR prepolymer.[10,11]

We also prepared aromatic PI-containing isocyanate prepolymers by reacting PMDA and polymeric aromatic isocyanates in **Chapter 6**, leading to PU elastomers with enhanced thermal properties. However, the viscosity of the prepolymer also dramatically increases with more imide structures present, which is due to the strong packing effect of aromatic imides. Therefore, maximum 5 wt% PMDA was used in the synthesis of imide-containing isocyanate prepolymer, leading to as low as 2 wt% imide structures in the final PU elastomer (PUI-1 in **Chapter 6**). Although this small number of imides did improve the flame retardancy of PU elastomer as shown in **Figure 6-5**, further studies could help to increase the imide content in order to get PU materials with even better flame retardancy. Additionally, we observed precipitation of imides during reaction between 4,4'-MDI and PMDA. On the other hand, the reaction between long-chain isocyanate-terminated prepolymer and PMDA avoids the precipitation of imides, but the reaction stops at the mono-imide formation. Overall, we have not yet found a way to prepare linear imide-containing PU polymers in bulk, which also needs to be further studied.

7.2 Future perspectives

7.2.1 Further directions of mechanism studies

In addition to many peer-reviewed literatures, we reported a detailed cyclotrimerization mechanism of aromatic isocyanates using acetate anion as a catalyst. During our study, we demonstrated that the qualitative mechanism is independent of the solvent polarity. We also proposed that it is possible for the catalytically active anionic species to change several times during the polymerization (*e.g.*, deprotonated amide, carbamate and urea). However, the effect that protic solvents may have on the relative stability of the corresponding anions needs to be further studied.

On the other hand, the mechanism of reaction between isocyanates and anhydrides needs to be investigated more in depth. As we discussed in section 7.1.1, we only studied the reaction of aromatic isocyanates and PMDA, which is the most industrially relevant monomer. Whereas it will be interesting to check other commercially available anhydrides such as BPTDA, OPDA and phthalic anhydrides, the reaction of these anhydrides and aromatic isocyanates hardly worked out. Therefore, model reactions, such as reaction between anhydrides and phenyl isocyanates, or reaction between anhydrides and hexyl isocyanates can be carried out to study the mechanisms. In addition, we found that the triethyl phosphate (TEP) additive has remarkable effect on reducing the reaction time (**Table 7-1**), while the quantum chemical calculations

show no significant energy lowering of the ionic species. We proposed that the role of TEP is to stabilize the anion on the deprotonated urea, but an accurate description of the solvation effects of TEP needs to be given. The dielectric constant of TEP may also play a role in the reaction mechanism, which demands further experimental and computational studies.

Table 7-1. Reaction time of model reaction 5-5 using 2 mol% *N*-methylaniline as a pre-catalyst, DMCHA as a co-catalyst and 10 vol% of different additives/solvents.

Solvent	b_p (°C)	DMCHA amount (mol%)	Reaction time[a]
Triethyl phosphate	215	0.4	4 h
Tetrahydrofuran	66	0.4	---
Cyclohexanone	156	0.4	4 h
Propylene carbonate	242	0.4	14 h
Propylene carbonate	242	1	8 h

[a] The time when there was only di-imide carbonyl peak in ^{13}C NMR spectra was defined as reaction time.

Moreover, we also found that alcohols, malonates, acetoacetates and special secondary amines can potentially be used as pre-catalysts for the reaction between isocyanate and anhydrides (**Table 7-2**). Carleton *et al*. also reported that the presence of 10 mol% ethanol accelerates the reaction between phthalic anhydride and phenyl isocyanate in pyridine.[2] This may be an interesting direction to explore better pre-catalysts than *N*-methylaniline.

Table 7-2. Reaction time of model reaction 5-5 using DMCHA as a co-catalyst and different pre-catalysts (dosing amount 2 mol%).

Pre-catalyst	DMCHA amount (mol%)	Reaction time[a]
Phenol	0.4	5 h
t-Butanol	0.4	4 h
Dimethyl malonate	0.2	Isocyanurate formation
Dimethyl malonate	--	>20 h
Ethyl acetoacetate	0.4	14 h
Cyanuric acid	0.4	8 h

[a] The time when there was only di-imide carbonyl peak in ^{13}C NMR spectra was defined as reaction time.

7.2.2 Further improvements of thermal stability and flame retardancy of PU materials

In order to increase the PIR content and reduce the viscosity of the PIR prepolymer, the molar ratio of mono- and di-functional isocyanates for co-cyclotrimerization can be optimized. Moreover, co-cyclotrimerization of aromatic and aliphatic diisocyanates can be adopted. For instance, Endo *et al*. prepared flexible PIR networks with T_{d5} >

440 °C *via* co-cyclotrimerization of 4,4'-MDI and hexamethylene diisocyanate (HDI).[12] Their work provides a solution for preparing flexible PIR prepolymer with higher thermal stability. We can also optimize our PIR network by changing some of the 4,4'-MDI to HDI before co-cyclotrimerization with mono-functional isocyanates.

According to **Chapter 3** and **Chapter 4**, we also found that the mono-functional alcohol plays an important role in tuning the physical properties of the PU materials. For example, we found that by using 2-ethyl-1-hexanol or octanol, the water uptake of the subsequent PU materials significantly decreased compared to those using *n*-butanol or *t*-butanol. This may be an interesting direction for preparing PU adhesives and aerogels. In **Chapter 4**, we showed that the use of diethyl(hydroxymethyl) phosphonate (DEHP) greatly improves the flame retardancy of the PU elastomers. Based on this modular study, various phosphorus-containing alcohols or polyols can be used in preparation of PIR prepolymers, which will further improve the flame retardancy of PU materials.[13–16]

In order to prepare isocyanate prepolymer with high imide content, diisocyanates monomers can be used to reduce the viscosity of the prepolymer. However, as mentioned in previous section, the reaction between 4,4'-MDI and PMDA leads to precipitation. To solve this problem, 2,4'-methylene diphenyl diisocyanate (2,4'-MDI) can be used in the reaction with PMDA. However, when *N*-methylaniline and DMCHA were used as a catalyst and a co-catalyst, isocyanurate formation was always observed after imide formation and additional acid was required to quench the deprotonated urea. A combination of polymeric MDI and 2,4'-MDI may produce an isocyanate prepolymer with high imide content and the isocyanurate formation may be avoided. Additionally, dianhydrides with more flexible spacers, such as anhydride functionalized oligomers, may be used to reduce the packing effect of the imide structures and prepare prepolymers with lower viscosity.

7.3 References

(1) Schwetlickt, K.; Noacks, R. Kinetics and Catalysis of Consecutive Isocyanate Reactions. Formation of Carbamates, Allophanates and Lsocyanurates. *J. Chem. Soc. Perkin Trans. 2* **1995**, No. 2, 395–402.
(2) Farrissey, W. J.; Rose, J. S.; Carleton, P. S. Preparation of a Polyimide Foam. *J. Appl. Polym. Sci.* **1970**, *14*, 1093–1101.
(3) Carleton, P. S.; Farrissey, W. J.; Rose, J. S. The Formation of Polyimides from Anhydrides and Isocyanates. *J. Appl. Polym. Sci.* **1972**, *16*, 2983–2989.
(4) Sroog, C. E. Polyimides. *J. Polym. sci., Macromol. Rev.* **1976**, *11*, 161–208.
(5) Mundhenke, R. F.; Willis, T. S. Chemistry and Properties of 4,4'-Oxydiphthalic Anhydride Based Polyimides. *High Perform. Polym.* **1990**, *2*, 57–66.
(6) Ghosh, M. *Polyimides: Fundamentals and Applications*; Plastics Engineering; CRC Press, 2018.
(7) Hurd, C. D.; Prapas, A. G. Preparation of Acyclic Imides. *J. Org. Chem.* **1959**, *24*, 388–392.
(8) Chattopadhyay, D. K.; Webster, D. C. Thermal Stability and Flame Retardancy of Polyurethanes. *Prog. Polym. Sci.* **2009**, *34*, 1068–1133.

(9) Lapprand, A.; Boisson, F.; Delolme, F.; Méchin, F.; Pascault, J. P. Reactivity of Isocyanates with Urethanes: Conditions for Allophanate Formation. *Polym. Degrad. Stab.* **2005**, *90*, 363–373.
(10) Moritsugu, M.; Sudo, A.; Endo, T. Development of High-Performance Networked Polymers Based on Cyclotrimerization of Isocyanates: Control of Properties by Addition of Monoisocyanates. *J. Polym. Sci. Part A Polym. Chem.* **2012**, *50*, 4365–4367.
(11) Moritsugu, M.; Sudo, A.; Endo, T. Development of High-Performance Networked Polymers Consisting of Isocyanurate Structures Based on Selective Cyclotrimerization of Isocyanates. *J. Polym. Sci. Part A Polym. Chem.* **2011**, *49*, 5186–5191.
(12) Moritsugu, M.; Sudo, A.; Endo, T. Cyclotrimerization of Diisocyanates toward High-Performance Networked Polymers with Rigid Isocyanurate Structure: Combination of Aromatic and Aliphatic Diisocyanates for Tunable Flexibility. *J. Polym. Sci. Part A Polym. Chem.* **2013**, *51*, 2631–2637.
(13) Rao, W. H.; Xu, H. X.; Xu, Y. J.; Qi, M.; Liao, W.; Xu, S.; Wang, Y. Z. Persistently Flame-Retardant Flexible Polyurethane Foams by a Novel Phosphorus-Containing Polyol. *Chem. Eng. J.* **2018**, *343*, 198–206.
(14) Zhang, K.; Hong, Y.; Wang, N.; Wang, Y. Flame Retardant Polyurethane Foam Prepared from Compatible Blends of Soybean Oil-Based Polyol and Phosphorus Containing Polyol. *J. Appl. Polym. Sci.* **2018**, *135*, 1–10.
(15) Yuan, Y.; Yang, H.; Yu, B.; Shi, Y.; Wang, W.; Song, L.; Hu, Y.; Zhang, Y. Phosphorus and Nitrogen-Containing Polyols: Synergistic Effect on the Thermal Property and Flame Retardancy of Rigid Polyurethane Foam Composites. *Ind. Eng. Chem. Res.* **2016**, *55*, 10813–10822.
(16) Sykam, K.; Meka, K. K. R.; Donempudi, S. Intumescent Phosphorus and Triazole-Based Flame-Retardant Polyurethane Foams from Castor Oil. *ACS Omega* **2019**, *4*, 1086–1094.

Summary

After the invention of polyurethane by Bayer in 1937, PU industry has developed rapidly. Due to their versatile chemical and physical properties, PUs are made into different types of materials (*e.g.*, rigid or flexible foams, compact thermosets, coatings, elastomers and adhesives). These PU materials are used in various applications, especially in construction and automotive applications, where thermal stability and flame retardancy are required. With the increasing market demands, further improvement of the physical properties of PU materials becomes more and more crucial.

Many efforts have been made to improve the thermal properties of the PU materials. A conventional way is to add flame retardant additives in PU materials, but they may lead to several problems such as poor compatibility, deterioration of mechanical properties and releases of toxic gas during combustion. An alternative way is to introduce reactive flame retardant motifs in PU materials *via* covalent bonds. As a result, the inherent thermal properties of the PU materials can be improved, and the use of conventional flame retardant additives can be reduced. This thesis focuses on incorporating aromatic isocyanurate or aromatic imide motifs in PU elastomers in order to enhance their thermal stability and flame retardancy.

In the first part of this thesis, the introduction of aromatic PIR motifs in PU elastomers is discussed, which is typically achieved by cyclotrimerization of isocyanates. In **Chapter 2**, we study the cyclotrimerization mechanism of aromatic isocyanates in the presence of catalytic amount of acetate anions by state-of-the-art experimental and computational methods. The study reveals that, although the cyclotrimerization still follows an anionic mechanism, the actual catalytically active species changes and the acetate anion only serves as a pre-catalyst. During the cyclotrimerization of isocyanates, the reaction of acetate anion with excess of isocyanates first forms anhydride. After intramolecular rearrangement and decarboxylation of the anhydride, a deprotonated amide species is formed irreversibly. This newly formed deprotonated amide actively catalyzes the isocyanurate formation *via* an anionic mechanism. It is also capable of deprotonating other protic groups such as urethane and urea, which in turn catalyze the cyclotrimerization of aromatic isocyanates. In addition, the carboxylate migration of anhydrides to amide anions takes place regardless of the size of the carboxylate anions (*e.g.*, acetate, 2-ethylhexanoate and pivalate). On the other hand, only when acetate anion was used as a cyclotrimerization catalyst, a side product, N-heterocyclic olefin, was formed with elimination of a water molecule.

Furthermore, PIR-containing PU elastomers were prepared applying an elegant synthetic pathway. In order to avoid the limitation of PIR content by rigidity of PIR structures, a liquid PIR-containing isocyanate prepolymer was first prepared *via* co-trimerization of 4,4'-MDI and mono-isocyanates, as described in **Chapter 3**. The mono-isocyanate was synthesized from reaction between 4,4'-MDI and 2-ethyl-1-hexanol. During the study of trimerization catalysts, TDMAMP turned out to be the most suitable catalyst for the preparation of prepolymers due to the high isocyanurate content after trimerization, mild reaction condition and more controllable trimerization process. After co-trimerization, the molar ratio of urethane, allophanate and isocyanurate in the PIR prepolymer was determined by quantitative ^{13}C NMR spectroscopy and the average functionality of the PIR prepolymer was calculated from average molecular weight and NCO content. The prepolymer was further used to prepare PIR elastomers in both solvent and solvent-free conditions. These elastomers exhibit good thermal stability with high char formation, and improved mechanical properties with much higher Young's modulus.

Based on the insights gained in **Chapter 3**, we discover that the physical properties of PU elastomers can be tuned by varying the mono-functional alcohol linked to the PIR network, which is shown in **Chapter 4**. In order to further improve the thermal stability and flame retardancy of PU elastomers, a phosphorus-containing compound, DEHP, was used to replace 2-ethyl-1-hexanol during the synthesis of PIR prepolymer. The PIR-DEHP prepolymer obtained was used to prepare elastomers in solvent and solvent-free conditions. The subsequent PIR-DEHP elastomers have a high stiffness and a high T_g, which increase with PIR and aromatic content. Moreover, the elastomers show enhanced thermal stability and flame retardancy in comparison with the elastomers without PIR and phosphorus motifs.

The second part of this thesis describes the incorporation of aromatic PI motifs in PU elastomers. A straightforward synthetic way to realize this is *via* reaction between isocyanate and anhydride. The underlying mechanism behind the reaction is reported in detail in **Chapter 5**. The reaction of isocyanate and anhydride in the presence of catalytic amount of water was first investigated. This study reveals that the actual catalyst in the reaction is urea, which is formed as the hydrolysis product from isocyanate. We further discovered that secondary amines, with the help of tertiary amine bases, are better pre-catalysts (or, rather, co-catalysts) than water. With *N*-methylaniline and DMCHA as pre-catalyst and co-catalyst respectively, the reaction time of polymeric MDI and PMDA significantly decreased to 4 h, which was much shorter than that using water as a pre-catalyst (24 h). Furthermore, the combination of our experimental studies and quantum chemical calculations reveals exclusive insights in the reaction of aromatic isocyanates and dianhydrides. The reaction starts from a deprotonated urea ring-opening an anhydride, forming an intermediate containing a

carboxylate group. In the next step, the carboxylate of the acid intermediate reacts with one more isocyanate molecule, followed by release of a CO_2 molecule and ring closure, resulting in an imide structure.

Based on our mechanistic study, the preparation of PUI elastomers *via* a two-step synthesis is reported in **Chapter 6**. An imide-containing isocyanate prepolymer was first synthesized *via* reaction of aromatic (or aliphatic isocyanates) with PMDA. With *N*-methylaniline (or dibutylamine) as a pre-catalyst and DMCHA as a co-catalyst, this reaction could be carried out without solvent. The prepolymer was further used to prepare PUI elastomers in bulk. Both aromatic and aliphatic isocyanate-based elastomers exhibit enhanced thermal stability and stiffness in comparison with those without imide structures. Moreover, the aromatic PUI elastomer has lower total heat release and total smoke production, which indicates improved intrinsic thermal stability and flame retardancy.

In conclusion, this thesis demonstrates that the use of PIR and PI containing isocyanate prepolymers is an exciting approach to introduce isocyanurate and imide motifs in PU. With these prepolymers, high-performance PU elastomers can be produced in a greener and more processable way, which holds great potential for other industrial applications, such as rigid foams, compact thermosets and adhesives.

Curriculum Vitae

Yunfei Guo (郭芸菲) was born on 8th of August 1991 in Shanghai, China. After finishing high school at Shanghai Gezhi High School, she began her bachelor's study in High Molecular Material and Engineering at East China University of Science and Technology in Shanghai. In 2013, she obtained B.Eng. degree and moved to Berlin to start a joint Polymer Science master program held by Freie Universität Berlin, Humblodt Universität zu Berlin, Technische Universität Berlin and Universität Potsdam. During her master, she went to Bundesanstalt für Materialforschung und -prüfung (BAM) for internship about thermoresponsive core-shell nanoparticles and finished her master thesis there with the topic "Non-ionic Hydrogels with Positive Thermoresponsivity in Water and Electrolyte Solution" under the supervision of Dr. Annabelle Bertin. In 2015, she obtained her M.Sc. degree and joined BASF advanced chemicals co. ltd in Shanghai as an associate chemist working on polyurethane for three years.

To pursue her research interests in polyurethanes, she commenced her Ph.D research in 2019 in Eindhoven University of Technology. She joined Polymer Performance Materials (SPM) group under the supervision of Prof. Željko Tomović and Prof. Rint Sijbesma. During her PhD research, she focused on investigating the formation of isocyanurates and imides, and applying these structures in polyurethane materials in order to improve their chemical and physical properties.

List of Publications

Journal publications

Guo, Y.[†]; Muuronen, M.[†]; Deglmann, P.; Lucas, F.; Sijbesma, R. P.; Tomović, Ž., Role of acetate anions in the catalytic formation of isocyanurates from aromatic isocyanates. *J. Org. Chem.* **2021**, *86*, 5651–5659 ([†] equal contribution).

Guo, Y.; Muuronen, M.; Lucas, F.; Sijbesma, R. P.; Tomović, Ž., Catalysts for isocyanate cyclotrimerization. *ChemCatChem* **2023**, e202201362.

Guo, Y.; Spicher, S.; Cristadoro, A.; Deglmann, P.; Sijbesma, R. P.; Tomović, Ž., Towards high-performance polyurethanes: A mechanism of amine catalyzed aromatic imide formation from the reaction of isocyanates with anhydrides, *Polym. Chem.* **2023**, *14*, 1773-1780.

Guo, Y.; Kleemann, J.; Bokern, S.; Kamm, A.; Sijbesma, R. P.; Tomović, Ž., Synthesis of polyisocyanurate prepolymer and the resulting flexible elastomers with tunable mechanical properties. *Polym. Chem.* **2023**, *14*, 1923-1932.

Guo, Y.; Kleemann, J.; Sijbesma, R. P.; Tomović, Ž., Phosphorus-containing polyisocyanurate (PIR) elastomers for flame retardant application, *under peer review*.

Guo, Y.; Cristadoro, A.; Kleemann J.; Bokern, S.; Sijbesma, R. P.; Tomović, Ž., Solvent-free preparation of thermally stable poly(urethane-imide) (PUI) elastomers, *under peer review*.

Patent application

Cristadoro, A.; Kleemann, J.; Bokern, S.; **Guo, Y.**; Tomović, Ž.; Sijbesma, R. P., Application No. 22212781.3, submitted on December 14, **2022**.

Acknowledgement 致谢

Time flies by quickly and now it's the end of my doctoral career. Looking back to the four years of my research and life in TU/e, it is impossible for me to imagine that I could have accomplished my PhD without the company and support from my friends, family and colleagues. In the end (and probably most read) of my thesis, I would like to give my appreciation to many people that contributed in numerous ways.

The first person I would like to thank is my first promoter, **Željko**. Thank you for having me as your first PhD student and starting this incredible journey. If it was not for you, I would not have been able to start, let alone finish my PhD in time. Thank you for your trust, your guidance and your supervision. You have taught me to work and think independently.

I would also like to express my gratitude for my second promoter, **Rint**, for your brilliant ideas and suggestions, and for your guidance and coaching. Our weekly meetings were often very fruitful and together we solved many problems. I admire your enthusiasm for research, your broad and deep knowledge in various fields, your kindness to every student, your patience with my failures, and your professional and beautiful scientific writing. It has been a privilege and a joy to work under your supervision.

Hans, your nice suggestions and questions during the group meetings often gave me a new perspective on my work. I can really sense your joy and love for polymers. Especially, your expertise on polymer characterizations was vital for some of my chapters. It is always fun to talk to you due to your insights and consistently good mood.

Anna, we met each other when I started my imide projects. I appreciate your initiation of this nice project, organization of the meetings and support on the patent application and my manuscripts.

I would also like to thank my committee members **Prof. Anja Palmans** and **Prof. Berend Eling** for evaluating my work and providing valuable feedback. **Anja**, it is so delightful to see your presentations, your enthusiasm for your work and various topics. **Berend**, I have heard your lecture in Shanghai BASF and I was so impressed. You have so much knowledge in polyurethane which has driven my further pursuit for my doctoral degree.

I would also like to give special thanks to **Prof. Albert Schenning** for chairing my defense.

My PhD projects and this thesis would not be possible without the sponsorship and support from BASF Polyurethane GmbH. I had the honor to collaborate with some really

smart and talented people. **Nadine**, I appreciate your help on my experiments and measurements so much. The materials and some test results in my thesis could not have been achieved without your cooperation. You took good care of me during my visits to BASF and I enjoyed the coffee breaks and chats with you. I would like to thank **Julian** for the guidance and suggestions on my PIR and imide projects. It was a nice cooperation and I wish you great success in your new position. I am especially grateful for the help from **Stefan**. You are one of the catalysts for me to start my PhD project and you recommended me to get this opportunity. I am glad to have been able to cooperate with you again in my fourth year of PhD and you provided a lot of nice suggestions on my projects, patent and manuscripts. I wish you great success in your research and joy with the new-born baby. I would also like to thank **Daniel**, **Martin** and **Volker** for their great support on my projects.

It is such a privilege to get great help and support from colleagues in BASF SE. **Mikko**, **Sebastian** and **Peter**, you are experts in quantum chemical calculations. Without your professional advice and insights, I would not have been able to verify the experimental results and finish my Chapter 2 and Chapter 5. Also, thank you **Mikko** for your contribution to our review manuscript about cyclotrimerization catalysts. I would also like to thank **Frederic** for supporting me with the GPC measurements in Chapter 3 and the collection of references for the review manuscript.

People say that PhD means working mostly in dull and sometimes lonely hours. Thankfully, when I was working on Saturdays in a nearly empty building, I had my Saturday partner **Muhabbat** who made it a bit less lonely. I enjoyed all of our Saturday delivery food (junk food forever!!!), and got more motivated and efficient after the lunch break. Thank you for your small gifts and your passion in life. Your encouragement helped me to go through many hard times and difficulties. I also enjoyed our game nights which kept me relaxed and motivated after a hard-working day. So, thank you Muhabbat, you are such a kind person and an amazing friend. I'm so happy that you are one of my amazing paranymphs. I wish you great success in your coming defense and all the best in your new job!

Patrick, the other fantastic paranymphs, you are a very smart, confident and reliable person. You stay calm in urgent situations, try to keep everything safe, and you volunteered as a first-aid person. You are always ready to help people, no matter machine-broken or heart-broken, you always try to fix them. You are the strongest person in our group who helps to open the bottles, lifts the heavy stuff, organizes the lab equipment, and installs the racks in my fume hood. You are the most calorie-dense person in our group and I am so impressed with your 1 kg-lasagna. Most importantly, you have broad knowledge of different topics. Some useful suggestions that you gave

me helped a lot in my experiments and my manuscripts. I am very glad to have you as my officemate in the third and fourth year of my PhD.

During my PhD journey, I had the pleasure of being part of two wonderful research groups (Sijbesma group and SPM group). I want to thank everybody from these groups for the warm atmosphere, the laughs we shared, encouragement, discussions and company. **Huiyi**, you are the most social person that I have ever met and it was always fun to have you around. Also, as a kind and helpful person, you took care of me a lot when I was a fresh PhD student and you encouraged me when I was in a bad mood. **Jie**, I appreciated you so much for your ideas and suggestions on my experiments and each of our "lunch meetings". You are always so interested in different research topics and express your exclusive insights. **Patricia**, your passion, enthusiasm and big smile always motivate me. I will never forget the time when we shared the fumehood in lab 4. **Annalore**, you are a colorful person with many cute and fun stuffs. I was also impressed by your beautiful presentations and your nice mechanochemistry experiments. **Souma**, you are the most talented PhD student I know. You not only have deep knowledge in dynamic covalent bonds, rheology and phosphorus chemistry, but also broad knowledge in other fields. **Diederik**, you have vast knowledge of chemistry. It is always useful to discuss with you. Thank you for your kindness and your help. I would also like to thank **Yinjun**, **Eveline**, **Roy**, **Fang** and **Shahzad** for the help, discussions and chats.

I would also like to express my respect to Dr. Türel. Every time, if I have questions on organic synthesis and manuscripts, **Tankut** is always ready to help. I would like to express my gratitude for your support in my research and your contribution in establishing the lab. **Changlin**, thank you for your help on SEM measurement of my samples and for your discussions on my experiments and storylines. Thank you for sharing the snacks, home-made delicious bread and cakes. **Keita**, I am often impressed by your beautiful figures, slides and of course, your beautiful experimental results. I am sure that you can have more and more nice papers. **Özgün**, you are a very kind person and full of ideas and motivation. You are always helpful whenever I have questions or I need help. I would also like to thank you for designing my cover image. **Fabian**, I learned a lot from your professional and colorful slides. You always stay calm when dealing with difficult situations and keep patient with your students. I am glad that you became the assistant professor in SPM group and you helped a lot in organizing our group. **Audrey (Fournier)**, thank you for your strong support and amazing contributions in organizing our lab. Thank you for arranging the lab cleaning, lab safety and waste disposal. It is a difficult job but you manage it very well. **Bengi** and **Ahsen**, although you joined our group less than one year ago, I can really feel your passion and enthusiasm for research. I wish you good luck and much success with your projects. I would also like to thank **Tom**, **Niels**, **Frederique**, **Yi-Ru** and **Christos**, it is nice to have you in our group.

It was a privilege to get help from experts with the analysis of various measurements. I would like to thank **Lou** and **Joost** for their help with the MS measurements and discussions, **Siyu** for the Raman spectroscopy and **Marcel** for discussions about NMR spectroscopy. In addition, without the support from the following people, our research would not run smoothly. **Martina**, you are such a wonder woman who makes everything possible. You are so experienced, so efficient and you know everything about Helix. **Léontine**, I will never forget how cozy the kitchen you organized. Thank you very much for organizing the meetings and daily group routines. I hope you do well in your new position. **Audrey (Debije)**, thank you for guiding my scientific writing, from manuscript to cover letter to Chapter 1 of this thesis, I have learned a lot of writing skills from you.

I also want to thank and acknowledge some of my friends in TU/e. **Jingyi**, you were a wonderful officemate in the first and second year of my PhD. You helped me a lot in my daily life and I really enjoy chatting with you. **Linlin**, we came to TU/e in the same batch and we supported each other through all sorts of difficulties and challenges. I wish you great success in finishing your thesis and the coming defense! I would also like to thank the support from **Jingxin**, **Hailin** and **Bingbing**.

I will look back to my days as a PhD student with great fondness because of numerous awesome people who supported me and helped me. I am grateful to you all.

最后我想感谢国内的小伙伴给与我精神上的支持。首先我想要感谢聪明伶俐机智过人的**小悦悦**，谢谢你对我的支持。这几年一直都无法一起旅行，希望等毕业之后我们可以重启我们的冒险之旅，享受各类美食。我还要感谢**蔡蔡**一直以来对我的鼓励，感谢你听我的倾诉，感谢你时时刻刻能想到我。希望我们能不负初心，一起加油努力，一起发现生活中的乐趣。**笑笑**，谢谢你时不时来找我聊天鼓励我，讨论我们最爱的话题。你说你想多学一些东西，努力永远不算晚，希望你每天都能进步一点点。感谢来自**彭彭**，**陶子**，**婧扬**，**丁一**，**小玥**，**秀秀**，**贞贞**（502 寝室是最棒的！），**璐璐**，**嘉玥**，**珺琳**，**小强**对我关心与鼓励，等回国再聚！我还要感谢**刘英豪**博士和**韩玮**博士对我的举荐和帮助，感谢你们的信任并给予我读博的机会！

当然，最重要的，我最想要感谢的是我的家人对我无条件的支持与鼓励。**爸妈**，感谢你们对我的养育和对我的信心，感谢你们让我选择了喜欢的理工科。我能坚持下来从本科一路读到博士都离不开你们一直以来的后勤保障和精神鼓励。**舅舅**，**舅妈**，**外公**，**外婆**，**倜瑜**，**小华**，感谢你们对我的关心与支持，同时也祝**小萌萌**快乐长大！

Love,

Yunfei (芸菲)